

Two new bamboo-feeding species of the genus *Kirbyana* Distant, 1906 from China (Hemiptera, Fulgoromorpha, Cixiidae)

Yan Zhi^{1,2}, Lin Yang^{2,3}, Xiang-Sheng Chen^{2,3}

1 Laboratory Animal Center, Guizhou Medical University, Guiyang, Guizhou, 550025, China **2** Institute of Entomology, Guizhou University, Guiyang, Guizhou, 550025, China **3** The Provincial Special Key Laboratory for Development and Utilization of Insect Resources of Guizhou, Guizhou University, Guiyang, Guizhou, 550025, China

Corresponding author: Xiang-Sheng Chen (chenxs3218@163.com)

Academic editor: Mike Wilson | Received 19 February 2021 | Accepted 8 April 2021 | Published 11 May 2021

<http://zoobank.org/A664D1F6-5F7F-4D00-B21F-20AD7563B602>

Citation: Zhi Y, Yang L, Chen X-S (2021) Two new bamboo-feeding species of the genus *Kirbyana* Distant, 1906 from China (Hemiptera, Fulgoromorpha, Cixiidae). ZooKeys 1037: 1–14. <https://doi.org/10.3897/zookeys.1037.64653>

Abstract

Two new bamboo-feeding species of the cixiid planthopper genus *Kirbyana* Distant, 1906 (Hemiptera: Fulgoromorpha: Cixiidae: Eucarpiini), *K. aspina* Zhi & Chen, **sp. nov.** and *K. furcata* Zhi & Chen, **sp. nov.**, are described and illustrated from southern China. A key to all known species and a map of their geographic distributions are provided.

Keywords

Auchenorrhyncha, Cixiidae, Fulgoromorpha, Oriental region, planthopper, taxonomy

Introduction

The planthopper genus *Kirbyana* was established by Distant (1906), with *Kirbya pagana* Melichar, 1903 as the type species. This genus belongs to the tribe Eucarpiini of subfamily Cixiinae (Hemiptera: Cixiidae) (Holzinger et al. 2002). Previously, eight species and one subspecies in this genus have been recorded: *Kirbyana australis* (Muir,

1913), *K. deusta* (Distant, 1911), *K. deventeri* (Kirkaldy, 1907), *K. javana* Muir, 1913, *K. lini* Tsaour & Hsu, 2003, *K. pacifica* Emeljanov & Hayashi, 2007, *K. pagana* (Melichar, 1903), *K. pratti* Muir, 1913 and *K. pratti thyas* Fennah, 1978 (Bourgoin 2021).

Recent study of some Chinese specimens has found two new bamboo-feeding species, *K. aspina* Zhi & Chen, sp. nov. and *K. furcata* Zhi & Chen, sp. nov., which are described here. So far, including the two new species, the genus currently now counts for ten valid species, all distributed in the Australian and Oriental regions (Australia, China, India, Indonesia, Japan, Malaysia, Sri Lanka and Vietnam).

Materials and methods

The morphological terminology follows Bourgoin (1987) for male genitalia, Bourgoin et al. (2015) for wing venation and Bourgoin (1993) for female genitalia. Body length was measured from apex of vertex to tip of forewing; vertex length represented the median length of the vertex (from the apical transverse carina to the tip of basal emargination). Fuchsin staining was used to highlight female genitalia structures studied. External morphology and drawings were done with the aid of a Leica MZ 12.5 stereomicroscope. Photographs were taken with a KEYENCE VHX-6000 system. Illustrations were scanned with a CanoScan LiDE 200 and imported into Adobe Photoshop 7.0 for labeling and plate composition. The dissected male and female genitalia are preserved in glycerin in small plastic tubes pinned together with the specimens.

The type specimens are deposited in the Institute of Entomology, Guizhou University, Guiyang, Guizhou Province, China (**GUGC**).

Taxonomy

Genus *Kirbyana* Distant, 1906

Kirbya Melichar, 1903: 37, preoccupied by *Kirbya* Robineau-Desvoidy, 1830 (Diptera).

Kirbyana Distant, 1906a: 262, nom. nov. for *Kirbya* Melichar, 1903.

Kirbyella Kirkaldy, 1906: 248, synonymised by Distant 1906b: 274.

Saccharias Kirkaldy, 1907: 125, synonymised by Fennah 1980: 239.

Commolenda Distant, 1911: 741, synonymised by Fennah 1978: 211.

Type species. *Kirbya pagana* Melichar, 1903 (original designation by Distant).

Diagnosis. Head. Head including eyes slightly narrower than pronotum. Vertex in profile horizontal, in same line as thorax, meeting frons abruptly nearly at 90°; sub-apical carina absent. Frons somewhat longer than broad or as long as wide; median carina present; anterior margin angularly emarginate or transverse; position of maximum width of frons more or less at the level of antennae. Median ocellus absent. Subapical segment of rostrum 2.5 times longer than apical segment.

Thorax. Pronotum very narrow, scarcely half as long as vertex in midline. Mesonotum nearly twice as long as pronotum and vertex together. Forewing with the eucarpian basal concavity of the anterior margin of the forewings, also slightly concave at node level. Hindwing with simple radius (R). Hind tibia lacking lateral spines. Metatibiotarsal formula: 6/8-11/9-11.

Male genitalia. Pygofer symmetrical and prolonged with symmetrical lateral lobes in lateral view. Medioventral process thumb-like in lateral view. Anal segment short and stout. Gonostyli relatively small and symmetrical. Aedeagus slender and endosoma of aedeagus with spinose processes.

Female genitalia. Ovipositor elongate, orthopteroid and slightly curved upwards; anal segment square or rectangular in dorsal view; 9th tergite without wax plate. Posterior vagina with sclerites.

Distribution. Australian and Oriental regions.

Checklist and distributions of species of *Kirbyana* Distant

- K. aspina* Zhi & Chen, sp. nov.; China (Hunan).
K. australis (Muir, 1913); Australia (Northern Territory; Queensland).
K. deusta (Distant, 1911); Central India.
K. deventeri (Kirkaldy, 1907); Indonesia (Java).
K. furcata Zhi & Chen, sp. nov.; China (Guangxi, Yunnan).
K. javana Muir, 1913; Indonesia (Java).
K. lini Tsaour & Hsu, 2003; China (Taiwan).
K. pacifica Emeljanov & Hayashi, 2007; China (Taiwan), Japan (Ryukyu Islands).
K. pagana (Melichar, 1903); Sri Lanka (Peradeniya).
K. pratti Muir, 1913; Malaysia (Parit Buntar).
K. pratti thyas Fennah, 1978; Vietnam (Cuc-phuong Province, Ninh Binh).

Key to the species (males) of *Kirbyana* Distant

- 1 Anterior margin of vertex transverse.....2
 – Anterior margin of vertex angularly excavated or incised at middle7
 2 Forewing with numerous small fuscous spots on basal half and several wavy fuscous lines on apical half..... ***K. deusta* (Distant, 1911)**
 – Forewing not so marked3
 3 Forewing with a transverse veinlet from M to CuA near Cu fork4
 – Forewing without transverse veinlet from M to CuA near Cu fork.....5
 4 Forewing without transverse veinlet from MP3+4 to CuA1 (Löcker et al. 2010: fig. 6C) ***K. australis* (Muir, 1913)**
 – Forewing with two transverse veinlets from MP3+4 to CuA1 (Kirkaldy 1907: fig. 1) ***K. deventeri* (Kirkaldy, 1907)**
 5 Ventral margin of periandrium without spinous processes near base (Tsaour and Hsu 2003: fig. 2D) ***K. lini* Tsaour & Hsu, 2003**
 – Ventral margin of periandrium with two spinous processes near base.....6

- 6 One of the two basal processes of ventral margin of perianthium bifurcate (Fig. 5I, J, L)..... *K. furcata* sp. nov.
- Both basal processes of ventral margin of perianthium unbifurcated (Fig. 2I, J, L) *K. aspina* sp. nov.
- 7 All tubercles of longitudinal veins in forewings colourless *K. javana* Muir, 1913
- Some tubercles of longitudinal veins in forewings dark 8
- 8 Forewing with MP joining CuA with crossvein M_{3+4} -CuA (Emeljanov and Hayashi 2007: fig. 25) *K. pacifica* Emeljanov & Hayashi, 2007
- Forewing with MP joining CuA directly without crossvein M_{3+4} -CuA 9
- 9 Forewing with a series of black spots on the claval vein and the inner bifurcating veins; mesonotum with a small dark spot near base of each lateral carina *K. pagana* (Melichar, 1903)
- Forewing not so marked; mesonotum without a spot on each side near base of lateral carina *K. pratti* Muir, 1913

***Kirbyana aspina* Zhi & Chen, sp. nov.**

<http://zoobank.org/9FF2E020-333D-4CCD-AFED-FA322162E171>

Figures 1–3

Type material. *Holotype*: ♂, CHINA: Hunan Province, Wugang City, Yunshan National Forest Park (26°40'N, 110°37'E), 5 June 2011, leg. Xiang-Sheng Chen; *Paratypes*: 8♂♂7♀♀, same data as holotype.

Description. Body length: male 5.6–6.1 mm ($N=9$), female 5.9–6.5 mm ($N=7$).

Coloration. General color light brown (Figs 1A–E, 3J, K). Eyes blackish brown, ocelli light yellow, semitransparent. Vertex generally yellowish white. Face generally dark brown; rostrum light brown. Pronotum with discal areas and mesonotum with area between lateral carinae yellowish white, lateral areas brown. Forewing light brown, semi-translucent. Stigma light brown. The basal half dotted with small dark brown spots and distal half with two large dark brown patches; small dark brown spots on the ends of longitudinal veins. Hind tibiae and abdominal sternites yellowish brown.

Head and thorax. Vertex (Figs 1C, 2A) broad, 2.2 times wider than long; anterior margin truncated, posterior margin arched and recessed. Frons (Figs 1D, 2B) widest at the level of antennae, as long as wide; frontoclypeal suture nearly concave into an arch; middle carina with basal half absent; lateral carinae distinct and slight elevated. Rostrum distinctly surpassing hind coxae, subapical segment 2.5 times longer than apical segment. Pronotum (Figs 1C, 2A) 2.4 times longer than vertex; median carina indistinct, posterior margin nearly at right angle. Mesonotum 1.7 times longer than pronotum and vertex combined. Forewing (Fig. 2C) 2.4 times longer than wide, with 10 apical and 6 subapical cells; fork Sc+RP slightly basad of fork CuA_1+CuA_2 , first crossvein r-m at same level of fork MP, RP two branches, MP

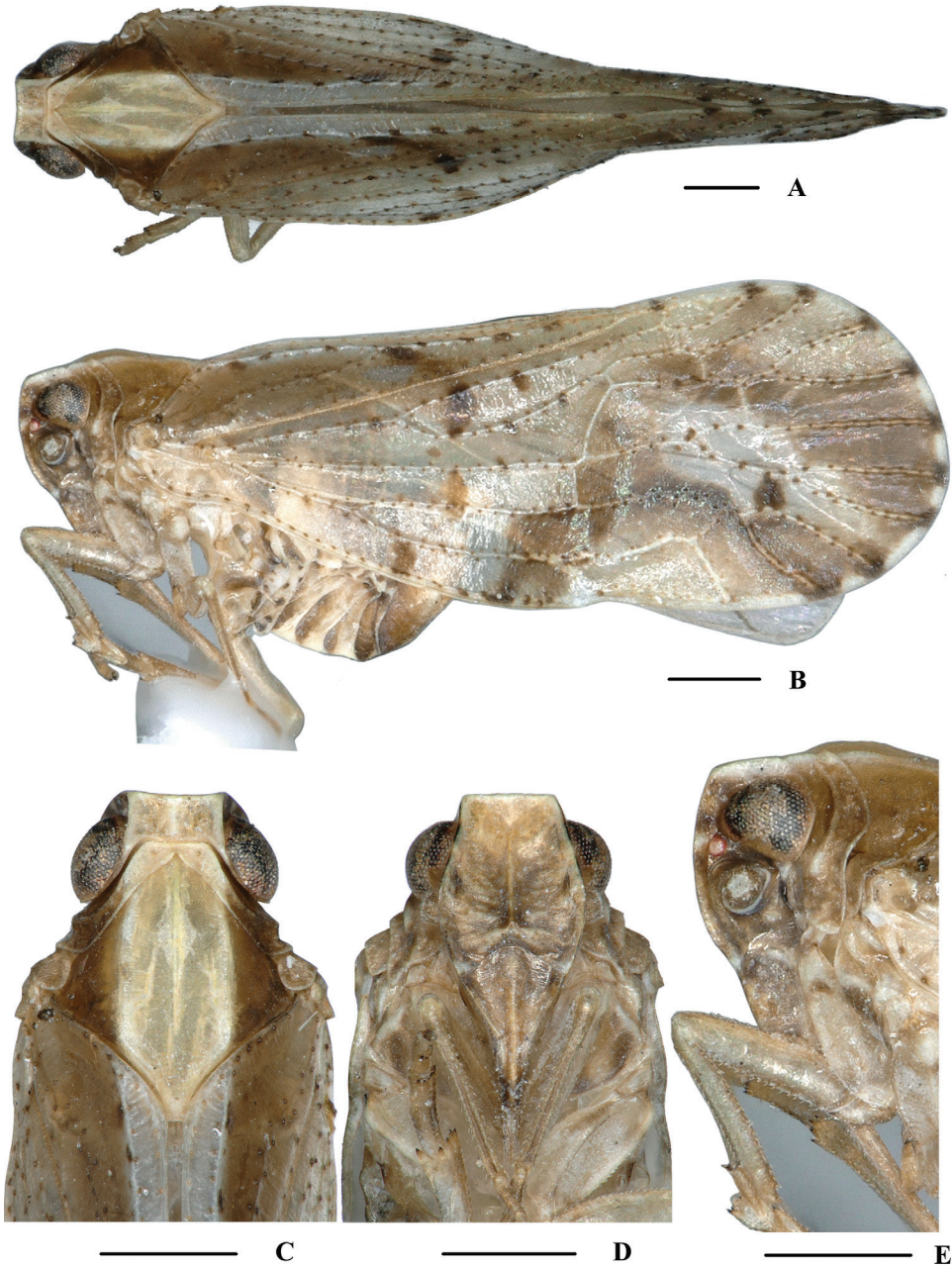


Figure 1. *Kirbyana aspina* sp. nov., male **A** habitus, dorsal view **B** habitus, lateral view **C** head and thorax, dorsal view **D** face, ventral view **E** head, lateral view. Scale bars: 0.5 mm.

with five terminals: MP_{11} , MP_{12} , MP_2 , MP_3 and MP_4 , fork MP_1+MP_2 basad of fork MP_3+MP_4 . Metatibiotarsal formula: 6/8–9/9, second segment of hind tarsus with four platellae (Fig. 2D).

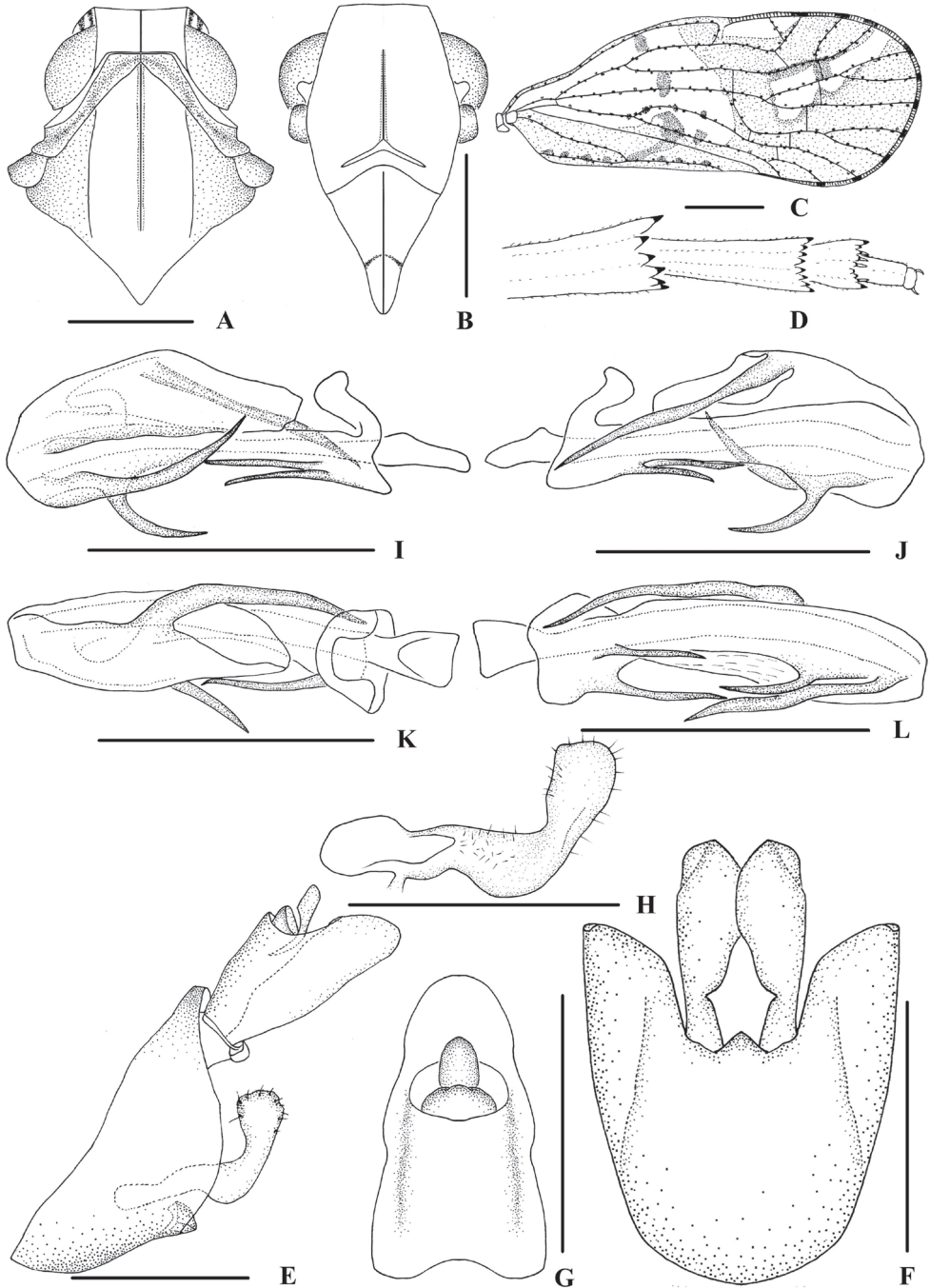


Figure 2. *Kirbyana aspina* sp. nov., male **A** head and thorax, dorsal view **B** face, ventral view **C** forewing **D** apex of left hind leg, ventral view **E** genitalia, lateral view **F** pygofer and gonostyli, ventral view **G** anal segment, dorsal view **H** gonostyli, inner lateral view **I** aedeagus, right side **J** aedeagus, left side **K** aedeagus, dorsal view **L** aedeagus, ventral view. Scale bars: 0.5 mm (**A, B, E–L**); 1.0 mm (**C**).

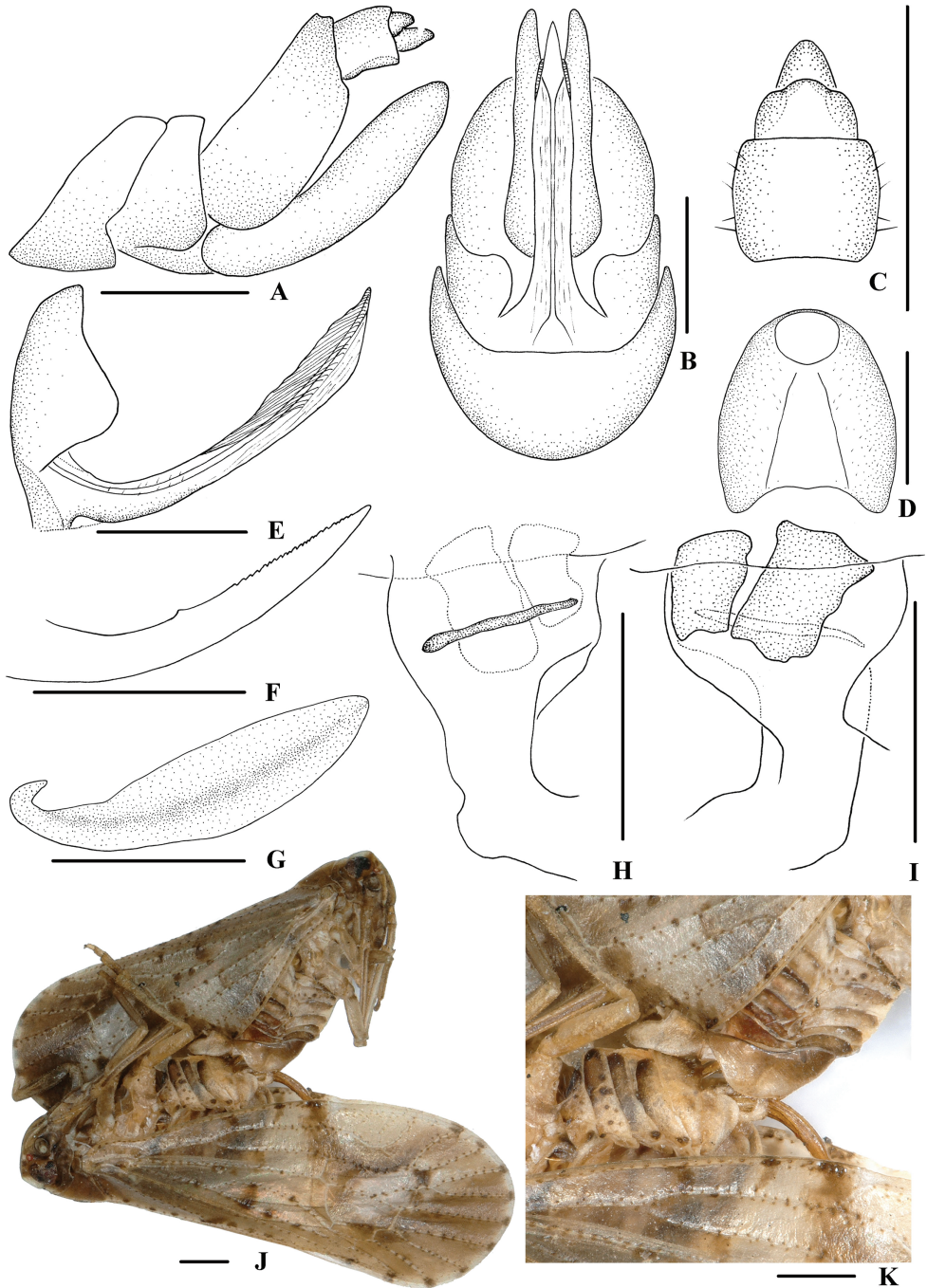


Figure 3. *Kirbyana aspina* sp. nov., **A–I** female **A** genitalia, lateral view **B** genitalia, ventral view **C** anal segment, dorsal view **D** tergite IX, caudal view **E** gonapophysis VIII and gonocoxa VIII, ventral view **F** gonapophysis IX, lateral view **G** gonoplac, lateral view **H** posterior vagina, dorsal view **I** posterior vagina, ventral view **J, K** mating. Scale bars: 0.5 mm.

Male genitalia. Pygofer (Fig. 2E, F) symmetrical, dorsal margin concave and U-shaped, slightly widened towards apex in ventral view; in lateral view, lateral lobes extended in an arc caudally, medioventral process triangular in ventral view. Anal segment (Fig. 2E, G) broad, dorsal margin almost straight, apical half of ventral margin convex, apical lobes round in lateral view; 1.7 times longer than wide in dorsal view; anal style strap-shaped, not beyond anal segment. Gonostyli (Fig. 2E, F, H) symmetrical in ventral view; in inner lateral view, base of ventral margin concave, dorsal margin bending inwards at a nearly right angle in the middle, apical part extended, apical margin round. Aedeagus (Fig. 2I–L) with total of five processes. On right side, apex of perianthrium with a long spinous process, sinuous, apex directed right-dorsocephalically; basal 1/4 of ventral margin with two short spinous processes, the longer one straight, directed caudally, the shorter one slightly curved and apex directed ventrocaudally; apical 1/3 of ventral margin with a curved spinous process, apex directed apically. Endosoma moderately sclerotised, relatively short, generally curved dorsally. The left dorsal margin with a long spinous process, slightly curved, and apex directed ventrocephalically.

Female genitalia. Posterior margin of pregenital sternite concave. Tergite IX (Fig. 3A, D) moderately sclerotised, with length almost equal to width in caudal view. Anal tube (Fig. 3A, C) short, nearly rectangular, slightly widened towards apex, 1.5 times longer than wide in dorsal view; dorsal and ventral margins nearly straight in lateral view, anal styles strap-shaped. Gonapophysis VIII (Fig. 3E) elongate, and slightly curved upwards. Gonapophysis IX (Fig. 3F), distance ratio between middle tooth to apex and length of denticulate portion is 1.50. Gonoplac (Fig. 3G) rod-like, 3.7 times longer than wide. Posterior vagina (Fig. 3H, I) elongate. The ventral wall of posterior vagina with two nearly oblong sclerites basally; the dorsal wall with a small long sclerite in the middle area.

Etymology. The specific name is derived from the Latin word “*aspina*”, referring to the apex of left side of perianthrium without process.

Host plant. Bamboo (Poaceae, Bambuseae).

Distribution. China (Hunan).

Remarks. The male genitalia of *K. aspina* sp. nov. is similar to *K. furcata* sp. nov., but differs in: (1) endosoma with one spinous process (endosoma with three spinous processes in *K. furcata*); (2) base of ventral margin of the perianthrium without a furcate process (base of ventral margin of perianthrium with a long furcate process in *K. furcata*) (3) apical margin of gonostyli round in lateral view (the latter transversal).

***Kirbyana furcata* Zhi & Chen, sp. nov.**

<http://zoobank.org/2DD2C8C6-5FF9-490F-AE20-0C70C0FE3CDB>

Figures 4, 5

Type material. Holotype: ♂, CHINA: Yunnan Province, Maguan County, Dulong Town, Jinzhuping Village (22°56'N, 104°30'E), 14 August 2017, leg. Yan Zhi, Qiang Luo and Nian Gong; **Paratypes:** 1♂1♀, Guangxi Zhuang Autonomous Region, Hechi City, Jinchengjiang Park (24°41'N, 108°3'E), 17 July 2015, leg. Ying-Jian Wang.

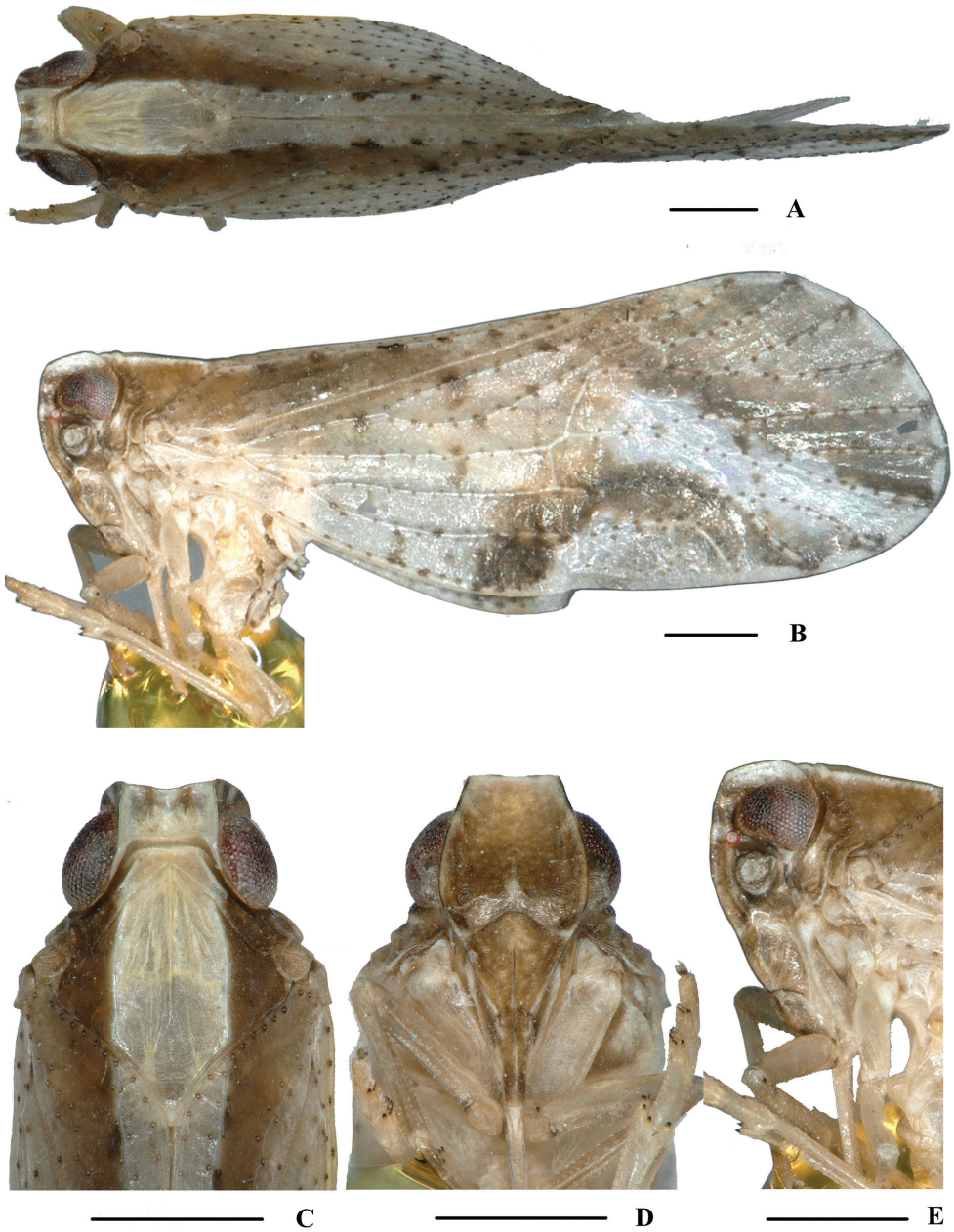


Figure 4. *Kirbyana furcata* sp. nov., male **A** habitus, dorsal view **B** habitus, lateral view **C** head and thorax, dorsal view **D** face, ventral view **E** head, lateral view. Scale bars: 0.5 mm.

Description. Body length: male 4.4–5.3 mm ($N = 2$), female 5.2 mm ($N = 1$).

Coloration. General color light brown (Fig. 4A–E). Eyes blackish brown, ocelli light yellow, semitransparent. Vertex generally yellowish white. Face generally brown;

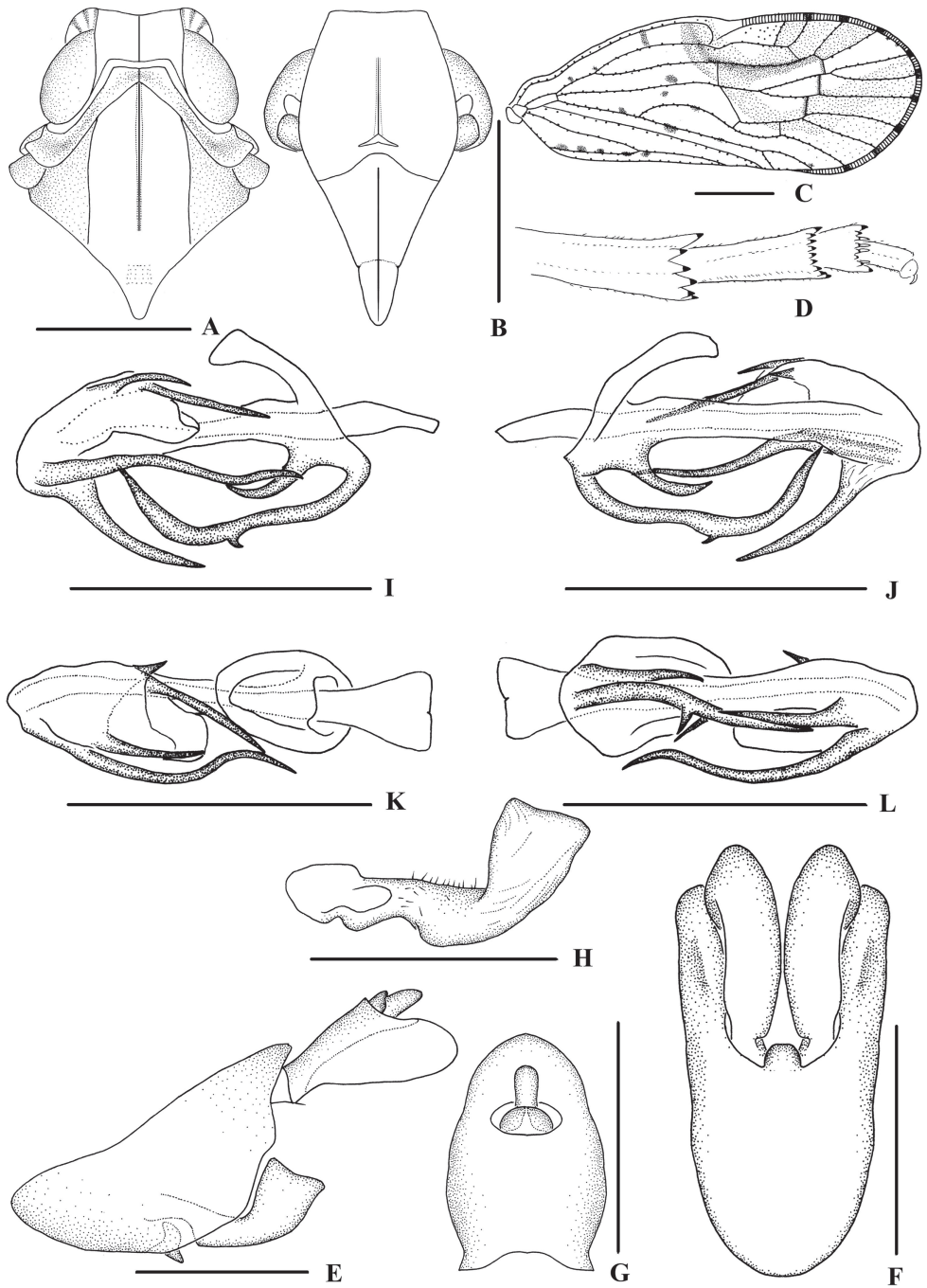


Figure 5. *Kirbyana furcata* sp. nov., male **A** head and thorax, dorsal view **B** face, ventral view **C** forewing **D** apex of left hind leg, ventral view **E** genitalia, lateral view **F** pygofer and gonostyli, ventral view **G** anal segment, dorsal view **H** gonostyli, inner lateral view **I** aedeagus, right side **J** aedeagus, left side **K** aedeagus, dorsal view **L** aedeagus, ventral view. Scale bars: 0.5 mm (**A, B, E-L**); 1.0 mm (**C**).

rostrum light brown. Pronotum with discal areas and mesonotum with area between lateral carinae yellowish white, lateral areas brown. Forewing light brown, semi-transparent, the basal half dotted with small dark brown spots and distal half with two large dark brown patches; small dark brown spots on the ends of longitudinal veins; stigma light brown. Hind tibiae yellowish brown and abdominal sternites dark brown.

Head and thorax. Vertex (Figs 4C, 5A) broad, 1.7 times wider than long; anterior margin truncated, posterior margin arched and recessed. Frons (Figs 4D, 5B) widest slightly below the level of antennae, 1.1 times as long as wide; frontoclypeal suture nearly concave into an arch; middle carina with basal half absent; lateral carinae distinct and slight elevated. Pronotum (Figs 4C, 5A) 1.8 times longer than vertex; median carina indistinct, posterior margin nearly at right angle. Mesonotum 1.6 times longer than pronotum and vertex combined. Forewing (Fig. 5C) 2.5 times longer than wide, with 11 apical and 6 subapical cells; fork Sc+RP basad of fork CuA₁+CuA₂, first cross-vein r-m slightly basad of fork MP, RP two branches, MP with five terminals: MP₁₁, MP₁₂, MP₂, MP₃ and MP₄, fork MP₁+MP₂ basad of fork MP₃+MP₄. Metatibiotarsal formula: 6/9/9, second segment of hind tarsus with four platellae (Fig. 5D).

Male genitalia. Pygofer (Fig. 5E, F) symmetrical, dorsal margin concave and U-shaped, slightly widened towards apex and concaved medially in ventral view; in lateral view, lateral lobes trapezoidally extended caudally, medioventral process round in ventral view. Anal segment (Fig. 5E, G) broad, dorsal margin almost straight, apical half of ventral margin convex, apical lobes round in lateral view; 1.5 times longer than wide in dorsal view; anal style strap-shaped, not beyond anal segment. Gonostyli (Fig. 5E, F, H) symmetrical in ventral view; in inner lateral view, base of ventral margin concave, dorsal margin bending inwards at a nearly right angle in the middle, apical part extended, apical margin transversal. Aedeagus (Fig. 5I–L) with total of seven processes. On right side, apex of periandrium with a long spinous process, sinuous, apex directed right-ventrocephally; base of ventral margin with a long furcate process, one ramus large, apex strongly curved and directed dorsocaudally, the other ramus rather small; a shorter curved spinous process on ventral margin near base, apex directed dorso-caudally; apex of periandrium with a medium-sized spinous process, slightly curved and directed ventrocephally. Endosoma moderately sclerotised, relatively short, generally curved dorsally. Three spinous processes on or near the apex, the right one medium-sized, slightly curved and directed ventrocephally; the middle one on the dorsal margin, longest and straight, apex directed right-ventrocephally; the left one extremely short, apex directed cephalad.

Etymology. The specific name is derived from the Latin word “*furcata*”, referring to the base of ventral margin of periandrium with a long furcate process.

Host plant. Bamboo (Poaceae, Bambuseae).

Distribution. China (Guangxi, Yunnan).

Remarks. This species can be distinguished from the other species of the genus by the following characters: ventral margin of periandrium with three spinous process, two on base and one on apex; apex of periandrium with a long spinous process on the right side; endosoma with three spinous processes on or near the apex.

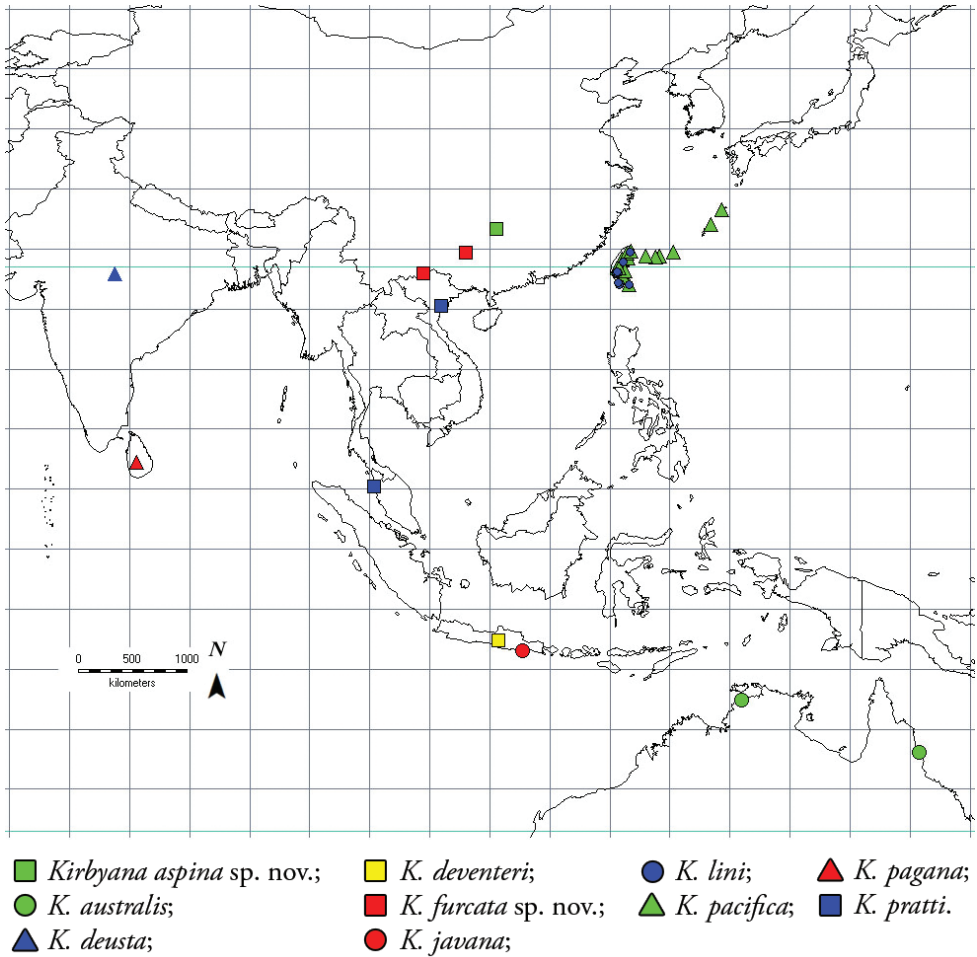


Figure 6. Distribution records of species from the genus *Kirbyana*: *K. aspina* sp. nov. (green square); *K. australis* (green circle); *K. deusta* (blue triangle); *K. deventeri* (yellow square); *K. furcata* sp. nov. (red square); *K. javana* (red circle); *K. lini* (blue circle); *K. pacifica* (green triangle); *K. pagana* (red triangle); *K. pratti* (blue square).

Discussion

Prior to this study, nothing had been reported on the host plants of *Kirbyana* except that *K. deventeri* (Kirkaldy, 1907) fed on *Saccharum officinarum* L. (Poales, Poaceae) (Kirkaldy 1907). As far as we have observed during our field trips, these two new species, *K. aspina* Zhi & Chen, sp. nov. and *K. furcata* Zhi & Chen, sp. nov. from southern China, were collected on bamboo (Poaceae, Bambuseae), which might be the plant on which they feed.

Based on data from published information and our field surveys, the distribution of *Kirbyana* is mostly restricted to the Australian and Oriental regions (Fig. 6) (Holt et al. 2013).

Acknowledgements

The authors are grateful to the specimen collectors for their hard work in the field collections. We wish to express our sincere thanks to Dr B. Löcker (Department of Primary Industries, Orange Agricultural Institute, Australia) for providing related literatures. This work was supported by the National Natural Science Foundation of China (No. 32060343, 31472033), the Science and Technology Support Program of Guizhou Province (grant no. 20201Y129), the Program of Excellent Innovation Talents, Guizhou Province (No. 20154021), the New Academic Talent Program of Guizhou Medical University (No. 19NSP066) and Doctoral Scientific Research Foundation of Guizhou Medical University (No. J[2020]019).

References

- Bourgoin T (1987) A new interpretation of the homologies of the Hemiptera male genitalia, illustrated by the Tettigometridae (Hemiptera, Fulgoromorpha). In: Proceedings of the 6th Auchenorrhyncha Meeting, Turin, Italy, 7–11 September 1987, 113–120.
- Bourgoin T (1993) Female genitalia in Hemiptera Fulgoromorpha, morphological and phylogenetic data. *Annales de la Société Entomologique France* 29(3): 225–244.
- Bourgoin T (2021) FLOW (Fulgoromorpha Lists on the Web): a world knowledge base dedicated to Fulgoromorpha. Version 8, updated 18 February 2021. <http://hemiptera-databases.org/flow/> [Accessed on: 2021-2-19]
- Bourgoin T, Wang RR, Asche M, Hoch H, Soulier-Perkins A, Stroiński A, Yap S, Szwedo J (2015) From micropterism to hyperpterism: recognition strategy and standardized homology-driven terminology of the forewing venation patterns in planthoppers (Hemiptera: Fulgoromorpha). *Zoomorphology* 134: 63–77. <https://doi.org/10.1007/s00435-014-0243-6>
- Distant WL (1906a) Rhynchota. III. (Heteroptera Homoptera). In: Bingham CT (Ed.) The fauna of British India including Ceylon and Burma. Taylor & Francis, London, 503 pp. <https://doi.org/10.1080/00222930608562592>
- Distant WL (1906b) Bibliographical and nomenclatorial notes on the Rhynchota. *The Entomologist* 39: 274–275.
- Distant WL (1911) LXXXV.—Descriptions of new genera and species of Oriental Homoptera. *Annals and Magazine of Natural History* (8), 48: 735–747. <https://doi.org/10.1080/00222931108693092>
- Emeljanov AF, Hayashi M (2007) New Cixiidae (Hemiptera, Auchenorrhyncha) from the Ryukyus, Japan. *Japanese Journal of Systematic Entomology* 13(1): 127–140.
- Fennah RG (1978) Fulgoroidea (Homoptera) from Vietnam. *Annales Zoologici (Warszawa)* 34(9): 207–279.
- Fennah RG (1980) The genus *Bajauana* and two allied new genera in New Guinea (Fulgoroidea: Cixiidae). *Pacific Insects* 22: 237–328.
- Holt BG, Lessard JP, Borregaard MK, Fritz SA, Araújo MB, Dimitrov D, Fabre PH, Graham CH, Graves GR, Jønsson KA, Nogués-Bravo D, Wang Z, Whittaker RJ, Fjeldså J,

- Rahbek C (2013) An update of Wallace's zoogeographic regions of the world. *Science* 339: 74–78. <https://doi.org/10.1126/science.1228282>
- Holzinger WE, Emeljanov AF, Kammerlander I (2002) The family Cixiidae Spinola, 1839 (Hemiptera: Fulgoromorpha)-a Review. *Denisia* 4: 113–138.
- Kirkaldy GW (1906) Bibliographical and nomenclatorial notes on the Hemiptera. No. 6. *The Entomologist* 39: 247–249. <https://doi.org/10.5962/bhl.part.1563>
- Kirkaldy GW (1907) Descriptions et remarques sur quelques Homoptères de la famille des Fulgoroidea vivant sur la canne à sucre. *Annales de la Société entomologique de Belgique. Bruxelles* 51: 123–127.
- Löcker B, Fletcher MJ, Gurr GM (2010) Taxonomic revision of the Australian Eucarpiini (Hemiptera: Fulgoromorpha: Cixiidae) with the description of nine new species. *Zootaxa* 2425: 1–31. <https://doi.org/10.11646/zootaxa.2425.1.1>
- Melichar L (1903) *Homopteren-Fauna von Ceylon*. Verlag von Felix L Dames, Berlin, 248 pp.
- Tsaur SC, Hsu TC (2003) The Cixiidae of Taiwan, Part VII: Tribe Pintaliini (Hemiptera: Fulgoroidea). *Zoological Studies* 42(3): 431–443.

The third species of the genus *Pachypaederus* Fagel, 1958 (Coleoptera, Staphylinidae, Paederinae) from the Oriental region

Xiaoyan Li¹, Yanpeng Cai², Haifeng Chen¹

1 Hebei Key Laboratory of Animal Diversity, Langfang Normal University Aiminxiadao 100, Anci Area, Langfang 065000, Hebei Province, China **2** Morphological Laboratory, Guizhou University of Traditional Chinese Medicine, Guiyang, 550025, Guizhou, China

Corresponding author: Haifeng Chen (chenhaifeng@lnu.edu.cn)

Academic editor: Adam Brunke | Received 13 April 2021 | Accepted 20 April 2021 | Published 11 May 2021

<http://zoobank.org/93FF955B-579D-45DF-B0A0-6FE818ECA665>

Citation: Li X, Cai Y, Chen H (2021) The third species of the genus *Pachypaederus* Fagel, 1958 (Coleoptera, Staphylinidae, Paederinae) from the Oriental region. ZooKeys 1037: 15–22. <https://doi.org/10.3897/zookeys.1037.67300>

Abstract

A new species of *Pachypaederus* Fagel, 1958, *P. kongshuhensis* Li, **sp. nov.**, is described from Yunnan Province, China. This species represents the third member of the genus from the Oriental region. Color plates of the habitus, labrum, mandibles, sternites VII–IX of the male and female, as well as the aedeagal structures are provided. A key to Oriental *Pachypaederus* species is provided.

Keywords

China, Paederina, taxonomy, Yunnan

Introduction

The genus *Pachypaederus* belongs to the subtribe Paederina, with *Paederus crassus* Boheman as the type species by original designation (Fagel 1958) and another 10 species originally included in this group (Fagel 1958). The group has a limited distribution and is only documented from the Ethiopian Region (South Africa, Guinea, Cameroon, D.R. Congo, Uganda, Rwanda, Tanzania, Zambia, Zimbabwe, Madagascar) (Fagel 1958; Janák 1998; Willers 2003; Janák 2012) and the Oriental Region (Chinese

provinces of Yunnan and Myanmar) (Willers 2001, 2002). So far, there are 27 species known, including 25 Ethiopian species and 2 Oriental species (Willers 2003; Janák 2012; Li et al. 2019).

Based on the original description by Fagel (1958) (large size, reduced hind wings, carinate prosternum, narrowly separate and parallel gular sutures, free and filiform parameres, robust aedeagus as in the genus *Allopaederus*), *Pachypaederus* is not well differentiated from the other genera of Paederina. Furthermore, *P. capillaris* does not have a carinate prosternum (V. Assing pers. comm.). In consideration of the morphological diagnosis, disjunct distribution between Afrotropical and Oriental regions, and preliminary phylogenetic work by Li and Zhou (2009), the monophyly of the genus *Pachypaederus* is doubtful and needs further assessment in future. Here, we follow the Catalog of Chinese Coleoptera edited by Li et al. (2019).

In 2016, some rove beetle specimens were collected from the border of Yunnan, China, and Myanmar. After close examination, some of these were discovered to belong to a new species of *Pachypaederus*. This study describes the new species and updates the information of this genus. As a result, the number of species in this genus from the Oriental Region increases to three.

Materials and methods

The dried specimens were softened in hot water at 60 °C for about 8 hours for dissection of the abdominal terminalia. The male genital was soaked in 10% KOH solution (30 °C) for about 20–40 minutes (depending on the degree of sclerotization). The surrounding soft tissues were immediately removed, and the dissected parts were preserved in glycerin in plastic microvials with stoppers for the subsequent observation and photography. Two specimens were dissected in this study.

Observation, dissection, and measurements were done under a Zeiss SteREO Discovery V20 stereomicroscope. Photos of the habitus, sternites, and genitalia were taken with Zeiss AxioCam MRc 5 camera attached to a Zeiss Axio Zoom V16 stereo zoom microscope. Photographs were synthesized and stacked with Zen 2012 (Blue version) and Helicon Focus imaging software. Inkscape v. 0.91 was used to make the line drawings.

All specimens listed in the present study were deposited in the Institute of Zoology, Chinese Academy of Sciences (IZ-CAS).

The following abbreviations are used in the descriptions:

- AEL** aedeagus length (base of median lobe to apical part);
- AEW** aedeagus width (greatest width of pronotum);
- BL** body length (from anterior margin of labrum to end of abdomen);
- EL** elytra length (from humeral angle to posterior margin);
- ESL** elytra suture length (apex of scutellum to apex of elytral suture);
- EW** elytra width (width of elytra across the widest part);
- EYL** eye length (longitudinal length of eye in dorsal view);

- FL** forebody length (from anterior margin of labrum to posterior margin of elytra);
HL head length (from anterior margin of clypeal to posterior constriction of head);
HW head width (greatest width of head, included eyes);
PL pronotum length (from anterior margin of pronotum to its posterior margin);
POL postocular length (from posterior margin of eye to posterior constriction of head);
PW pronotum width (greatest width of pronotum).

Taxonomy

Pachypaederus Fagel, 1958: 68, 70

Type species. *Paederus crassus* Boheman, fixed by original designation.

Key to *Pachypaederus* of the Oriental region

- 1 Body black including antennae, pronotum and abdomen *P. pallitarsis* Willers
 – Body with pronotum and at least first four abdominal segments reddish brown **2**
 2 Interior armature complex, with more sclerites; apex of dorsal plate in aedeagus curved to the right in ventral (parameral) view (Figs 2A, 3A) *P. kongshubensis* sp. nov.
 – Interior armature with fewer sclerites; apex of dorsal plate in aedeagus curved to the left in ventral (parameral) view (Willers 2001: 191) *P. capillaris* Fauvel

Pachypaederus kongshubensis Li, sp. nov.

<http://zoobank.org/4C2A985F-8470-4D0F-BA60-9AAE5A8ADA56>

Figures 1–3

Type material. *Holotype:* ♂, CHINA: Yunnan Province: Tengchong County, Mingguang Town, Kongshuhe County (空树河村), 2100 m elev., 25.7245°N, 98.6341°E, 30.VI.2016, coll. by Xiaoyan Li (IZ-CAS). *Paratypes:* ♂, 2 ♀♀, same data as holotype (IZ-CAS).

Description. BL: 8.7–9.0 mm; FL: 3.6–3.8 mm. HL: 1.08 mm; HW: 1.25 mm; PL: 1.39 mm; PW: 1.17 mm; EL: 1.08 mm; EW: 1.39 mm; EYL: 0.36 mm; POL: 0.50 mm.

Body glossy with typical “*Paederus*” color pattern; head and two apical segments of abdomen, the apical half of femora, and basal two-thirds of elytra dark blue; other parts brown; antennomeres 1 and 2 and 9–12 brownish yellow. Abdominal segments 4–6 with black patches in middle, and patches decreasing in size anteriorly.

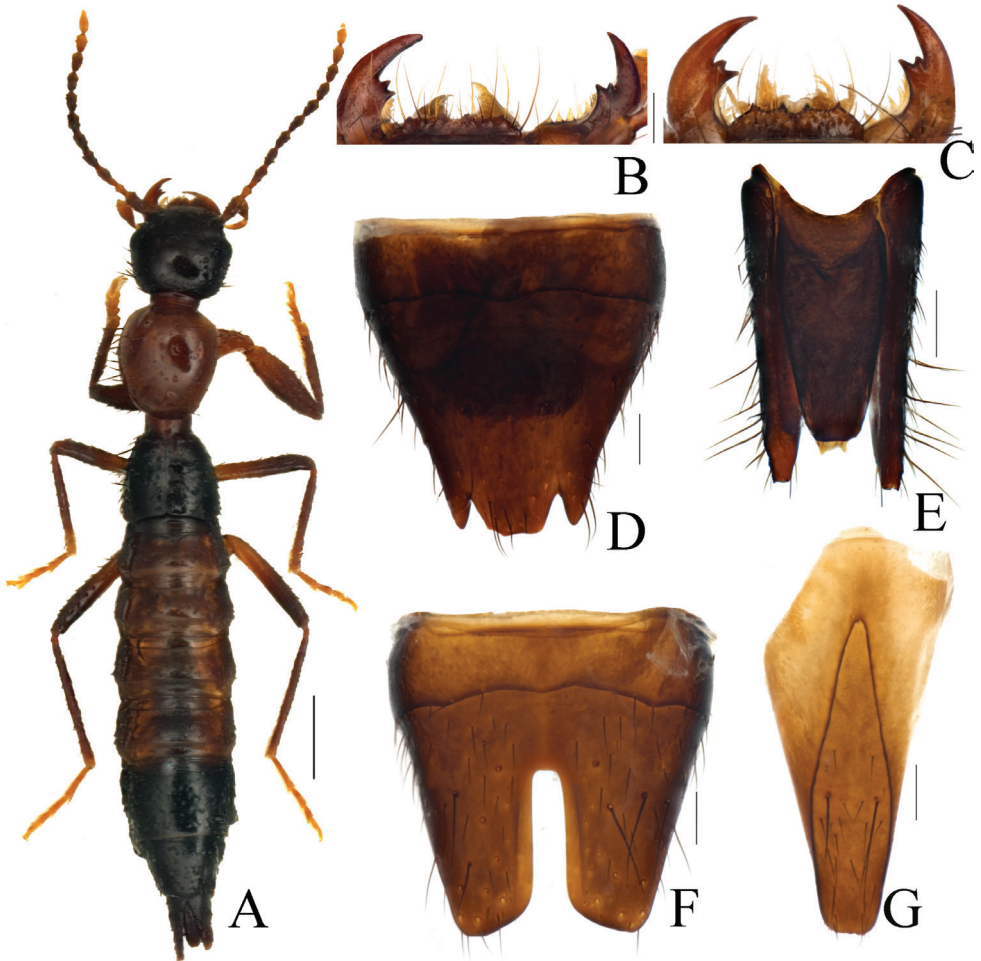


Figure 1. *Pachypaederus kongshubensis* Li, sp. nov., morphology **A** habitus **B** labrum and mandibles in male **C** labrum and mandibles in female **D** sternite VIII in female **E** sternite IX and lateral proctiger in female **F** sternite VIII in male **G** sternite IX in male. Scale bars: 1.0 mm (**A**); 0.2 mm (**B–G**).

Head wider than long (average HL/HW = 0.86). Eyes moderately large (average HL/EYL = 3.0), protruding laterally. Diameter of eye longer than gena and shorter than temple (average ratio, gena: eye: temple = 0.70: 1: 1.38). Surface of head smooth. Vertex and frons glabrous with sparse punctures, lateral portions of head with more denser, shallower, and coarser punctures which are irregularly distributed and of variable size.

Antennae filiform and densely pubescent, starting from antennomere 9. Ventral portion of neck with a reversed V-shaped protrusions.

Pronotum slightly longer than wide (average PL/PW = 1.12). Scutellum glossy with reticulate microsculpture and fine setiferous punctation. Mesoventrite pressed,

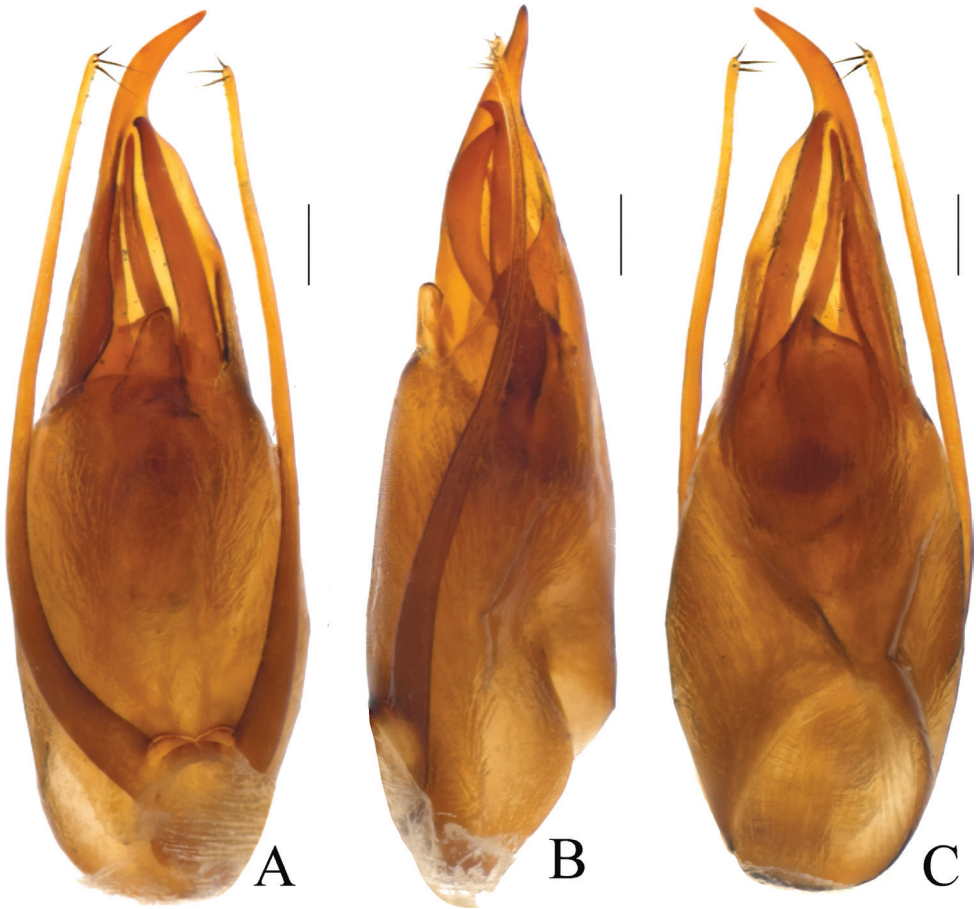


Figure 2. *Pachypaederus kongshubensis* Li, sp. nov., morphology **A** aedeagus, in ventral view **B** aedeagus, in lateral view **C** aedeagus, in dorsal view. Scale bars: 0.2 mm.

surface smooth, with fine microsculpture, and anterior margins ridged. Metaventricle small with anterior portion even and posterior surface pressed with fine microsculpture.

Elytra trapezoidal-sided, longer than wide (average $EL/EW = 0.79$ and $ESL/EL = 0.68$), wings reduced completely. Surface uneven, lustrous, with fine reticulate microsculpture, punctures smaller and denser than that on pronotum, diameter of a puncture usually shorter than interval between punctures.

Tergites III–VI of abdomen with setiferous punctures small and sparse; basal area of each tergite without distinct punctate row. Sternites with punctuation similar to that on tergites.

Male. Labrum (Fig. 1B) narrower than in female, with two small pairs of teeth on anterior margin. Tergite VIII with punctures denser and larger than those on tergites III–VII. Sternites III–VII with setae slightly directed mediad. Sternite VII with microsculpture and punctures much denser than those on sternites III–VI, posterior

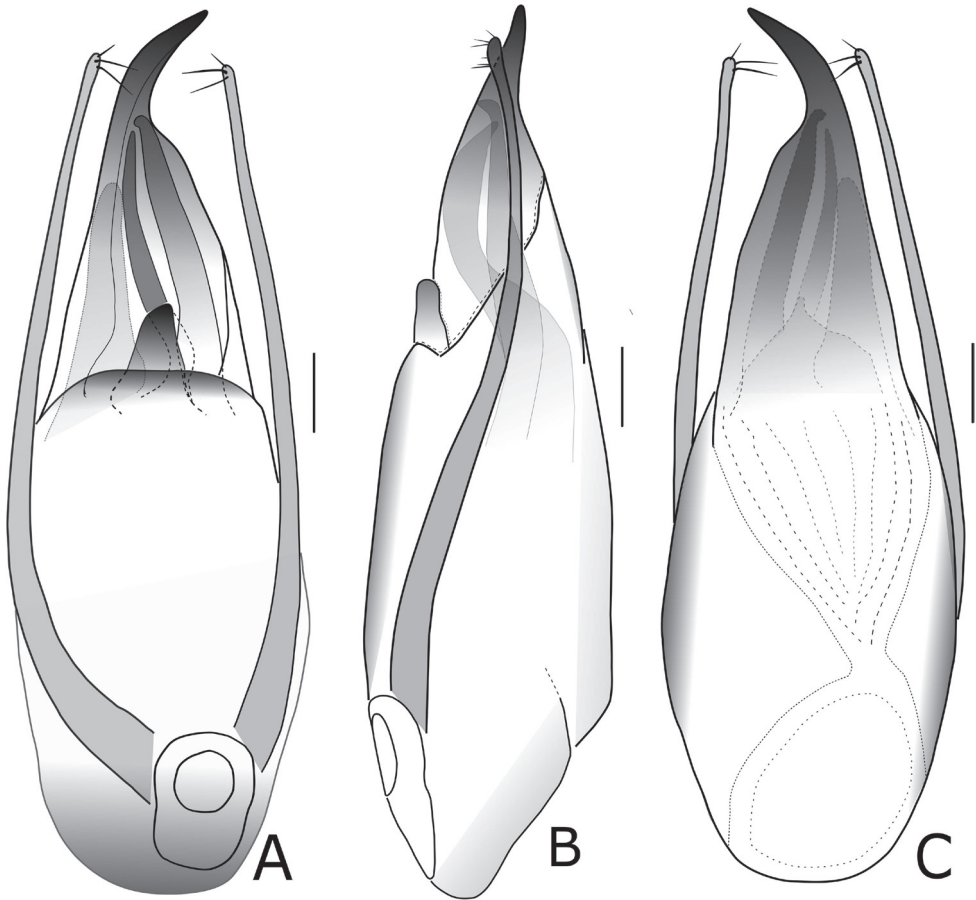


Figure 3. *Pachypaederus kongshubensis* Li, sp. nov., morphology **A** aedeagus, in ventral view **B** aedeagus, in lateral view **C** aedeagus, in dorsal view. Scale bars: 0.2 mm.

margin broadly notched. Sternite VIII with deep, parallel-sided, median incision, base of incision truncate, depth longer than half the length of sternite (Fig. 1F). Sternite IX asymmetrical, apex slightly emarginate and inner ridge symmetrical (Fig. 1G).

Female. Labrum (Fig. 1C) well developed, distinctly wider than that in male, two pairs of anterior teeth distinctly larger and sharper. Sternite VIII deeply notched as in Figure 1D. Sternite IX (Fig. 1E) with basal part bilobed and gradually narrowed apically, posterior margin shallowly emarginated in middle.

Aedeagus (Figs 2A–C, 3A–C), robust and asymmetrical. AEL = 2.27 mm, AEW = 0.5 mm. Parameres symmetrical and filiform in shape; posterior part slightly clavate. Dorsal plate long and asymmetrical, gradually narrower posteriad and apical part rather sharp and curved leftward in dorsal view. Ventral plate short, with apex broadly round. Internal sac complex and exposed in ventral side, the interior armature with several elongate sclerites and several broad and lamelliform sclerites.

Diagnosis. The new species *Pachypaederus kongshuhensis* sp. nov. can be easily distinguished from the two Oriental congeners by a combination of bicolored body and the morphology of the aedeagus. *Pachypaederus pallitarsis* is completely black, while in *P. capillaris*, the apex of the dorsal plate faces to the left and there are fewer sclerites in the internal sac of the aedeagus.

Distribution. The species is known only from westernmost Yunnan Province, China, at an altitude of 2100 m. The specimens were collected in June as they were moving under fresh grass along the sides of a river.

Etymology. The specific epithet is derived from the type locality, Kongshuhe, a mountain village in westernmost Yunnan Province, China, near the border between Myanmar and China.

Acknowledgements

We express our gratitude to the editor, Dr. Adam J. Brunke (Canadian National Collection of Insects, Arachnids and Nematodes, Agriculture and Agri-Food Canada, Ontario, Canada), Dr. Volker Assing (Hannover, Germany) for their sincere comments on this manuscript and Dr. Chengbin Wang (王成斌, Mianyang Normal University, Mianyang, China) for assistance with collecting the specimens in 2016. This study was financially supported by the Fundamental Research Funds for the Universities in Hebei Province (C2019408016, ZD2020123, JYT202001, A202002007) and the National Natural Science Foundation of China (NSFC-31501883, NSFC-31760629).

References

- Fagel G (1958) Paederini (Coleoptera Polyphaga) Fam. Staphylinidae. Exploration du Parc National de l'Upemba (Mission G. F. de Witte) 51: 1–470.
- Li XY, Zhou HZ (2009) Phylogenetic analysis and taxonomy of the subgenus *Gnathopaederus* Chapin and related groups of *Paederus* s. l. (Coleoptera: Staphylinidae: Paederinae). Invertebrate Systematics 23: 422–444. <https://doi.org/10.1071/IS09015>
- Li XY, Solodovnikov A, Zhou HZ (2013) Five new species of the genus *Paederus* Fabricius from mainland China, with a review of the Chinese fauna of the subtribe Paederina (Coleoptera: Staphylinidae: Paederinae). Annals of the Entomological Society of America 106(5): 562–574. <https://doi.org/10.1603/AN13008>
- Li LZ, Hu JY, Peng Z, Tang L, Yin ZW, Zhao MJ (2019) Staphylinidae. In: Yang XK (Ed.) Catalogue of Chinese Coleoptera (Vol. 3). Science Press, Beijing, 343–406.
- Willers J (2001) Systematisch-nomenklatorische Änderungen in der Gattung *Paederus* Fabricius s.l. (Coleoptera, Staphylinidae). Veröffentlichungen Naturkundemuseum Erfurt 2001(20): 189–192.
- Willers J (2002) Three new species of *Paederus* and related genera from Thailand, Vietnam and South China (Coleoptera: Staphylinidae). Zoosystematica Rossica 11: 155–162.

- Willers J (2003) Two new species of *Paederus* Fabricius sensu lato (Coleoptera: Staphylinidae: Paederinae) from Guinea and South Africa. *Cimbebasia* 19: 25–30.
- Janák J (1998) *Pachypaederus anita* sp. nov. aus Madagaskar (Coleoptera: Staphylinidae: Paederinae). *Klapalekiana* 34: 61–64.
- Janák J (2012) A description of four new species of the genus *Pachypaederus* Fagel from South Africa with a key to southern African species (Coleoptera: Staphylinidae: Paederinae). *Studies and Reports, Taxonomical Series* 8(1–2): 193–212.

Redescription of *Gnorimosphaeroma oregonense* (Dana, 1853) (Crustacea, Isopoda, Sphaeromatidae), designation of neotype, and 16S-rDNA molecular phylogeny of the north-eastern Pacific species

Regina Wetzer¹, Adam Wall¹, Niel L. Bruce^{2,3}

1 Research and Collections Branch, Natural History Museum of Los Angeles County, 900 Exposition Boulevard, Los Angeles, California 90007, USA **2** Queensland Museum, Brisbane, Australia **3** North-West University, Water Research Group, Unit for Environmental Sciences and Management, Private Bag C6001, Potchefstroom 2520, South Africa

Corresponding author: Regina Wetzer (rwetzer@nhm.org)

Academic editor: T. Horton | Received 12 January 2021 | Accepted 15 March 2021 | Published 13 May 2021

<http://zoobank.org/4BB4E90C-0EB8-47D6-B5AF-C6F5E954140F>

Citation: Wetzer R, Wall A, Bruce NL (2021) Redescription of *Gnorimosphaeroma oregonense* (Dana, 1853) (Crustacea, Isopoda, Sphaeromatidae), designation of neotype, and 16S-rDNA molecular phylogeny of the north-eastern Pacific species. ZooKeys 1037: 23–56. <https://doi.org/10.3897/zookeys.1037.63017>

Abstract

Gnorimosphaeroma oregonense (Dana, 1852) is revised, a male neotype is designated, photographed, and illustrated; the species occurs from Vancouver British Columbia to the central California coast. 16S-rDNA sequences (~650 bp) for all available ethanol preserved species of *Gnorimosphaeroma* were used to hypothesize their relationships. Our analyses revealed a sister taxon relationship between the fully marine *G. oregonense* and the brackish to freshwater species, *G. noblei*. The oyster associated and introduced *G. rayi* is sister to a previously not recognized or identified, but genetically distinct, *Gnorimosphaeroma* sp. collected at two sites in San Francisco Bay. *Gnorimosphaeroma* sp. is probably also a western Pacific species based on its genetic relationship to *G. rayi*. Photographic comparisons are offered for *G. oregonense* (marine), *G. noblei* (freshwater), *G. rayi* (introduced), *G. sp.* (presumably introduced), and *G. insulare* (San Nicolas Island). Records of the holdings at the Los Angeles County Museum of Natural History are summarized. Without material available north of Vancouver through Alaska, the range of *G. oregonense* could not be genetically verified. This review includes a diagnosis and description of the genus *Gnorimosphaeroma* Menzies, 1954.

Keywords

Brackish, California, East Pacific, freshwater, intertidal, San Francisco Bay, Tomales Bay, Washington

Introduction

In the temperate region of the East Pacific, the sphaeromatid isopod fauna is limited to shallow coastal waters and is represented by eight genera (*Dynoides* Barnard, 1914, *Dynamenella* Hansen, 1905, *Exosphaeroma* Stebbing, 1900, *Gnorimosphaeroma* Menzies, 1954, *Paracerceis* Hansen, 1905, *Paradella* Harrison & Holdich, 1982, *Pseudosphaeroma* Chilton, 1909, and *Sphaeroma* Bosc, 1801). The genus *Gnorimosphaeroma* Menzies, 1954 was erected for three species and a subspecies. *Gnorimosphaeroma oregonense* (Dana, 1853) was designated as the type species. Menzies (1954) further distinguished *G. oregonense oregonense* from *G. oregonense lutea*, a new subspecies, from the west coast of North America from, “very brackish to almost freshwater”. In his 1954 paper, Menzies included *G. insulare* (Van Name, 1940) collected from freshwater on San Nicolas Island (California Channel Islands); described *G. noblei* from marine waters in Tomales Bay, California; *G. chinensis* (Tattersall, 1921) from freshwater in Shanghai, China; *G. ovata* (Gurjanova, 1933) from marine environments off Japan; and recognized a *Gnorimosphaeroma* sp. an undescribed species from Japanese seashores. Today 26 species are accepted by the World Register of Marine Species (Boyko et al. 2008). The genus is restricted to the northern Pacific from Japan and China to Alaska and California. *Gnorimosphaeroma* is unusual among sphaeromatids as it contains marine as well as fresh- and brackish-water species (Menzies 1954).

Dana’s (1853) redescription and accompanying figures for the type species of *Gnorimosphaeroma oregonense* are inadequate to distinguish the species. All of Dana’s isopod specimens were lost when the sloop, the USS ‘Peacock’, sank at the mouth of the Columbia River on July 18, 1841 (Hanable 2003; Bruce 2009: 211) and the type material is unequivocally lost. Menzies (1954) erected *Gnorimosphaeroma* for Dana’s species, but did not designate a neotype for *Gnorimosphaeroma oregonense* (Dana, 1853), providing only a redrawn figure of a portion of the pleotelson. Menzies’ attribution of the species range from the Bering Islands, Alaska to and including San Francisco Bay, further precludes precise inclusion of what constitutes the taxon, as this large geographical range likely includes more than one species.

Here we review specimens attributed to *Gnorimosphaeroma* from Vancouver, Canada and the state of Washington to Santa Barbara, California and to the southern California offshore island San Nicolas, from fully marine to freshwater habitats. We provide a 16S-rDNA phylogenetic hypothesis of the relationships for all of the material at hand, designate a replacement for the lost *Gnorimosphaeroma oregonense* type specimen, and redescribe the species. Furthermore, we provide comparative photographs of *G. oregonense*, *G. noblei*, *G. rayi*, *G. insulare*, and *Gnorimosphaeroma* sp.

Materials and methods

The redescription of *Gnorimosphaeroma oregonense* is based on the male neotype (here designated) and additional material as described below. Specimens examined have LACM numbers preceded by RW which are field station numbers. Collections

so labelled are readily retrieved from the LACM collections as are those denoted as DISCO. Setal terminology broadly follows Watling (1989).

Examined specimens were obtained from 49.294°N (British Columbia) to ~33.262°N (California). *Gnorimosphaeroma* material held in the LACM collections and available for morphological study is presented in Table 1. Some material is available for both morphological and genetic examination (Table 2). We sequenced all material preserved and useful for molecular analysis resulting in Figures 10 and 11 and photographed representatives of these four species including a fifth species discovered during the genetic analyses (Figs 12–15).

Specimens for SEM were prepared as described in Wall et al. (2015). Drawings were made with the aid of a camera lucida and illustrations were electronically “inked” with Affinity Designer, Serif Labs. Appendages were illustrated by dissecting off the appendage and placing them in glycerol on a depression slide and then imaged using a Nikon Labophot-2 compound scope. Specimens were measured with a micrometer. The lengths given in the “Material examined” are of the largest specimen of each species and sex. Not all specimens were measured. If a length is provided and multiple specimens were present in a lot, the length refers to the largest specimen.

Molecular data was generated according to the protocols described in Wetzer et al. (2013). Voucher specimens are held in the LACM Crustacea Collections. Sequences have been published in GenBank and are summarized in Table 2. Complete metadata is provided in Table 2 for specimens used in the molecular analysis. Our numbering scheme readily allows identification to a specific specimen. Table 1 summarizes specimens examined for morphology. The lot from which the neotype was selected is deposited in the LACM Crustacea Collections. Nexus data will be added to Open Tree of Life upon publication. Wetzer (2015) describes isopod collecting and preservation methods. 16S-rDNA Palumbi et al. (1991) universal 16Sar and 16Sbr primers were used for the 16S-rRNA fragment (~650 bp). Tissue extraction, amplification, sequence editing, sequence assembly as well as alignment protocols are detailed in Wetzer et al. (2013, 2018). The online MAFFT (Multiple Alignment Program for amino acid or nucleotide sequences, Katoh et al. (2002, 2005) alignment tool was used to create separate datasets using LINS, EINS, or GINS alignment protocols. RAxML and MrBayes analyses were performed on CIPRES (Miller et al. 2010).

Abbreviations

| | |
|-------------------|--|
| DISCO | Diversity Initiative of the Southern California Ocean; |
| LACM / NHM | Natural History Museum of Los Angeles County; |
| MBPC | Marine Biodiversity Center; |
| NWU | North-West University; |
| PMS | plumose marginal setae; |
| RS | robust seta/e; |
| SEM | scanning electron microscopy. |

Latitudes and longitudes denoted with “~” are approximate and estimated from Google Earth or otherwise estimated and not recorded during specimen collection.

Table 1. Museum collections examined morphologically and not included in the molecular analyses. Taxa are grouped by species and sorted by latitude. Label data and associated notes are transcribed here. Note that in some instances latitude and longitude are approximate and are indicated as “-”. Although we attempted to extract and amplify DNA, some were unsuccessful.

| Species | Specimen label |
|------------------------------------|---|
| <i>Gnorimosphaeroma insulare</i> | California, Ventura County, San Nicolas Island, -33.262°N; -119.502°W, fresh water pond with pulmonate mollusk, <i>Physa virgata</i> Gould, 1938, Types at AMNH 8092, one syntype at LACM CR 1938-270.1, Coll. T.A.D. Cockerell, Collection ID: RW17.013 |
| <i>Gnorimosphaeroma noblei</i> | California, Humboldt County, Humboldt Bay, <i>Salicornia</i> flats, 3/4 mi N of Samoa, -40.858°N; -124.153°W, mud banks, preserved in 70% ethanol, 29 Apr 1972, I72-30, MBPC 6774, Coll. R. Talmadge & E. Iverson, Collection ID: RW17.044 |
| | California, Mendocino/Sonoma County, 100 yds. up from mouth of Russian River, -38.437°N; -123.11°W, preserved in 75% ethanol, 19 Aug 1971, EI-1969, Coll. J. Carlton, Collection ID: RW17.047 |
| | California, Sacramento County, central San Joaquin Delta (freshwater), -38.33°N; -121.3°W, collected before May 2003, fixed in formalin, preserved in 70% ethanol, Coll. Wayne Fields, Collection ID: RW03.218 |
| | California, Sacramento County, central San Joaquin Delta (freshwater), -38.33°N; -121.3°W, collected before May 2003, fixed in formalin, preserved in 70% ethanol, Coll. Wayne Fields, Collection ID: RW03.217 |
| | California, Marin County, Tomales Bay, at the Marconi Marina, -38.143°N; -122.879°W, under rocks with <i>Armadilloniscus</i> at high tide line, preserved in 75% ethanol, 21 Feb 1972, C72-19, SDNHM A.0030, NHM36, MBPC 6783, Coll. Ernie Iverson and J. Carlton, Collection ID: RW14.069 |
| | California, San Joaquin County, Delta-Mendota Canal, mile post 11.35, -37.991°N; -121.263°W, freshwater; Isopods very abundant in clusters and as individuals all along surface (concrete wall) and in mass congregation in darkened cracks/crevices. These scooped up in one small hand-full. Canal running at high-water and fully operating; water at high velocities (12?-13? mph surface velocity). Some isopods observed crawling slowly against this current. Some of the larger specimens collected also by hand elsewhere in the same area along concrete wall, preserved in 75% ethanol, 6 Jun 1972, Coll. J. Chapman & E. Iverson, Collection ID: RW17.046 |
| | California, Marin County, creek at Bolinas Lagoon immediately north of Audubon Canyon Ranch where creek goes under road, 37.925°N; 122.676°W, under rocks, preserved in 75% ethanol, 21 Feb 1972, C72-14, Coll. E. Iverson & J. Carlton, Collection ID: RW17.052 |
| | California, Marin County, creek at Bolinas Lagoon immediately north of Audubon Canyon Ranch, 37.924°N; 122.675°W, brackish creek mouth, preserved in 75% ethanol, 21 Feb 1972, C72-13, Coll. E. Iverson & J. Carlton, Collection ID: RW17.050 |
| | California, Santa Cruz County, San Lorenzo River, City of Santa Cruz, 200–250 m downstream of Laurel Street, 1.5 mi. above ocean, 36.969°N; 122.022°W, fixed in formalin and preserved in 75% ethanol, 22 May 2004, CCS2004-18, Coll. Camm Swift and Steve Howard, Collection ID: RW04.268 |
| | California, Santa Cruz County, San Lorenzo River, -36.58°N; -122.03°W, collected before May 2003, fixed in formalin, preserved in 70% ethanol, Coll. Christopher Rogers, rcvd. from Wayne Fields, Collection ID: RW03.216 |
| | California, San Luis Obispo County, Diablo Cove, -35.211°N; -120.86°W, preserved 75% ethanol, 19 Apr 1976, Coll. D. W. Behrens, Collection ID: RW17.037 |
| | California, Santa Barbara County, El Capitan State Beach in kelp debris at mouth of Cañada del Capitan, 34.458°N; 120.022°W, preserved in 75% ethanol, 28 Dec 1971, I71-90, Coll. E. Iverson, Collection ID: RW17.051 |
| | California, Santa Barbara County, San Miguel Island, -34.101°N; -120.379°W, preserved in 70% ethanol, 11 Oct 1978, Coll. Eric Hochberg, Collection ID: RW17.030 |
| | California, Ballona Creek Estuary, 33.971°N; 118.439°W, Van Veen, 1.5 m, fixed in 10% formalin, preserved in 70% ethanol, 16 Sep 2003, MBPC 10271, Bight '03, Sta. 4053, Coll. Aquatic Bioassay and Consulting Laboratories, Inc., Collection ID: RW17.027 |
| | California, Dominguez Channel, 33.802°N; 118.228°W, VanVeen, 4 m, fixed in 10% formalin, preserved in 70% ethanol, 17 Sep 2003, MBPC 10592, Bight '03, Sta. 5108, Coll. Kinetic Laboratories, Inc, Collection ID: RW17.028 |
| <i>Gnorimosphaeroma oregonense</i> | Washington, San Juan County, Friday Harbor, Ocean Labs, -48.546°N; -22.013°W, marine, night light, 27 Aug 1949, Coll. J.L. Mohr, Collection ID: RW17.039 |
| | Washington, San Juan County, Puget Sound, Seattle Puget Sound Naval Supply Depot, Smith Cove, 47.631°N; 122.386°W, under rocks in sand. LT2, preserved in 75% ethanol, 11 Aug 1973, I73-17, Coll. E. Iverson, Collection ID: RW17.045 |
| | Washington, Grays Harbor County, Grays Harbor, Westport floats, 46.9°N; 124.094°W, on floats among fouling organisms, fixed in isopropyl, preserved in 75% ethanol, 22 Mar 1976, Coll. J. T. Carlton & D. A. Fishlyn, Collection ID: RW17.038 |
| | Oregon, Lincoln County, Cape Perpetua, Strawberry Hill, 44.254°N; 124.112°W, under seaweed at high tide mark, fixed and preserved in 70% ethanol, 9 Jul 1971, rcvd. from Robert Hessler, MBPC 13410, Coll. Fred Schram, Collection ID: RW17.041 |

| Species | Specimen label |
|------------------------------------|---|
| <i>Gnorimosphaeroma oregonense</i> | Oregon, Coos County, Squaw Island, off Cape Argo Light, 43.339°N; 124.376°W, intertidal, -1.6 ft. tide, rocky reef, some loose rocks kelp covered, preserved in 95% ethanol, 27 Jul 1942, Sta. 1488-42, LACM 42-46.5, Coll. R/V Veleró, Collection ID: RW17.033 |
| | California, San Francisco County, San Francisco Bay, Aquatic Park, west of Scout Hut, -37.8°N; -122.362°W, under rocks, fixed and preserved in 75% ethanol, 17 Nov 1971, Coll. E. Iverson & J. Carlton, Collection ID: RW17.032 |

Table 2. Sequences used in the 16S-rDNA analyses are associated with their taxon names in alphabetical order and GenBank accession number. The molecular identification number identifies the specimen on the phylogenetic tree. In several instances multiple individuals were extracted and sequenced from the specimen lot. An asterisk denotes the lot from which neotype was selected.

| Species | GenBank No. | Mol. Id. | Specimen label |
|--------------------------------|-------------|---|---|
| <i>Gnorimosphaeroma</i> sp. | MH427743 | 2550 | California, San Mateo County, Redwood Shores, 631 Marlin Court, -37.535°N; -122.249°W, from floating styrofoam boat dock, amongst bases of <i>Ciona</i> , salinity 24 ppt, fixed and preserved in 95% ethanol, 9 Nov 2002, Coll. R. Wetzter, N. D. Pentcheff, C. Wetzter, Collection ID: RW02.060 |
| | MH427746 | 2551 | |
| | MH427744 | 2550 | |
| | MH427750 | 3124 | |
| | MH427749 | 3122 | California, Alameda County, San Francisco Bay, off Doolittle Road near Oakland Airport, 37.079°N; 122.224°W, high intertidal, salinity 30 ppt, fixed and preserved in 95% ethanol MBPC: Fixed and preserved in 95% ethanol, 5 Jun 2002, Coll. R. Wetzter and S. Boyce, Collection ID: RW02.030 |
| MH427747 | 3120 | | California, Alameda County, San Francisco Bay, off Doolittle Road near Oakland Airport, 37.731°N; 122.21°W, from high intertidal under rocks, isopods found under rocks most commonly without grapsid crabs – upper intertidal occurring with <i>Ligia</i> , salinity 30 ppt, fixed in 95%, preserved in 95% ethanol, 5 Jun 2002, Coll. R. Wetzter, T. Haney, and S. Boyce, Collection ID: RW02.028 |
| MH427748 | 3121 | | |
| <i>Gnorimosphaeroma noblei</i> | MH427755 | 2546 | California, Santa Barbara County, lagoon at mouth of Refugio Creek, Refugio Creek State Park, 14–15 km E. of Gaviota, salinity 0‰, -34.465°N; -120.069°W, probably fixed in 95%, preserved in 70% ethanol, 22 Oct 1999, Coll. Camm Swift and Todd Haney, Collection ID: RW00.017 |
| | MH427770 | 3113 | |
| | MH427771 | 3114 | |
| | KU248168 | 1541 | California, Marin County, Tomales Bay, head of bay near channel (man-made) adjacent to Hwy. 1, 38.091°N; 122.825°W, from under algae and barnacle covered rocks, salinity 20 ppt, fixed and preserved in 95% ethanol, 4 Jun 2002, Coll. R. Wetzter, S. Boyce, and T. Haney, Collection ID: RW02.021 |
| | MH427772 | 3115 | |
| | MH427773 | 3116 | |
| | MH427761 | 3104 | California, Santa Cruz County, San Lorenzo River at Laurel Street bridge, 36.97°N; 122.023°W, freshwater, probably fixed and preserved in 95% ethanol, 22 Mar 2002, Coll. D. Christopher Rogers, Collection ID: RW03.010 |
| | MH427762 | 3105 | |
| | MH427753 | 2543 | California, Humboldt County, Arcata Bay Margin, mouth of Mad River Slough and tributary at crossing Hwy. 255, -2 mi. W. of Arcata, -40.833°N; -124.133°W, CCS99-69, fixed and preserved in 75% ethanol, 19 Oct 1999, salinity 25‰, Coll. Camm Swift, Todd Haney, Dave Jacobs, Collection ID: RW00.009 |
| | MH427759 | 3102 | |
| | MH427760 | 3103 | |
| | MH427751 | 2541 | California, Del Norte County, Lake Earl, -2 mi NNE of Crescent City at end Buzzini Road along E side, salinity 5‰, 41.831°N; 124.188°W, probably fixed in 95%, preserved in 70% ethanol, 18 Oct 1999, CCS99-71, Coll. Camm Swift, Todd Haney, Dave Jacobs, Collection ID: RW00.011 |
| | MH427763 | 3106 | |
| | MH427756 | 2549 | California, Marin County, Walker Creek, US Hwy. 1, -100 m above mouth of Keyes Creek, 1.5 km SW of Tomales, salinity 1–12‰, 38.232°N; 122.912°W, probably fixed in 95%, preserved in 70% ethanol, 21 Oct 1999, Coll. Camm Swift and Todd Haney, Collection ID: RW00.015 |
| | MH427768 | 3111 | |
| MH427769 | 3112 | | |
| MH427752 | 2542 | California, Del Norte County, Smith River, at mouth of Tillas Slough and Rittman Creek at tide gate, -2 m W of town of Smith River, stream to 30 m, -41.931°N; -124.185°W, probably fixed in 95%, preserved in 70% ethanol, 18 Oct 1999, CCS99-70, Coll. Camm Swift, Todd Haney, Dave Jacobs, Collection ID: RW00.010 | |
| MH427764 | 3107 | California, Sonoma County, Salmon Creek at Hwy. 1, -4.8 km N of N edge of Bodega Bay, salinity 9–23‰, -38.17°N; -122.28°W, probably fixed in 95%, preserved in 70% ethanol, 19 Oct 1999, CCS99-76, Coll. Camm Swift and Todd Haney, Collection ID: RW00.013 | |
| MH427765 | 3108 | | |
| MH427774 | 3117 | California, Marin County, Tomales Bay, off Hwy. 1, Alan Sieroty State Park, Millerton Point, -38.109°N; -122.851°W, fixed and preserved in 95% ethanol, 4 Jun 2002, Coll. R. Wetzter, S. Boyce, and T. Haney, Collection ID: RW02.022 | |
| MH427775 | 3118 | | |

| Species | GenBank No. | Mol. Id. | Specimen label |
|--------------------------------------|-------------|--|--|
| <i>Gnorimosphaeroma noblei</i> | MH427765 | 3109 | California, Marin County, Schooner Bay at crossing of Sir Francis Drake road to coast of Drakes Bay, 5.5 km W Inverness (airline), salinity 9–23‰, 38.232°N; 122.912°W, probably fixed in 95%, preserved in 70% ethanol, 20 Oct 1999, CCS99-82, Coll. Camm Swift and Todd Haney, Collection ID: RW00.014 |
| | MH427767 | 3110 | |
| | KU248165 | 1174 | California, San Mateo County, San Gregorio Creek, lagoon, just W of US Hwy, stream width 30–40 m, 37.321°N; 122.402°W, fixed and preserved in 75% ethanol, 17 Oct 1999, CCS99-68, Coll. Camm Swift, Dave Jacobs, Todd Haney, Collection ID: RW00.008 |
| | MH427754 | 2544 | |
| MH427757 | 3100 | | |
| MH427758 | 3101 | | |
| <i>Gnorimosphaeroma oregonense</i> * | MH427781 | 3131 | British Columbia, Vancouver, Stanley Park, 49.294°N; 123.155°W, mid intertidal, hand, fixed and preserved in 95% ethanol, 7 Jul 2010, Coll. R. Wetzer & N. D. Pentcheff, Collection ID: RW10.003 |
| <i>Gnorimosphaeroma oregonense</i> | AF260866 | 324 | British Columbia, University of British Columbia, -49.256°N; -123.257°W, nude, rocky intertidal, among mussels, fixed and preserved in 95% ethanol, 25 Jun 1998, Coll. T. J. Hilbisch, Collection ID: RW98.033 |
| | MH427778 | 3099 | |
| | KU248218 | 1496 | Washington, northeast of San Juan Island, Reuben Tarte County Park, 48.612°N; 123.098°W, underside of rocks in intertidal, hand, fixed and preserved in 95% ethanol, 9 Apr 2004, #7, Coll. R. Wetzer & N. D. Pentcheff, Collection ID: RW04.040 |
| | MH427780 | 3126 | |
| | KU248217 | 1151 | Washington, westside of San Juan Island, Deadman Bay, 48.513°N; 123.008°W, cobble/sand beach washes, hand, fixed and preserved in 95% ethanol, 8 Apr 2004, #5, Coll. R. Wetzer & N. D. Pentcheff, Collection ID: RW04.038 |
| | MH427779 | 3125 | |
| | KU248330 | 1477 | Washington, north end of Whidbey Island, Deception Pass, -48.405°N; -122.646°W, rocky intertidal among mussels, fixed and preserved in 95% ethanol, 25 Jun 1998, Coll. T. J. Hilbisch, Collection ID: RW98.031 |
| | MH427776 | 3096 | |
| MH427777 | 3097 | | |
| <i>Gnorimosphaeroma rayi</i> | MH427784 | 2567 | California, Marin County, Tomales Bay, north end of bay across from Hog Island, boat launch parking lot, 38.201°N; 122.922°W, intertidal, from underside of rocks, hand, fixed and preserved in 95% ethanol, 9 Jan 2009, #2, Coll. R. Wetzer, Collection ID: RW09.002 |
| | MH427785 | 2567 | |
| | MH427790 | 3129 | |
| | MH427786 | 2568 | California, Marin County, Tomales Bay, Marshall, beach in front of Tomales Bay Oyster Company, 15479 Highway One, 38.116°N; 122.854°W, intertidal, from under rocks on sandy beach, hand, fixed and preserved in 95% ethanol, 9 Jan 2009, #1, Coll. R. Wetzer, Collection ID: RW09.001 |
| | MH427787 | 2568 | |
| | MH427789 | 3128 | |
| | MH427783 | 2566 | California, Marin County, Tomales Bay, north end of bay across from Hog Island, boat launch parking lot, 38.201°N; 122.922°W, intertidal, from empty <i>Balanus glandula</i> testes, hand, fixed and preserved in 95% ethanol, 9 Jan 2009, #2, Coll. N. D. Pentcheff, Collection ID: RW09.006 |
| | MH427791 | 3130 | |
| MH427783 | 2566 | | |
| MH427788 | 2958 | California, Marin County, Bolinas Beach, 37.902°N; 122.686°W, intertidal, hand, fixed and preserved in 95% ethanol, 3 Sep 2009, Coll. Martin Hauser and Darolyn Striley, Collection ID: RW09.072 | |

Results

Taxonomy

Gnorimosphaeroma Menzies, 1954

Isopoda: Sphaeromatidea: Sphaeromatoidea: Sphaeromatidae

Gnorimosphaeroma Menzies, 1954: 5; Kussakin 1979: 406; Harrison and Ellis 1991: 939.

Nishimuraia Nunomura, 1988: 1.

Type species. *Spheroma oregonensis* Dana, 1853; now *Gnorimosphaeroma oregonense* (Dana, 1853); by original designation.

Diagnosis. *Body* vaulted, dorsal surfaces smooth or polished in appearance, without setae. *Eyes* lateral, simple, without posterior lobe. *Pleon* consisting of 4 visible

segments (as determined by lateral sutures), sutures (except first) long extending from lateral margin, separated medially by 24–28% pleon width; pleonite 1 entire, posterior margin even, narrower than remainder of pleon, not extending to pleon lateral margins. *Pleotelson* vaulted, anteriorly as wide as pleon, without dorsal process; posterior margin entire, simple, arcuate. *Maxilliped* palp articles 2–4 medial margins lobate, article 2 not expanded. *Penial processes* entirely separate, basally close set, short (not extending beyond pleopod peduncles). *Uropod* rami lamellar, similar in size, exopod shorter than endopod, inserted near anterolateral angle of peduncle; endopod lateral margin simple, finely serrate or smooth, distally broadly rounded; both rami distally broadly rounded or narrowly rounded.

Description. *Body* vaulted, dorsal surfaces smooth or polished in appearance, without setae; coxal and other margins smooth, with ability to conglobate; not or weakly sexually dimorphic. *Head* with rostral point present, dorsally visible, simple, not separating antennular bases; without paired incisions in front of eyes, lateral margins not laterally extended to body outline (antennules more or less ventral). *Eyes* lateral, simple. Pereonite 1 lateral margins not anteriorly produced, not laterally enclosing head, pereonites 2–7 with posterior margin not raised, pereonite 1 anteriorly with keys. *Sternite 1* without cuticular mesial extensions. *Pereonite 6* simple, without bosses, processes or marginal extensions. *Pereonite 7* as wide as pereonite 6, forming part of body outline, dorsally without bosses, processes, or marginal extensions. *Coxae* distally narrow, those of pereonites 2–7 overlapping the one behind, rounded, with ventral ‘lock and key’ processes, with grooved articulation; those of pereonite 6 not large, not overlapping those of pereonite 7. *Pleon* consisting of 4 visible segments (as determined by lateral sutures); pleonite 1 entire, posterior margin even, narrower than remainder of pleon, not extending to pleon lateral margins; sutures (except first) running to lateral margin, all separate, sutures long (separated medially by 24–28% pleon width); pleonal sternite absent; dorsal surface without process; posterior margin even, with ‘keys’. Pleonite 5 posterior margin entire (not fused with pleotelson). *Pleotelson* vaulted, anteriorly as wide as pleon, without dorsal process; posterior margin entire, simple, arcuate; ventro-lateral margins forming ridge.

Marsupium formed from four pairs of oostegites, arising from pereonites 1–4; anterior pocket absent, posterior pocket absent, oostegites overlapping at mid-line (except 1).

Antennule peduncle with basal articles medially not in contact, 1 and 2 robust, article 3 slender; article 1 not produced, without anterior lobe; article 2 approximately 0.5 as long as article 1; with articles 2 and 3 colinear, article 3 longer than article 2; article(s) not flattened; flagellum shorter than peduncle, longer than peduncular article 3. *Antenna* peduncle articles all colinear (or curving regularly), less robust than antennule, peduncular articles all of similar thickness.

Epistome anteriorly narrow, with median weak constriction, anteriorly flush with head, not projecting; elongate. *Mandible* incisor wide, 4-cuspid; lacinia mobilis present; spine row normal; present, molar process gnathal surface with transverse ridges, rounded. *Maxillula* lateral lobe robust setae with some or all serrate, mesial lobe with major robust setae, these setae being heavily serrate. *Maxilla* with setae on middle and

lateral lobes serrate. *Maxilliped* palp articles 2–4 medial margins lobate, article 2 not expanded; endite distal margin rounded, anteromesial (upper) marginal ridge without long curved serrate robust setae.

Mouthparts of female not metamorphosed.

Pereopod 1 ambulatory; dactylus secondary unguis short, robust, simple; setae on superodistal corner of merus only very long. *Pereopod 2* similar in proportion to *pereopod 3*; dactylus with secondary unguis simple, short and stout. *Pereopods 3–7* dactylus with secondary unguis simple. *Pereopods* with inferior margins of ischium to carpus without dense setulose fringe, ischium superior margin without sinuate acute robust seta, *pereopods 1–3* or *4* ischium superior margin with few long stiff slender setae. *Pereopods 1* (or *1–3*), inferior margins of merus, carpus and propodus palm *pereopod 1* only with robust setae on propodus inferior margin.

Penial processes entirely separate, basally close set, short (not extending beyond pleopod peduncles), widest near base, apex bluntly rounded.

Pleopod 1 rami not operculate; exopod lamellar; rami exopod with longitudinal axis weakly oblique; endopod of similar proportions to exopod, mesial margin lamellar, distally triangular, endopod proximomedial heel absent; exopod distally rounded or distally subtruncate or truncate, exopod distal margins not serrate. *Pleopod 2* endopod ca. as long as exopod; exopod distal margins not deeply serrate; appendix masculina inserted basally, with straight margins, distally abruptly narrowed, longer than and extending beyond endopod ($1.14 \times$ as long as endopod), distally narrowly rounded. *Pleopod 3* exopod transverse suture present, endopod of similar proportions to exopod. *Pleopod 4* rami with PMS; exopod transverse suture present, incomplete, thickened transverse ridges absent, lateral margin not thickened, with short simple marginal setae; endopod thickened transverse ridges absent; mesial margin without deep distal notch; endopod without proximomedial lobe. *Pleopod 5* exopod transverse suture present, entire, thickened transverse ridges absent, lateral margin with short simple setae, lateral margin not thickened, with 3 discrete scale patches; scale patches flush or weakly domed; endopod with thickened transverse ridges absent, endopod without proximomedial lobe.

Uropod rami not strongly flattened, not forming part of continuous body outline; exopod shorter in length than endopod, exopod lamellar, inserted near anterolateral angle of peduncle-endopod, lateral margin simple, finely serrate or smooth, distally broadly rounded; endopod lamellar, distally broadly rounded or narrowly rounded. *Uropod* endopods not in contact posteriorly.

Remarks. *Gnorimosphaeroma* is in a general sense quite unremarkable in appearance, with no species showing any sort of dorsal ornamentation of tubercles, processes, or pereonal and pleonal ridges that characterize so many genera of Sphaeromatidae. As such, there is a lack of readily obvious characters by which to identify the genus. *Gnorimosphaeroma*, on morphological criteria, is most similar to the genera *Bilistra* Sket & Bruce, 2004, *Exosphaeroma* Stebbing, 1900, *Lekanesphaera* Verhoeff, 1943, *Neosphaeroma* Baker, 1926 and *Sphaeroma* Bosc, 1802. The latter three genera can be

differentiated from *Gnorimosphaeroma* in the first instance by having the uropodal exopod lateral margin with one or more serrations or notches (among other characters).

Exosphaeroma is a large genus with 40 species at the last count (Boyko et al. 2008) that, as presently constituted, contains both smooth bodied species as well as some with coarsely pitted or ridged dorsal surfaces (e.g., see Kensley 1978; Espinosa-Pérez and Hendrickx 2001; Bruce 2003), and also species with greatly enlarged uropodal rami (e.g., see Kensley 1978; Bruce 2003; Wall et al. 2015). Some of the smooth-bodied species of *Exosphaeroma* are superficially similar to *Gnorimosphaeroma*, but can be distinguished by the pleonal sutures running to the posterior margin (to the free lateral margin in *Gnorimosphaeroma*), as well as pleonite 1 having two flat sub-median lobes on the posterior margin (see Bruce 2003: figs 14E, 18F).

Bilistra is similar in gross morphology and also occupies coastal freshwater habitats. *Bilistra* differs from *Gnorimosphaeroma* in having a far shorter uropodal exopod (ca. half as long as endopod), shorter pleonal sutures that run to the pleon posterior margin (not lateral margin); the inferior margins of pereopods ischium or merus to propodus have a dense setulose (fur-like) fringe while the superior margins lack long setae altogether. *Bilistra* is presently restricted to New Zealand, but there is also one species in South Africa, from supralittoral brackish pools and tidal streams that is currently classified as *Pseudosphaeroma barnardi* Monod, 1931 that is in need of redescription and formal reassignment to *Bilistra* (NLB, pers. obs.).

Gnorimosphaeroma pereopod setation is inconsistently illustrated, even within species, despite being a potentially significant character. The redescription given here, and figures of Hoestlandt (1975) show long setae on the superior or superodistal margin of the merus and long setae on the inferior margin of the ischium and merus. Such setae were not mentioned or figured in Menzies' (1954) genus diagnosis or species descriptions. Such setae are also apparently absent from all northwestern species (e.g., Hoestlandt 1975, 1977; Kwon and Kim 1985; Nunomura 1998, 1999a, 2007).

Neotype designation. It has been long established that all of Dana's (1852) isopod material, and therefore all the type material for the many species of isopod that he named, was lost with the sinking of the ship USS 'Peacock' on the bar of the Columbia River in 1841 (Bruce 1986: 220; 2004: 228; 2009: 211; Poore and LewTon 1993: 234). *Gnorimosphaeroma oregonense* (Dana, 1853) is one such species.

Species of *Gnorimosphaeroma* are uniform in appearance, and to date no assessment has been made of intrinsic variability within species. Some species of *Gnorimosphaeroma* occur sympatrically and there are many exceedingly similar species. At present few species have been described in full detail. Furthermore, records of *G. oregonense* are somewhat inconsistent in the details presented and the material is not always available for re-examination, so that it is not always possible to confirm the correct identity of previous records and indeed also on occasion, new material. We consider that designating a neotype is necessary to clearly characterize the identity of this species, to allow for the genus to be precisely diagnosed based on the type species and to permit unambiguous identification and separation from other sympatric congeneric species.

Dana (1853) did not indicate a specific type locality, but stated that the species had been obtained from “Puget’s Sound, Oregon; also, Bay of San Francisco, California”. One may infer that the first mentioned location is the type locality but that remains an inference, and furthermore one cannot be certain that the material consists of only one species, given that there are four species in the region and also that the morphology of purported species apparently changes from low to high latitudes (present study). The neotype has been chosen from specimens collected as near as practically possible to the original type locality, and is now Stanley Park, 49.294°N, 123.155°W (British Columbia, Canada), ca. 150 km north of Puget Sound.

Included species. *Gnorimosphaeroma albicauda* Nunomura, 2005, *G. akanense* Nunomura, 1998, *G. anchialos* Jang & Kwon, 1993, *G. boninense* Nunomura & Satake, 2006, *G. chejuense* Kim & Kwon, 1988, *G. chinense* (Tattersall, 1921), *G. hachijoense* Nunomura, 1999b, *G. hoestlandti* Kim & Kwon, 1985, *G. hokurikuense* Nunomura, 1998, *G. insulare* (Van Name, 1940), *G. iriei* Nunomura, 1998, *G. kurilense* Kussakin, 1974, *G. naktongense* Kwon & Kim, 1987, *G. noblei* Menzies, 1954, *G. oregonense* (Dana, 1853), *G. ovatum* (Gurjanova, 1933), *G. paradoxa* (Nunomura, 1988), *G. pulchellum* Nunomura, 1998, *G. rayi* Hoestlandt, 1969, *G. rebunense* Nunomura, 1998, *G. saiyoense* Nunomura, 2013, *G. shikinense* Nunomura, 1999b, *G. tondaense* Nunomura, 1999b, *G. trigonocaudum* Nunomura, 2011, *G. tsutshimaense* Nunomura, 1998.

Notes. The original diagnosis of the genus was provided by Menzies (1954: 5). A more complete diagnosis of the genus is provided here (see above). Menzies (1954) suggested that *Neosphaeroma pentaspina* Baker, 1926 could possibly be attributed to *Gnorimosphaera* were it to be redescribed, while Harrison and Holdich (1984) indicated some shared characters, notably the pleon suture, but the species is presently considered as *incertae sedis*. Smooth-bodied Sphaeromatidae similar to *Gnorimosphaeroma* are summarized in the genus remarks above and reoccur in several sphaeromatid clades. In their molecular analysis Wetzer et al. (2018) demonstrated that this a plesiomorphic trait and that *Neosphaeroma* is basal to or nested within the *Cymodoce* clade and is not closely related to *Gnorimosphaeroma*.

***Gnorimosphaeroma oregonense* (Dana, 1853)**

Figures 1–9

Abbreviated synonymy (detailed synonymies given by Richardson (1905), Menzies (1954), and Kussakin (1979)).

Spheroma oregonensis Dana, 1853: 778, Atlas plate 52x.

Exosphaeroma oregonensis.— Richardson, 1905: 296, figs 315, 316.

Neosphaeroma oregonense.— Monod, 1932: 76, fig. 74.

Gnorimosphaeroma oregonensis oregonensis.— Menzies, 1954: 406, figs 5, 7A–E, 12.

Material examined. *Neotype* ♂ (8.5 mm): Canada, British Columbia, Vancouver, Stanley Park, 49.294°N, 123.155°W, mid intertidal, hand, fixed and preserved in

95% ethanol. 7 Jul 2010, coll. Regina Wetzer & N. Dean Pentcheff. Collection ID: RW10.003. LACM:DISCO:7028.

Additional material examined from the same lot as the neotype. ♀ Non-type with mancas (6.0 mm) LACM:DISCO:11164; ♂ (8.5 mm) LACM:DISCO:11161; subadult ♂ with penes beginning, without appendix masculina (6.0 mm) LACM:DISCO:11162; plus additional 20+ adults, juveniles, and mancas in this lot.

Body parts and appendages figured are as indicated in figure legends.

Description of male neotype. *Body* length $2.4 \times$ width; widest at pereonite 6; pleotelson length $0.6 \times$ width, distal margin broad and weakly convex. (Figs 1A, B, 2A). *Pleotelson* length $0.66 \times$ width.

Antennula peduncle article 1 length $1.3 \times$ width; article 2 as long as wide; article 3 length $2.6 \times$ width, inferior distal margin with one palm seta; flagellum with 13 articles, 11 basal articles with aesthetascs and small simple seta (Figs 2A, 3A, 4A). *Antenna* reaching slightly beyond anterior margin of pereonite 2; peduncle article 4 length $2.3 \times$ width, flagellum with 14 articles, setation as figured (Figs 2A, 3B, 4B). *Clypeus* and *labrum* as in Figs 3A, 8B.

Left mandible incisor with 4 cusps; lacinia mobilis with a single cusp; lacinia mobilis spine row comprised of 4 serrate spines; crushing surfaces ridged (Fig. 4C). *Right mandible* incisor with 3 cusps, spine row comprised of 7 serrate spines (Fig. 4D). *Maxillula* mesial lobe with ca. 4 spines; lateral lobe with ca. 8 spines (Fig. 4F, E, respectively). *Maxilla* mesial lobe with 5 simple setae and 6 plumose RS on gnathal surface; middle lobe with 2 simple setae and 1 pectinate RS; lateral lobe with 2 simple setae, and 1 pectinate RS (Fig. 4G). *Maxilliped* endite distal surface with 7 plumose setae; distomesial margin with 3 plumose setae; palp article 2 distal apex with 9 long, simple RS; article 3 distal apex with 11 long, simple RS, lateral distal angle with 2 long, simple RS; article 4 distal apex with 15 long, simple RS, lateral distal angle with 1 long, simple RS; article 5 distal apex with 13 long, simple RS (Fig. 4H).

Pereopod 1 (Figs 5A, 7C) *basis* inferior distal angle with 1 long, RS, inferior proximal margin with setal patch; *ischium* length $1.6 \times$ width, inferior medial margin with setal patch; *merus* lobate, $0.74 \times$ ischium length, superior distal angle with 4 long, RS; *carpus* inferior medial margin with 1 robust, serrate, trident seta; *propodus* length $2.1 \times$ width, $1.1 \times$ ischium length, inferior margin with 3 robust, serrate, trident seta, and 3 plumose setae; *dactylus* length $1.2 \times$ width, length $0.33 \times$ propodus length, distal margin with 4 simple setae (Figs 5A, 7C). *Pereopod 2* (Fig. 5B) *basis* inferior distal angle with 1 long, simple RS, inferior medial margin with setal patch; *ischium* length $2.2 \times$ width, inferior medial margin with 12 long, simple RS, inferior distal angle with single simple RS; *merus* lobate, length $1.6 \times$ width, $0.69 \times$ ischium length, superior distal angle with cluster of 7 simple RS, distal medial margin with one palm seta; *carpus* length $1.2 \times$ merus length, $2.5 \times$ width, superior margin with 4 robust, biserrate setae on distal angle, inferior margin 2 palm setae; *propodus* weakly curved, length $2.6 \times$ width, $1.2 \times$ carpus length, superior distal margin with a palm seta; *dactylus* length $1.2 \times$ width, length $0.27 \times$ propodus length, inferior margin with scales, distal margin with 3 long, simple setae (Fig. 5B). *Pereopods 3–6* progressively less setose (not figured). *Pereopod 7* (Figs 5C, 7B) *basis* inferior medial margin with setal patch, inferior distal angle with 1 long, simple seta; *ischium* length 3.2

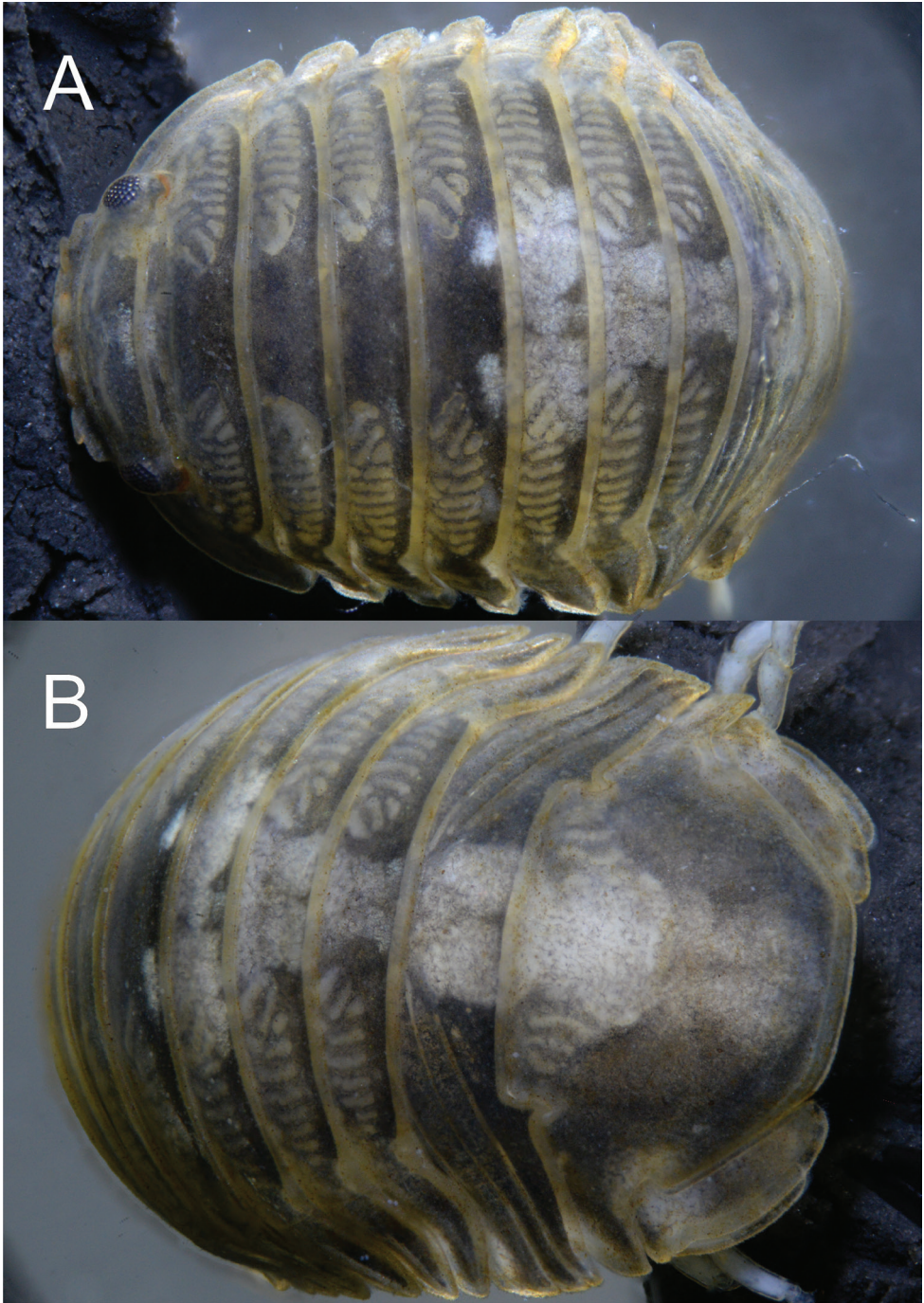


Figure 1. *Gnorimosphaeroma oregonense*. ♂ Neotype. LACM:DISCO:7028 **A** anterior dorsal **B** posterior dorsal and pleotelson.

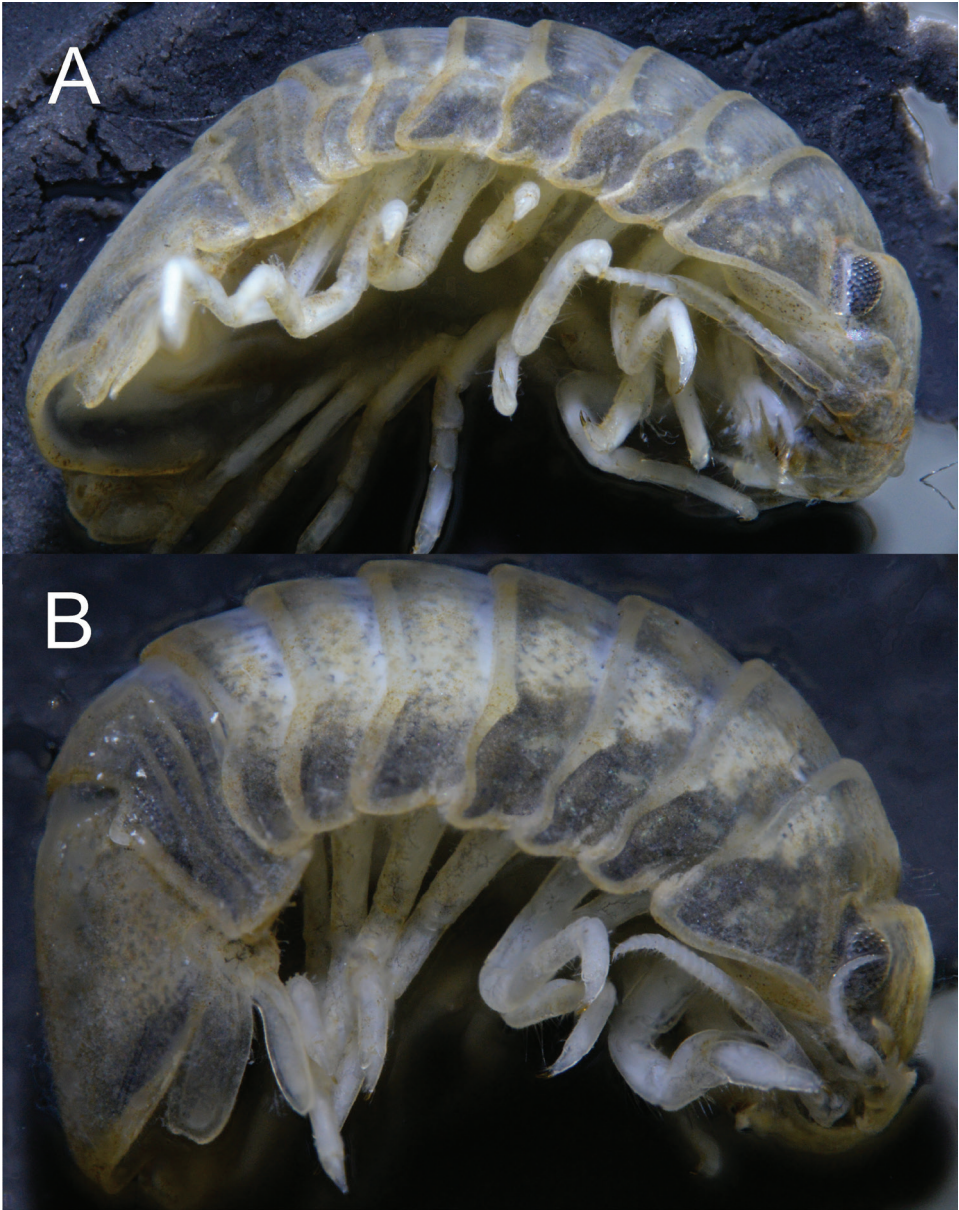


Figure 2. *Gnorimosphaeroma oregonense* **A** ♂ neotype. LACM:DISCO:7028, lateral **B** ♀ non-type LACM:DISCO:11164, lateral.

× width, inferior distal angle with 1 palm seta; *merus* lobate, merus length $1.3 \times$ width, merus length $0.42 \times$ ischium length, superior distal angle with 1 trident seta, inferior distal angle with 1 biserrate seta and 1 palm seta; *carpus* length $1.8 \times$ width, carpus length $1.3 \times$ merus length, superior distal angle with a cluster of 5 long, biserrate setae, inferior

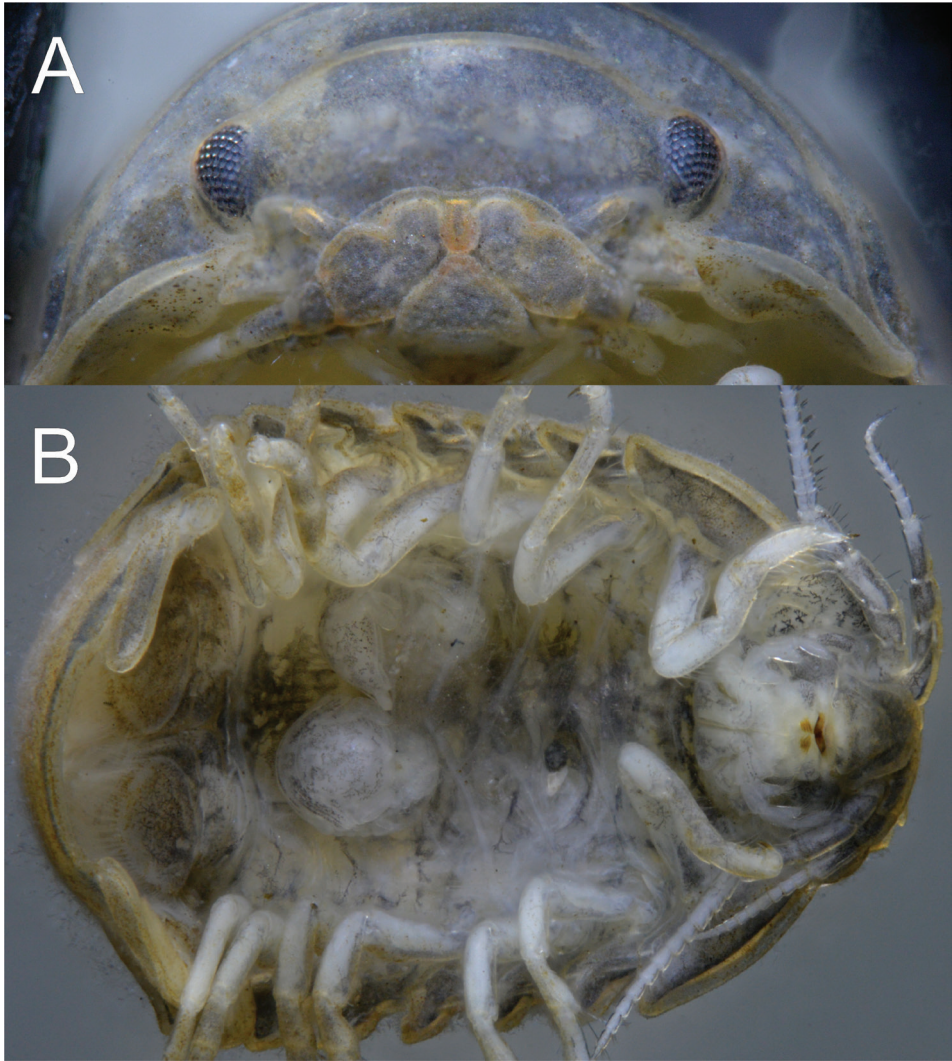


Figure 3. *Gnorimosphaeroma oregonense* ♀ Non-type. LACM:DISCO:11164 **A** clypeus and labrum **B** marsupium with three mancas.

distal angle with a cluster of 1 long, biserrate seta, and 1 long, trident seta; *propodus* weakly curved, length 3.2 width, length 1.5 carpus length, superior distal angle with 1 simple seta, and 1 palm seta, inferior margin with 2 long, trident setae; *dactylus* length 1.3 × width, dactylus length 0.21 × propodus length, distal margin with 3 simple setae (Figs 5C, 7B).

Penial processes length 3.8 × basal width; close set (Fig. 6A).

Pleopod 1 (Fig. 6B) peduncle length 0.38 × width with 4 coupling hooks; exopod length 1.5 × width, 1.1 × endopod length. *Pleopod 2* (Fig. 6C) peduncle length 0.34 × width with 3 coupling hooks, *appendix masculina* length 8.5 × width, 1.1 × length of endopod, straight, proximally and medially slightly swollen, distally narrowing. *Pleopod 3*

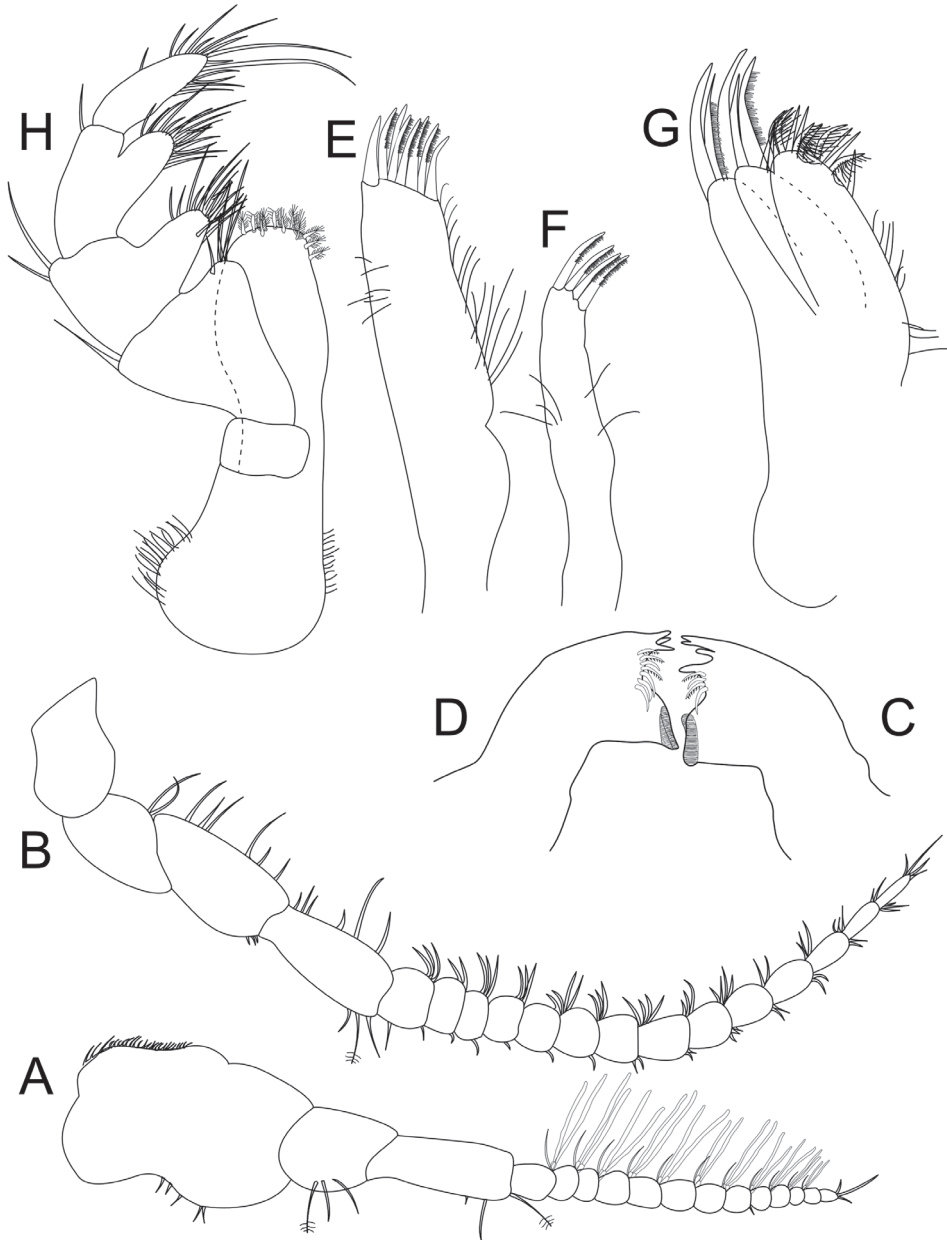


Figure 4. *Gnorimosphaeroma oregonense* ♂ Neotype LACM:DISCO:7028. All appendages from right, unless otherwise indicated **A** antennula **B** antenna **C** left mandible **D** right mandible **E** maxillula lateral lobe **F** maxillula medial lobe **G** maxilla **H** maxilliped.

(Fig. 6D) peduncle length $0.34 \times$ width with 3 coupling hooks. *Pleopods 1–4* exopods and endopods with PMS as figured (note: not all drawn, but indicated). *Pleopod 4* (Fig. 6E) endopod and exopod subequal, exopod with transverse suture. *Pleopod 5* (Fig. 6F)



Figure 5. *Gnorimosphaeroma oregonense* ♂ Neotype LACM:DISCO:7028. All appendages from right **A** pereopod **B** pereopod **C** pereopod 7.

endopod and exopod subequal, endopod length $1.5 \times$ width, exopod length $2.1 \times$ width with 1 distal scale patch and 2 medial lateral scale patches.

Uropod extending to posterior margin of pleotelson. *Exopod* $0.83 \times$ as long as endopod, $2.7 \times$ as wide; apex narrowly rounded; mesial margin with continuous row of PMS. *Endopod* $3.8 \times$ as long as wide, lateral margin weakly convex, apex bluntly rounded.

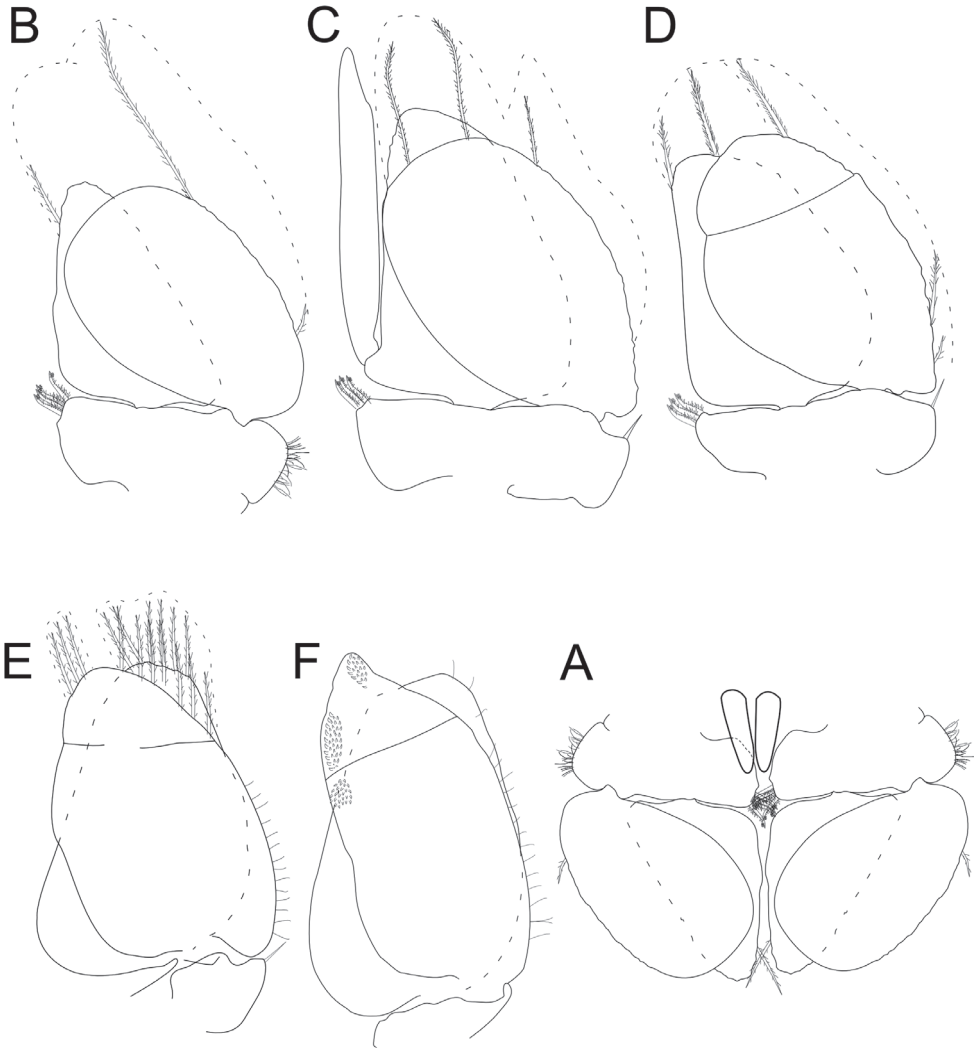


Figure 6. *Gnorimosphaeroma oregonense* ♂ Non-type LACM:DISCO:11161 **A** penes in ventral view with relative position to pleopods. ♂ Neotype. LACM:DISCO:7028. All appendages from right **B–F** pleopods 1–5.

Description of female. *Body* length $2.4 \times$ width (Figs 2B, 3A, B, 7A, 8A–C, 9A, B). *Pleotelson* length $0.66 \times$ width (Fig. 8C). *Uropodal* endopod (Figs 8C, 9B) as in male, longer than exopod, endopod just barely extending to posterior margin of pleotelson. Gravid female (Figs 3B, 9B) estimated to be able to brood 8–10 manca.

Size. Largest ♂ to 8.5 mm, largest ♀ to 6 mm. Dana (1853) gave no measurements. Fee (1926: 8, 9) records the largest specimens as being “ca. 1 cm. long; one-half as long as wide.”

Color. When preserved in ethanol, specimens quickly become pale buff to whitish.

Distribution. British Columbia, Vancouver to California, San Francisco.

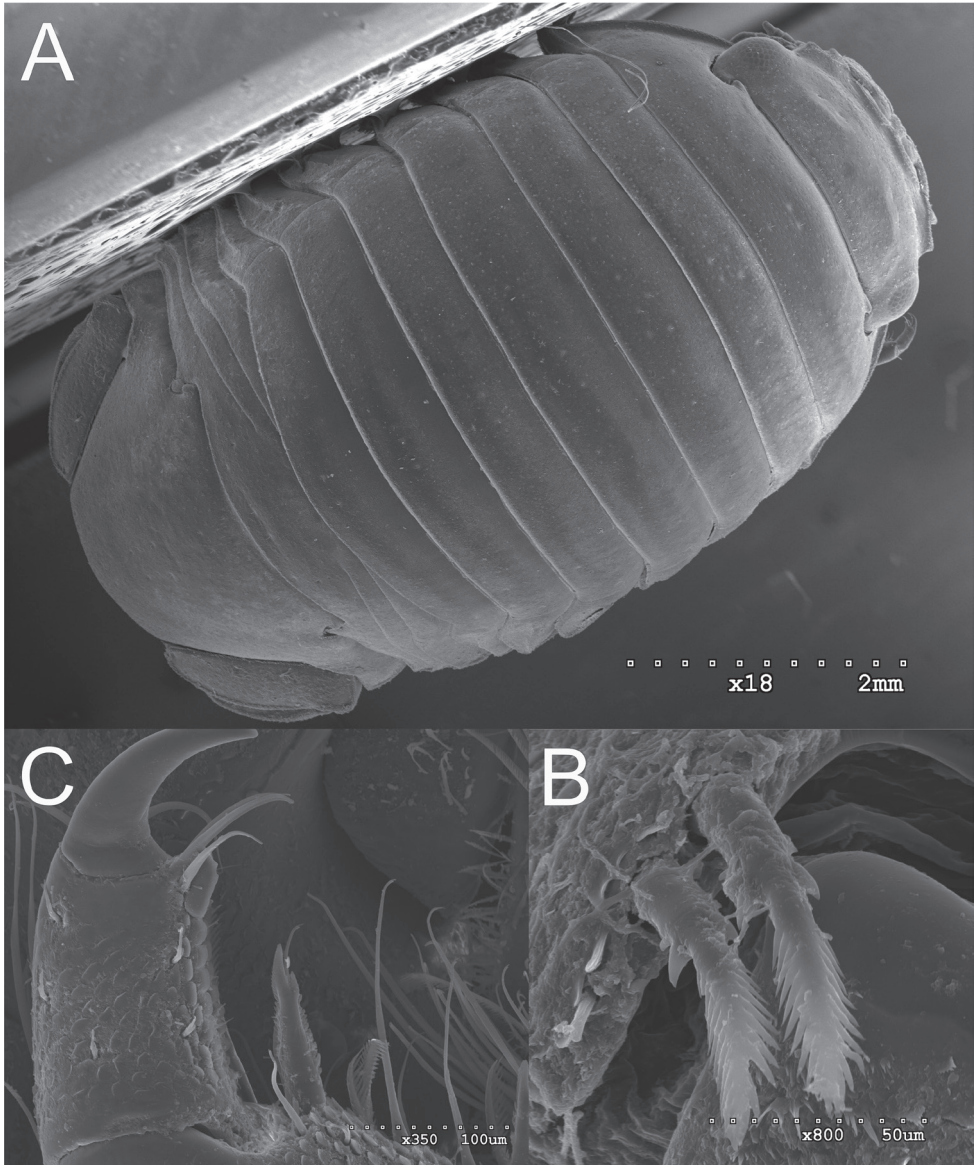


Figure 7. *Gnorimosphaeroma oregonense* ♀ Non-type SEM. LACM:DISCO:11164 **A** dorsum **B** pereopod 1 seta **C** pereopod 7 setae.

Remarks. The species occurs only in fully marine habitats in the intertidal to an unknown depth. A single lot indicated that it was collected by night light, and another that specimens were collected on floats among fouling organisms. None of the material examined indicates depth.

Kussakin (1979) reported *G. oregonense* from Alaska, Popov Island to San Francisco Bay, California. Kussakin (1979) figured *G. oregonense* from the collections of the

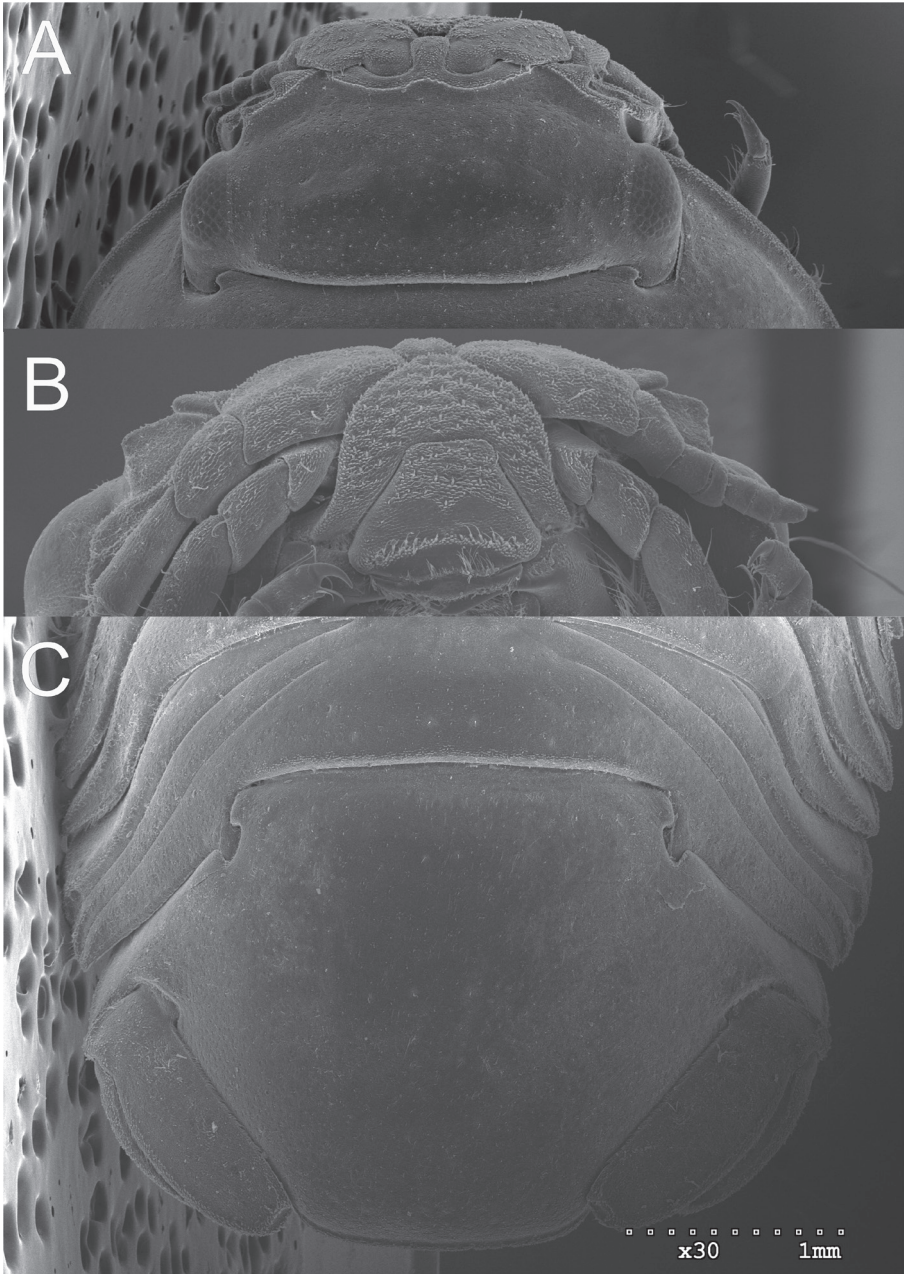


Figure 8. *Gnorimosphaeroma oregonense* ♀ Non-type SEM. LACM:DISCO:11164 **A** head dorsum **B** clypeus and labrum ventral **C** pleotelson dorsal.

Zoological Institute of the Academy of Sciences of the USSR. He noted that it is widely distributed with males reaching a length of 12 mm and females up to 8 mm, and that it occurred widely from Alaska to California. It is not clear what the specific localities of

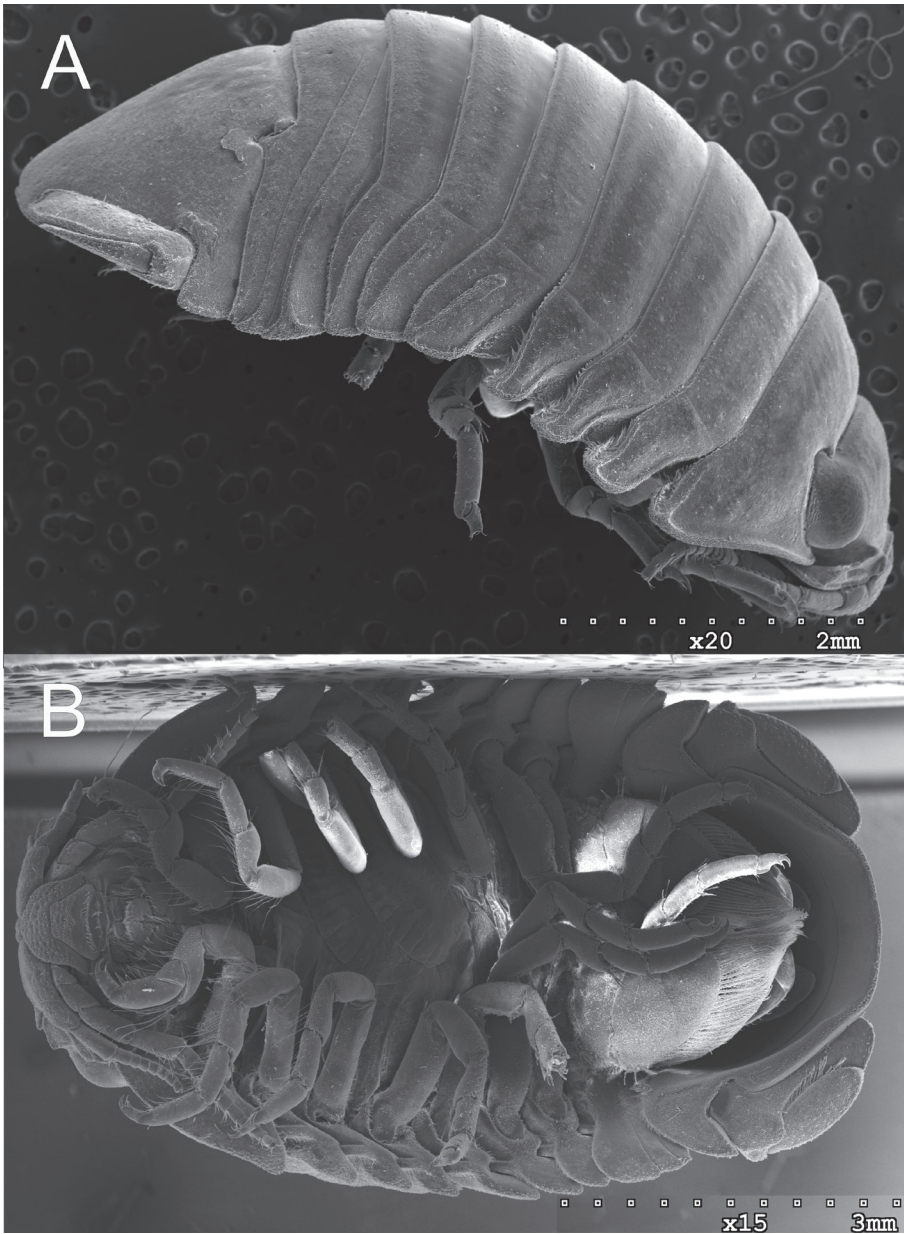


Figure 9. *Gnorimosphaeroma oregonense* Non-type SEM. LACM:DISCO:11164 **A** ♀ LACM:DISCO:11164 lateral **B** ♀ LACM:DISCO:11164 ventral view with oostegites.

the figured specimens were (Kussakin 1979: 407) nor of those deposited in the Russian collections. We were unable to locate and access these specimens. Kussakin reported that the specimens he examined were predominantly littoral, but can be sublittoral to

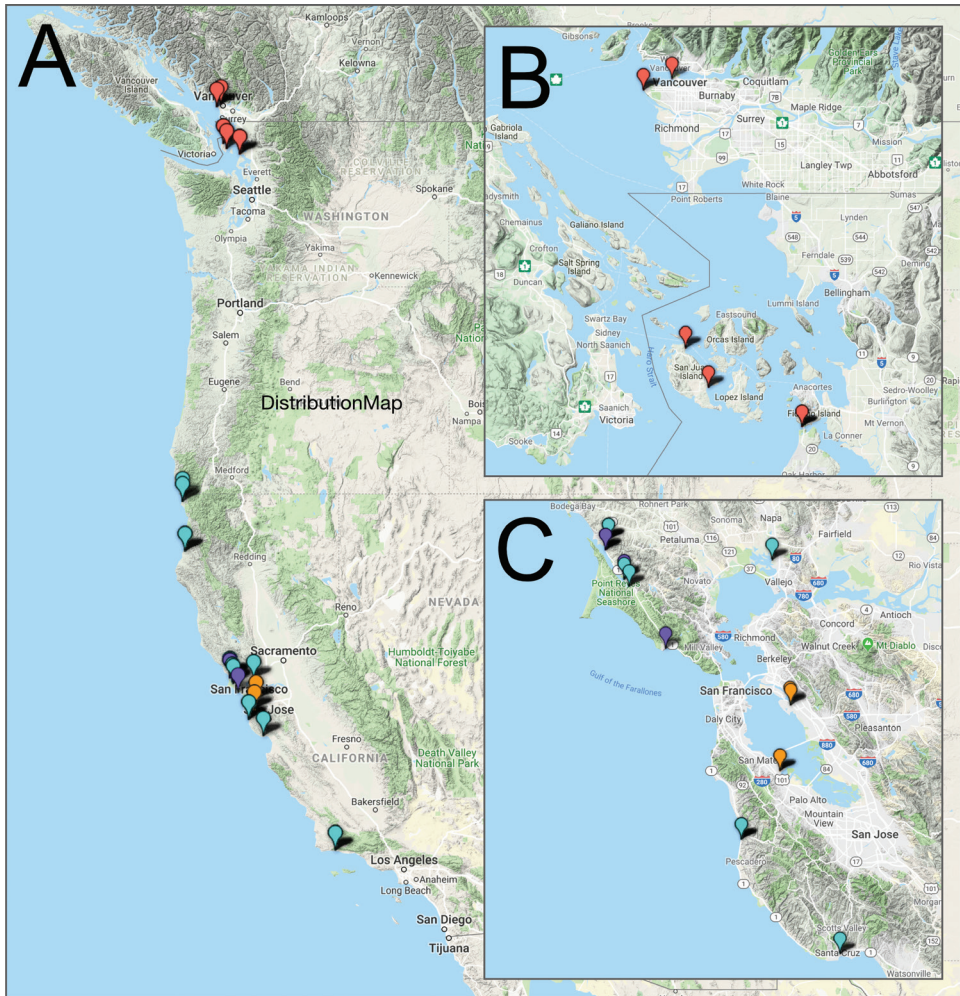


Figure 10. **A** West Coast distribution of *Gnorimosphaeroma* for which genetic material was available. Red = *G. oregonense*, light blue = *G. noblei*, purple = *G. rayi*, orange = *Gnorimosphaeroma* sp. **B** *Gnorimosphaeroma oregonense* distribution in Puget Sound for which genetic material was available **C** *Gnorimosphaeroma noblei*, *G. rayi*, and *Gnorimosphaeroma* sp. Distribution in San Francisco Bay region.

22 m, on rocks, under rocks, less often on sand, and sometimes in empty shipworm tubes. Kussakin remarked it is a good swimmer, and sometimes turns up in night light samples. It can tolerate salinities as low as 9‰. Since we were not able to re-examine Kussakin's specimens, we cannot verify that the *Gnorimosphaeroma* he identified are the same species as *G. oregonense* from the type locality and described here. Furthermore, our genetic data clearly distinguishes between fully marine and low salinity specimens and recognizes these as distinct species (see below). We do not include Kussakin's specimens in the synonymy (*Gnorimosphaeroma oregonense*: Kussakin, 1979: 406, figs 260–262.)

Molecular analysis

The molecular analyses include *G. oregonense* from Vancouver and the San Juan Islands, Washington (49.256°N–48.513°N). There are no specimens north of Vancouver in our collections. *Gnorimosphaeroma noblei* material came from Del Norte to Santa Barbara Counties (40.833°N–34.46°N), *G. rayi* from Marin County (38.201°N–37.902°N), and the unidentified *Gnorimosphaeroma* sp. were collected only in San Francisco Bay (San Mateo and Alameda Counties, latitude 37.079°N–37.535°N). Figure 10 indicates the localities of the sequenced material. Alignment differences resulting from the LINS, EINS, or GINS alignment algorithms had insignificant effect on RAxML and Fasttree analyses and the phylogenetic hypotheses. *Ancinus* sp. (Sphaeromatoidea: Ancinidae) was used as the outgroup based on the basal position of *Gnorimosphaeroma* within the Sphaeromatidae (Wetzer et al. 2013). Both analyses resulted in the same 1 tree. Only the RAxML tree (Fig. 11) is shown.

Our molecular analyses (Fig. 11) clearly distinguish *G. oregonense* and *G. noblei*. They are always sister taxa. *Gnorimosphaeroma rayi*, is always sister to an unidentified *Gnorimosphaeroma* species collected from the two localities in San Francisco Bay.

***Gnorimosphaeroma noblei* Menzies, 1954**

Gnorimosphaeroma noblei Menzies, 1954 was described from the town of Marshall in Tomales Bay, California (~38.162°N, ~122.89°W). Hoestlandt (1969) synonymized *G. oregonense lutea* with *G. noblei*. Menzies noted the species was associated with the terrestrial isopod *Armadilloniscus* in the upper intertidal, and that they were excellent swimmers. This association indicates likely freshwater input and possible lower salinity. This species has the largest range of all of the *Gnorimosphaeroma* species studied here (California, Del Norte County, ~41.931°N to Los Angeles County, 33.802°N). This species also has the broadest salinity tolerance – brackish to freshwater, a characteristic found in only a few sphaeromatid genera. *Gnorimosphaeroma noblei* has been collected from a full range of high intertidal, brackish to fully freshwater habitats including Sacramento, central San Joachin Delta, ~38.33°N, ~121.3°W collections by Wayne Fields. Fields' specimens were preserved in formalin and their collection date is unknown. They have been in the LACM collections since before 2003. Specimens of *G. noblei* can be comparable in size to *G. oregonense*, but more commonly are slightly smaller. *Gnorimosphaeroma noblei* is purported to occur as far south as Los Angeles County, Dominguez Channel, 33.802°N, 118.228°W. Three very small specimens from 4 m depth were collected 17 September 2003 (MBPC 10592, Collection ID: RW17.028). These were also preserved in formalin and were unavailable for genetic analysis, but based on all of the other material examined (Table 2) are presumed to be *G. noblei*.

Their very similar appearance to *G. oregonense* makes morphological identifications ambiguous, yet genetically they are easy to distinguish from *G. oregonense* (Figs 11–13, 15). Sequence divergence between the two species for the 16SrDNA fragment sequenced here is 16.5–20.9%. *Gnorimosphaeroma noblei* is always the sister taxon to *G. oregonense* in all of our genetic analyses (Fig. 11; Wetzer et al. 2018).

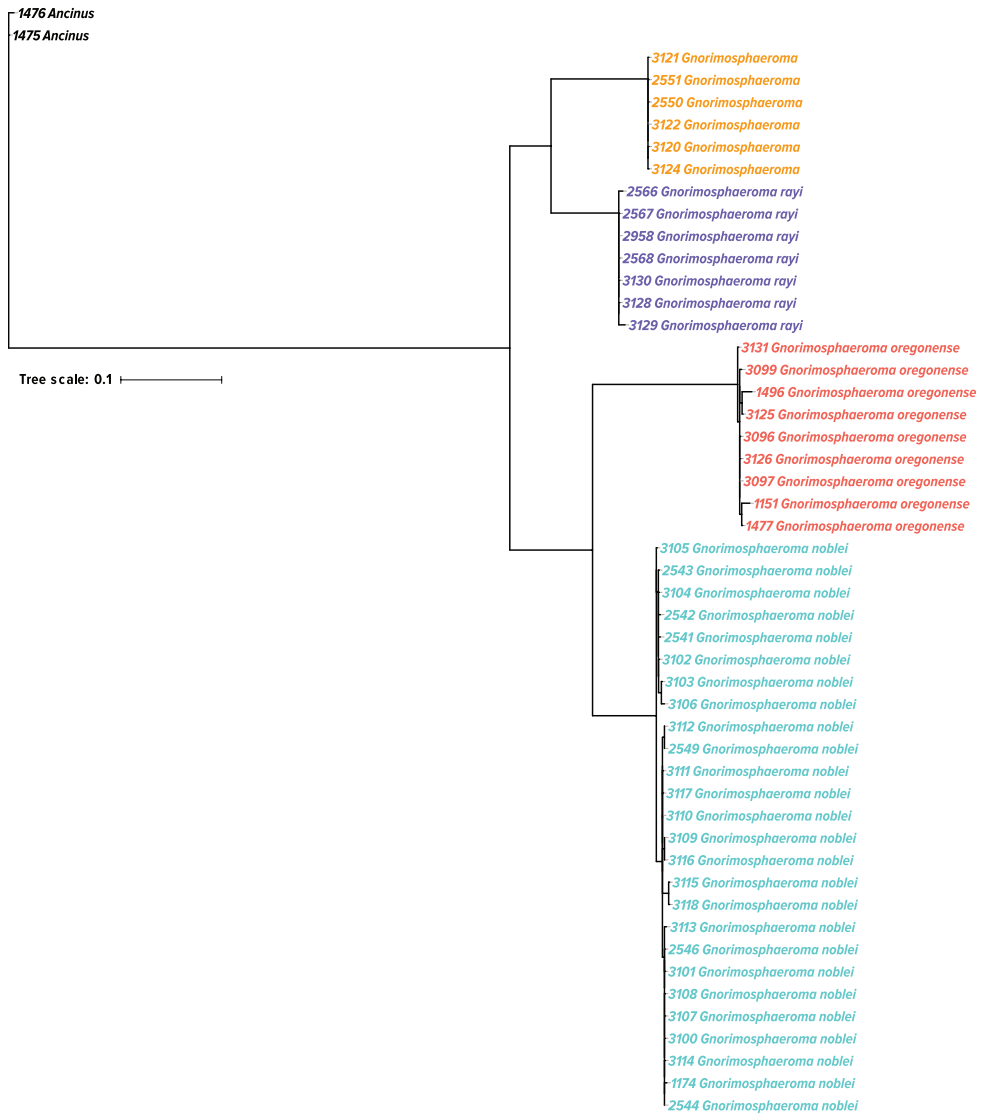


Figure 11. *Gnorimosphaeroma* 16SrDNA phylogeny based on maximum likelihood and 54 sequences. *Gnorimosphaeroma oregonense* (6 localities), *G. noblei* (11 localities), *G. rayi* (4 localities), and 2 localities within San Francisco Bay for the unidentified *Gnorimosphaeroma* sp. Red = *G. oregonense*, light blue = *G. noblei*, purple = *G. rayi*, orange = *Gnorimosphaeroma* sp. (same color coding as in Fig. 10).

Gnorimosphaeroma rayi Hoestlandt, 1969

Gnorimosphaeroma rayi arrived in Tomales Bay in 1928 with oysters (*Crassostrea gigas* now accepted as *Magallana gigas* (Thunberg, 1793) from Japan (Bonnot 1935; Barrett 1963; James Carlton pers. comm. 2019). The type locality for this species is California, Marin County, Tomales Bay, Shallow Beach, 38.14°N, 122.881°W (Hoestlandt 1969). In addition to Japan, Hoestlandt (1975, 1977) reported this species from eastern

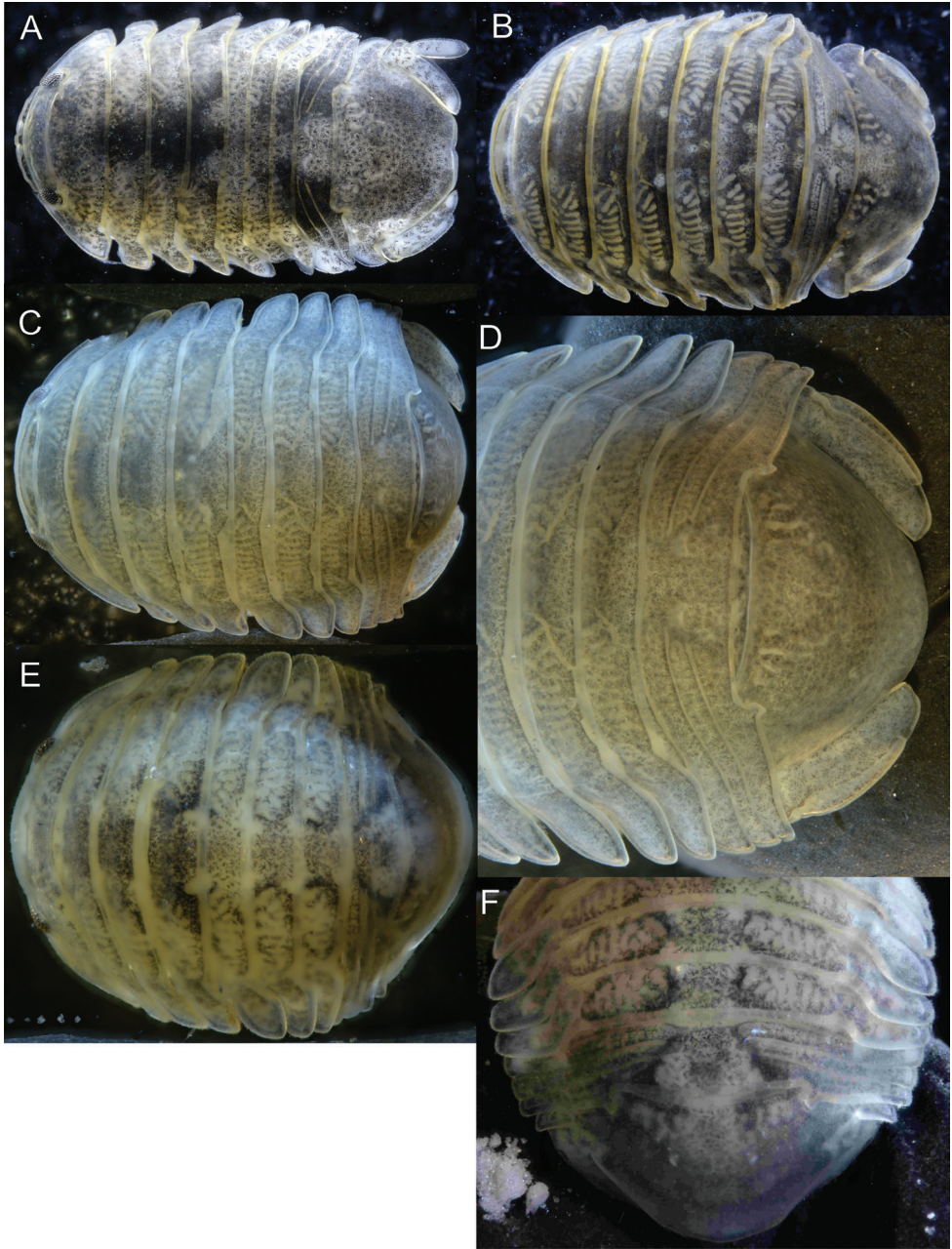


Figure 12. ♂ *Gnorimosphaeroma* spp. Dorsal **A** *Gnorimosphaeroma noblei* LACM:DISCO:220 **B** *Gnorimosphaeroma oregonense* LACM:DISCO:11161 **C** *Gnorimosphaeroma rayi* LACM:DISCO:2707 anterior end **D** *Gnorimosphaeroma rayi* posterior LACM:DISCO:2707 **E** LACM:DISCO:232 *Gnorimosphaeroma* sp. anterior **F** LACM:DISCO:232 *Gnorimosphaeroma* sp. posterior.

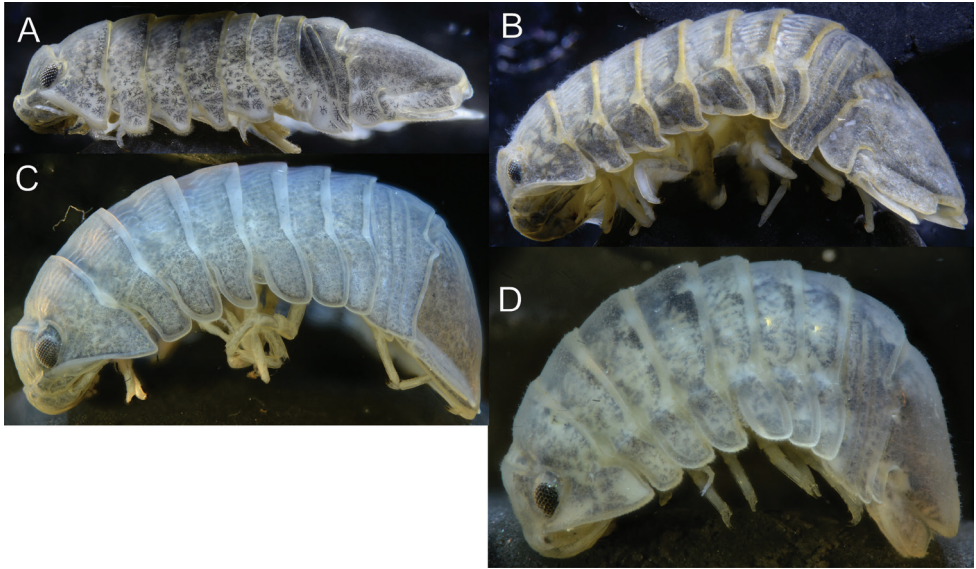


Figure 13. ♂ *Gnorimosphaeroma* spp. Lateral view **A** *Gnorimosphaeroma noblei* LACM:DISCO:220 **B** *Gnorimosphaeroma oregonense* LACM:DISCO:11161 **C** *Gnorimosphaeroma rayi* LACM:DISCO:2707 **D** LACM:DISCO:232 *Gnorimosphaeroma* sp.

Siberia and Hawaii. Hoestlandt too acknowledged the differences between *G. rayi* and *G. oregonense* are subtle. Hoestlandt's (1975) key attempts to disambiguate the four species (*G. oregonense*, *G. noblei*, *G. rayi*, and *G. insulare*). However, we urge caution as his key may only be applicable to the largest specimens of each species, and we were unable to use it consistently.

Based on all of the material in the LACM collections available for genetic analysis, we could only confirm that the species occurs in Tomales Bay (three lots) and one lot from Bolinas Beach. Bolinas Beach is just 43.5 km south of Tomales Bay (Fig. 11, Table 1). It does not appear that this species is broadly distributed or quickly expanding its range (Figs 11–13, 15). A further assessment of its distribution awaits future genetically appropriately collected material and analyses. Additionally, we recognized a previously unidentified *Gnorimosphaeroma* sp. in San Francisco Bay. Genetically *Gnorimosphaeroma* sp. and *G. rayi* are readily distinguished and are always sister taxa in our analyses. However, we were unable to identify any reliable morphological characters to distinguish the two species. Based on the phylogenetic relationship between *Gnorimosphaeroma* sp. to *G. rayi*, it is presumed it too has a western Pacific origin.

***Gnorimosphaeroma* sp.**

Morphologically this species cannot be distinguished from *G. rayi*. However, it is clearly genetically distinct with 13.9–16.5% sequence divergence for the 16S-rDNA

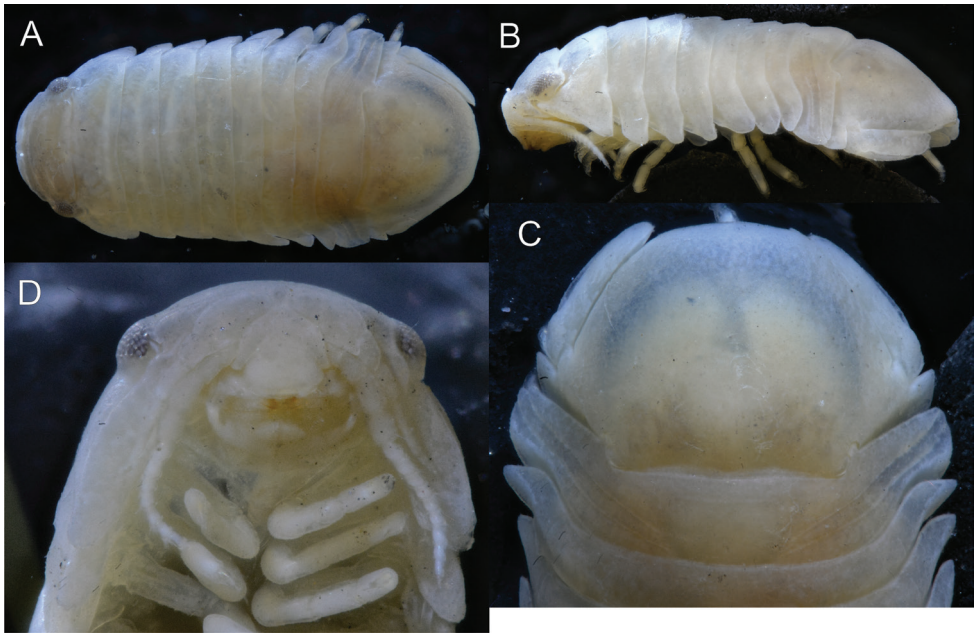


Figure 14. *Gnorimosphaeroma insulare*. Paratype. Male LACM:DISCO:6963 **A** dorsal **B** lateral **C** clypeus and labrum **D** pleotelson dorsal.

fragment that was sequenced. Since we know *G. rayi* is an introduction from the western Pacific, this species is also likely a trans-Pacific traveler. San Francisco Bay, a biodiversity hotspot, is infamous for non-native and invasive species. At this time, there are no sequences available for western Pacific *Gnorimosphaeroma* that would allow identification of this species and clarification of their relationships (Figs 11–13). Many western Pacific species are poorly described and in need of redescription, making it impossible at this time to identify these specimens further.

***Gnorimosphaeroma insulare* (Van Name, 1940)**

Gnorimosphaeroma insulare was described from freshwater on San Nicolas Island. San Nicolas is part of the Channel Island Archipelago off the Southern California Coast, today located nearly 100 km from the nearest point on the mainland coast. Menzies' (1954) redescription detailed the *G. oregonense* distribution and compared *G. oregonense* to Van Name's (1940) *Exosphaeroma insulare*, which Menzies moved to *Gnorimosphaeroma*. Menzies (1954) noted that the largest *G. insulare* is 8 mm in length. Some confusion then ensues with the description of *G. noblei* Menzies, 1954. *Gnorimosphaeroma noblei* is described from Tomales Bay from the high intertidal found in association with *Armadilloniscus*, hence associated with possible freshwater input and thus lower salinity. To the best of our knowledge, the only material of *G. insulare* is that from the original collections and type locality on San Nicolas Island.

Eleven specimens were collected from freshwater where they were associated with the freshwater gastropod pulmonate, *Physa virgata* (Gould, 1855). The LACM collections hold a single male syntype which is photographed here (Fig. 14). Additional specimens are at the American Museum of Natural History. The specific collecting locality on San Nicolas is not known and it is unclear if any freshwater still runs today. Accessing this US Navy-controlled island, which is used for weapons testing and training, is difficult.

Key

- 1 Body length 2 × width. Body widest at pereonite 7 and anterior portion of pleon (Fig. 14A). Known only from a freshwater pond on San Nicolas Island.....*Gnorimosphaeroma insulare*
- Body more than 2 × width. Body widest at pereonite 6 or pereonites 2–7 similar in width **2**
- 2 In lateral view, pereonite coxal plates 2, 3, and 4 anterior margins raised, posterior margin not raised, giving coxae a somewhat “s-shaped” appearance (Fig. 15A, C). Species is fully marine *Gnorimosphaeroma oregonense*
- In lateral view, pereonite coxal plates 2, 3, and 4 anterior margins not raised. Species may occur in marine, brackish, or freshwater **3**
- 3 Pereonites 1–4 coxal plates margins with setose fringe (Fig. 15B). Posterior pleotelson margin with slight indentation (Fig. 12A). Species occurs in brackish or freshwater.....*Gnorimosphaeroma noblei*
- Pereonites 1–4 without setose fringe on coxal plate margins. Posterior pleotelson margin without indentation (Fig. 12D, F). Species are fully marine..... **4**
- 4 Pleonites lateral margins acute. Pleon lateral anterior margin smooth, without ornamentation (Fig. 12D) *Gnorimosphaeroma rayi*
- Pleonites lateral margins rounded. Pleonal lateral anterior margin with short acute lobe (Fig. 12F) *Gnorimosphaeroma* sp.

Discussion

The genus *Gnorimosphaeroma* is a temperate-water clade occurring only on the shores of the northwestern Pacific (China, Japan), east through Alaska, and along the East Pacific coast to southern California shores. The genus is most speciose in the north western Pacific with 26 described species. Many of these species descriptions are inadequate, in need of critical evaluation, and redescription. In the eastern Pacific, *G. oregonense* is the most wide-ranging species, apparently occurring from Alaska to San Francisco, California. However, in this study we were only able to verify morphologically and genetically the species occurrences from Vancouver to San Francisco Bay. Adult specimens of *G. oregonense* become larger and more robust with increasing latitude. Along the Washington to California coast this species commonly co-occurs with *Exosphaeroma inornata* Dow, 1958. The latter is known from Puget Sound, Washington to

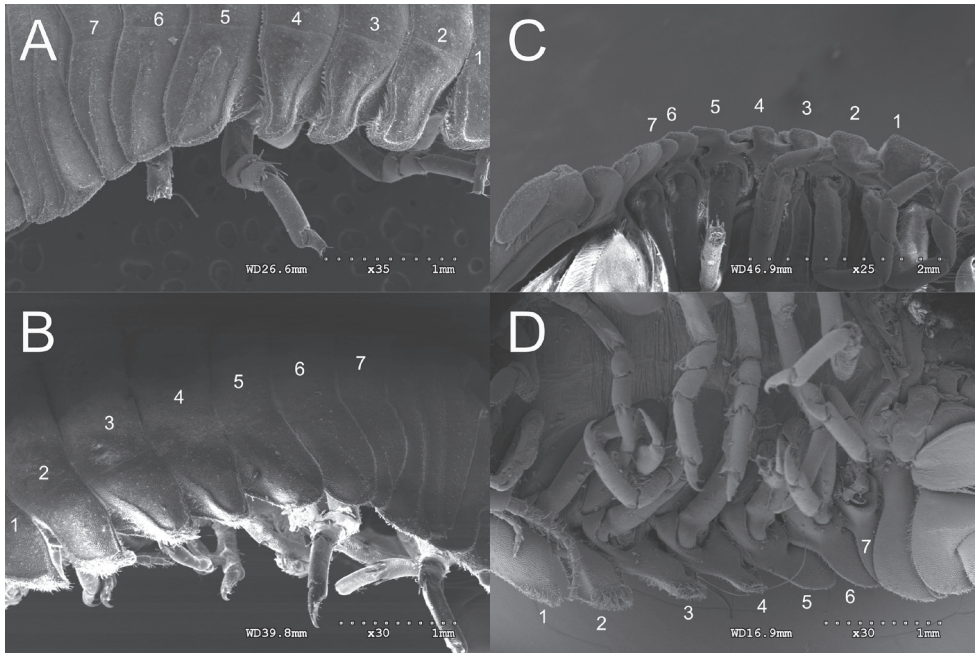


Figure 15. SEM comparison of *G. oregonense* LACM:DISCO:11164 and *G. noblei* LACM:DISCO:11168 coxae **A** *G. oregonense* lateral **B** *G. noblei* lateral **C** *G. oregonense* ventral, and **D** *G. noblei* ventral.

central-southern Baja California Norte, Mexico (Wall et al. 2015). When specimens are very small and/or subadults, not only do the species of *Gnorimosphaeroma* get readily confused, but sometimes they are misidentified as *E. inornata* if the most careful attention is not paid. Any distinctive color patterns are lost in preserved material.

However, we have demonstrated that regardless of their size, species of *Gnorimosphaeroma* and *Exosphaeroma inornata* are readily distinguished based on their genetics (Wetzer et al. 2018). For both molecular analyses and morphological study, we had a very restricted distribution of *G. oregonense* specimens available. Kussakin 1979 had similarly struggled with resolving the identity of Northern Pacific *Gnorimosphaeroma*. He recognized that the genus contains fully freshwater, brackish, and marine species. *Gnorimosphaeroma kurilense* (Gurjanova, 1933) occurs in freshwater. It would be informative to be able to compare genetic sequences of our material with specimens from north of Vancouver, British Columbia to Alaska, fully marine to freshwater, and verify that the specimens observed and figured by Kussakin and others are genetically similar. Kussakin's specimen(s) were from Popov Island, Primorsky Krai, near Vladivostok northwestern Pacific. The dorsal view (fig. 260, pg. 407) does look very similar to the *G. oregonense* from the eastern Pacific. It possesses the same distinctive rather heavily calcified coxal plates with strong carinae on coxae 2, 3, 5, and 6. Coxa 1 is acute, coxa 2 is subquadrate, with coxae 3–7 becoming more acute posteriorly. Kussakin's figures (fig. 262) differ from our specimens in that antenna 1 has 15 flagellar articles

and antenna 2 has ten flagellar articles compared to most of the specimens which we observed, which have 13 and 14, respectively. Also, the mandible of the Kussakin specimen has three long setae at the base of the molar incisor. Our specimens lack such setae (Fig. 4C, D). Pereopod 1 of the Popov specimen (fig. 261) appears more setose than the Washington specimen (Fig. 5A).

Since we only had specimens of *G. oregonense* available from a restricted range of Vancouver to Washington, we cannot assess the genetic diversity across the species' larger range (Figs 10, 11). Our *Exosphaeroma amplicauda* (Wall et al. 2015) review resulted in the recognition of five species with Alaska and Washington specimens recognized as distinct from the type locality (Central California), and distinct from those from the Southern California coast. It would not be surprising if future studies based on broader sampling revealed greater genetic diversity than we have observed here.

We also had available for study a single male syntype of *G. insulare* Van Name, 1940 (Fig. 14). As noted previously by Van Name, *G. insulare* and *G. oregonense* are very similar. Examination of the specimens we had available, dorsally *G. insulare* appears oblong and is ca. twice as long as wide compared to *G. oregonense*, *G. noblei*, *G. rayi*, and the unidentified *Gnorimosphaeroma* sp. from San Francisco Bay. These species are all broader than *G. insulare* and therefore have a more globular appearance. The largest *G. insulare* specimen observed was 8 mm in length, whereas the largest known individuals of *G. oregonense*, *G. noblei*, and *G. rayi* had been previously recorded as 12 mm in length. *Gnorimosphaeroma insulare* is distinguished from all other *Gnorimosphaeroma* species in that it appears to have been entirely restricted to a freshwater pond and only known from the type locality. It is unknown whether this pond still exists today. Since it is the sole specimen (syntype) and fragile, no dissections were undertaken, but rather the specimen was photographed (Fig. 14). A collection made on San Miguel Island by E. Hochberg and identified by E.W. Iverson was reidentified here as *G. noblei*. Sadly, no habitat information was provided for this collection and it had been formalin fixed and is not available for genetic study. San Miguel Island is the northernmost of the Channel Islands and 74 miles distant from San Nicolas Island. The only specimens known from offshore islands were these two lots.

Future genetic comparisons of marine, brackish, and freshwater *Gnorimosphaeroma* species occurring north of Vancouver, through Alaska to Primorsky Krai (north-west Pacific) may reveal either multiple invasions or a single invasion to brackish and freshwater and may change the current phylogenetic relationship of brackish/freshwater species and marine species in the Eastern Pacific. Phylogenetic placement of *G. insulare* would also be most interesting should populations at this locality still exist today.

Identification keys for west coast *Gnorimosphaeroma* species are available in Menzies (1954) and Hoestlandt (1975, 1977). Kussakin (1979) provides a key for north Pacific species, Kwon and Kim (1987) for Korean species, and Nunomura (1998) for the Japanese species. Difficulty arises in using them as differences between species can be very subtle and may only apply to very large adult specimens. In some instances, the largest specimens possible for the species may not have been available at the time

of description (e.g., *G. noblei* Hoeslandt, 1975). However, the differences in the lateral and ventral appearance of the coxal plates of *G. oregonense* and *G. noblei* are distinct in large adult males and females (Figs 13A, B, 15). In *G. oregonense* lateral view the anterior margins of coxal plates 2, 3, and 4 are raised, posterior margin not raised, giving coxae a somewhat “s-shaped” appearance (Fig. 15A, C). Ventrally these appear as interlocking units. *Gnorimosphaeroma noblei* which can co-occur with *G. oregonense* lacks these (ventrally coxae not interlocking) (Fig. 15B, D). The two species are also readily distinguished based on habitat and salinity. *Gnorimosphaeroma oregonense* is always in fully marine waters and *G. noblei* inhabits high intertidal, brackish to fully freshwaters.

As molecular phylogenetic studies allow more and deeper sampling, cryptic species in marine environments are being recognized with ever greater frequency. Organisms as diverse as foraminiferans (Aurahs et al. 2009), copepods (Bláha et al. 2010), hydroids (Moura et al. 2008), and valviferan isopods (Xavier et al. 2012) are revealing much greater diversity than previously recognized. This diversity is and cannot always be recognized morphologically. The recent detailed study of the sphaeromatid isopod *Dynamene* by Vieira et al. (2019) demonstrated that not only can large sequence divergences exist over small spatial scales, but that repeated invasions leave their genetic mark on populations, and that population diversification can be recognized over shorter time scales than previously thought for organisms with limited dispersal abilities. Based on the putative cryptic species in their study, they estimate a 300% under-estimation of known species in *Dynamene*, a species-poor genus. As more *Gnorimosphaeroma* species and specimens for genetic analysis become available, this genus has the potential to provide interesting insights into not only the evolution of the rare marine to freshwater invasion of species within the genus, but also human induced species relocations across the Pacific Ocean. If *G. insulare* still exists on San Nicolas Island and possibly on other Channel Islands too, this genus could reveal a very interesting phylo-biogeographic history.

Acknowledgements

We thank Camm Swift and Todd Haney for their invaluable specimen contributions and careful locality annotations. Additionally, this review benefited from specimen donations made by Don Cadien and Ernie Iverson and input from James Carlton. The authors acknowledge the gracious support of the NHM Marine Biodiversity Center infrastructure from colleagues Kathy Omura and Jenessa Wall. Dean Pentcheff is thanked for field support, help with maps, tree figures, and all-round technical support. Jessica Carrillo is credited for preparing the stacked photographs. Tammy Horton is thanked for her meticulous editing, and an anonymous reviewer is acknowledged for their thoughtful comments. This is Contribution Number 5 of the NHM Diversity Initiative of the Southern California Ocean (DISCO) and NWU-Water Research Group Contribution Number 516.

References

- Aurahs R, Grimm GW, Hemleben V, Hemleben C, Kucera M (2009) Geographic distribution of cryptic genetic types in the planktonic foraminifer *Globigerinoides ruber*. *Molecular Ecology* 18: 1692–1705. <https://doi.org/10.1111/j.1365-294X.2009.04136.x>
- Baker WH (1926) Species of the isopod family Sphaeromidae, from the eastern, southern, and western coasts of Australia. *Transactions of the Royal Society of South Australia* 50: 247–279.
- Barrett EM (1963) The California oyster industry. California Department of Fish and Game, Fish Bulletin 123: 1–103.
- Bláha M, Hulák, M, Slouková J, Těšitel J (2010) Molecular and morphological patterns across *Acanthocyclops vernalis-robustus* species complex (Copepoda, Cyclopoida). *Zoologica Scripta* 39(3): 259–268. <https://doi.org/10.1111/j.1463-6409.2010.00422.x>
- Bonnot P (1935) A recent introduction of exotic species of molluscs into California water from Japan. *Nautilus* 49: 1–2.
- Bosc LAG (1802) Histoire naturelle des Crustacés, contenant leur description et leurs moeurs, avec figures dessinées d'après nature (Vol. 2). Deterville, Paris, 296 pp. [pls 9–18] <https://doi.org/10.5962/bhl.title.39831>
- Boyko CB, Bruce NL, Hadfield KA, Merrin KL, Ota Y, Poore GCB, Taiti S, Schotte M, Wilson GDF [Eds] (2008 onwards) World Marine, Freshwater and Terrestrial Isopod Crustaceans database. *Gnorimosphaeroma oregonense* (Dana, 1853). <http://www.marinespecies.org/aphia.php?p=taxdetails&cid=1264222> [accessed on 03 Oct 2018]
- Bruce NL (1986) Cirolanidae (Crustacea: Isopoda) of Australia. *Records of the Australian Museum Supplement* 6: 1–239. <https://doi.org/10.3853/j.0812-7387.6.1986.98>
- Bruce NL (2003) New genera and species of sphaeromatid isopod crustaceans from Australian marine coastal waters. *Memoirs of Museum Victoria* 60(2): 309–369. <https://doi.org/10.24199/j.mmv.2003.60.28>
- Bruce NL (2004) Reassessment of the isopod crustacean *Aega deshaysiana* (Milne Edwards, 1840) (Cymothoidea: Aegidae) a world-wide complex of 21 species. *Zoological Journal of the Linnean Society* 142: 135–232. <https://doi.org/10.1111/j.1096-3642.2004.00127.x>
- Bruce NL (2009) A new genus and new species of Sphaeromatidae (Crustacea: Isopoda) from the Great Barrier Reef, Australia. *Memoirs of Museum Victoria* 66: 35–42. <https://doi.org/10.24199/j.mmv.2009.66.5>
- Brusca RC, Coelho VR, Taiti S (2007) Isopoda. In: Carlton JT (Ed.) *The Light and Smith Manual: Intertidal Invertebrates from Central California to Oregon* (4th edn.). University of California Press Berkeley, California, 503–542.
- Dana JD (1852) Crustacea. Part I. United States Exploring Expedition. During the years 1838, 1839, 1840, 1841, 1842. Under the command of Charles Wilkes, U.S.N. Sherman, Philadelphia 13: 1–685. <https://doi.org/10.5962/bhl.title.61409>
- Dana JD (1853) Crustacea. Part II. In: United States Exploring Expedition. During the years 1838, 1839, 1840, 1841, 1842. Under the command of Charles Wilkes. U.S.N.C. Sherman, Philadelphia 14: 689–1618.
- Dow TG (1958) Description of a new isopod from California, *Exosphaeroma inornata*. *Bulletin of the Southern California Academy of Sciences* 57(2): 93–97.

- Espinosa-Pérez MC, Hendrickx ME (2001) A new species of *Exosphaeroma* Stebbing (Crustacea: Isopoda: Sphaeromatidae) from the Pacific coast of Mexico. *Proceedings of the Biological Society of Washington* 114(3): 640–648.
- Fee AR (1926) The Isopoda of Departure Bay and vicinity, with descriptions of new species, variations and colour notes. *Contributions to Canadian Biology and Fisheries* 3(2): 13–47. <https://doi.org/10.1139/f26-002>
- Gurjanova EF (1933) Contributions to the Isopoda fauna of the Pacific Ocean. I. New species Valvifera and Flabellifera. *Gosudarstvennyi Gidrologicheskii Institut, Isseldovaniya Morei SSSR* 17: 87–106.
- Hanable WS (2003) USS *Peacock* wrecks at the mouth of the Columbia River, giving her name to Peacock Spit, on July 18, 1841. <http://www.historylink.org/File/5624>
- Harrison K, Ellis JP (1991) The genera of the Sphaeromatidae (Crustacea: Isopoda): a key and distribution list. *Invertebrate Taxonomy* 5: 915–952. <https://doi.org/10.1071/IT9910915>
- Hoestlandt H (1969) Sur un Sphérome nouveau de la côte pacifique américaine, *Gnorimosphaeroma rayi* n. sp. (Isopode Flabellifère). *Comptes rendus hebdomadaires des séances de l'Académie des sciences, série D* 268: 325–327.
- Hoestlandt H (1975) Occurrences of the Isopoda Flabellifera *Gnorimosphaeroma rayi* Hoestlandt on the coast of Japan, eastern Siberia and Hawaii, with a brief note on its genetic polychromatism. *Publications of the Seto Marine Biological Laboratory* 22(1/4): 31–46. <https://doi.org/10.5134/175891>
- Hoestlandt H (1977) Description complémentaire de l'isopode flabellifère *Gnorimosphaeroma insulare* Van Name et synonymie de *G. luteum* avec cette espèce. *Crustaceana* 32(1): 45–54. <https://doi.org/10.1163/156854077X00863>
- Jang IK, Kwon DH (1993) A new species of the genus *Gnorimosphaeroma* (Crustacea, Isopoda, Sphaeromatidae) from a brackish-water lake in Korea. *Korean Journal of Zoology* 36(3): 402–407.
- Katoh K, Kuma K, Toh H, Miyata T (2005) MAFFT version 5: improvement in accuracy of multiple sequence alignment. *Nucleic Acids Research* 33: 511–518. <https://doi.org/10.1093/nar/gki198>
- Katoh K, Misawa K, Kuma K, Miyata T (2002) MAFFT: a novel method for rapid multiple sequence alignment based on fast Fourier transform. *Nuclei Acids Research* 30: 3059–3066. <https://doi.org/10.1093/nar/gkf436>
- Kensley B (1978) *Guide to the Marine Isopods of Southern Africa*. Trustees of the South African Museum, Cape Town, 173 pp.
- Kim HS, Kwon DH (1988) Marine isopod crustaceans from Cheju Island, Korea. *Inje Journal* 4: 195–220.
- Kussakin OG (1974) Fauna and Ecology of isopods (Crustacea) from the intertidal zone of the Kurile Islands. *Transactions of the Academy of Science of the USSR, Far East Center, Institute of Marine Biology* 1: 227–275.
- Kussakin OG (1979) Marine and brackish-water Isopoda of cold and temperate (boreal) waters of the Northern Hemisphere. Part 1. Flabellifera, Valvifera, and Tyloidea. *National Academy of Sciences, USSR, Zoology [Opredeliteli po Faune SSR, Akademiya Nauk, SSSR]* 122: 1–470.
- Kwon DH, Kim HS (1985) The systematic study of the family Sphaeromatidae (Crustacea, Isopoda, Flabellifera) from Korea. *Inje Journal* 1(2): 143–165.

- Kwon DH, Kim HS (1987) A new species of the genus *Gnorimosphaeroma* (Crustacea, Isopoda, Sphaeromatidae) from the Naktong River, with a key to the Korean species of the genus. *The Korean Journal of Systematic Zoology* 3: 51–56.
- Menzies RJ (1954) A review of the systematics and ecology of the genus “*Exosphaeroma*,” with the description of a new genus, a new species, and new subspecies (Crustacea, Isopoda, Sphaeromatidae). *American Novitates* 1683: 1–24.
- Miller MA, Pfeiffer W, Schwartz T (2010) Creating the CIPRES Science Gateway for inference of large phylogenetic trees. In: *Proceedings of the Gateway Computing Environments Workshop (GCE)*, 14 Nov. 2010, New Orleans, Louisiana, 8 pp. <https://doi.org/10.1109/GCE.2010.5676129>
- Monod T (1931) Tanaidacés et Isopodes subantarctique de la collection Kohl-Larsen du Senckenberg Museum. *Senckenbergiana* 13(1): 10–30.
- Moura C, Harris DJ, Cunha MR, Rogers AD (2008) DNA barcoding reveals cryptic diversity in marine hydroids (Cnidaria, Hydrozoa) from coastal and deep-sea environments. *Zoological Scripta* 37: 93–108.
- Nunomura N (1988) Description of *Nishimuraia paradoxa* gen. et sp. nov., and the first record of the genus *Paracerceis* in Japan (Isopoda, Sphaeromatidae). *Bulletin of the Toyama Science Museum* 12: 1–7.
- Nunomura N (1998) On the genus *Gnorimosphaeroma* (Crustacea, Isopoda, Sphaeromatidae) in Japan with descriptions of six new species. *Bulletin of the Toyama Science Museum* 21: 23–54.
- Nunomura N (1999a) A new species of the genus *Gnorimosphaeroma* (Isopoda, Sphaeromatidae) from the mouth of Tonda River, Kii Peninsula, southern Japan. *Bulletin of the Toyama Science Museum* 22: 1–5.
- Nunomura N (1999b) Sea shore isopod crustaceans from Izu Islands, Middle Japan. *Bulletin of the Toyama Science Museum* 22: 7–38.
- Nunomura N (2005) Sea shore isopod crustaceans from Bonin Islands. *Bulletin of the Toyama Science Museum* 314: 33–57.
- Nunomura N (2007) A new species of *Gnorimosphaeroma* (Crustacea: Isopoda) from a freshwater stream of Izu Peninsula, middle Japan. *Bulletin of the Toyama Science Museum* 30: 37–42.
- Nunomura N (2011) A new species of the genus *Gnorimosphaeroma* (Crustacea: Isopoda: Sphaeromatidae) from brackish waters in Nagasaki, western Japan. *Bulletin of the Toyama Science Museum* 34: 61–65.
- Nunomura N (2013) Isopod crustaceans from Shikoku, western Japan – 1, specimens from Ehime Prefecture. *Contributions from the Toyama Science Museum* 446: 19–78.
- Nunomura N, Satake K (2006) A new species of the genus *Gnorimosphaeroma* (Crustacea, Isopoda) from Hahajima, Bonin Islands, southern Japan. *Contributions from Toyama Science Museum No. 320*. Palumbi SR, Martin A, Romano S, McMillan WO, Stice L, Grabowski G (1991) *The Simple Fool’s Guide to PCR*, version 2. University of Hawaii, Honolulu, Hawaii, Department of Zoology and Kewalo Marine Laboratory, 43 pp.
- Poore GCB, LewTon HM (1993) Idoteidae of Australia and New Zealand (Crustacea: Isopoda: Valvifera). *Invertebrate Taxonomy* 7: 197–278. <https://doi.org/10.1071/IT9930197>
- Sket B, Bruce NL (2004) Sphaeromatids (Isopoda, Sphaeromatidae) from New Zealand fresh and hypogean waters, with description of *Bilistra* n. gen. and three new species. *Crustaceana* 76[for 2003](11): 1347–1370. <https://doi.org/10.1163/156854003323009858>

- Stebbing TRR (1900) Arctic Crustacea: Bruce collection. The Annals and Magazine of Natural History, series 7 5: 1–16. <https://doi.org/10.1080/00222930008678236>
- Tattersall WM (1921) Mysidacea, Tanaidacea, and Isopoda. Pt. 7. In: Zoological Results of a Tour in the Far East. Memoires of the Asiatic Society of Bengal 6: 403–443. Van Name WG (1940) A supplement to the American land and fresh-water isopod Crustacea. Bulletin of the American Museum of Natural History 77: 109–142.
- Verhoeff KW (1943) Zur Morphologie, Oekologie und Systematik von *Sphaeroma*, *Eurosphaera* und *Jaera*. Zeitschrift für Morphologie und Oekologie der Tiere 40(2): 276–290. <https://doi.org/10.1007/BF00421684>
- Vieira PE, Desiderato A, Holdich DM, Soares P, Creer S, Carvalho GR, Costa FO, Queiroga H (2019) Deep segregation in the open ocean: Macaronesia as an evolutionary hotspot for low dispersal marine invertebrates. Molecular Ecology 1–17. <https://doi.org/10.1111/mec.15052>
- Wall AR, Bruce NL, Wetzer R (2015) Status of *Exosphaeroma amplicauda* (Stimpson, 1857), *E. aphrodita* (Boone, 1923) and description of three new species (Crustacea, Isopoda, Sphaeromatidae) from the north-eastern Pacific. ZooKeys 504: 11–58. <https://doi.org/10.3897/zookeys.504.8049>
- Watling L (1989) A classification system for crustacean setae based on the homology concept. In: Felgenhauer B, Watling L, Thistle AB (Eds) Functional Morphology of Feeding and Grooming in Crustacea. [Schram FR (series Ed.) Crustacean Issues] A.A. Balkema, Rotterdam, 6: 15–26. <https://doi.org/10.1201/9781003079354-2>
- Wetzer R (2015) Collecting and preserving marine and freshwater Isopoda (Crustacea: Peracarida). Biodiversity Data Journal 3: e4912. <https://doi.org/10.3897/BDJ.3.e4912>
- Wetzer R, Pérez-Losada M, Bruce NL (2013) Phylogenetic relationships of the family Sphaeromatidae Latreille, 1825 (Crustacea: Peracarida: Isopoda) within Sphaeromatidea based on 18S-rDNA molecular data. Zootaxa 3599: 161–177. <https://doi.org/10.11646/zootaxa.3599.2>
- Wetzer R, Bruce NL, Pérez-Losada M (2018) Relationships of the Sphaeromatidae genera (Peracarida: Isopoda) based on 18SrDNA and 16SrDNA genes. Arthropod Systematics and Phylogeny 76: 1–30. https://figshare.com/authors/Regina_Wetzer/5346782
- Xavier R, Santos AM, Harris DJ, Sezgin M, Machado M, Branco M (2012) Phylogenetic analysis of the north-east Atlantic and Mediterranean species of the genus *Stenosoma* (Isopoda, Valvifera, Idoteidae). Zoological Scripta 41: 386–399. <https://doi.org/10.1111/j.1463-6409.2012.00537.x>

Three new species of the primitively segmented spider genus *Songthela* (Araneae, Mesothelae) from Guizhou Province, China

Zhaoyang Chen¹, Dengqing Li¹, Daiqin Li², Xin Xu¹

1 College of Life Sciences, Hunan Normal University, Changsha 410081, Hunan Province, China **2** Department of Biological Sciences, National University of Singapore, 14 Science Drive 4, 117543, Singapore

Corresponding author: Xin Xu (xuxin@hunnu.edu.cn)

Academic editor: Jeremy Miller | Received 8 January 2021 | Accepted 19 April 2021 | Published 13 May 2021

<http://zoobank.org/A5455CAB-4230-4B84-8B83-AC2F10EF34FC>

Citation: Chen Z, Li D, Li D, Xu X (2021) Three new species of the primitively segmented spider genus *Songthela* (Araneae, Mesothelae) from Guizhou Province, China. ZooKeys 1037: 57–71. <https://doi.org/10.3897/zookeys.1037.62916>

Abstract

We diagnose and describe three new species of the primitively segmented spider genus *Songthela* from Guizhou Province, China, based on morphological characters and molecular data: *S. liui* **sp. nov.** (♂♀), *S. tianzhu* **sp. nov.** (♂♀), and *S. yuping* **sp. nov.** (♂♀). We provide the genetic distances within and among the three new species based on the DNA barcode gene, cytochrome c oxidase subunit I (COI) to support our descriptions. We also provide the COI GenBank accession codes for the three new species for future identification.

Keywords

COI, Heptathelinae, Liphistiidae, morphology, taxonomy, trapdoor spiders

Introduction

Liphistiidae is the only living family of the suborder Mesothelae. As the sister lineage to all other extant spiders, it retains several unique plesiomorphies, such as abdominal tergites (Fig. 1D, E, I, M, N) and spinnerets projected from the middle of the ventral abdomen (Haupt 2003; Schwendinger and Ono 2011; Xu et al. 2015a). Liphistiid spiders live in their underground borrow, which is closed by a silk-based trapdoor.

The family contains 142 species belonging to eight genera in two subfamilies, Hepthathelinae and Liphistiinae (World Spider Catalog 2021). Hepthathelinae is confined to East Asia, while Liphistiinae is restricted to Southeast Asia (World Spider Catalog 2021). Liphistiinae contains the single genus *Liphistius* Schiödte, 1849, while Hepthathelinae comprises the other seven genera (Xu et al. 2015a, b, 2021; World Spider Catalog 2021).

The genus *Songthela* includes 16 described species, 15 of which are distributed in southern China, and the remaining species, *S. sapana* (Ono, 2010), is found in northern Vietnam (World Spider Catalog 2021). Out of the 15 species from southern China, only one species, *S. pluma* Yu, Li & Zhang, 2018, is described from Guizhou Province. In this study, we diagnose and describe three new *Songthela* species from Guizhou Province based on both male and female genital morphology. To support our descriptions, we provide estimations of the intraspecific and interspecific genetical distances within and among the three new species as well as the interspecific genetic distances between the new species and other *Songthela* species based on the animal bar-coding gene, cytochrome c oxidase subunit I (COI). For future identification, we also provide the GenBank accession codes of the COI for the three species.

Material and methods

All specimens were collected from Guizhou Province, China (Fig. 2). We took the subadults back to the laboratory and reared them until they reached adulthood. We removed the right four legs of adults, preserved them in 100% ethanol and kept them at -80°C for molecular work. We preserved the remains of each specimen in 80% ethanol for morphological examination. All the type and voucher specimens are deposited at the College of Life Sciences, Hunan Normal University (HNU), Changsha, Hunan Province, China.

We examined and dissected the specimens using an Olympus SZ51 stereomicroscope. The soft tissues of female genitalia were degraded using 10 mg/ml trypsinase (Bomei Biotech Company, Hefei, Anhui, China) for at least three hours at room temperature. We photographed male and female genitalia using a CCD digital camera mounted on an Olympus BX53 compound microscope, and then generated compound focused images using Helicon Focus v6.7.1. All measurements were made using a digital camera MC170HD mounted on a Leica M205C stereomicroscope and given in millimeters. Leg and palp measurements are given in the following order: leg total length (femur + patella + tibia + metatarsus + tarsus), palp total length (femur + patella + tibia + tarsus).

Abbreviations used: ALE = anterior lateral eyes; AME = anterior median eyes; BL = body length; CL = carapace length; Co = conductor; CT = contrategulum; CW = carapace width; E = embolus; OL = opisthosoma length; OW = opisthosoma width; PC = paracymbium; PLE = posterior lateral eyes; PME = posterior median eyes; RC = receptacular cluster; T = tegulum.

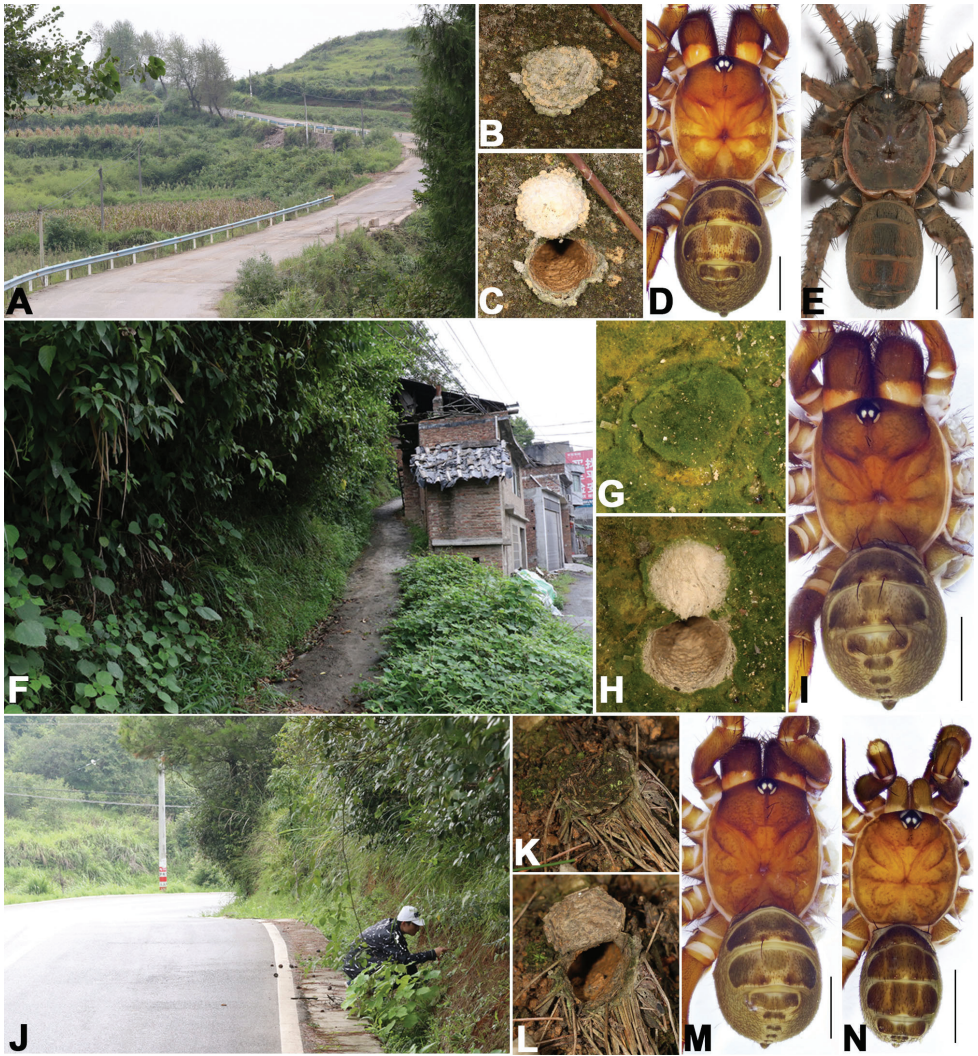


Figure 1. Microhabitat and general somatic morphology of three new *Songthela* species **A–E** *Songthela liui* sp. nov.: **D** XUX–2018–381, female **E** XUX–2018–375A, male **F–I** *Songthela tianzhu* sp. nov.: **I** XUX–2018–339, female **J–N** *Songthela yuping* sp. nov.: **M** XUX–2018–380, female **N** XUX–2018–380A, male **A, F, J** microhabitat **B, C, G, H, K, L** the trapdoor with the door closed and open **D, E, I, M, N** dorsal view. Scale bars: 3 mm (**D, E, I, M, N**).

We extracted the total genomic DNA from spider legs using the Animal Genomic DNA Isolation Kit (Kangwei Biotech, Beijing, China). We used the primer pair LCO1490/HCO2198 (Folmer et al. 1994) to amplify COI. We used the following PCR reaction protocol: initial denaturation at 95 °C for 5 min; 35 cycles of denaturation at 95 °C for 1 min, annealing at 40 °C for 1 min, and elongation at 72 °C for 30 s; and final extension at 72 °C for 7 min (Xu et al. 2015c). The 25 µl PCR reaction



Figure 2. Map showing the type localities of the four *Songthela* species that are distributed in Guizhou Province, China.

contained 12.5 μ l of 2 \times Taq MasterMix (KangWei Biotech, Beijing, China), 1 μ l of each forward and reverse 10 μ M primer, 1 μ l of genomic DNA, and 9.5 μ l of double-distilled H₂O. The PCR products were visualized by agarose gel electrophoresis (1% agarose). All PCR products were purified and sequenced at Tsingke Biotechnology Company (Changsha, China).

Since only five known species (*S. goulouensis*, *S. huangyang*, *S. pyriformis*, *S. shuyuan* and *S. xiangnan*) have sequence data available from the holotype specimen (making the identification unambiguous), we obtained the publicly available COI sequences for these five species from the GenBank (for their GenBank accession codes, see Table 1) for comparison.

We estimated intraspecific and interspecific genetic distances based on COI sequences using Kimura 2-parameter (K2P) and *p*-distance substitution models with MEGA v.6 (Tamura et al. 2013).

Taxonomy

Genus *Songthela* Ono, 2000

Type species. *Heptathela hangzhouensis* Chen, Zhang & Zhu, 1981

Diagnosis. *Songthela* males can be distinguished from those of all other Heptathelinae genera by the contrategulum with serrated edges (Figs 3A, D, G, 4B, D, G, 5C, D, G); by the proximal portion of the conductor relatively narrow and smooth, the distal portion gradually narrowed into one long apical spine (Figs 4D, E, 5D, E) or two apical spines (Fig. 3A, B, D, E); and by the distal portion of the embolus slightly

sclerotized with a wide and flat opening (Figs 3A, D, 4B, D, 5C, D). *Songthela* females differ from those of all other Heptathelinae genera by four receptacular clusters separated from each other, the median pair situated along the anterior margin of the bursa copulatrix or close to the dorsal wall of the bursa copulatrix with distinct tubular stalks, the lateral ones located dorsolaterally (Figs 3I–P, 4H–O, 5H–W).

Composition. *Songthela bristowei* (Gertsch, 1967), *S. ciliensis* (Yin, Tang & Xu, 2003), *S. goulouensis* (Yin, 2001), *S. hangzhouensis* (Chen, Zhang & Zhu, 1981), *S. huangyang* Li, Liu, Li & Xu, 2020, *S. jiangnanensis* (Chen, Gao, Zhu & Luo, 1988), *S. mangshan* (Bao, Yin & Xu, 2003), *S. pluma* Yu, Li & Zhang, 2018, *S. pyriformis* Li, Liu & Xu, 2019, *S. sapana* (Ono, 2010), *S. shei* (Xu & Yin, 2001), *S. shuyuan* Li, Liu & Xu, 2019, *S. wosanensis* (Wang & Jiao, 1995), *S. xiangnan* Li, Liu, Li & Xu, 2020, *S. xianningensis* (Yin, Tang, Zhao & Chen, 2002), *S. yunnanensis* (Song & Haupt, 1984).

Distribution. Southern China (Guizhou, Hubei, Hunan, Sichuan, Yunnan, Zhejiang Provinces) and northern Vietnam (Lao Cai Province).

Songthela liui sp. nov.

<http://zoobank.org/D485CADB-3AC6-49BA-BF06-805D00DB9390>

Figure 3

Type material. Holotype: CHINA · 1 ♂; Guizhou Province, Tongren City, Yuping Autonomous County, Zhujiachang Town, Yutang Village; 27.30°N, 108.89°E; alt. 542 m; 17 August 2018; D. Li, F.X. Liu, X. Xu, D.Q. Li and L. Yu leg.; XUX–2018–375A (matured on 5 May 2019 at HNU). **Paratypes:** CHINA · 1 ♀; same data as for the holotype; XUX–2018–381 · 9 ♀♀; Guizhou Province, Qiandongnan Autonomous Prefecture, Cengong County, Xiajiao Village; 27.46°N, 108.83°E; alt. 552–553 m; 17 August 2018; D. Li, F.X. Liu, X. Xu, D.Q. Li and L. Yu leg.; XUX–2018–383, 383A, 385, 386, 387, 387A, 387C, 387D, 387E.

Diagnosis. Male of *S. liui* sp. nov. resembles that of *S. hangzhouensis*, but can be distinguished from the latter by the base of the lower spine of the conductor wider and with a small spur (Fig. 3A, B, D–F), and by the tegulum with a small terminal apophysis (Fig. 3B, C, E, G, H); from that of *S. goulouensis* by the conductor with a shorter upper spine and the base of the lower spine of the conductor wider with a small spur (Fig. 3A, B, D–F), and by the marginal regular apophysis with a slightly helicoid edge (Fig. 3B, C, E, G, H); from that of *S. shuyuan* by the contrategulum with an apophysis proximally (Fig. 3A, D), and by the base of the lower spine of the conductor wider with a small spur (Fig. 3B, E, F); from that of *S. yuping* sp. nov. by the conductor with two apical spines (Fig. 3A, B, D, E), by the contrategulum with smaller marginal teeth (Fig. 3A, D); from those of other *Songthela* species by the conductor with two conspicuous apical spines (Fig. 3A, B, D, E). Females of *S. liui* sp. nov. can be distinguished from those of *S. hangzhouensis* by the bases of the median receptacular clusters separated from each other (Fig. 3I–P); from those of *S. shuyuan* by the median receptacular clusters with shorter stalks (Fig. 3I–P); from those of *S. yuping* sp. nov. by

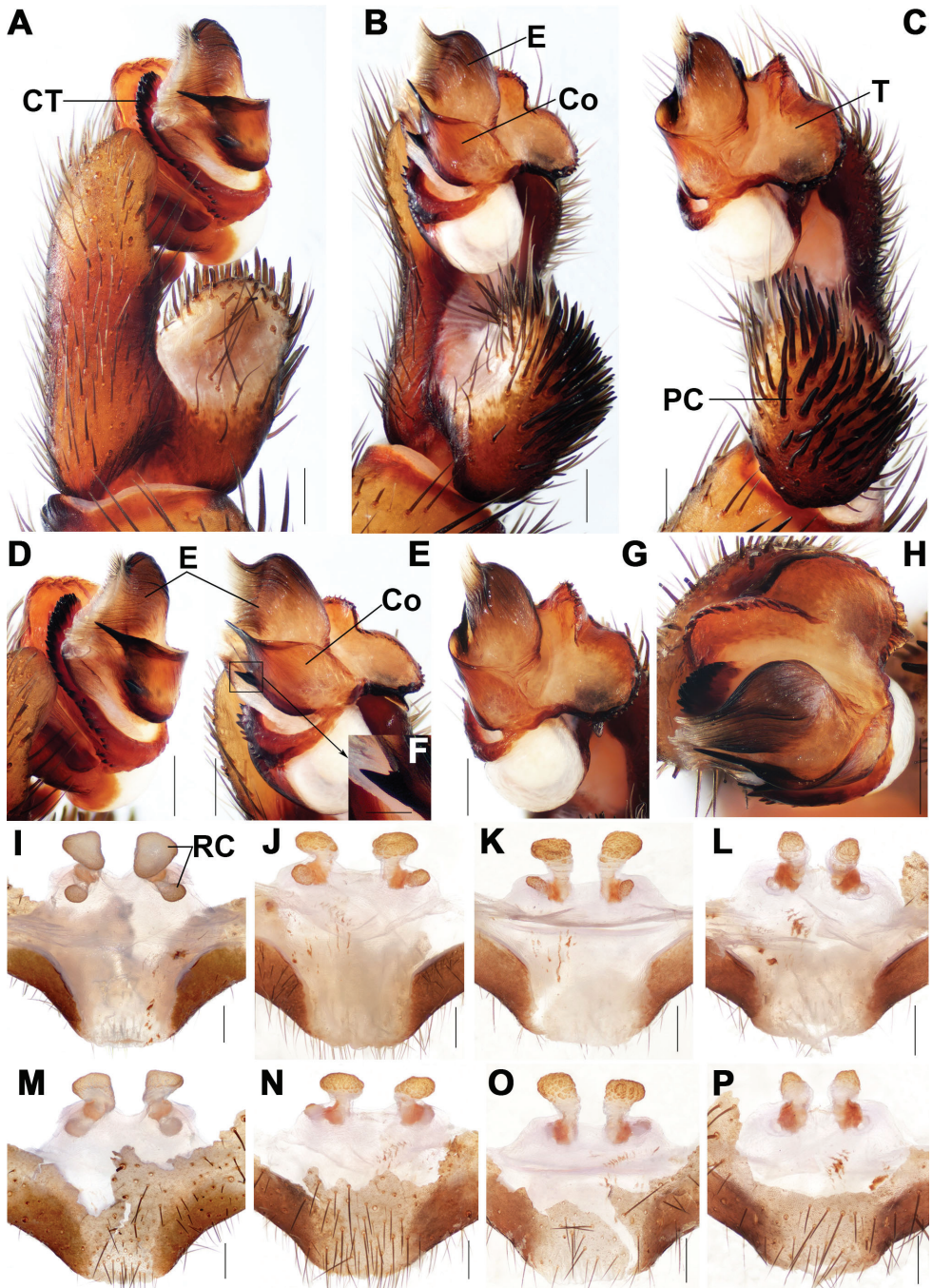


Figure 3. Male and female genital anatomy of *Songhela liui* sp. nov. **A, D** palp prolateral view **B, E** palp ventral view **C, G** palp retrolateral view **H** palp distal view **I–L** vulva dorsal view **M–P** vulva ventral view **A–H** XUX–2018–375A (holotype) **I, M** XUX–2018–381 **J, N** XUX–2018–383A **K, O** XUX–2018–387D **L, P** XUX–2018–387. Scale bars: 0.3 mm (**A–E, G–P**); 0.1 mm (**F**).

the middle receptacular clusters situated at anterior margin of the bursa copulatrix, and distinctly larger than the lateral ones, and by the middle genital stalks separated from each other basally (Fig. 3I–P); and from those of other *Songthela* species by the middle receptacular clusters larger than the lateral ones and the bases of the middle ones close to the lateral ones (Fig. 3I–P).

Description. Male (holotype; Fig. 1E). Carapace dark reddish brown, opisthosoma slightly reddish brown, with 12 dark reddish brown tergites, close to each other, 2–6 larger than others, and the 4th largest; sternum narrow, much longer than wide; a few pointed hairs running over ocular area; chelicerae robust with promargin of cheliceral groove with 9 denticles of variable size; legs with hairs and spines; 7 spinnerets. Measurements: BL 14.25, CL 6.33, CW 5.21, OL 6.78, OW 4.62; ALE > PLE > PME > AME; leg I 18.44 (5.26 + 2.44 + 4.01 + 4.40 + 2.33), leg II 18.95 (4.72 + 2.54 + 4.02 + 4.95 + 2.72), leg III 21.33 (5.10 + 2.22 + 4.48 + 6.48 + 3.05), leg IV 27.85 (6.44 + 2.64 + 5.65 + 9.24 + 3.88).

Palp. Paracymbium with numerous setae and spines at the tip, with an apophysis ventrally (Fig. 3B). Contrategulum with a small apophysis and three teeth proximally, the marginal teeth arranged sparsely and gradually split into two edges distally (Fig. 3A, D). The marginal regular apophysis and the dorsal extension of terminal regular apophysis with helicoid edges, and with a small triangular terminal regular apophysis retrolaterally (Fig. 3B, C, E, G, H). Conductor smooth, fused with embolus basally, with two apical spines and a spur at the base of the lower spine from ventral view (Fig. 3A, B, D–F). Embolus with a flat opening distally and numerous ribbed ridges in middle and distal portion (Fig. 3A–E, G).

Female (XUX–2018–381; Fig. 1D). Carapace dark reddish brown, opisthosoma slightly brown, with 12 dark brown tergites, close to each other, 2–6 larger than others, and the 4th largest; sternum narrow, much longer than wide; a few pointed hairs running over ocular area; chelicerae robust with promargin of cheliceral groove with 13 denticles of variable size; legs with hairs and spines; 7 spinnerets. Measurements: BL 14.97, CL 6.81, CW 5.66, OL 7.17, OW 5.13; ALE > PLE > PME > AME; palp 10.96 (3.67 + 1.81 + 2.46 + 3.02), leg I 13.70 (4.08 + 2.33 + 2.79 + 2.74 + 1.76), leg II 13.40 (4.01 + 2.28 + 2.45 + 2.79 + 1.87), leg III 14.66 (4.17 + 2.28 + 2.73 + 3.39 + 2.09), leg IV 20.35 (5.57 + 2.74 + 3.72 + 5.57 + 2.75).

Female genitalia. Two pairs of receptacular clusters with tubular stalks. The middle pair of receptacular clusters situated at anterior margin of bursa copulatrix, separated from each other, larger than the lateral ones. The lateral ones ellipsoidal, situated dorsolaterally with short genital stalks. The bases of the middle receptacular clusters close to those of the lateral ones (Fig. 3I–P).

Variation. Females vary in body size. The range of measurements as follows ($N = 10$): BL 10.51–14.76, CL 4.84–6.24, CW 4.08–5.95, OL 4.71–7.39, OW 3.86–5.48. The number of promargin of cheliceral groove varies from 11–13 ($N = 10$). There are 7 or 8 spinnerets. Moreover, female genitalia are somewhat variable: the median pair of receptacular clusters are different in shape, mushroom-like (Fig. 3J, K,

N, O), triangular (Fig. 3I, M), or ovoid (Fig. 3L, P); the genital stalks of the middle receptacular clusters slightly vary in length (Fig. 3I–P).

Etymology. The specific name is dedicated to Mr Fengxiang Liu for his kind instructions on all our collection.

Distribution. Guizhou (Tianzhu, Cengong) Province, China.

GenBank accession number. Holotype, XUX–2018–375A: MW450989; Paratypes, XUX–2018–383: MW808998; XUX–2018–383A: MW808999; XUX–2018–385: MW809000; XUX–2018–386: MW809001; XUX–2018–387: MW809002; XUX–2018–387A: MW809003; XUX–2018–387B: MW809004; XUX–2018–381: MW809005.

Remarks. Although liphistiid spiders are known to have a high level of endemism with the increasing number of our collected liphistiid specimens, we have found more than one species in a few localities and also a few widespread species in the genus *Songthela* (unpublished data). In this study, we diagnosed two new *Songthela* species, *S. liui* sp. nov. and *S. yuping* sp. nov., after examining the specimens collected from Yutang Village, Zhujiachang Town, Yuping Autonomous County, Tongren City, Guizhou Province, based not only on male and female genital morphology, but also the genetic distances of COI. We provide the intraspecific genetic distances of *S. liui* sp. nov., and the interspecific genetic distances among the three new species, as well as among the new species and other known species (*S. goulouensis*, *S. huangyang*, *S. pyriformis*, *S. shuyuan* and *S. xiangnan*) (Table 1). The interspecific genetic distances were estimated based on the holotype of each species, except for *S. goulouensis*, which was based on the publicly available COI sequence from the GenBank along with its descriptions (Li et al. 2019, 2020).

***Songthela tianzhu* sp. nov.**

<http://zoobank.org/9430C186-894D-4A77-ACDC-2C1955F2216B>

Figure 4

Type material. Holotype: CHINA · 1 ♂; Guizhou Province, Qiandongnan Autonomous Prefecture, Tianzhu County, Qinxiang Village; 26.92°N, 109.26°E; alt. 380 m; 16 August 2018; D. Li, F.X. Liu, X. Xu, D.Q. Li and L. Yu leg.; XUX–2018–340A (matured on 10 September 2019 at HNU). **Paratypes:** CHINA · 10 ♀♀; same data as for holotype; XUX–2018–336, 336A, 337, 338, 339, 340, 340B, 341, 345, 345A · 17 ♀♀; Guizhou Province, Qiandongnan Autonomous Prefecture, Tianzhu County, Mixi Village; 26.94°N, 109.08°E; alt. 543–552 m; 16 August 2018; D. Li, F.X. Liu, X. Xu, D.Q. Li and L. Yu leg.; XUX–2018–346, 346A, 347, 348, 349, 350, 351, 352, 353, 354, 354A, 354B, 355, 356, 356A, 357, 357A.

Diagnosis. Male of *S. tianzhu* sp. nov. resembles that of *S. ciliensis*, but can be distinguished from the latter by the apical spine of the conductor with a spinule basally (Fig. 4D, E), and by the embolus with a curved margin ventrally (Fig. 4B, E, G); from those of other *Songthela* species by the smooth conductor with an apical

Table 1. Genetic distances within and among the three new species in this study and among the three new species and five known species based on COI sequences (K2P/*p*-distance). The GenBank accession codes of the known species and the number of specimens of each new species that were used to calculate the genetic distances are provided in parentheses. The specimen code and the GenBank accession code of the new species are provided in the descriptions.

| | <i>S. liui</i> sp. nov. (<i>N</i> = 9) | <i>S. tianzhu</i> sp. nov. (<i>N</i> = 21) | <i>S. yuping</i> sp. nov. (<i>N</i> = 9) | <i>S. goulouensis</i> | <i>S. huangyang</i> | <i>S. pyriformis</i> | <i>S. shuyuan</i> |
|----------------------------------|--|--|--|-----------------------|---------------------|----------------------|-------------------|
| <i>S. liui</i> sp. nov. | 0.1/0.1% | – | – | – | – | – | – |
| <i>S. tianzhu</i> sp. nov. | 18.4/16.2% | 0.9/0.9% | – | – | – | – | – |
| <i>S. yuping</i> sp. nov. | 17.3/15.3% | 6.6/6.2% | 0/0% | – | – | – | – |
| <i>S. goulouensis</i> (MT102211) | 14.4/12.9% | 23.4/19.8% | 21.5/18.5% | – | – | – | – |
| <i>S. huangyang</i> (MT102213) | 19.8/17.3% | 20.2/17.6% | 21.1/18.2% | 23.0/19.5% | – | – | – |
| <i>S. pyriformis</i> (MN400625) | 17.7/15.6% | 18.0/15.9% | 17.3/15.3% | 17.8/15.8% | 19.2/16.8% | – | – |
| <i>S. shuyuan</i> (MN400635) | 12.6/11.4% | 19.6/17.1% | 19.7/17.1% | 16.5/14.4% | 18.8/16.5% | 17.9/15.8% | – |
| <i>S. xiangnan</i> (MT102212) | 19.5/17.0% | 14.2/12.7% | 11.2/10.3% | 23.3/19.7% | 20.0/17.4% | 19.7/17.3% | 20.2/17.4% |

spine, and the apical spine with a spinule basally (Fig. 4D, E). Females of *S. tianzhu* sp. nov. resemble those of *S. pluma* and *S. yuping* sp. nov., but can be distinguished from those of *S. pluma* by the stalks of the median pair receptacular clusters fused together basally (Fig. 4H–K); from those of *S. yuping* sp. nov. by the trapeziform genital area and the shallower depressions (Fig. 4H–O); from those of other *Songthela* species by two pairs of receptacular clusters situated on the dorsal wall of the bursa copulatrix (Fig. 4H–O).

Description. Male (holotype). Carapace yellow brown; opisthosoma light brown, with 12 dark brown tergites, close to each other, 2–6 larger than others, and the 4th largest; sternum narrow, much longer than wide; a few pointed hairs running over ocular area; chelicerae robust with promargin of cheliceral groove with 9 denticles of variable size; legs with sturdy hairs and spines; 7 spinnerets. Measurements: BL 12.16, CL 5.77, CW 5.02, OL 5.56, OW 3.50; ALE > PLE > PME > AME; leg I 18.02 (5.11 + 2.28 + 3.73 + 4.57 + 2.33), leg II 17.09 (4.63 + 1.88 + 3.18 + 5.08 + 2.32), leg III 19.40 (4.59 + 1.96 + 3.90 + 5.76 + 3.19), leg IV 25.91 (6.29 + 2.50 + 5.23 + 8.05 + 3.84).

Palp. Paracymbium unpigmented and unsclerotized in prolateral view, with several setae and spines on the tip (Fig. 4A–C). Contrategulum with a distinct apophysis on the proximal portion and a regular dentate edge (Fig. 4D, E). Tegulum with a slightly dentate marginal apophysis and the dorsal extension of the terminal apophysis, and with a thumb-like terminal tegular apophysis retrolaterally (Fig. 4F, G). Conductor with a wide base and fused with embolus, the distal portion gradually narrow to a long apical spine with a spinule basally (Fig. 4D, E). Embolus with a flat opening distally, numerous ribbed ridges in middle and distal portion, and with a curved margin ventrally (Fig. 4B–G).

Female (XUX–2018–339; Fig. 11). Carapace dark reddish brown; opisthosoma light brown, with 12 dark brown tergites, close to each other, 2–6 larger than others, and the 4th largest; sternum narrow, much longer than wide; a few pointed hairs running over ocular area; chelicerae robust with promargin of cheliceral groove with 10 denticles of variable size; legs with sturdy hairs and spines; 7 spinnerets. Measurements:

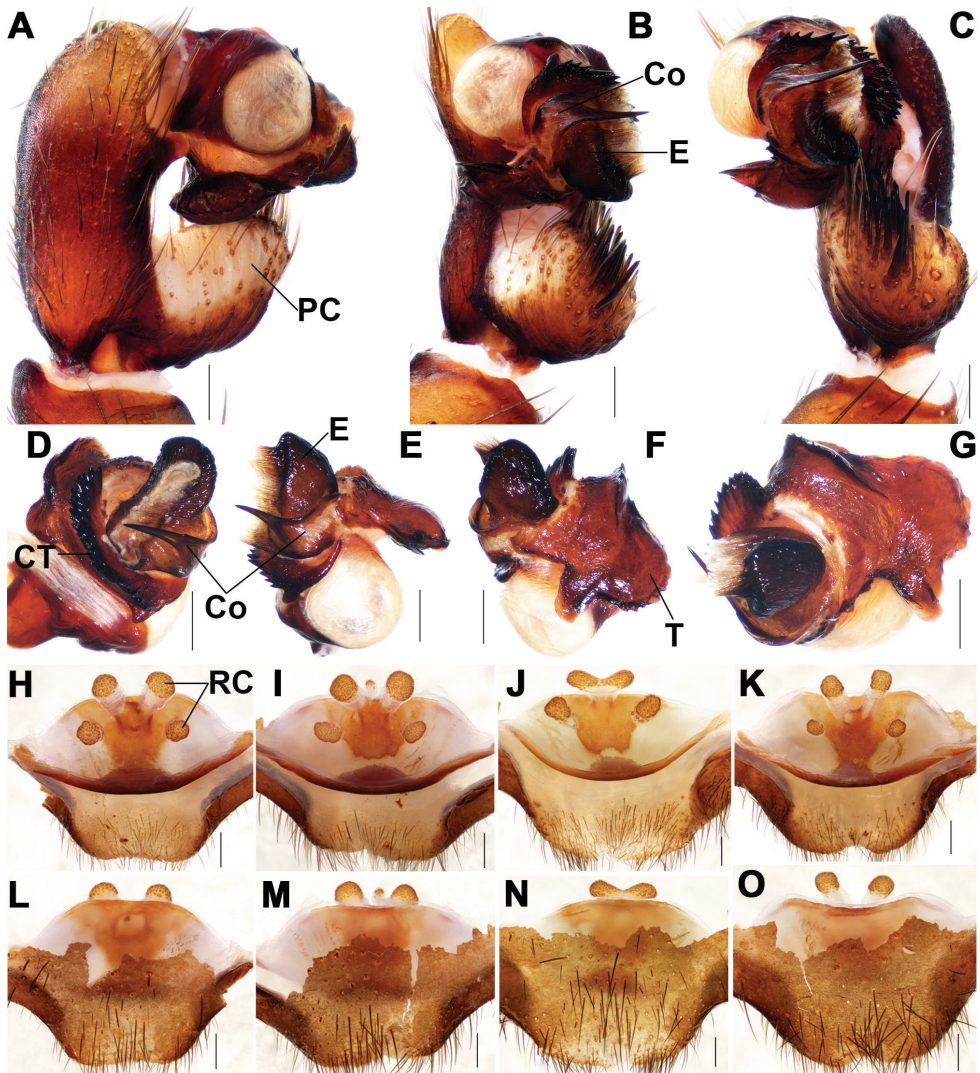


Figure 4. Male and female genital anatomy of *Songthela tianzhu* sp. nov. **A, D** palp prolatateral view **B, E** palp ventral view **C, F** palp retrolateral view **G** palp distal view **H–K** vulva dorsal view **L–O** vulva ventral view **A–G** XUX–2018–340A (holotype) **H, L** XUX–2018–339 **I, M** XUX–2018–338 **J, N** XUX–2018–340 **K, O** XUX–2018–341. Scale bars: 0.3 mm.

BL 11.68, CL 5.52, CW 4.81, OL 5.40, OW 4.33; ALE > PLE > PME > AME; palp 10.32 (3.45 + 1.74 + 2.19 + 2.66), leg I 11.28 (3.62 + 1.98 + 2.20 + 2.03 + 1.45), leg II 10.90 (3.62 + 1.98 + 2.20 + 2.03 + 1.45), leg III 12.09 (3.55 + 2.09 + 2.22 + 2.47 + 1.76), leg IV 17.92 (5.02 + 2.52 + 3.53 + 4.53 + 2.32).

Female genitalia. Two pairs of ovoid receptacular clusters with tubular stalks, situated on the dorsal wall of the bursa copulatrix. The median pair slightly larger than (Fig. 4H, I, K) or similar to (Fig. 4J) the lateral ones, and the bases of the middle stalks fused together (Fig. 4H–K).

Variation. Females vary in body size. The range of measurements as follows ($N = 27$): BL 10–13.82, CL 4.57–6.94, CW 4.14–6.10, OL 4.54–6.57, OW 3.77–6.00. The number of promargin of cheliceral groove varies from 10–13 ($N = 27$). There are 7 or 8 spinnerets. In addition, female genitalia show somewhat intraspecific variation: there is an additional receptacular cluster situated at the middle of the median pair (Fig. 4I, M); the genitalia stalks of the median pair are fused together basally (Fig. 4H, I, K) or the middle receptacular clusters are fused together (Fig. 4J); some specimens have slightly longer middle genital stalks than others (Fig. 4K).

Etymology. The species epithet, a noun in apposition, refers to the type locality.

Distribution. Guizhou (Tianzhu), China.

GenBank accession number. Holotype, XUX–2018–340A: MW450988; Paratypes, XUX–2018–336: MW809006; XUX–2018–337: MW809007; XUX–2018–338: MW809008; XUX–2018–339: MW809009; XUX–2018–340: MW809010; XUX–2018–341: MW809011; XUX–2018–342: MW809012; XUX–2018–343: MW809013; XUX–2018–345: MW809014; XUX–2018–346: MW809015; XUX–2018–347: MW809016; XUX–2018–348: MW809017; XUX–2018–349: MW809018; XUX–2018–350: MW809019; XUX–2018–352: MW809020; XUX–2018–353: MW809021; XUX–2018–354: MW809022; XUX–2018–355: MW809023; XUX–2018–356: MW809024; XUX–2018–357: MW809025.

Remarks. The intraspecific genetic distances of the new species and the interspecific genetic distances between the new species and the other two new species and five known species are shown in Table 1.

Songthela yuping sp. nov.

<http://zoobank.org/1B725706-AC1A-4B8D-8F90-B5AE5FC920E1>

Figure 5

Type material. *Holotype*: CHINA · 1 ♂; Guizhou Province, Tongren City, Yuping Autonomous County, Zhujiachang Town, Yutang Village; 27.30°N, 108.89°E; alt. 546 m; 17 August 2018; D. Li, F.X. Liu, X. Xu, D.Q. Li and L. Yu leg.; XUX–2018–380A. *Paratypes*: CHINA · 10 ♀♀; same data for the holotype; XUX–2018–373, 374, 375, 376, 377, 378, 379, 380, 382, 382A.

Diagnosis. Male of *S. yuping* sp. nov. resembles that of *S. pluma* and *S. xiangnan*, but can be distinguished from that of *S. pluma* by the apical spine of the conductor with a spinule basally (Fig. 5C, D, E), the contrategulum with fewer teeth (Fig. 5D); from that of *S. liui* sp. nov. by the conductor with only a long apical spine, and the middle part of conductor covered with numerous small spines (Fig. 5C–E); from that of *S. xiangnan* by the blade-shaped spine of the conductor with one tip (Fig. 5C–E), by the semielliptical contrategulum (Fig. 5D, G), and by the tegulum with a small terminal apophysis retrolaterally (Fig. 5B, F); from that of other *Songthela* species by the conductor covered with several short spines on the middle part (Fig. 5C–E). Females of *S. yuping* sp. nov. resemble those of *S. pluma* and *S. tianzhu* sp. nov., but can be distinguished from those of *S. pluma* by the arc-shaped anterior margin of the bursa

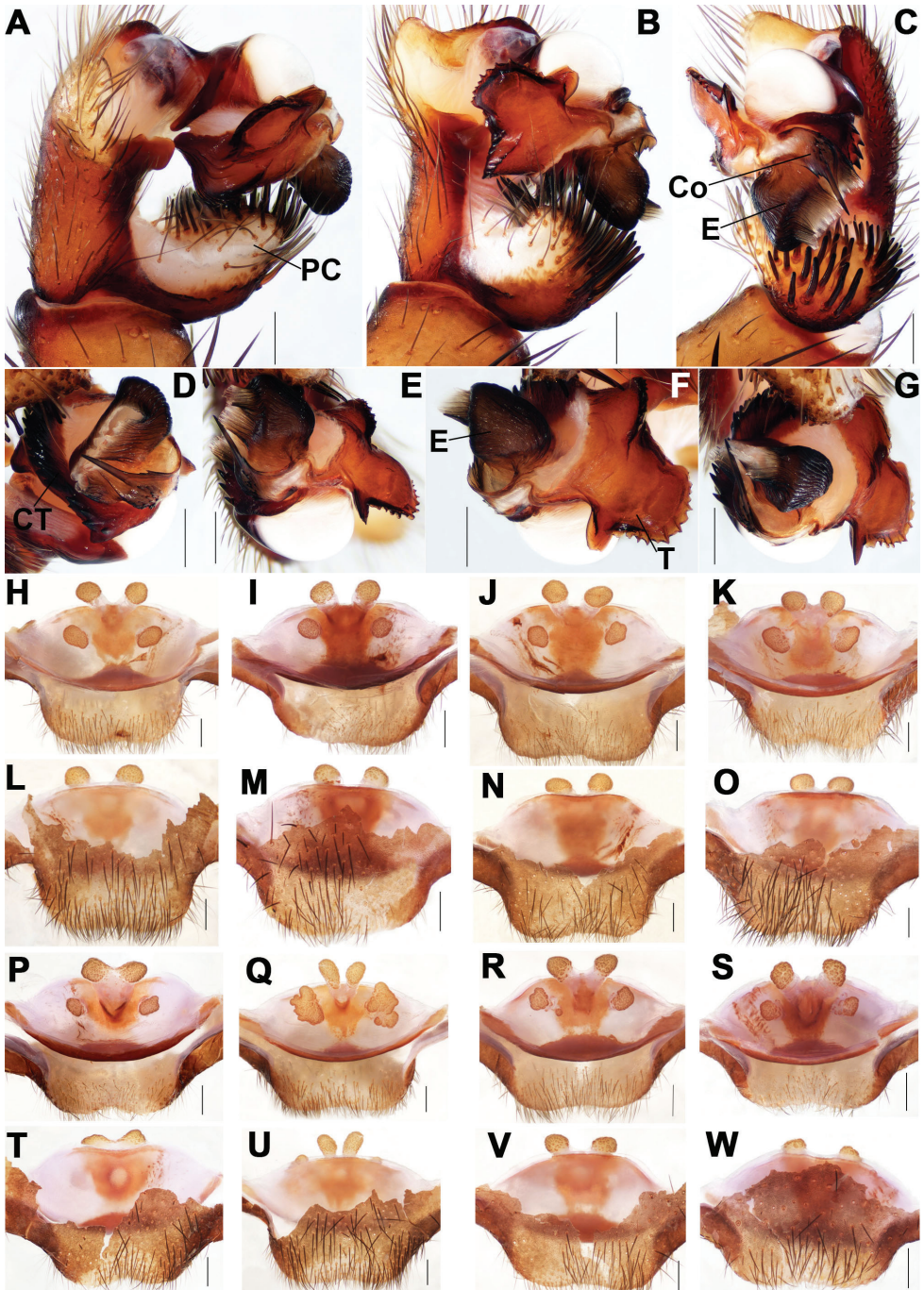


Figure 5. Male and female genital anatomy of *Songthela yuping* sp. nov. **A, D** palp prolateral view **B, E** palp ventral view **C, F** palp retrolateral view **G** palp distal view **H–K** vulva dorsal view **L–O** vulva ventral view **A–G** XUX–2018–380A (holotype) **H, L** XUX–2018–380 **I, M** XUX–2018–374 **J, N** XUX–2018–377 **K, O** XUX–2018–382 **P, T** XUX–2018–382A **Q, U** XUX–2018–375 **R, V** XUX–2018–379 **S, W** XUX–2018–373. Scale bars: 0.3 mm.

copulatrix (Fig. 5H–K, P–S); from those of *S. tianzhu* sp. nov. by the slightly longer middle genital stalks (Fig. 5H–W), and by the rectangular genital area and the slightly deeper depressions (Fig. 5H–K, P–S); from those of *S. liui* sp. nov. by the two pairs of receptacular clusters situated on the dorsal wall of the bursa copulatrix, and the middle genital stalks fused together basally (Fig. 5H–W); from those of other *Songthela* species by four receptacular clusters situated on the dorsal wall of the bursa copulatrix (Fig. 5H–W).

Description. Male (holotype; Fig. 1N). Carapace yellow brown, opisthosoma slightly brown, with 12 dark brown tergites, close to each other, 2–6 larger than others, and the 4th largest; sternum narrow, much longer than wide; a few pointed hairs running over ocular area; chelicerae robust with promargin of cheliceral groove with 9 denticles of variable size; legs with sturdy hairs and spines; 7 spinnerets. Measurements: BL 9.65, CL 4.53, CW 3.62, OL 4.63, OW 3.28; ALE > PLE > PME > AME; leg I 15.40 (4.42 + 2.00 + 3.43 + 3.73 + 1.82), leg II 14.06 (4.15 + 1.85 + 3.48 + 2.90 + 1.68), leg III 17.08 (4.26 + 1.88 + 3.38 + 5.25 + 2.31), leg IV 23.05 (5.66 + 2.18 + 4.59 + 7.37 + 3.25).

Palp. Paracymbium with numerous setae and spines at the distal portion (Fig. 5A). Contrategulum with an irregular dentate edge and an apophysis proximally (Fig. 5D). Tegulum with a serrated marginal apophysis and a dorsal extension of terminal apophysis, and with a small thumb-like terminal tegular apophysis retrolaterally (Fig. 5B, F, G). Conductor fused with embolus basally, covered with several small spines in the middle part, and a long blade-shaped apical spine with a spinule basally (Fig. 5C, D, E). Embolus with a flat opening in distal portion and numerous ribbed ridges in middle and distal portion (Fig. 5C–G).

Female (XUX–2018–382A; Fig. 1M). Carapace yellow brown, opisthosoma slightly brown, with 12 dark brown tergites, close to each other, 2–6 larger than others, and the 4th largest; sternum narrow, much longer than wide; a few pointed hairs running over ocular area; chelicerae robust with promargin of cheliceral groove with 12 denticles of variable size; legs with sturdy hairs and spines; 7 spinnerets. Measurements: BL 13.67, CL 6.60, CW 5.43, OL 6.28, OW 5.06; ALE > PLE > PME > AME; palp 11.50 (3.75 + 2.05 + 2.42 + 3.28), leg I 13.37 (4.41 + 2.32 + 2.53 + 2.57 + 1.54), leg II 13.00 (3.85 + 2.30 + 2.27 + 2.79 + 1.79), leg III 13.21 (3.95 + 2.42 + 2.09 + 2.94 + 1.81), leg IV 19.08 (5.35 + 2.64 + 3.35 + 5.38 + 2.36).

Female genitalia. Two pairs of receptacular clusters with tubular stalks, situated on the dorsal wall of the bursa copulatrix. The median ones similar to or slightly larger than the lateral ones, with smooth genital stalks and fused together basally (Fig. 5H–W).

Variation. Females vary in body size. The range of measurements as follows ($N = 10$): BL 9.65–14.14, CL 4.53–6.60, CW 3.62–5.68, OL 4.59–6.71, OW 3.28–5.30. The number of promargin of cheliceral groove varies from 9–12 ($N = 10$). Moreover, the female genitalia show somewhat intraspecific variation: the genital stalks of the median receptacular clusters are different in shape, either “Y” shaped (Fig. 5K, Q, R, S), “V” (Fig. 5H–J), or fused together (Fig. 5P); the lateral receptacular clusters are irregular, and larger than the median ones (Fig. 5Q).

Etymology. The species epithet, a noun in apposition, refers to the type locality.

Distribution. Guizhou (Yuping), China.

GenBank accession number. Holotype, XUX–2018–380A: MW450990; Paratypes, XUX–2018–373: MW809026; XUX–2018–374: MW809027; XUX–2018–375: MW809028; XUX–2018–376: MW809029; XUX–2018–377: MW809030; XUX–2018–378: MW809031; XUX–2018–379: MW809032; XUX–2018–380: MW809033.

Remarks. The intraspecific genetic distances of *S. yuping* sp. nov., and the inter-specific genetic distances between *S. yuping* sp. nov. and the other two new species and the five known species are shown in Table 1.

Acknowledgements

We thank Fengxiang Liu and Li Yu for their help in field collection of specimens. We thank Braxton Jones for helping edit the language, Jeremy Miller and Ono Hirotsugu for insightful comments on the manuscript. We are also grateful to the Animal Nutrition and Human Health Laboratory, the Mineral Nutrition Laboratory, as well as the Gene Function and Regulation Laboratory at the College of Life Sciences, Hunan Normal University, for assistance in molecular work. This study was supported by the National Natural Sciences Foundation of China (NSFC-32070430) to XX, and the Singapore Ministry of Education AcRF Tier 1 grant (R-154-000-A52-114) to DL.

References

- Folmer O, Black M, Hoeh W, Lutz R, Vrijenhoek R (1994) DNA primers for amplification of mitochondrial cytochrome c oxidase subunit I from diverse metazoan invertebrates. *Molecular Marine Biology and Biotechnology* 3: 294–299.
- Haupt J (2003) The Mesothelae – monograph of an exceptional group of spiders (Araneae: Mesothelae) (Morphology, behaviour, ecology, taxonomy, distribution and phylogeny). *Zoologica* 154: 1–102.
- Li DQ, Liu FX, Li D, Xu X (2020) Two new species of the primitively segmented spider genus *Songthela* from Hunan Province, China (Mesothelae, Liphistiidae). *ZooKeys* 937: 1–19. <https://doi.org/10.3897/zookeys.937.50548>
- Li DQ, Liu H, Xu X (2019) Three new species of the primitively segmented spiders from Mt. Yuelu, Hunan, China (Mesothelae, Liphistiidae). *Zootaxa* 4691: 139–152. <https://doi.org/10.11646/zootaxa.4691.2.3>
- Schwendinger PJ, Ono H (2011) On two *Heptathela* species from southern Vietnam, with a discussion of copulatory organs and systematics of the Liphistiidae (Araneae: Mesothelae). *Revue suisse de Zoologie* 118: 599–637. <https://doi.org/10.5962/bhl.part.117818>
- Tamura K, Stecher G, Peterson D, Filipowski A, Kumar S (2013) MEGA6: Molecular evolutionary genetics analysis version 6.0. *Molecular Biology and Evolution* 30: 2725–2729. <https://doi.org/10.1093/molbev/mst197>

- World Spider Catalog (2021) World Spider Catalog, Version 22.0. Natural History Museum Bern. <http://wsc.nmbe.ch> [access on 27 April 2021]
- Xu X, Liu FX, Cheng RC, Chen J, Xu X, Zhang ZS, Ono H, Pham DS, Norma-Rashid Y, Arnedo MA, Kuntner M, Li D (2015a) Extant primitively segmented spiders have recently diversified from an ancient lineage. *Proceedings of the Royal Society B: Biological Sciences* 282: e20142486. <https://doi.org/10.1098/rspb.2014.2486>
- Xu X, Liu FX, Chen J, Ono H, Li D, Kuntner M (2015b) A genus-level taxonomic review of primitively segmented spiders (Mesothelae, Liphistiidae). *ZooKeys* 488: 121–151. <https://doi.org/10.3897/zookeys.488.8726>
- Xu X, Liu FX, Chen J, Li D, Kuntner M (2015c) Integrative taxonomy of the primitively segmented spider genus *Ganthela* (Araneae: Mesothelae: Liphistiidae): DNA barcoding gap agrees with morphology. *Zoological Journal of the Linnean Society* 175: 288–306. <https://doi.org/10.1111/zoj.12280>
- Xu X, Su YC, Ho SYW, Kuntner M, Ono H, Liu FX, Chang CC, Warrit N, Sivayyapram V, Aung KPP, Pham DS, Norma-Rashid Y, Li D (2021) Phylogenomic analysis of ultraconserved elements resolves the evolutionary and biogeographic history of segmented trapdoor spiders. *Systematic Biology*: syaa098. <https://doi.org/10.1093/sysbio/syaa098>

Composition and diversity of butterflies (Lepidoptera, Papilionoidea) along an atmospheric pollution gradient in the Monterrey Metropolitan Area, Mexico

Edmar Meléndez-Jaramillo¹, César Martín Cantú-Ayala¹,
Eduardo Javier Treviño-Garza¹, Uriel Jeshua Sánchez-Reyes²,
Bernal Herrera-Fernández³

1 *Facultad de Ciencias Forestales, Universidad Autónoma de Nuevo León, Ap. Postal 41, Linares, Nuevo León, C.P. 67700, México* **2** *Tecnológico Nacional de México - Instituto Tecnológico de Cd. Victoria. Boulevard Emilio Portes Gil No.1301, C.P. 87010, Ciudad Victoria, Tamaulipas, México* **3** *Fundación para el Desarrollo de la Cordillera Volcánica Central (Fundecor), Costa Rica e Instituto Internacional para la Conservación y Manejo de la Vida Silvestre (Icomvis), Universidad Nacional, Heredia, Costa Rica*

Corresponding author: Edmar Meléndez-Jaramillo (edmel.jar09@gmail.com)

Academic editor: M. Wiemers | Received 16 March 2021 | Accepted 18 April 2021 | Published 14 May 2021

<http://zoobank.org/1C44098E-4ABC-4F9C-A780-657997E37A9A>

Citation: Meléndez-Jaramillo E, Cantú-Ayala CM, Treviño-Garza EJ, Sánchez-Reyes UJ, Herrera-Fernández B (2021) Composition and diversity of butterflies (Lepidoptera, Papilionoidea) along an atmospheric pollution gradient in the Monterrey Metropolitan Area, Mexico. ZooKeys 1037: 73–103. <https://doi.org/10.3897/zookeys.1037.66001>

Abstract

This study compares the variation of richness, abundance and diversity of butterfly species along an atmospheric pollution gradient and during different seasons in the Monterrey Metropolitan Area, Mexico. Likewise, we analyse the influence of environmental variables on the abundance and richness of butterfly species and quantify the indicator species for each atmospheric pollution category. Based on spatial analysis of the main atmospheric pollutants and the vegetation cover conditions, four permanent sampling sites were delimited. The sampling was carried out monthly in each of the sites using aerial entomological nets and ten Van Someren-Rydon traps during May 2018 to April 2019. A total of 8,570 specimens belonging to six families and 209 species were collected. Both species richness and abundance were significantly different between all sites, except for the comparison between the moderate contamination site and the high contamination site; diversity decreased significantly with increasing levels of contamination. The seasonality effect was absent on species richness; however, for species abundance the differences between dry season and rainy season were significant in each site excepting the moderate contamination site. Regarding diversity, the seasonal effect showed different distribution patterns according to each order. Relative humidity, vegetation cover and three pollution variables were highly correlated with both abundance and

species richness. From the total number of species found, only 47 had a significant indicator value. This study constitutes the first faunistic contribution of butterflies as indicators of the environmental quality of urban areas in Mexico, which will help in the development of strategies for the management, planning and conservation of urban biodiversity.

Keywords

Atmospheric pollution, community patterns, indicator species, Papilionoidea, seasonality

Introduction

The dynamics of the demographic growth that cities are facing represents a serious threat to the environment, to the health and quality of life of its inhabitants (Vlahov and Galea 2002). The excessive exploitation of the natural resources, land use changes, industrial and urban concentrations and the large quantity of pollutants being emitted to the atmosphere, damage the environment in a process that seems irreversible (García et al. 2013). These effects not only harm living beings, but also generate phenomena that affect the ecosystem (López et al. 2001). This unregulated urbanisation process and ecosystems degradation occurs more rapidly in countries located in regions classified as developing economies, particularly in Latin America, where it is estimated that 75% of the population lives in cities (UN–HABITAT 2010).

In Mexico, atmospheric pollution has deteriorated air quality in various cities, including the Valle de México Metropolitan Zone, the Guadalajara Metropolitan Zone and the Monterrey Metropolitan Zone (MMZ) (García et al. 2012; Cerón et al. 2014; Mancilla et al. 2015; Menchaca et al. 2015). It should be noted that the main problem is the perception of society which often does not realise the severity of the problem, mainly because there is no clear awareness of pollutant emissions, their concentrations and the damage they cause to health, urban infrastructure, ecosystems and biodiversity (Lezama 2010). The State of Nuevo León, in the northeast of Mexico, has an unregulated urban growth. Its main city, the Monterrey Metropolitan Zone, presents serious environmental problems: geological and hydrological risks, water scarcity, green areas loss, air pollution, amongst many others (Cantú et al. 2013; Badillo et al. 2015; Orta et al. 2016; Sanchez-Castillo et al. 2016; Sisto et al. 2016; Sanchez-Castillo et al. 2017).

Studies on species diversity in urban ecosystems with air pollution problems are necessary to understand the effect of anthropogenic development on the integrity and livelihood of the ecosystem (Mukherjee et al. 2015). However, arthropods in such environments are poorly studied despite being crucial components and indicators of urban ecosystems and biodiversity (McIntyre 2000; Magle et al. 2012; Bonebrake and Cooper 2014). Butterflies, in general, are very sensitive to changes in temperature, humidity and solar radiation produced by disturbances in their habitat, for which the inventory of their communities, through measures of diversity and richness, represents a valid tool for evaluating the state of alteration between an urbanised area with pollution problems and a natural environment (Kremen 1993; Wagner et al.

2003; García et al. 2007; Settele et al. 2008; Li et al. 2009). In this way, these insects act as biological indicators, which can reflect the state of the biota in terms of biodiversity, its variation along gradients, endemism or the degree of human intervention, including air pollution (Fagua 2001; Moreno et al. 2007; Butchart et al. 2010; Defra 2016). Various studies demonstrate that butterfly species richness decreases as urbanisation increases (Blair and Launer 1997; Blair 1999; Hardy and Dennis 1999; Brown and Freitas 2002; Di Mauro et al. 2007; Konvička and Kadlec 2011; Bonebrake and Cooper 2014; Ramírez and MacGregor 2016), not only because the construction of buildings and roads replaces or reduces the area of natural and semi-natural habitats, but because the quality of residual habitats is affected by various forms of pollution (Corke 1998; Hardy and Dennis 1999; Mulder et al. 2005; Jones and Leather 2012; Philips et al. 2017).

Some other studies have yielded results that support the intermediate disturbance hypothesis, in which species diversity peaked in areas with an intermediate level of habitat alteration (Dial and Roughgarden 1998; Niell 2001; Giuliano et al. 2004; Koh and Sodhi 2004; Jones and Leather 2012). On the other hand, most insect studies investigating seasonality are based on relatively pristine ecosystems and few have examined the relationship between urban ecosystems seasonality and their butterfly assemblages. Only very few studies have explored the seasonality of urban butterflies, including Brown and Freitas (2002) in Sao Paulo, Brazil; Shapiro (2002) in California, USA; Koh and Sodhi (2004) in Singapore; Chowdhury et al. (2017) in Dhaka, Bangladesh; Gupta et al. (2019) in Delhi, India. The objectives presented here have the caveat that urban gradient studies are clearly a simplification of the complex patterns produced by urbanisation, such as pollution (Alberti et al. 2001; Hahs and McDonnell 2006; McKinney 2008). Therefore, the objectives of this study are: (1) Identify the butterfly species richness in the Monterrey Metropolitan Zone, Mexico; (2) Compare the variation in richness, abundance and diversity of butterfly species along an atmospheric pollution gradient and during the seasons of the year; (3) Analyse the influence of environmental variables (atmospheric pollutants, temperature, relative humidity, solar radiation and vegetation cover) on the abundance and richness of butterfly species; and (4) quantify the indicator value of the species per atmospheric pollution category.

Methods

Study area

The Monterrey Metropolitan Zone (**MMZ**) is the largest urban area in northeast Mexico and the third largest urban centre in the country, extending from 25°15' to 26°30' of north latitude and from 99°40' to 101°10' of west longitude (Figure 1A, B). The area is limited by the coastal plain of the Gulf of Mexico and the Sierra Madre Oriental mountain range. The MMZ urban sprawl integrates the Municipality of Monterrey in the central portion, the Municipalities of Guadalupe, San Nicolas de los Garza and San

Pedro Garza Garcia in the pericentral portion, Apodaca, Escobedo and Santa Catarina Municipalities in the periphery and El Carmen, Garcia, Santiago, Juarez, Cadereyta and Salinas Victoria in the surrounding area (Alanís 2005; González et al. 2011; Mancilla et al. 2015; Ybáñez and Barboza 2017). The MMZ has a vehicle fleet of 1.7 million (INEGI 2010) and 4.1 million of inhabitants (INEGI 2011), which is probably higher nowadays. Likewise, there is a variety of industrial complexes that include the production of glass, steel, cement and paper, amongst others (Menchaca et al. 2015). The centre of the city has an average altitude of 540 m a.s.l, its steppe climate is dry and warm with temperatures above 35 °C during the summer and below 8 °C during the winter (Alanís 2005; González et al. 2011; Menchaca et al. 2015).

Delimitation of the pollution and vegetation cover gradients

Since November 1992, the MMZ operates a network of air quality monitoring stations known as the Integral Environmental Monitoring System (SIMA). The SIMA network currently consists of 13 registration stations, located following the criteria of meteorological, epidemiological, land use and population density studies. The concentrations registered in the monitoring stations are: PM₁₀ (particulate matter of less than 10 µm), PM_{2.5} (particulate matter of less than 2.5 µm), carbon monoxide (CO), ozone (O₃), nitrogen dioxide (NO₂), nitrogen oxides (NO_x) and sulphur dioxide (SO₂). In addition, some meteorological variables are reported, such as barometric pressure (Bp), rainfall (R), relative humidity (Rh), solar radiation (Sr), temperature (T) and the direction (Wd) and magnitude of wind (Ws) (Arreola and González 1999; González et al. 2011; Mancilla et al. 2015). The data recorded by SIMA stations for air quality and meteorological variables during the period from 2008 to 2017 were obtained from the website of the National System of Air Quality Information (SINAICA). Descriptive measures for each of the months and each registered year were obtained in the Statistica 13.3 software (TIBCO Software Inc. 2017).

To identify the main air quality descriptor pollutants in the MMZ during the period 2008–2017, a Principal Component Analysis (PCA) was carried out. Subsequently, to differentiate the changes in the spatial distribution of the air quality indicator pollutants in the MMZ, maps were prepared using the annual average information per monitoring station. The creation of maps was carried out using Inverse Distance Weighting Interpolation (IDW), with a value of 2 as Coefficient of Distance and the pixel size of the output raster re-defined to 10 metres. As reference of the extension for each interpolation, the minimum and maximum distances were taken from the vector sections corresponding to the urban areas that form the MMZ; such vectors were obtained from the National Land Use and Vegetation Series 6 layer (INEGI 2016). The procedures described above were performed using the QGIS 3.2 software (QGIS Development Team 2018). As a result, three categories of air pollution were generated: low (0.19 to 26.51 µg/m³ of NO_x; 3.22 to 10.56 µg/m³ of PM_{2.5}), moderate (26.51 to 52.83 µg/m³ of NO_x; 10.56 to 17.92 µg/m³ of PM_{2.5}) and elevated (52.83 to 79.19 µg/m³ of NO_x; 17.92 to 25.3 µg/m³ of PM_{2.5}) (Figure 1C).

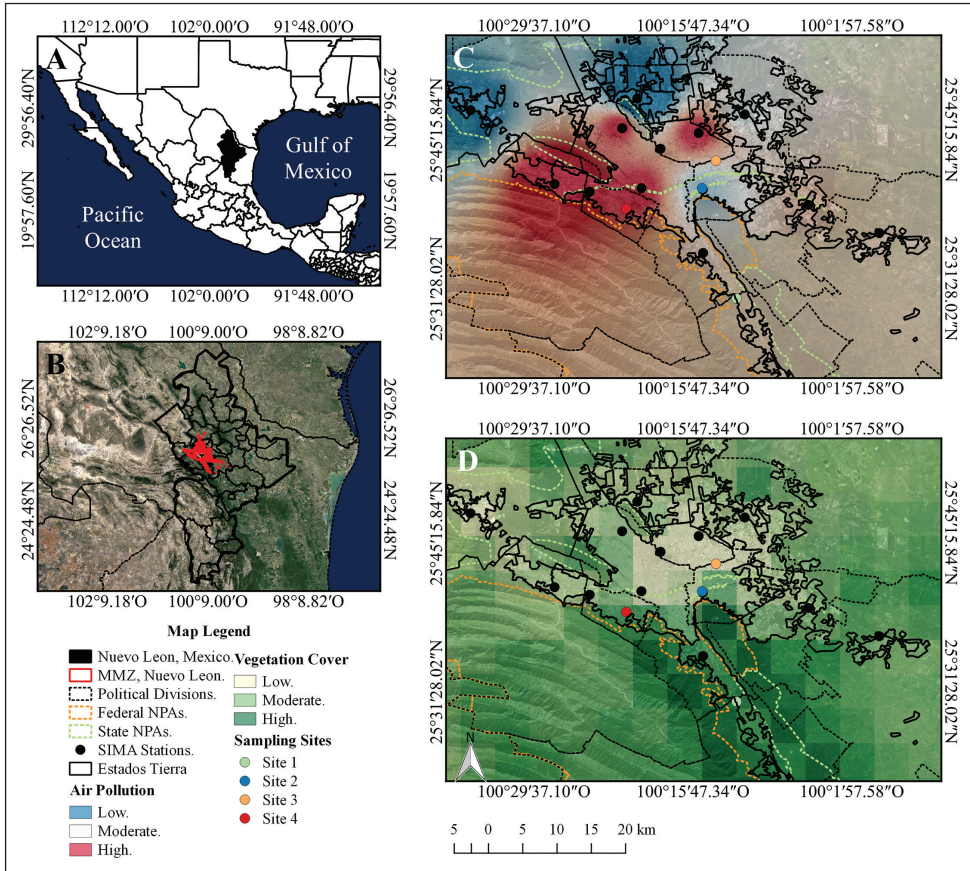


Figure 1. Study area and location of sampling sites **A** location of Nuevo Leon in Mexico **B** location of MMZ inside of Nuevo Leon **C** location of the sampling sites according to the level of atmospheric pollutant **D** location of the sampling sites according to the levels of vegetation cover.

Percentage of vegetation cover was determined through an analysis of MODIS images for the period 2008–2017, obtained from GIOVANNI online server. Consequently, three categories of vegetation cover were designated: low (23 to 40%), moderate (40 to 57%) and high (57 to 74%) (Figure 1D).

Selection of sampling sites

Four permanent sampling sites were delimited, based on the spatial overlapping of four geographic elements: (1) the IDW analysis of the main atmospheric pollutants (Figure 1C), (2) the vegetation cover (Figure 1D), (3) images obtained from Google Earth Pro software and (4) a mesh with a grid size of 150 × 150 metres. The procedures of superimposition and selection were performed in QGIS 3.2 software. Site 1 is found in the Municipality of Santiago, an atmospheric pollution-free area with sec-

Table 1. Descriptive synthesis of the sampling sites.

| Site | Vegetation | Frequent species | General description |
|------|--------------------------------|--|--|
| 1 | Secondary submontane scrub | <i>Ehretia anacua</i> , <i>Ebenopsis ebano</i> , <i>Havardia pallens</i> , <i>Prosopis glyulosa</i> , <i>Celtis laevigata</i> , <i>Sideroxylon celastrinum</i> and <i>Eragrostis barrelieri</i> . | Vacant site located in the Municipality of Santiago, with elevation of 530 m a.s.l. The site is outside the limits of registration of atmospheric pollution and with vegetation cover of 71.06%. |
| 2 | Secondary submontane scrub | <i>Ehretia anacua</i> , <i>Ebenopsis ebano</i> , <i>Prosopis glyulosa</i> , <i>Fraxinus americana</i> , <i>Celtis laevigata</i> , <i>Leucaena leucocephala</i> and <i>Euphorbia hirta</i> . | Site inside La Pastora Park Zoo in the Municipality of Guadalupe. Elevation of 492 m a.s.l, as well as low levels of atmospheric pollution and a vegetation cover of 53.47%. |
| 3 | Secondary submontane scrub | <i>Ebenopsis ebano</i> , <i>Leucaena leucocephala</i> , <i>Fraxinus americana</i> , <i>Cordia boissieri</i> , <i>Parkinsonia aculeata</i> , <i>Caesalpinia mexicana</i> and <i>Eragrostis barrelieri</i> . | Vacant site in the northern limit of the Municipality of Guadalupe, at an elevation of 486 m a.s.l. It presents moderate levels of atmospheric pollution, and a vegetation cover of 46.3%. |
| 4 | Anthropogenic submontane scrub | <i>Fraxinus americana</i> , <i>Ligustrum lucidum</i> , <i>Populus tremuloides</i> and <i>Phyla nodiflora</i> . | Abandoned square in the Municipality of San Pedro Garza García. Site with an elevation of 663 m a.s.l., high levels of atmospheric pollution and a vegetation cover of 58.03%. |

ondary vegetation of submontane scrub (25°30'41.184"N, 100°11'53.159"W). Site 2 is located in the central zone of the Municipality of Guadalupe with low values of atmospheric pollution and secondary vegetation of submontane scrub (25°40'4.944"N, 100°14'45.564"W). Site 3 is located in the northern zone of the Municipality of Guadalupe with moderate atmospheric pollution and secondary vegetation of submontane scrub (25°42'44.017"N, 100°13'58.825"W). Site 4 is in the Municipality of San Pedro Garza García with high atmospheric pollution and anthropogenic vegetation of submontane scrub (25°38'11.112"N, 100°21'30.815"W) (Table 1, Figure 1).

Sampling and processing of specimens

Monthly samplings were carried out for each of the sites, during the period from May 2018 to April 2019, resulting in a total of six samplings per season: dry season (November, December, January, February, March and April) and rainy season (May, June, July, August, September and October). The seasons were defined based on historical data of monthly total values of temperature and rain (average from 2008 to 2017), which were obtained from the SIMA stations located within the study area (Figure 2). Therefore, a total of 48 samplings were considered (six samplings for two seasons and four sites).

The sampling of individuals was carried out using an entomological aerial net. In each of the sites, tours were made inside a pre-established quadrant of 150 m × 150 m, following the techniques recommended by Villarreal et al. (2006). The sampling time at each site was nine hours in the period from 08:00 h to 17:00 h. Furthermore, along with the use of aerial nets, Van Someren-Rydon traps were used (Rydon 1964). Ten traps were placed, five at one end of the quadrant and five at the opposite end, at a distance of 30 m from each other and between 1 and 2.5 m from the ground, with an exposure time of nine hours (08:00 h to 17:00 h). The bait used for the traps consisted of a fermented mixture of seasonal fruits: banana (*Musa paradisiaca*), pineapple (*Ananas comosus*), mango (*Mangifera indica*) and guava (*Psidium guajava*).

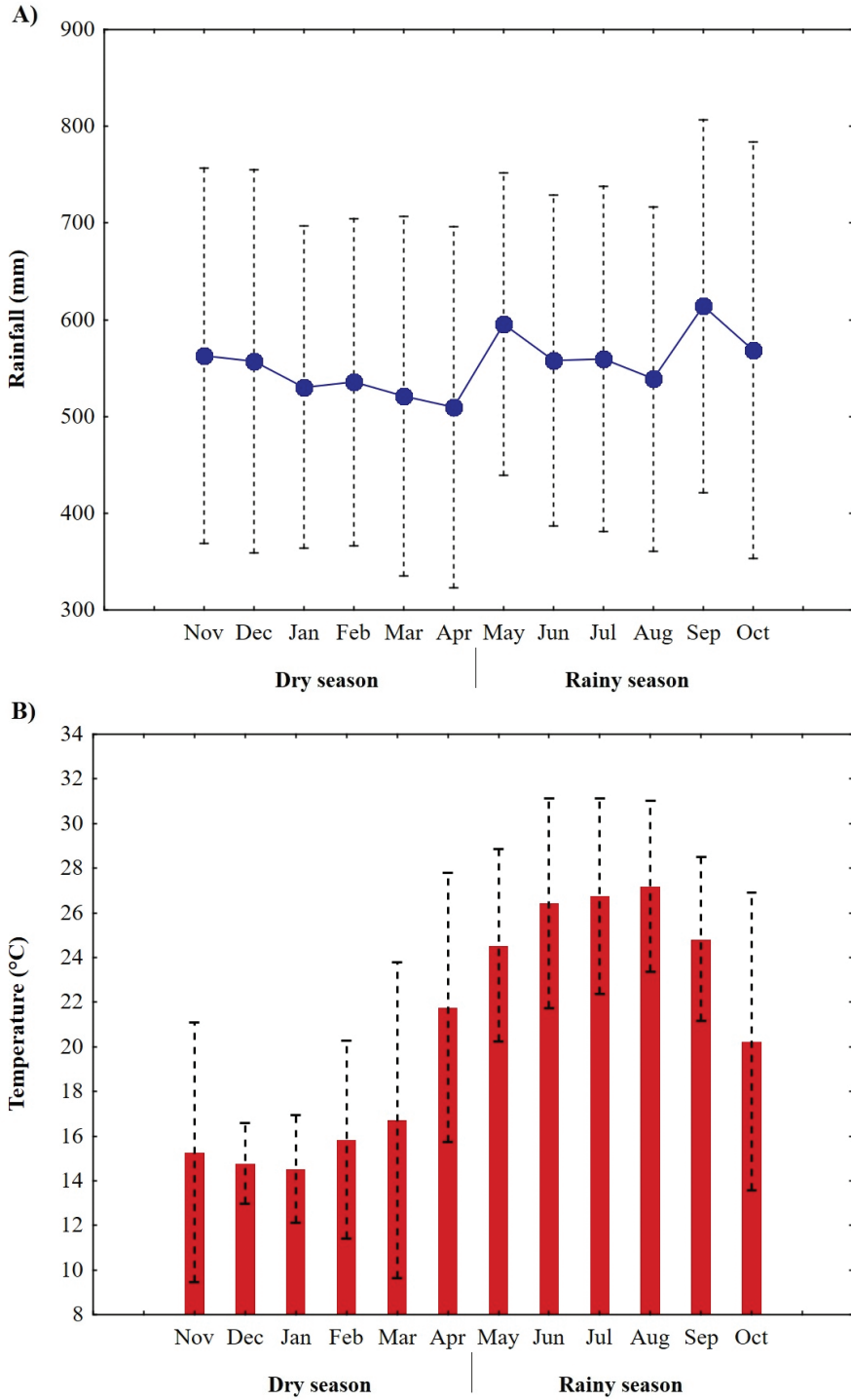


Figure 2. Average monthly variation of temperature and accumulated rain in the MMZ.

The collected specimens were mounted according to the described procedure of Andrade et al. (2013). For taxonomic identification of specimens, the works of Scott (1986), Llorente et al. (1997), Luis et al. (2003), Garwood and Lehman (2005), Vargas et al. (2008), Luis et al. (2010) and Glassberg (2018) were consulted. The interactive list and the phylogenetic ordering of Warren et al. (2012) were taken as reference. All the specimens were labelled and deposited in the entomological collection of the Conservation Department of the Forestry Sciences Faculty at the Autonomous University of Nuevo León, Linares, Nuevo León, Mexico.

Data analysis

The observed species richness was measured as the total number of species in the study area, as well as at each of the sites. The constancy index was determined and the species were classified as: constant (species found more than 50% of the time during sampling), accessory (species present between 25 to 50%) and accidental (species in less than 25%) (Sackis and Morais 2008). Significant differences in the number of species between sites were determined using a generalised linear model (GLM) (they were modelled as Poisson-distributed variables with a log link) and one-way ANOVA, with Statistica software 13.3. The sampling efficiency was calculated for the entire study area and for each study site using the interpolation and extrapolation methodology proposed by Chao and Jost (2012), available in the package iNEXT (Hsieh et al. 2016).

Five species categories were considered according to the total registered abundance: rare (species with one individual), scarce (from 2 to 5), frequent (from 6 to 21), common (from 22 to 81) and abundant (with 82 or more individuals) (Luna et al. 2010). Differences in the abundance of butterfly communities at the sites were calculated with a GLM and one-way ANOVA. For the analysis of alpha diversity, we adopted the analytical method of Chao and Jost (2015) to obtain diversity profiles in which diversity is evaluated in terms of “effective numbers of species” (qD), an approach that is equivalent to Hill's numbers (Hill 1973). The analysis was made for all the study area and for each study site using the 3.5.3 version of R (R Development Core Team 2019), with the package SpadeR (Chao et al. 2016). To examine the differences in species composition amongst the four sites, we performed a non-metric multidimensional scaling analysis (NMDS), based on the similarity matrix using the Bray-Curtis Index. A one-way PERMANOVA was also performed to test for differences in species composition between sites. Both analyses were performed using R 3.5.3 with the package Vegan (Oksanen et al. 2019).

The seasonal effect was measured separately, comparing the species richness, abundance and diversity observed per study site during the rainy season (May to October 2018) and dry season (November of 2018 to April 2019). The indexes and statistical tests mentioned above were used for such comparisons: GLM and nested ANOVA tests for differences in species richness and abundance, estimation of species richness and alpha diversity index, which were performed in Statistica 13.3 and R 3.5.3. In addition, a two-way PERMANOVA and NMDS analyses were carried out, to include the seasonal

effect in the species composition, with the aim of grouping sites and seasons. These analyses were performed in Statistica 13.3 and R 3.5.3. A Canonical Correlation Test was applied between the community parameters (number of species and abundance) and the different environmental variables: monthly averages of the main variables of atmospheric pollution (with the highest loading values in the PCA previously obtained) (NO_2 , NO_x , CO and $\text{PM}_{2.5}$), climatological variables (temperature, relative humidity and solar radiation) and vegetation cover variables extracted from the SIMA stations and from MODIS images nearest to the sampling sites, using Statistica 13.3.

Finally, to calculate the association value of each butterfly species with the habitat type, the Indicator Value Index, or IndVal, was used (Dufrêne and Legendre 1997). This index is based on the degree of specificity (exclusivity of the species to a particular site, based on its abundance) and the degree of fidelity (frequency of occurrence within the same habitat) (Tejeda et al. 2008), expressed in a percentage value. The analysis was performed with the *lapsdv* package on platform R 3.5.3, using 1,000 random permutations to define the level of significance. The indicator species with an index equal to or greater than 75% were classified as “characteristics”, which are defined by their high specificity for a given habitat; species with a value less than 75%, but equal to or greater than 50% are considered as “detectors”, which show different degrees of preference for diverse habitats (McGeoch et al. 2002).

Results

Variation of butterflies per pollution category

A total of 8,570 Papilionoidea specimens were collected, distributed in six families, 19 subfamilies, 31 tribes, 138 genera and 209 species. From this total, only 26 species (499 individuals) were registered exclusively with Van Someren-Rydon baited traps, while the remaining 183 species (8,071 individuals) were collected with entomological nets (Appendix 1). Nymphalidae was the most abundant family with 3,008 individuals, which represents 35.1% of total abundance in the study area. A lower abundance was recorded in Hesperidae (23.2%), Pieridae (19.5%), Lycaenidae (11.9%), Papilionidae (6.6%) and Riodinidae (3.6%). The highest species richness was found in the Hesperidae family with 32.5% of the total obtained species, followed by Nymphalidae (31.1%), Lycaenidae (14.4%), Pieridae (11%), Papilionidae (6.7%) and Riodinidae (4.3%). Twenty-two species were categorised as abundant (with more than 82 individuals) and represented 25.9% of the total abundance. *Kricogonia lyside* (Godart, 1819) (142 individuals), *Anaea aidea* (Guérin-Méneville, 1844) (122), *Phoebis sennae marcellina* (Cramer, 1777) (120), *Pyrisitia proterpia* (Fabricius, 1775) (117) and *Libytheana carinenta larvata* (Strecker, 1878) (113), amongst others, showed the highest abundance. One hundred and three species were considered as common, being 65.2% of the total number of individuals recorded. Fifty-four species were considered as frequent, occupying 8.2% of the total abundance. Seventeen were scarce (0.7% of total

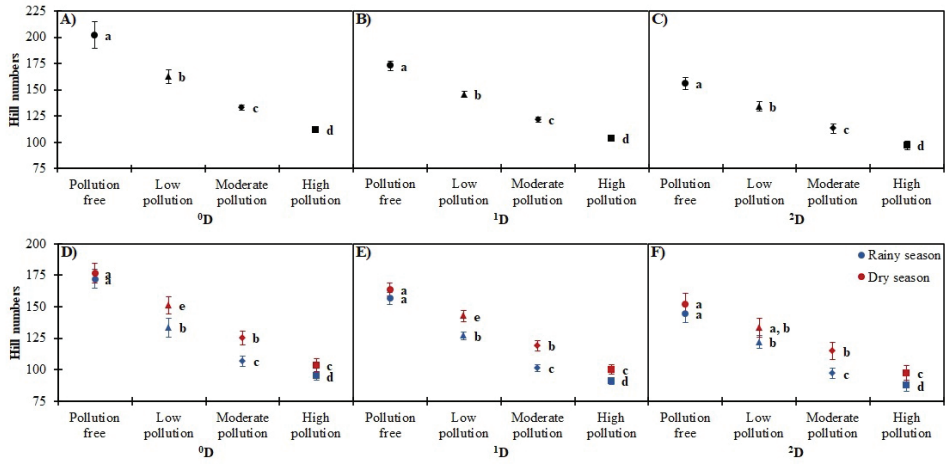


Figure 3. Alpha diversity profiles (0D , 1D and 2D) of butterflies along the pollution gradient and by season (dry and rainy) in the MMZ. The error bars represent 95% confidence intervals.

Table 2. Summary of ANOVA (GLM) results for butterfly abundance and species richness by pollution categories in the MMZ.

| Pollution categories | Estimate | 95%Lower | 95%Upper | p-Value |
|--------------------------|----------|----------|----------|---------|
| Species richness | | | | |
| Intercept | | | | |
| Pollution free | 0.266 | 0.218 | 0.313 | < 0.001 |
| Low pollution | 0.112 | 0.063 | 0.162 | < 0.001 |
| Moderate pollution | -0.128 | -0.182 | -0.074 | < 0.001 |
| Species abundance | | | | |
| Intercept | 5.168 | 5.146 | 5.190 | < 0.001 |
| Pollution free | 0.242 | 0.207 | 0.276 | < 0.001 |
| Low pollution | 0.102 | 0.067 | 0.138 | < 0.001 |
| Moderate pollution | -0.116 | -0.155 | -0.077 | < 0.001 |

abundance) and three were rare (0.04%) (Appendix 1). On the other hand, 93 species (44.5%) were categorised as constant, 47 (22.5%) were accessory species and 69 (33%) were accidental. *Kricogonia lyside* and *Phoebis sennae marcellina* were the most frequent species (87.5%) during all the samplings.

The sample coverage estimator indicated that our inventory for the MMZ is 99.7% complete. In Figure 3, we plotted the proposed diversity with the method of Chao and Jost (2015) and the confidence intervals for $q = 0, 1$ and 2 for each pollution category and station.

Both species richness and abundance were significantly different ($p < 0.05$) between all sites, except for the comparison between Site 3 (moderate pollution) and Site 4 (high pollution) (Table 2, Figure 4A, B). Both parameters (species richness and abundance) decreased with increasing levels of pollution. In Site 1 (pollution free) 2,683 individuals and 199 species were registered, representing a sampling coverage of 99.7%. In Site 2 (low pollution), the values were reduced to 2,334 individuals and

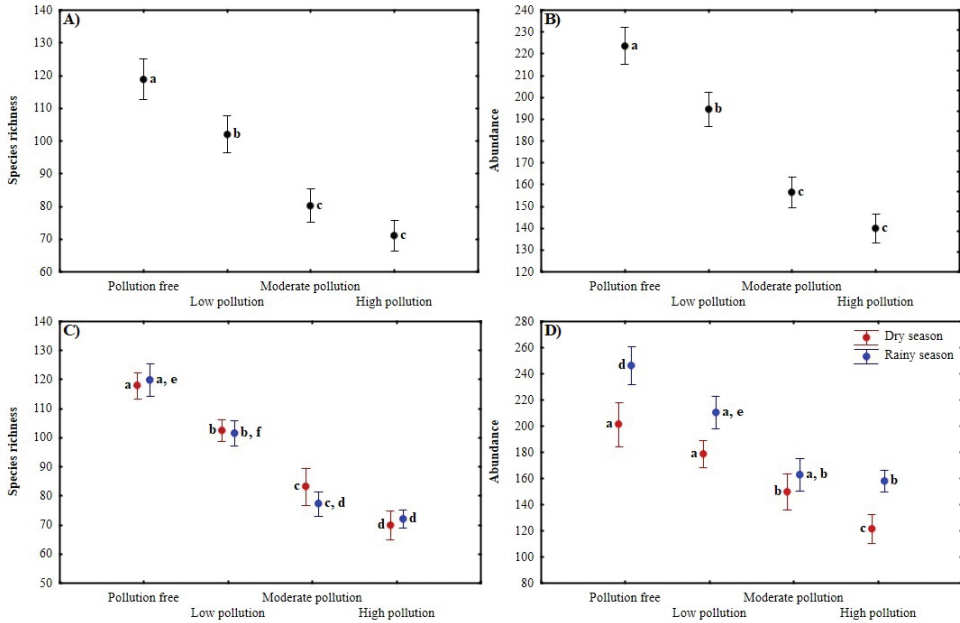


Figure 4. Effect of pollution and seasonality on species richness and abundance of butterflies (mean \pm standard errors) of the MMZ. Different letters represent significant differences between categories ($p < 0.05$).

162 species (coverage of 99.9%). For Site 3 (moderate pollution), 1,876 individuals and 133 species were registered (coverage of 99.9%), while for Site 4 (high pollution), 1,677 individuals and 112 species (coverage of 100%).

For 0D , 1D and 2D , Site 1 (pollution free) had the highest diversity. All comparisons between sites were significantly different (with 95% confidence intervals) (Figure 3A, B and C). The one-way PERMANOVA test detected significant differences in species composition amongst Sites 1, 2 and 3 (free, low and moderate contamination) ($SS_{\text{total}} = 6.63$; $SS_{\text{within-group}} = 5.05$; $F = 4.575$, $p < 0.001$). Butterflies collected during each month for Sites 1, 2 and 3 (free, low and moderate contamination) formed separate groups in the NMDS diagram (Stress = 0.23) (Figure 5A).

Effect of seasonality on butterfly changes per pollution category

In the MMZ, the highest abundance was registered during the rainy season, while the highest species richness was shown during the dry season. The highest completeness of the inventory was recorded during the rainy season (Table 2).

The differences in the abundance of the dry and rainy season were significant ($p < 0.05$) in each site with the exception of Site 3 (moderate contamination) (Table 3, Figure 4D). Regarding diversity, the seasonal effect was absent in Site 1 (pollution free) for 0D and 1D , while for 2D , Site 1 (pollution free), 2 (low contamination) and 4 (high contamination) did not show significant differences between seasons (Figure 3D, F).

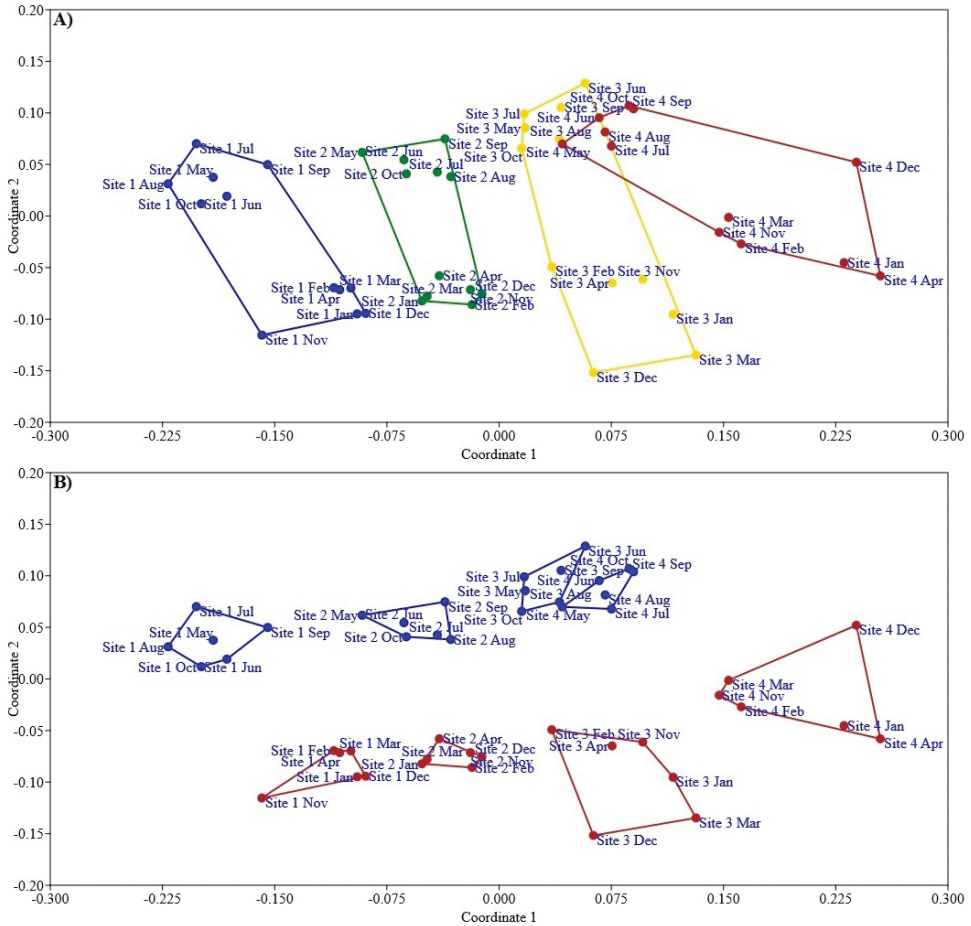


Figure 5. Non-metric multidimensional scaling ordination (NMDS) of the butterfly communities for contamination categories and seasons of the year of the MMZ **A** pollution free (blue colour), low pollution (green colour), moderate pollution (yellow colour) and high pollution (red colour) **B** rainy season (blue colour) and dry season (red colour).

Two-way PERMANOVA allowed us to identify a significant effect of season ($F = 7.702, df = 1, p < 0.001$) and pollution (site) ($F = 5.682, df = 3, p < 0.001$) on species composition, as well as an interaction effect between the two factors ($F = 2.315, df = 3, p < 0.001$). Butterflies collected each month in each of the study sites formed separated groups by seasons in the NMDS ordination diagram (Stress = 0.23) (Figure 5B).

The variables NO_2 , NO_x , $PM_{2.5}$, relative humidity and vegetation cover were highly correlated, both with abundance and species richness. The individual interaction of NO_2 , NO_x , $PM_{2.5}$ and relative humidity with abundance and species richness resulted negative, while the interaction of vegetation cover with both ecological parameters resulted positive (Table 4).

Table 3. Summary of the nested ANOVA (GLM) for the species richness and abundance of butterflies by categories of contamination and seasons of the year in the MMZ.

| Pollution categories | Estimate | 95% Lower | 95% Upper | p-Value |
|-----------------------------------|----------|-----------|-----------|---------|
| Species richness | | | | |
| Intercept | 4.277 | 4.182 | 4.371 | < 0.001 |
| Dry season (Pollution free) | -0.017 | -0.121 | 0.087 | > 0.05 |
| Rainy season (Pollution free) | 0.000 | | | |
| Dry season (Low pollution) | 0.008 | -0.104 | 0.120 | > 0.05 |
| Rainy season (Low pollution) | 0.000 | | | |
| Dry season (Moderate pollution) | 0.075 | -0.052 | 0.201 | > 0.05 |
| Rainy season (Moderate pollution) | 0.000 | | | |
| Dry season (High pollution) | -0.031 | -0.165 | 0.104 | > 0.05 |
| Rainy season (High pollution) | 0.000 | | | |
| Species abundance | | | | |
| Intercept | 5.063 | 4.999 | 5.126 | < 0.001 |
| Dry season (Pollution free) | -0.201 | -0.277 | -0.125 | < 0.001 |
| Rainy season (Pollution free) | 0.000 | | | |
| Dry season (Low pollution) | -0.165 | -0.246 | -0.083 | < 0.001 |
| Rainy season (Low pollution) | 0.000 | | | |
| Dry season (Moderate pollution) | -0.083 | -0.174 | 0.007 | > 0.05 |
| Rainy season (Moderate pollution) | 0.000 | | | |
| Dry season (High pollution) | -0.263 | -0.359 | -0.166 | < 0.001 |
| Rainy season (High pollution) | 0.000 | | | |

Table 4. Correlation analysis between environmental variables with the abundance and richness of butterfly species in the MMZ. The marked correlations (*) are significant ($p < 0.05$).

| | Abundance | Species richness |
|--|-----------|------------------|
| CO (ppm) | 0.046 | 0.137 |
| NO ₂ (ppm) | -0.725 * | -0.590 * |
| NO _x (ppm) | -0.595 * | -0.418 * |
| PM _{2.5} (µg/m ³) | -0.652 * | -0.580 * |
| Temperature (°C) | -0.003 | 0.047 |
| Relative humidity (%) | -0.487 * | -0.603 * |
| Solar radiation (Klux) | -0.007 | 0.027 |
| Vegetation cover (%) | 0.492 * | 0.481 * |

Indicator value of butterflies in a gradient of pollution

From the 209 species found in the study area, only 47 had a significant indicator value ($p < 0.05$). The highest proportion included detector species, with an IndVal between 50 and 75% (30 species). The remaining 17 were characteristic, with values greater than 75% (Table 5). *Anteros carausius* Westwood, 1851 was considered the only indicator (detector) species at Site 4 (high pollution). In Site 2 (low pollution), the species *Polygonia interrogationis* (Fabricius, 1798), *Lasaia agesilas callaina* Clench, 1972; *Cyanophrys miserabilis* (Clench, 1946), *Panoquina lucas* (Fabricius, 1793), *Strymon jojoa* (Reakirt, 1867) and *Heraclides thoas autocles* Rothschild & Jordan, 1906 were considered as detector indicator species. Likewise, 23 species were considered as detector indicators of Site 1 (free pollution), amongst which, *Quinta cannae* (Herrich-Schäffer, 1869) and *Memphis pithyusa pithyusa* (R. Felder, 1869) have the highest values of Ind-

Table 5. Butterfly species with a significant indicator value in the pollution gradient of the MMZ. Index values are expressed as a percentage. Legend: C = characteristic; D = detector; p = probability. The marked species (*) were collected with Van Someren-Rydon traps.

| Taxon | Site 1 | Site 2 | Site 3 | Site 4 | p | Indicator category |
|---|--------|--------|--------|--------|-------|--------------------|
| <i>Anteros carausius carausius</i> Westwood, 1851 | 0.0 | 0.0 | 18.2 | 53.0 | 0.001 | D |
| * <i>Polygonia interrogationis</i> (Fabricius, 1798) | 2.8 | 69.4 | 0.0 | 0.0 | 0.000 | D |
| <i>Lasaia agesilas callaina</i> Clench, 1972 | 20.8 | 63.9 | 0.0 | 0.0 | 0.004 | D |
| <i>Cyanophrys miserabilis</i> (Clench, 1946) | 18.2 | 60.6 | 0.0 | 0.0 | 0.017 | D |
| <i>Panoquina lucas</i> (Fabricius, 1793) | 9.5 | 59.5 | 0.0 | 0.0 | 0.001 | D |
| <i>Strymon yojoa</i> (Reakirt, 1867) | 13.1 | 51.8 | 0.0 | 0.0 | 0.018 | D |
| <i>Heraclides thoas autocles</i> Rothschild & Jordan, 1906 | 31.7 | 51.6 | 0.0 | 0.0 | 0.001 | D |
| <i>Quinta cannae</i> (Herrich-Schäffer, 1869) | 75.0 | 8.3 | 0.0 | 0.0 | 0.000 | D |
| * <i>Memphis pithyusa pithyusa</i> (R. Felder, 1869) | 68.5 | 0.0 | 0.0 | 0.0 | 0.001 | D |
| <i>Protographium epidaus epidaus</i> (Doubleday, 1846) | 66.7 | 0.0 | 0.0 | 0.0 | 0.001 | D |
| <i>Heraclides anchisiades idaeus</i> Fabricius, 1793 | 66.7 | 0.0 | 0.0 | 0.0 | 0.013 | D |
| <i>Atlixes halesus corcorani</i> Clench, 1942 | 66.7 | 0.0 | 0.0 | 0.0 | 0.001 | D |
| <i>Michaelus hecate</i> (Godman y Salvin, 1887) | 66.7 | 0.0 | 0.0 | 0.0 | 0.000 | D |
| * <i>Temenis laotboe</i> (Cramer, 1777) | 66.7 | 0.0 | 0.0 | 0.0 | 0.001 | D |
| <i>Thorybes pylades albosuffusa</i> H. Freeman, 1943 | 66.7 | 0.0 | 0.0 | 0.0 | 0.001 | D |
| <i>Autochton cellus</i> (Boisduval & Le Conte, 1837) | 66.7 | 0.0 | 0.0 | 0.0 | 0.018 | D |
| <i>Calephelis rawsoni</i> McAlpine, 1939 | 64.8 | 11.1 | 0.0 | 0.0 | 0.020 | D |
| * <i>Asterocampa idyja argus</i> (H. Bates, 1864) | 64.3 | 21.4 | 0.0 | 0.0 | 0.001 | D |
| <i>Strymon bazochii bazochii</i> (Godart, 1824) | 61.1 | 0.0 | 0.0 | 0.0 | 0.001 | D |
| * <i>Limenitis arthemis astyanax</i> (Fabricius, 1775) | 59.5 | 0.0 | 0.0 | 0.0 | 0.021 | D |
| <i>Eurema daira eugenia</i> (Wallengren, 1860) | 56.9 | 35.9 | 0.0 | 0.0 | 0.002 | D |
| <i>Anteos clorinde</i> (Godart, 1824) | 56.8 | 23.8 | 0.0 | 0.0 | 0.002 | D |
| <i>Polyctor enops</i> (Godman & Salvin, 1894) | 56.7 | 0.0 | 0.0 | 0.0 | 0.006 | D |
| <i>Anthanassa tulcis</i> (H. Bates, 1864) | 55.2 | 37.4 | 0.0 | 0.0 | 0.000 | D |
| <i>Rekoa zebina</i> (Hewitson, 1869) | 54.8 | 19.0 | 0.0 | 0.0 | 0.011 | D |
| <i>Eurema boisduvaliana</i> (C. Felder & R. Felder, 1865) | 51.0 | 10.3 | 25.6 | 0.0 | 0.004 | D |
| * <i>Megisto rubricata rubricata</i> (W. H. Edwards, 1871) | 50.0 | 0.0 | 0.0 | 0.0 | 0.009 | D |
| <i>Carrhenes canescens canescens</i> (R. Felder, 1869) | 50.0 | 0.0 | 0.0 | 0.0 | 0.008 | D |
| <i>Wallengrenia otho otho</i> (J. E. Smith, 1797) | 50.0 | 0.0 | 0.0 | 0.0 | 0.009 | D |
| <i>Anatrytone mazai</i> (H. Freeman, 1969) | 50.0 | 0.0 | 0.0 | 0.0 | 0.009 | D |
| <i>Pyrisitia dina westwoodii</i> (Boisduval, 1836) | 100.0 | 0.0 | 0.0 | 0.0 | 0.000 | C |
| <i>Heliconius erato petiverana</i> (E. Doubleday, 1847) | 100.0 | 0.0 | 0.0 | 0.0 | 0.000 | C |
| <i>Timochares ruptifasciata</i> (Plötz, 1884) | 100.0 | 0.0 | 0.0 | 0.0 | 0.000 | C |
| <i>Eumaeus childrenae</i> (G. Gray, 1832) | 90.7 | 0.0 | 0.0 | 0.0 | 0.000 | C |
| <i>Dymasia dymas dymas</i> (W. H. Edwards, 1877) | 90.7 | 0.0 | 0.0 | 0.0 | 0.002 | C |
| <i>Leptophobia aripa elodia</i> (Boisduval, 1836) | 90.4 | 0.0 | 0.0 | 0.0 | 0.001 | C |
| <i>Cyanophrys herodotus</i> (Fabricius, 1793) | 83.3 | 0.0 | 0.0 | 0.0 | 0.000 | C |
| <i>Anthanassa ardyis</i> (Hewitson, 1864) | 83.3 | 0.0 | 0.0 | 0.0 | 0.004 | C |
| <i>Sostrata nordica</i> Evans, 1953 | 83.3 | 0.0 | 0.0 | 0.0 | 0.000 | C |
| <i>Parides erithalion polyzelus</i> (C. Felder & R. Felder, 1865) | 83.3 | 0.0 | 0.0 | 0.0 | 0.000 | C |
| <i>Allosmaitia strophius</i> (Godart, 1824) | 83.3 | 0.0 | 0.0 | 0.0 | 0.003 | C |
| <i>Strymon bebrycia</i> (Hewitson, 1868) | 83.3 | 0.0 | 0.0 | 0.0 | 0.000 | C |
| <i>Timolus ecbion ecbiolus</i> (Draudt, 1920) | 83.3 | 0.0 | 0.0 | 0.0 | 0.000 | C |
| <i>Heliopterus macaira macaira</i> (Reakirt, 1867) | 83.3 | 0.0 | 0.0 | 0.0 | 0.000 | C |
| <i>Cynaenes trebius</i> (Mabille, 1891) | 83.3 | 0.0 | 0.0 | 0.0 | 0.000 | C |
| <i>Staphylus azteca</i> (Scudder, 1872) | 83.3 | 0.0 | 0.0 | 0.0 | 0.003 | C |
| <i>Pterourus palamedes leontis</i> Rothschild & Jordan, 1906 | 76.5 | 0.0 | 0.0 | 0.0 | 0.001 | C |

Val. In Site 1, 17 species were considered as characteristic indicator species, those being *Pyrisitia dina westwoodii* (Boisduval, 1836), *Heliconius erato petiverana* (E. Doubleday, 1847) and *Timochares ruptifasciata* (Plötz, 1884) with the highest IndVal (Table 5).

Discussion

This study constitutes the first faunistic contribution of butterflies as indicators of the environmental quality of an urban area in Mexico and the first inventory of butterflies systematically carried out in the State of Nuevo León. The 209 registered species in the MMZ constitute 78.6% of the described richness so far in Nuevo Leon, according to Luz and Madero (2011) in collaboration with the North American Butterfly Association (NABA) and 10.2% to what was recorded for Mexico (Warren 2000; Llorente et al. 2006). However, it should be noted that urban gradient studies are clearly a simplification of the complex patterns produced by urbanisation (Alberti et al. 2001; Hahs and McDonnell 2006; McKinney 2008). The specific impacts of urbanisation on species richness vary, depending on variables, such as geographic location and many historical and economic factors that are unique to each city (McKinney 2008).

Urbanisation intensity is correlated with increased disturbance and structural simplification of the remaining vegetation through landscaping practices that remove woody plants, leaf litter and other microhabitats from natural communities (Marzluff and Ewing 2001). Combination of all these factors reduces the area and quality of animal habitat and tends to increase with the intensity of urbanisation (Alberti et al. 2001; Hahs and McDonnell 2006). Studies using spatial gradients in urban areas have shown that the development of these areas can strongly and negatively affect many sensitive butterfly species (Blair and Launer 1997; Blair 1999; Clark et al. 2007). The close relationship between the abundance of host plants and the persistence status of butterflies suggests that the decline of plants may cause the co-extinction of some associated butterflies (Koh et al. 2004) or the host plant's own rarity (rather than decrease) could be associated with another trait of the butterfly that makes it vulnerable to extirpation (Harrison 1991). Corke (1999), Mulder et al. (2005) and Öckinger et al. (2006) suggest that the butterfly decline in urban areas could be a secondary effect of heavy metal stress presence on local plants, not resulting in a decrease in the number of host-plants, but in a selective pressure of pollutants on the plant vigour, subsequently affecting their associated fauna. Either way, our results corroborate similar studies of declining butterfly populations, suggesting that habitat degradation may be a devastating threat to the persistence of certain sensitive taxa, such as butterflies characteristic of unpolluted and low-pollution sites (Schultz and Dlugosch 1999; Weiss 1999; Wagner and Van Driesche 2010; Bonebrake and Cooper 2014).

A study of butterfly communities in fragments of urban forests in Brazil (Brown and Freitas 2002) similarly found that the most important factors affecting diversity and composition, excluding site size and sampling time, were connectivity, vegetation, flowers and negative human impact, such as pollution (indirect effect of urbanisation). Observations of butterfly diversity provide information on variations in species richness and abundance formed by vegetation throughout the landscape and the interaction between species (Öckinger et al. 2009). Although local determinants of diversity, such as competition and predation, remained undetermined in these studies, to a large extent, landscape characteristics influence butterfly richness and abundance in different geographic areas (Öckinger et al. 2006; Öckinger et al. 2009). Spatial scale differ-

ences in butterfly diversity can be attributed to heterogeneity at the landscape level, while timescale differences can be attributed to changes in climatic conditions at both local and regional scales (Mukherjee et al. 2015). In the current context, it can be assumed that butterfly diversity varies in the four sampling sites as a matter of differences in pollutants concentration and composition of vegetation.

In general, the differences in species distribution in the four areas were prominent, although the abundance of the different species was not profound (indirect effect of the high degree of urbanisation), possibly due to the high concentrations of the contaminants, as well as the corresponding abundance of host plants in the affected areas. The observed variations in species richness in areas without apparent pollution provide an impression of differences in food plants abundance and landscape characteristics in the region. Previous studies on the diversity of butterflies in landscapes with high pollution in contrast to the regions of moderate and low pollution show that the richness increased with the availability of green space and the heterogeneity of habitats in terms of the available plant species and dominant microenvironmental conditions (Kuussaari et al. 2007). According to these studies, our observations register a greater diversity in the areas with no apparent pollution and low urbanisation, followed by the areas of low, moderate and high pollution and urbanisation (Blair and Launer 1997; Kitahara and Sei 2001; Hogsden and Hutchinson 2004).

Regardless of variations between different landscapes, observations of butterfly diversity in the study area suggest that conservation management is necessary to ensure the livelihood of the different ecosystem services derived from butterflies. The abundance of butterflies in urban landscapes will promote the pollination and hence the propagation of different plant species that can reduce the decrease in vegetation, consequently diminishing other variables, such as noise and mainly pollution levels (Mukherjee et al. 2015; Selmi et al. 2016; Alfie and Salinas 2017). To understand the ways these insects respond to urbanisation, different authors have suggested three ecological patterns that are related to our results: (1) there are fewer butterfly species in highly urbanised areas (Knapp et al. 2008; Soga et al. 2014); (2) the number of specialised butterflies decreases with increasing urbanisation, a case demonstrated by the number of indicator species in each gradient category (Bergerot et al. 2011; Lizée et al. 2011; Soga and Koike 2012, 2013); and (3) urbanisation can lead to local disappearance of rare and not abundant, specialised butterfly species, as shown in this study (Fattorini 2011; Soga and Koike 2012).

We found that the variables associated with the increase in urbanisation (NO_2 , NO_x and $\text{PM}_{2.5}$) were negatively correlated with the richness of butterflies, while the measures associated with less developed areas (green space) were positively correlated. These results are consistent with those of Ruszczyk (1986), Ruszczyk and DeAraujo (1992) and Stefanescu et al. (2004), who found lower diversity of species with higher urbanisation. Growing more trees and shrubs that provide nectar for adult butterflies and using a greater variety of larval food plants species in planting schemes, may be more effective in maintaining populations of these insects than simply increasing the amount of plant cover cultivated (Koh and Sodhi 2004).

The richness and distribution of butterfly species fluctuates according to their life cycle, which is linked to seasonal changes. However, compared to butterflies in temperate climates, seasonal variation generally does not have a great impact on tropical butterflies, which are reported as well distributed throughout the year, the case corresponding to the present study, as there is no seasonal differentiation for most of the comparisons (Hamer et al. 2005). In the MMZ, the butterflies showed a highest species richness during the dry season with 88% of the total species observed during the evaluation period. This finding is contrary to other studies, which report higher numbers in the rainy season (Devries et al. 1997; Hamer et al. 2005; Hernández-Mejía et al. 2008; Meléndez-Jaramillo et al. 2019). This can be attributed to human intervention, when irrigation provides higher food resources for butterflies and also attracts a higher number of species than normal during the dry season.

Biodiversity inventories provide crucial reference information for future ecological and conservation studies. The existence of species lists at various stages of the urbanisation process allows documentation of changes in species composition over time. However, few lists of butterfly species have been published in cities, most of which are restricted to few countries, for example, Brasil, Argentina or India (Núñez 2008; Chowdhury and Soren 2011; Silva et al. 2012). Until now, significant efforts have been made in and around cities to conserve endangered butterfly species (Daniels 2009; Ramírez and MacGregor 2016). Butterfly conservation in urban areas is a feasible task, since many species can thrive in these areas. Hopefully, creative urban planning and management, such as habitat design and planting of native, nectar-rich plants, could improve urban habitats for butterflies. However, all actions must be monitored and must build on prior knowledge about the biology and ecology of the target species to be successful (Snep et al. 2006; Kadlec et al. 2008).

Conclusions

For the first time in Mexico, butterflies were systematically sampled in order to monitor the environmental quality in an urban area. A total of 8,570 specimens belonging to six families, 19 subfamilies, 31 tribes, 138 genera and 209 species of butterflies were collected for the study area. The highest species abundance and richness, as well as alpha diversity, are recorded at the site free from air pollution, that is associated with a less impacted landscape. Both species richness and abundance were significantly different between all sites, except for the comparison between the moderate contamination site and the high contamination site, while diversity decreased significantly with increasing levels of contamination. The overall trend of distribution of butterflies to the levels of air pollution shown in the Monterrey Metropolitan Area is a decrease, this being in agreement with the general disturbance hypothesis.

The seasonality effect was absent on species richness; however, for species abundance, the differences between dry season and rainy season were significant in each site, excepting the moderate contamination site. Regarding diversity, the seasonal effect

showed different distribution patterns according to each order. The variables NO_2 , NO_x , $\text{PM}_{2.5}$, relative humidity and vegetation cover, were highly correlated, both with species abundance and richness, so they could be the main reasons for the variation of butterfly communities in this study.

This work is one of the first studies of butterflies in a specific area of northeast Mexico, in which the environmental quality and seasonality in an urban area were analysed. The information presented here provides benchmarks that allow the comparison of the diversity and richness of Papilionoidea species at regional and national levels. This information can be used as an initial step to analyse the possible use of butterflies as an indicator group of the biodiversity in Mexico.

Acknowledgements

The first author recognises the great support of the Cantú Bendeck family for their kindness during the development of the collections. Bernal Herrera Fernández provided support and recommendations during the planning of this investigation. Consejo Nacional de Ciencia y Tecnología of Mexico (CONACYT) gave financial support to carry out this study (Doctoral scholarship No. 704911).

References

- Alanís GJ (2005) El arbolado urbano en el área metropolitana de Monterrey. *Ciencias UANL* 8(1): 20–32.
- Alberti M, Botsford E, Cohen A (2001) Quantifying the urban gradient: linking urban planning and ecology. In: Marzluff JM, Bowman R, Donnelly R (Eds) *Avian Ecology in an Urbanizing World*. Kluwer, Norwell, Massachusetts, 68–85. https://doi.org/10.1007/978-1-4615-1531-9_5
- Alfie CM, Salinas CO (2017) Ruido en la ciudad. *Contaminación auditiva y ciudad caminable. Estudios demográficos y urbanos* 32(1): 65–96.
- Andrade MG, Bañol ERH, Triviño P (2013) Técnicas y procesamiento para la recolección, preservación y montaje de mariposas diurnas en estudios de biodiversidad y conservación (Lepidoptera: Hesperioidea y Papilionoidea). *Revista de la Academia Colombiana de Ciencias* 37(144): 311–325. <https://doi.org/10.18257/raccefyn.12>
- Arreola JL, González G (1999) Análisis espectral del viento y partículas menores de 10 micrómetros (PM10) en el área Metropolitana de Monterrey México, *Revista Internacional de Contaminación Ambiental* 15(2): 95–102.
- Badillo CT, Garza L, Garza MCH, Zanatta MT, Caballero A (2015) Heavy metal content in PM2.5 air samples collected in the Metropolitan Area of Monterrey, México. *Human and Ecological Risk Assessment* 21(8): 2022–2035. <https://doi.org/10.1080/10807039.2015.1017873>
- Bergerot B, Fontaine B, Julliard R, Baguette M (2011) Landscape variables impact the structure and composition of butterfly assemblages along an urbanization gradient. *Landscape Ecology* 26(1): 83–94. <https://doi.org/10.1007/s10980-010-9537-3>

- Blair RB (1999) Birds and butterflies: surrogate taxa for assessing biodiversity? *Ecological Applications* 9(1): 164–170. [https://doi.org/10.1890/1051-0761\(1999\)009\[0164:BABAAU\]2.0.CO;2](https://doi.org/10.1890/1051-0761(1999)009[0164:BABAAU]2.0.CO;2)
- Blair RB, Launer AE (1997) Butterfly diversity and human land use: species assemblages along an urban gradient. *Biological Conservation* 80: 113–125. [https://doi.org/10.1016/S0006-3207\(96\)00056-0](https://doi.org/10.1016/S0006-3207(96)00056-0)
- Bonebrake TC, Cooper DS (2014) A Hollywood drama of butterfly extirpation and persistence over a century of urbanization. *Journal of Insect Conservation* 18(4): 683–692. <https://doi.org/10.1007/s10841-014-9675-z>
- Brown Jr KS, Freitas AVL (2002) Butterfly communities of urban forest fragments in Campinas, São Paulo, Brazil: Structure, instability, environmental correlates, and conservation. *Journal of Insect Conservation* 6(4): 217–231.
- Butchart SH, Walpole M, Collen B, van Strien A, Scharlemann JPW, Almond REA, Baillie JEM, Bomhard B, Brown C, Bruno J, Carpenter KE, Carr GM, Chanson J, Chenery AM, Csirke J, Davidson NC, Dentener F, Foster M, Galli A, Galloway JN, Genovesi P, Gregory RD, Hockings M, Kapos V, Lamarque J-F, Leverington F, Loh J, McGeoch MA, McRae L, Minasyan A, Morcillo MH, Oldfield TEE, Pauly D, Quader S, Revenga C, Sauer JR, Skolnik B, Spear D, Stanwell-Smith D, Stuart SN, Symes A, Tierney M, Tyrrell TD, Vié J-C, Watson R (2010) Global biodiversity: indicators of recent declines. *Science* 328: 1164–1168. <https://doi.org/10.1126/science.1187512>
- Cantú C, Rovalo M, Marmolejo J, Ortiz S, Serriñá F (2013) Historia natural del Parque Nacional Cumbres de Monterrey. Universidad Autónoma de Nuevo León, Conanp, Pronatura. Monterrey, N.L, México.
- Cerón JG, Cerón RM, Kahl JDW, Ramírez LE, Guarnaccia C, Aguilar CA, Montalvo RC, Anguebes F, López CU (2014) Diurnal and seasonal variation of BTEX in the air of Monterrey, Mexico: preliminary study of sources and photochemical ozone pollution. *Air Quality, Atmosphere & Health* 8(5): 469–482. <https://doi.org/10.1007/s11869-014-0296-1>
- Chao A, Gotelli NJ, Hsieh TC, Sander EL, Ma KH, Colwell, RK, Ellison AM (2014) Rarefaction and extrapolation with Hill numbers: a framework for sampling and estimation in species diversity studies. *Ecological Monographs* 84: 45–67. <https://doi.org/10.1890/13-0133.1>
- Chao A, Jost L (2012) Coverage-based rarefaction and extrapolation: standardizing samples by completeness rather than size. *Ecology* 93(12): 2533–2547. <https://doi.org/10.1890/11-1952.1>
- Chao A, Jost L (2015) Estimating diversity and entropy profiles via discovery rates of new species. *Methods in Ecology and Evolution* 6(8): 873–882. <https://doi.org/10.1111/2041-210X.12349>
- Chao A, Ma KH, Hsieh TC, Chiu CH (2016) SpadeR (Species-richness prediction and diversity estimation in R): an R package in CRAN. Program and User's Guide also published at http://chao.stat.nthu.edu.tw/wordpress/software_download/.
- Chowdhury S, Hesselberg T, Böhm M, Islam MR, Aich U (2017) Butterfly diversity in a tropical urban habitat (Lepidoptera: Papilionoidea). *Oriental Insects* 51(4): 417–430. <https://doi.org/10.1080/00305316.2017.1314230>
- Chowdhury S, Soren R (2011) Butterfly (Lepidoptera: Rhopalocera) fauna of East Calcutta wetlands, West Bengal, India. *Check List* 7: 700–703. <https://doi.org/10.15560/10960>

- Clark PJ, Reed JM, Chew FS (2007) Effects of urbanization on butterfly species richness, guild structure, and rarity. *Urban Ecosystems* 10(3): 321–337. <https://doi.org/10.1007/s11252-007-0029-4>
- Corke D (1999) Are Honeydew/Sap-feeding Butterflies (Lepidoptera: Rhopalocera) affected by particulate air-pollution? *Journal of Insect Conservation* 3(1): 5–14.
- Daniels JC (2009) Cooperative conservation efforts to help recover an endangered south Florida butterfly. *Insect Conservation and Diversity* 2(1): 62–64. <https://doi.org/10.1111/j.1752-4598.2008.00039.x>
- Defra (2016) UK Biodiversity Indicators 2015. Department for Environment, Food and Rural Affairs, London.
- Devries PJ, Murray D, Lande R (1997) Species diversity in vertical, horizontal, and temporal dimensions of a fruit-feeding butterfly community in an Ecuadorian rainforest. *Biological Journal of the Linnean Society* 62(3): 343–364. <https://doi.org/10.1111/j.1095-8312.1997.tb01630.x>
- Di Mauro D, Dietz T, Rockwood L (2007) Determining the effect of urbanization on generalist butterfly species diversity in butterfly gardens. *Urban Ecosystems* 10(4): 427–439. <https://doi.org/10.1007/s11252-007-0039-2>
- Dial R, Roughgarden J (1998) Theory of marine communities: the intermediate disturbance hypothesis. *Ecology* 79(4): 1412–1424. [https://doi.org/10.1890/0012-9658\(1998\)079\[1412:TOMCTI\]2.0.CO;2](https://doi.org/10.1890/0012-9658(1998)079[1412:TOMCTI]2.0.CO;2)
- Dufrene M, Legendre P (1997) Species assemblages and indicator species: the need for a flexible asymmetrical approach. *Ecological Monographs* 67(3): 345–366. <https://doi.org/10.2307/2963459>
- Fagua G (2001) Manual de metodologías para el desarrollo de Inventarios y Monitoreo de la Biodiversidad: Mariposas diurnas (Lepidoptera) Grupo de Exploración y Monitoreo ambiental, Bogotá, Colombia.
- Fattorini S (2011) Insect extinction by urbanization: A long term study in Rome. *Biological Conservation* 144(1): 370–375. <https://doi.org/10.1016/j.biocon.2010.09.014>
- García JF, Ospina LA, Villa FA, Reinoso G (2007) Diversidad y distribución de mariposas Satyrinae (Lepidoptera: Nymphalidae) en la cuenca del río Coello, Colombia. *Revista de Biología Tropical* 55(2): 645–653. <https://doi.org/10.15517/rbt.v55i2.6039>
- García M, Ramírez H, Ulloa H, García O, Meulenert Á, Alcalá J (2013) Concentración de contaminantes SO₂, NO₂ y correlación con H⁺, SO₄²⁻ y NO₃⁻ durante la temporada de lluvias en la Zona Metropolitana de Guadalajara, Jalisco, México. *Revista chilena de enfermedades respiratorias* 29(2): 81–88. <https://doi.org/10.4067/S0717-73482013000200004>
- García M, Sánchez HUR, Godínez HU, Pérez A, Arias S (2012) Las inversiones térmicas y la contaminación atmosférica en la zona Metropolitana de Guadalajara (México) *Investigaciones geográficas* (58): 9–29. <https://doi.org/10.14198/INGEO2012.58.01>
- Garwood K, Lehman R (2005) Butterflies of Northeastern Mexico. Nuevo León, San Luis Potosí and Tamaulipas. A Photographic Checklist (2nd edn.) Eye Scry Publishing, McAllen, Texas, 194 pp.
- Giuliano WM, Accamando AK, Mcadams EJ (2004) Lepidoptera-habitat relationships in urban parks. *Urban Ecosystems* 7(4): 361–370. <https://doi.org/10.1007/s11252-005-6835-7>

- Glassberg J (2018) *A Swift Guide to the Butterflies of Mexico and Central America*. Sunstreak books, Morristown, 304 pp. <https://doi.org/10.1515/9781400889860>
- González SO, Badillo CT, Kahl JD, Ramírez LE, Balderas RI (2011) Temporal Analysis of PM₁₀ in Metropolitan Monterrey, México. *Journal of the Air & Waste Management Association* 61(5): 573–579. <https://doi.org/10.3155/1047-3289.61.5.573>
- Gupta H, Tiwari C, Diwakar S (2019) Butterfly diversity and effect of temperature and humidity gradients on butterfly assemblages in a sub-tropical urban landscape. *Tropical Ecology* 60(1): 150–158. <https://doi.org/10.1007/s42965-019-00019-y>
- Hahs AK, McDonnell MJ (2006) Selecting independent measures to quantify Melbourne's urban-rural gradient. *Landscape and Urban Planning* 78(4): 435–448. <https://doi.org/10.1016/j.landurbplan.2005.12.005>
- Hamer KC, Hill JK, Mustafa N, Benedick S, Sherratt TN, Chey VK, Maryati M (2005) Temporal variation in abundance and diversity of butterflies in Bornean rain forests: opposite impacts of logging recorded in different seasons. *Journal of Tropical Ecology* 21(4): 417–425. <https://doi.org/10.1017/S0266467405002361>
- Hardy PB, Dennis RL (1999) The impact of urban development on butterflies within a city region. *Biodiversity and Conservation* 8(9): 1261–1279. <https://doi.org/10.1023/A:1008984905413>
- Harrison S (1991) Local extinction in a metapopulation context: an empirical evaluation. *Biological Journal of the Linnean Society* 42(1-2): 73–88. <https://doi.org/10.1111/j.1095-8312.1991.tb00552.x>
- Hernández-Mejía C, Llorente JB, Vargas IF, Luis AM (2008) Las mariposas (Papilionoidea y Hesperioidea) de Malinalco, Estado de México. *Revista Mexicana de Biodiversidad* 79: 117–130.
- Hill MO (1973) Diversity and Evenness: A unifying notation and its consequences. *Ecology* 54(2): 427–432. <https://doi.org/10.2307/1934352>
- Hogsden KL, Hutchinson TC (2004) Butterfly assemblages along a human disturbance gradient in Ontario, Canada. *Canadian Journal of Zoology* 82(5): 739–748.
- Hsieh TC, Ma KH, Chao A (2016) iNEXT: An R package for interpolation and extrapolation of species diversity (Hill numbers). To appear in *Methods in Ecology and Evolution*.
- INEGI (2010) Estadísticas de vehículos de motor registrados en circulación. Información estadística. Instituto Nacional de Estadística y Geografía, México D. F.
- INEGI (2011) XIII Censo de Población y Vivienda de México, Resultados definitivos. Instituto Nacional de Estadística y Geografía. México, D. F.
- INEGI (2016) Conjunto de Datos Vectoriales de Uso de Suelo y Vegetación. Escala: 1: 250 000. Serie VI (Capa Union) Edición: 1. Instituto Nacional de Estadística y Geografía. Aguascalientes, México.
- Jones EL, Leather SR (2012) Invertebrates in urban areas: A review. *European Journal of Entomology* 109(4): 463–478. <https://doi.org/10.14411/eje.2012.060>
- Kadlec T, Benes J, Jarosik V, Konvička M (2008) Revisiting urban refuges: Changes of butterfly and bumblebee fauna in Prague reserves over three decades. *Landscape and Urban Planning* 85(1): 1–11. <https://doi.org/10.1016/j.landurbplan.2007.07.007>

- Kitahara M, Sei K (2001) A comparison of the diversity and structure of butterfly communities in semi-natural and human-modified grassland habitats at the foot of Mt. Fuji, central Japan. *Biodiversity and Conservation* 10(3): 331–351. <https://doi.org/10.1023/A:1016666813655>
- Knapp S, Kühn I, Mosbrugger V, Klotz S (2008) Do protected areas in urban and rural landscapes differ in species diversity? *Biodiversity and Conservation* 17(7): 1595–1612.
- Koh LP, Sodhi NS (2004) Importance of reserves, fragments, and parks for butterfly conservation in a tropical urban landscape. *Ecological Applications* 14(6): 1695–1708. <https://doi.org/10.1890/03-5269>
- Koh LP, Sodhi NS, Brook BW (2004) Ecological correlates of extinction proneness in tropical butterflies. *Conservation Biology* 18(6): 1571–1578. <https://doi.org/10.1111/j.1523-1739.2004.00468.x>
- Konvička M, Kadlec T (2011) How to increase the value of urban areas for butterfly conservation? A lesson from Prague nature reserves and parks. *European Journal of Entomology* 108(2): 219–229. <https://doi.org/10.14411/eje.2011.030>
- Kremen CRK, Colwell TL, Erwin DD, Murphy RF, Sanjayan MA (1993) Terrestrial arthropod assemblages: their use in conservation planning. *Conservation Biology* 7: 796–808. <https://doi.org/10.1046/j.1523-1739.1993.740796.x>
- Kuussaari M, Heliölä J, Luoto M, Pöyry J (2007) Determinants of local species richness of diurnal Lepidoptera in boreal agricultural landscapes. *Agriculture, Ecosystems Environment* 122(3): 366–376. <https://doi.org/10.1016/j.agee.2007.02.008>
- Lezama JL, Graizbord B (2010) Los Grandes Problemas de México. IV Medio Ambiente. 1a. Edición. El Colegio de México. México, D. F. <https://www.jstor.org/stable/j.ctt1657t3w>
- Li X Luo Y, Zhang Y, Schweiger O, Settele J, Yang Q (2009) On the conservation biology of a Chinese population of the birdwing *Troides aeacus* (Lepidoptera: Papilionidae) *Journal of Insect Conservation* 14(3): 257–268. <https://doi.org/10.1007/s10841-009-9254-x>
- Lizée M, Bonardo R, Mauffrey J, Bertaudière V, Taton T, Deschamps-Cottin M (2011) Relative importance of habitat and landscape scales on butterfly communities of urbanizing areas. *Comptes Rendus Biologies* 334(1): 74–84. <https://doi.org/10.1016/j.crv.2010.11.001>
- Llorente JB, Luis AM, Vargas IF (2006) Apéndice general de Papilionoidea: Lista sistemática, distribución estatal y provincias biogeográficas. In: Morrone JJ, Llorente JB (Eds) Componentes bióticos principales de la entomofauna mexicana, vol. II. Las Prensas de Ciencias, Facultad de Ciencias, UNAM, México, D. F., 945–1009.
- Llorente JB, Oñate LO, Luis AM, Vargas IF (1997) Papilionidae y Pieridae de México: distribución geográfica e ilustración. Facultad de Ciencias, Universidad Nacional Autónoma de México/ Comisión Nacional para el Uso y Conocimiento de la Biodiversidad, México, 235 pp.
- López E, Bocco G, Mendoza M, Duhau E (2001) Predicting land-cover and land-use change in the urban fringe. *Landscape and Urban Planning* 55(4): 271–285. [https://doi.org/10.1016/S0169-2046\(01\)00160-8](https://doi.org/10.1016/S0169-2046(01)00160-8)
- Luis AM, Llorente JB, Vargas IF (2003) Nymphalidae de México I. Danainae, Apaturinae, Biblidinae y Heliconiinae: distribución geográfica e ilustración. Comisión Nacional para el Conocimiento y Uso de la Biodiversidad/ Universidad Nacional Autónoma de México, México, 249 pp.

- Luis AM, Llorente JB, Vargas IF, Pozo C (2010) Nymphalidae de México III. Nymphalinae: distribución geográfica e ilustración. Las Prensas de Ciencias, Facultad de Ciencias, UNAM, México, 196 pp.
- Luna MR, Llorente JB, Luis AM, Vargas IF (2010) Composición faunística y fenología de las mariposas (Rhopalocera: Papilionoidea) de Cañón de Lobos, Yautepec, Morelos, México. *Revista Mexicana de Biodiversidad* 81: 315–342. <https://doi.org/10.22201/ib.20078706e.2010.002.257>
- Luz M de la, Madero A (2011) Guía de mariposas de Nuevo León. Fondo Editorial de Nuevo León, UANL, México, 366 pp.
- Magle SB, Hunt VM, Vernon M, Crooks KR (2012) Urban wildlife research: Past, present, and future. *Biological Conservation* 155: 23–32. <https://doi.org/10.1016/j.biocon.2012.06.018>
- Mancilla Y, Herckes P, Fraser MP, Mendoza A (2015) Secondary organic aerosol contributions to PM_{2.5} in Monterrey, Mexico: Temporal and seasonal variation. *Atmospheric Research* 153: 348–359. <https://doi.org/10.1016/j.atmosres.2014.09.009>
- Marzluff JM, Ewing K (2001) Restoration of fragmented landscapes for the conservation of birds: A general framework and specific recommendations for urbanizing landscapes. *Restoration Ecology* 9(3): 280–292. <https://doi.org/10.1046/j.1526-100x.2001.009003280.x>
- McGeoch MA, Rensburg BJV, Botes A (2002) The verification and application of bioindicators: a case study of dung beetles in a savanna ecosystem. *Journal of Applied Ecology* 39: 661–672. <https://doi.org/10.1046/j.1365-2664.2002.00743.x>
- McIntyre NE (2000) Ecology of urban arthropods: a review and a call to action. *Annals of the Entomological Society of America* 93: 825–835. [https://doi.org/10.1603/0013-8746\(2000\)093\[0825:EOUAAR\]2.0.CO;2](https://doi.org/10.1603/0013-8746(2000)093[0825:EOUAAR]2.0.CO;2)
- McKinney ML (2008) Effects of urbanization on species richness: A review of plants and animals. *Urban Ecosystems* 11(2): 161–176. <https://doi.org/10.1007/s11252-007-0045-4>
- Meléndez-Jaramillo E, Cantú-Ayala C, Sánchez-Reyes UJ, Sandoval-Becerra FM, Herrera-Fernández B (2019) Altitudinal and seasonal distribution of butterflies (Lepidoptera, Papilionoidea) in Cerro Bufo El Diente, Tamaulipas, Mexico. *ZooKeys* 900: 31–68. <https://doi.org/10.3897/zookeys900.36978>
- Menchaca HL, Mercado R, Mendoza A (2015) Diurnal and seasonal variation of volatile organic compounds in the atmosphere of Monterrey, Mexico. *Atmospheric Pollution Research* 6(6): 1073–1081. <https://doi.org/10.1016/j.apr.2015.06.004>
- Moreno CE, Sánchez-Rojas G, Escobar F, Pineda E (2007) Atajos para la evaluación de la biodiversidad: una revisión de la terminología y recomendaciones para el uso de grupos objetivo, bioindicadores y sustitutos. *IJEnvH's* 1: 71–86. <https://doi.org/10.1504/IJENVH.2007.012225>
- Mukherjee S, Banerjee S, Saha GK, Basu P, Aditya G (2015) Butterfly diversity in Kolkata, India: An appraisal for conservation management. *Journal of Asia-Pacific Biodiversity* 8(3): 210–221. <https://doi.org/10.1016/j.japb.2015.08.001>
- Mulder C, Aldenberg T, de Zwart D, van Wijnen HJ, Breure AM (2005) Evaluating the impact of pollution on plant-Lepidoptera relationships. *Environmetrics* 16(4): 357–373. <https://doi.org/10.1002/env.706>

- Niell RS (2001) Butterfly community change in response to rural residential development. Masters Thesis, University of Nevada, Reno, NV.
- Núñez E (2008) Las especies urbanas de Rhopalocera de la Reserva Ecológica Costanera Sur, Ciudad de Buenos Aires, Argentina (Lepidoptera: Hesperioidea y Papilionoidea) SHILAP Revista de Lepidopterología 36: 435–447.
- Öckinger E, Dannestam A, Smith HG (2009) The importance of fragmentation and habitat quality of urban grasslands for butterfly diversity. *Landscape and Urban Planning* 93(1): 31–37. <https://doi.org/10.1016/j.landurbplan.2009.05.021>
- Öckinger E, Eriksson AK, Smith HG (2006) Effects of grassland abandonment, restoration and management on butterflies and vascular plants. *Biological Conservation* 133(3): 291–300. <https://doi.org/10.1016/j.biocon.2006.06.009>
- Öckinger E, Hammarstedt O, Nilsson SG, Smith HG (2006) The relationship between local extinctions of grassland butterflies and increased soil nitrogen levels. *Biological Conservation* 128(4): 564–573. <https://doi.org/10.1016/j.biocon.2005.10.024>
- Oksanen J, Blanchet FG, Friendly M, Kindt R, Legendre P, McGlenn D, Minchin PR, O’Hara RB, Simpson GL, Solymos P, Stevens MHH, Szoecs E, Wagner H (2019) vegan: Community Ecology Package. R package version 2.5–4. <https://CRAN.R-project.org/package=vegan>
- Orta ST, Ochoa AC, Carrizalez L, Varela JA, Pérez FJ, Pruneda LG, Torres A, Guzmán JL, Pérez IN (2016) Persistent organic pollutants and heavy metal concentrations in soil from the Metropolitan Area of Monterrey, Nuevo Leon, Mexico. *Archives of Environmental Contamination and Toxicology* 70(3): 452–463. <https://doi.org/10.1007/s00244-015-0239-3>
- Philips KH, Kobiela ME, Snell EC (2017) Developmental lead exposure has mixed effects on butterfly cognitive processes. *Animal Cognition* 20(1): 87–96. <https://doi.org/10.1007/s10071-016-1029-7>
- Quantum GIS Development Team (2018) Quantum GIS Geographic Information System. Open Source Geospatial Foundation Project. <https://qgis.org/es/site/>
- R Development Core Team (2019) R: a language and environment for statistical computing. R Foundation for Statistical Computing, Vienna.
- Ramírez L, MacGregor-Fors I (2016) Butterflies in the city: a review of urban diurnal Lepidoptera. *Urban Ecosystems* 20(1): 171–182. <https://doi.org/10.1007/s11252-016-0579-4>
- Ruszczyk A (1986) Distribution and abundance of butterflies in the urbanization zones of Porto Alegre, Brazil. *Journal of Research on the Lepidoptera* 25(3): 157–178.
- Ruszczyk A, de Araujo AM (1992) Gradients in butterfly species diversity in an urban area in Brazil. *Journal of the Lepidopterists’ Society* 46: 255–264.
- Rydon AHB (1964) Notes on the use of butterfly traps in East Africa. *Journal of the Lepidopterists’ Society* 18(1): 57–58.
- Sackis GD, Morais ABB (2008) Borboletas (Lepidoptera: Hesperioidea e Papilionoidea) do campus da Universidade Federal de Santa Maria, Santa Maria, Rio Grande do Sul. *Biota Neotropica* 8(1): 21–28. <https://doi.org/10.1590/S1676-06032008000100018>
- Sanchez-Castillo L, Kubota T, Cantú I, Moriyama T, Hasnawir (2016) A probability method of rainfall warning for sediment-related disaster in developing countries: a case study in Sierra Madre Oriental, Mexico. *Natural Hazards* 85(3): 1893–1906. <https://doi.org/10.1007/s11069-016-2669-2>

- Sanchez-Castillo L, Kubota T, Cantu I, Yanez M, Hasnawir, Pequeno M (2017) Comparisons of the root mechanical properties of three native Mexican tree species for soil bioengineering practices. *Botanical Sciences* 95(2): 259–269. <https://doi.org/10.17129/botsci.802>
- Schultz CB, Dlugosch KM (1999) Nectar and host plant scarcity limit populations of an endangered Oregon butterfly. *Oecologia* 119(2): 231–238. <https://doi.org/10.1007/s004420050781>
- Scott JA (1986) *The Butterflies of North America. A Natural History and Field Guide*. Stanford University Press, Stanford, 583 pp.
- Selmi W, Weber C, Rivière E, Blond N, Mehdi L, Nowak D (2016) Air pollution removal by trees in public green spaces in Strasbourg city, France. *Urban Forestry & Urban Greening*, 17: 192–201. <https://doi.org/10.1016/j.ufug.2016.04.010>
- Settele J, Kudrna O, Harpke A, Kühn I, van Swaay C, Verovnik R, Warren M, Wiemers M, Hanspach J, Hickler T, Kühn E, van Halder I, Veling K, Vliegthart A, Wynhoff I, Schweiger O (2008) *Climatic risk Atlas of European Butterflies*. *BioRisk* 1: 1–712. <https://doi.org/10.3897/biorisk.1>
- Shapiro AM (2002) The Californian urban butterfly fauna is dependent on alien plants. *Diversity Distributions* 8(1): 31–40. <https://doi.org/10.1046/j.1366-9516.2001.00120.x>
- Silva ARM, Castro COD, Mafia PO, Mendonça MOC, Alves TCC, Beirão MDV (2012) Borboletas frugívoras (Lepidoptera: Nymphalidae) de uma área urbana (Área de Proteção Especial Manancial Cercadinho) em Belo Horizonte, Minas Gerais, Brasil. *Biota Neotropica* 12: 292–297. <https://doi.org/10.1590/S1676-06032012000300028>
- Sisto NP, Ramírez AI, Aguilar I, Magaña V (2016) Climate threats, water supply vulnerability and the risk of a water crisis in the Monterrey Metropolitan Area (Northeastern Mexico) *Physics and Chemistry of the Earth, Parts A/B/C* 91: 2–9. <https://doi.org/10.1016/j.pce.2015.08.015>
- Snep R, Opdam P, Baveco J, Devries PJ, Timmermans W, Kwak R, Kuypers V (2006) How peri-urban areas can strengthen animal populations within cities: A modeling approach. *Biological Conservation* 127(3): 345–355. <https://doi.org/10.1016/j.biocon.2005.06.034>
- Soga M, Koike S (2012) Relative importance of quantity, quality and isolation of patches for butterfly diversity in fragmented urban forests. *Ecological Research* 27(2): 265–271. <https://doi.org/10.1007/s11284-011-0896-2>
- Soga M, Koike S (2013) Mapping the potential extinction debt of butterflies in a modern city: implications for conservation priorities in urban landscapes. *Animal Conservation* 16(1): 1–11. <https://doi.org/10.1111/j.1469-1795.2012.00572.x>
- Soga M, Yamaura Y, Koike S, Gaston KJ (2014) Land sharing vs. land sparing: does the compact city reconcile urban development and biodiversity conservation? *Journal of Applied Ecology* 51(5): 1378–1386. <https://doi.org/10.1111/1365-2664.12280>
- Stefanescu C, Herrando S, Páramo F (2004) Butterfly species richness in the north-west Mediterranean Basin: the role of natural and human-induced factors. *Journal of Biogeography* 31(6): 905–915. <https://doi.org/10.1111/j.1365-2699.2004.01088.x>
- Tejeda-Cruz C, Mehlreter K, Sosa VJ (2008) Indicadores ecológicos multi-taxonómicos. In: Manson RH, Hernández-Ortiz V, Gallina S, Mehlreter K (Eds) *Agroecosistemas Cafetaleros de Veracruz: Biodiversidad, Manejo y Conservación*. Instituto Nacional de Ecología A. C., México: 123–134.

- TIBCO Software Inc. (2017) Statistica (data analysis software system): version 13.3. Palo Alto, CA. <https://www.tibco.com/products/tibco-statistica>
- UN-HABITAT (2010) State of the World's Cities 2010/2011: Bridging the Urban Divide. London: Earthscan and UN-Habitat. <https://doi.org/10.4324/9781849774864>
- Vargas IF, Llorente JB, Luis AM, Pozo C (2008) Nymphalidae de México II. Libytheinae, Ithomiinae, Morphinae y Charaxinae: Distribución Geográfica e Ilustración. Facultad de Ciencias, Universidad Nacional Autónoma de México/ Comisión Nacional para el Uso y Conocimiento de la Biodiversidad, México, 225 pp.
- Villarreal H, Álvarez M, Córdoba S, Escobar F, Fagua G, Gast F, Mendoza H, Ospina M, Umaña AM (2006) Manual de Métodos Para el Desarrollo de Inventarios de Biodiversidad. Programa de Inventarios de Biodiversidad. Instituto de Investigación de Recursos Biológicos Alexander von Humboldt, Bogotá, 236 pp.
- Vlahov D, Galea S (2002) Urbanization, urbanicity, and health. *Journal of Urban Health: Bulletin of the New York Academy of Medicine* 79(Suppl. 1): 1–12. https://doi.org/10.1093/jurban/79.suppl_1.S1
- Wagner DL, Nelson MW, Schweitzer DF (2003) Shrubland Lepidoptera of southern New England and southeastern New York: ecology, conservation, and management. *Forest Ecology and Management* 185(1-2): 95–112. [https://doi.org/10.1016/S0378-1127\(03\)00249-4](https://doi.org/10.1016/S0378-1127(03)00249-4)
- Wagner DL, Van Driesche RG (2010) Threats Posed to Rare or Endangered Insects by Invasions of Non-native Species. *Annual Review of Entomology* 55(1): 547–568. <https://doi.org/10.1146/annurev-ento-112408-085516>
- Warren AD (2000) Hesperioidea (Lepidoptera). In: Llorente JB, González ES, Papavero N (Eds) Biodiversidad, taxonomía y biogeografía de artrópodos de México: hacia una síntesis de su conocimiento (Vol. II). Las Prensas de Ciencias, Facultad de Ciencias, UNAM, México, D. F., 535–580.
- Warren AD, Davis KJ, Grishin NV, Pelham JP, Stangeland EM (2012) Interactive Listing of American Butterflies. <http://www.butterfliesofamerica.com/>
- Weiss SB (1999) Cars, cows, and checkerspot butterflies: nitrogen deposition and management of nutrient-poor grasslands for a threatened species. *Conservation Biology* 13: 1476–1486. <https://doi.org/10.1046/j.1523-1739.1999.98468.x>
- Ybáñez E, Barboza C (2017) Trayectorias recientes de la migración interna en la Zona Metropolitana de Monterrey: características, orígenes y destinos a nivel municipal, 2010. *Estudios Demográficos y Urbanos* 32(2): 245–281. <https://doi.org/10.24201/edu.v32i2.1722>

Appendix I

Taxonomic list of Papilionoidea by season in each pollution category in the Monterrey Metropolitan Area. Legend: S 1 = Site 1 (Pollution free), S 2 = Site 2 (Low pollution), S 3 = Site 3 (Moderate pollution), S 4 = Site 4 (High pollution). The marked species (*) were collected with Van Someren-Rydon traps.

| Taxon | Dry season | | | | Rainy season | | | | General (MMZ) |
|---|------------|-----|-----|-----|--------------|-----|-----|-----|---------------|
| | S 1 | S 2 | S 3 | S 4 | S 1 | S 2 | S 3 | S 4 | |
| Papilionidae Latreille, 182 | | | | | | | | | |
| Papilioninae Latreille, 182 | | | | | | | | | |
| Troidini Talbot, 1939 | | | | | | | | | |
| <i>Parides photinus</i> (Doubleday, 1844) | | | | 3 | | 3 | | | 6 |
| <i>Parides erithalion polyzelus</i> (C. Felder & R. Felder, 1865) | | | | 5 | | | | | 5 |
| <i>Battus philenor philenor</i> (Linnaeus, 1771) | 8 | 12 | 13 | 8 | 17 | 16 | 10 | 16 | 100 |
| <i>Battus polydamas polydamas</i> (Linnaeus, 1758) | 9 | 11 | 11 | 6 | 11 | 17 | 8 | 13 | 86 |
| Leptocircini W. F. Kirby, 1896 | | | | | | | | | |
| <i>Protographium epidaus epidaus</i> (Doubleday, 1846) | 4 | | | | | | | | 4 |
| <i>Protographium philolaus philolaus</i> (Boisduval, 1836) | 4 | 3 | | | 5 | 6 | | | 18 |
| Papilionini Latreille, 182 | | | | | | | | | |
| <i>Papilio polyxenes asterius</i> (Stoll, 1782) | 4 | 5 | 10 | 7 | 12 | 7 | 8 | 11 | 64 |
| <i>Pterourus pilumnus</i> Boisduval, 1836 | 12 | 10 | | | 8 | 9 | 9 | 7 | 55 |
| <i>Pterourus palamedes leontis</i> Rothschild & Jordan, 196 | 10 | | | | 7 | | | | 17 |
| <i>Heracles crespontes</i> Cramer, 1777 | 12 | 9 | 5 | 10 | 6 | 8 | 9 | 7 | 66 |
| <i>Heracles thoas autocles</i> Rothschild & Jordan, 196 | 8 | 13 | | | | | | | 21 |
| <i>Heracles astyalus pallas</i> G. Gray, 1853 | 7 | 8 | 7 | | 12 | 10 | 11 | | 55 |
| <i>Heracles ornithion</i> Boisduval, 1836 | 13 | 9 | | | 5 | 12 | 7 | 8 | 54 |
| <i>Heracles anchisiades idaeus</i> Fabricius, 1793 | 8 | | | | 10 | | | | 18 |
| Pieridae Swainson, 182 | | | | | | | | | |
| Coliadinae Swainson, 1821 | | | | | | | | | |
| <i>Kricogonia lyside</i> (Godart, 1819) | 14 | 14 | 21 | 16 | 23 | 12 | 16 | 26 | 142 |
| <i>Nathalis iole iole</i> Boisduval, 1836 | 12 | 17 | 7 | 12 | 20 | 13 | 18 | 9 | 108 |
| <i>Eurema daiva eugenia</i> (Wallengren, 186) | 13 | 14 | | | 20 | 11 | | | 58 |
| <i>Eurema boisduvaliana</i> (C. Felder & R. Felder, 1865) | 9 | 8 | 16 | | 19 | | | | 52 |
| <i>Eurema mexicana mexicana</i> (Boisduval, 1836) | 13 | 16 | 11 | 15 | | 14 | 15 | 17 | 101 |
| <i>Abaeis nicippe</i> (Cramer, 1779) | 20 | 12 | 14 | 13 | 14 | 16 | 7 | 9 | 105 |
| <i>Pyrisitia proterpia</i> (Fabricius, 1775) | 19 | 23 | 9 | 13 | 13 | 10 | 12 | 18 | 117 |
| <i>Pyrisitia lisa centralis</i> (Herrich-Schäffer, 1865) | 12 | 10 | 14 | 12 | 7 | 11 | 16 | 16 | 98 |
| <i>Pyrisitia nise nelphe</i> (R. Felder, 1869) | 4 | 14 | | | 12 | 18 | 18 | 11 | 77 |
| <i>Pyrisitia dina westwoodii</i> (Boisduval, 1836) | 17 | | | | 21 | | | | 38 |
| <i>Colias eurytheme</i> Boisduval, 1832 | | | 9 | 11 | 12 | | | | 32 |
| <i>Zerene cesonia cesonia</i> (Stoll, 179) | 15 | 9 | 16 | 9 | 10 | 19 | 17 | 14 | 109 |
| <i>Anteos clorinde</i> (Godart, 1824) | 14 | 9 | | | 23 | 15 | | | 61 |
| <i>Anteos maerula</i> (Fabricius, 1775) | 20 | 15 | 16 | | 15 | 11 | 9 | 16 | 102 |
| <i>Phoebis sennae marcellina</i> (Cramer, 1777) | 11 | 19 | 11 | 9 | 20 | 23 | 15 | 12 | 120 |
| <i>Phoebis philea philea</i> (Linnaeus, 1763) | 10 | 6 | 9 | | 14 | 13 | | | 52 |
| <i>Phoebis agarithe agarithe</i> (Boisduval, 1836) | 16 | 11 | 6 | 14 | 7 | 18 | 15 | 13 | 100 |
| Pierinae Swainson, 182 | | | | | | | | | |
| Pierini Swainson, 182 | | | | | | | | | |
| <i>Glutophrissa drusilla tenuis</i> (Lamas, 1981) | 8 | 4 | 4 | 5 | 8 | 9 | 6 | 3 | 47 |
| <i>Catantix nimbice nimbice</i> (Boisduval, 1836) | 6 | 4 | | | 6 | | | | 16 |
| <i>Leptophobia aripa elodia</i> (Boisduval, 1836) | 8 | | | | 11 | | | | 19 |
| <i>Pontia protodice</i> (Boisduval & Le Conte, 183) | 7 | 6 | | | 10 | 13 | 12 | 8 | 56 |
| <i>Ascia monuste monuste</i> (Linnaeus, 1764) | 4 | 1 | 5 | | 7 | 6 | 12 | 13 | 48 |
| <i>Ganyra josephina josepha</i> (Salvin & Godman, 1868) | 4 | 2 | 5 | 6 | | | | | 17 |

| Taxon | Dry season | | | | Rainy season | | | | General (MMZ) |
|---|------------|-----|-----|-----|--------------|-----|-----|-----|---------------|
| | S 1 | S 2 | S 3 | S 4 | S 1 | S 2 | S 3 | S 4 | |
| Heliconiini Swainson, 1822 | | | | | | | | | |
| <i>Agraulis vanillae incarnata</i> (N. Riley, 1926) | 8 | 5 | 3 | 2 | 5 | 11 | 11 | 10 | 55 |
| <i>Dione moneta poeyii</i> Butler, 1873 | 5 | 5 | | | | | | | 10 |
| <i>Dryas iulia moderata</i> (N. Riley, 1926) | 7 | 3 | 6 | 7 | 8 | 12 | 11 | 10 | 64 |
| <i>Heliconius charithonia vazquezae</i> W. Comstock & F. Brown, 195 | 6 | 8 | 11 | 3 | 6 | 7 | 11 | 7 | 59 |
| <i>Heliconius erato petiverana</i> (E. Doubleday, 1847) | | | | | 7 | | | | 7 |
| Argynnini Swainson, 1833 | | | | | | | | | |
| <i>Euptoieta claudia</i> (Cramer, 1775) | 6 | 6 | | 8 | 11 | 9 | 5 | 9 | 54 |
| <i>Euptoieta hegesia meridiania</i> Stichel, 1938 | 10 | 6 | 10 | 9 | 7 | 8 | 10 | 10 | 70 |
| Limenitidinae Behr, 1864 | | | | | | | | | |
| Limenitidini Behr, 1864 | | | | | | | | | |
| * <i>Limenitis arthemis astyanax</i> (Fabricius, 1775) | 4 | | | | 3 | | | | 7 |
| * <i>Adelpha paroecca paroecca</i> (H. Bates, 1864) | | | | | 9 | 8 | | | 17 |
| * <i>Adelpha fessonia fessonia</i> (Hewitson, 1847) | 7 | 9 | 5 | 6 | 9 | 11 | 7 | 16 | 70 |
| * <i>Adelpha basiloides</i> (H. Bates, 1865) | 9 | 6 | | | 8 | 3 | 8 | | 34 |
| Apaturinae Boisduval, 184 | | | | | | | | | |
| * <i>Asterocampa celtis antonia</i> (W. H. Edwards, 1878) | 9 | 14 | 7 | 6 | 6 | 7 | 6 | 13 | 68 |
| * <i>Asterocampa leilia</i> (W. H. Edwards, 1874) | 8 | 11 | 10 | 4 | 7 | 8 | 10 | 15 | 73 |
| * <i>Asterocampa clyton louisa</i> D. Stallings & Turner, 1947 | 4 | 7 | 10 | 9 | 9 | 12 | 8 | 11 | 70 |
| * <i>Asterocampa idyja argus</i> (H. Bates, 1864) | 13 | | | | 6 | 9 | | | 28 |
| * <i>Doxocopa pavon theodora</i> (Lucas, 1857) | 9 | 11 | | | | | | | 20 |
| <i>Doxocopa laure laure</i> (Drury, 1773) | 6 | 9 | 9 | | 11 | 5 | 10 | | 50 |
| Biblidinae Boisduval, 1833 | | | | | | | | | |
| Biblidini Boisduval, 1833 | | | | | | | | | |
| * <i>Biblis hyperia aganisa</i> Boisduval, 1836 | 9 | 3 | 6 | 9 | 14 | 12 | 10 | 5 | 68 |
| <i>Mestra amydone</i> (Ménétriés, 1857) | 10 | 13 | 9 | 7 | 15 | 11 | 5 | 10 | 80 |
| Catonephelini Orfila, 1952 | | | | | | | | | |
| * <i>Eunica tatila tatila</i> (Herrich-Schäffer, 1855) | 10 | 5 | 10 | | 9 | 14 | | | 48 |
| * <i>Eunica monima</i> (Stoll, 1782) | 9 | 10 | | | 10 | | | | 29 |
| * <i>Myscelia ethusa ethusa</i> (Doyère, 184) | 9 | 9 | 8 | 8 | 7 | 8 | 4 | 8 | 61 |
| Ageroniini E. Doubleday, 1847 | | | | | | | | | |
| * <i>Hamadryas februa ferentina</i> (Godart, 1824) | 9 | 6 | 5 | 5 | 10 | 13 | 11 | 10 | 69 |
| * <i>Hamadryas glauconome glauconome</i> (H. Bates, 1864) | 4 | 4 | 11 | | 5 | 5 | | | 29 |
| Epiphelini Jenkins, 1987 | | | | | | | | | |
| * <i>Epiphile adrasta adrasta</i> Hewitson, 1861 | 2 | 3 | | | 7 | | | | 12 |
| * <i>Temenis laothoe</i> (Cramer, 1777) | | | | | 4 | | | | 4 |
| Eubagini Burmeister, 1878 | | | | | | | | | |
| <i>Dynamine postverta mexicana</i> d'Almeida, 1952 | 5 | 4 | 2 | 6 | 3 | 5 | 3 | 5 | 33 |
| Cyrestinae Guenée, 1865 | | | | | | | | | |
| Cyrestini Guenée, 1865 | | | | | | | | | |
| <i>Marpesia petreus</i> (Cramer, 1776) | 3 | 3 | | | 1 | | | | 7 |
| Nymphalinae Rafinesque, 1815 | | | | | | | | | |
| Nymphalini Rafinesque, 1815 | | | | | | | | | |
| <i>Vanessa virginiensis</i> (Drury, 1773) | 6 | 5 | | | 6 | | | | 17 |
| <i>Vanessa cardui</i> (Linnaeus, 1758) | 8 | 10 | 4 | | 10 | 8 | 8 | 6 | 54 |
| * <i>Vanessa atalanta rubria</i> (Fruhstorfer, 199) | 3 | 3 | 2 | 6 | 3 | 6 | 4 | 4 | 31 |
| * <i>Polygonia interrogationis</i> (Fabricius, 1798) | 1 | 5 | | | | | | | 6 |
| Victorini Scudder, 1893 | | | | | | | | | |
| <i>Anartia jatrophae luteipicta</i> (Fruhstorfer, 197) | 3 | 3 | 6 | 4 | 9 | 7 | 6 | 10 | 48 |
| <i>Anartia fatima fatima</i> (Fabricius, 1793) | 4 | 6 | 6 | 5 | 6 | 11 | 9 | 9 | 56 |
| <i>Siproeta stelenes biplagiata</i> (Fruhstorfer, 197) | 7 | 4 | 7 | 5 | 4 | 11 | 10 | 13 | 61 |
| Junoniini Reuter, 1896 | | | | | | | | | |
| <i>Junonia coenia coenia</i> Hübner, 1822 | | 4 | 1 | 1 | | 4 | 3 | 4 | 17 |
| Melitaeini Newman, 187 | | | | | | | | | |
| <i>Chlosyne janais janais</i> (Drury, 1782) | 10 | 9 | 8 | 8 | 5 | 13 | 16 | 15 | 84 |
| <i>Chlosyne definita definita</i> (E. Aaron, 1885) | 3 | 9 | 7 | 7 | | | | | 26 |

| Taxon | Dry season | | | | Rainy season | | | | General (MMZ) |
|---|------------|-----|-----|-----|--------------|-----|-----|-----|---------------|
| | S 1 | S 2 | S 3 | S 4 | S 1 | S 2 | S 3 | S 4 | |
| <i>Chlosyne endeis pardelina</i> Scott, 1986 | 11 | 8 | 7 | | 9 | 8 | 7 | | 50 |
| <i>Chlosyne rosita browni</i> Bauer, 1961 | 8 | 13 | 7 | 9 | 10 | 11 | 4 | 11 | 73 |
| <i>Chlosyne theona bollii</i> (W. H. Edwards, 1877) | 9 | 12 | 7 | 13 | 5 | 14 | 17 | | 77 |
| <i>Chlosyne lacinia adjutrix</i> Scudder, 1875 | 7 | 8 | 5 | 10 | 12 | 15 | 11 | 13 | 81 |
| <i>Microtia elva elva</i> H. Bates, 1864 | 12 | 4 | 7 | 11 | 17 | 13 | 9 | 10 | 83 |
| <i>Dymasia dymas dymas</i> (W. H. Edwards, 1877) | 8 | | | | 10 | | | | 18 |
| <i>Texola elada ulrica</i> (W. H. Edwards, 1877) | 5 | 9 | 8 | 10 | | | | | 32 |
| <i>Anthanassa texana texana</i> (W. H. Edwards, 1863) | 11 | 7 | 12 | 7 | 11 | 14 | 12 | 17 | 91 |
| <i>Anthanassa ardyi</i> (Hewitson, 1864) | 12 | | | | 12 | | | | 24 |
| <i>Anthanassa ptolyca</i> (H. Bates, 1864) | 10 | 10 | 8 | | | | | | 28 |
| <i>Anthanassa argentea</i> (Godman & Salvin, 1882) | 6 | 7 | 12 | 7 | 15 | 12 | 9 | 18 | 86 |
| <i>Anthanassa tulcis</i> (H. Bates, 1864) | | | | | 16 | 13 | | | 29 |
| <i>Phyciodes graphica</i> (R. Felder, 1869) | 6 | 8 | 8 | 10 | | | | | 32 |
| <i>Phyciodes phaon phaon</i> (W. H. Edwards, 1864) | 11 | 13 | 6 | | | | | | 30 |
| <i>Phyciodes tharos tharos</i> (Drury, 1773) | 6 | 10 | 8 | 9 | 5 | 12 | 12 | 14 | 76 |
| Charaxinae Guenée, 1865 | | | | | | | | | |
| Anaeini Reuter, 1896 | | | | | | | | | |
| * <i>Anaea aidea</i> (Guérin-Méneville, 1844) | 15 | 11 | 12 | 12 | 12 | 20 | 22 | 18 | 122 |
| * <i>Fountainaea glycerium glycerium</i> (E. Doubleday, 1849) | 2 | 5 | 3 | | 9 | 6 | | | 25 |
| * <i>Memphis pithyusa pithyusa</i> (R. Felder, 1869) | 5 | | | | 4 | | | | 9 |
| Satyrinae Boisduval, 1833 | | | | | | | | | |
| Satyrini Boisduval, 1833 | | | | | | | | | |
| * <i>Cyllopsis dospassosi</i> L. Miller, 1974 | 3 | | | | 4 | 7 | | | 14 |
| * <i>Cyllopsis gemma freemani</i> (D. Stallings & Turner, 1947) | 7 | 8 | 7 | 8 | 20 | 14 | 17 | 13 | 94 |
| * <i>Megisto rubricata rubricata</i> (W. H. Edwards, 1871) | 3 | | | | | | | | 3 |
| <i>Hermeuptychia hermes</i> (Fabricius, 1775) | 8 | 9 | 8 | 8 | 11 | 13 | 5 | 8 | 70 |
| Hesperiidae Latreille, 189 | | | | | | | | | |
| Eudaminae Mabilie, 1877 | | | | | | | | | |
| <i>Phocides polybius lilea</i> (Reakirt, 1867) | 1 | | | | | | | | 1 |
| <i>Phocides urania urania</i> (Westwood, 1852) | 4 | 2 | | | 1 | 5 | | | 12 |
| <i>Polygonus leo arizonensis</i> (Skinner, 1911) | | | | | 2 | | | | 2 |
| <i>Chioiodes albofasciatus</i> (Hewitson, 1867) | 6 | 5 | 5 | 8 | 5 | 6 | 8 | 11 | 54 |
| <i>Chioiodes zilpa</i> (Butler, 1872) | 6 | 5 | 7 | 8 | 5 | 7 | 15 | 9 | 62 |
| <i>Aguna asander asander</i> (Hewitson, 1867) | | 3 | 1 | 4 | | 4 | 2 | 4 | 18 |
| <i>Aguna metophis</i> (Latreille, 1824) | 2 | 5 | 3 | 3 | | | | | 13 |
| <i>Typhedanus undulatus</i> (Hewitson, 1867) | | | | | 1 | 1 | 3 | | 5 |
| <i>Urbanus proteus proteus</i> (Linnaeus, 1758) | 7 | 4 | 7 | | 6 | 11 | 11 | 10 | 56 |
| <i>Urbanus dorantes dorantes</i> (Stoll, 179) | 7 | 6 | 7 | | 10 | 7 | 7 | | 44 |
| <i>Urbanus procne</i> (Plötz, 1881) | 8 | 8 | 9 | 5 | 11 | 14 | 8 | 4 | 67 |
| <i>Astraptes fulgerator azul</i> (Reakirt, 1867) | 3 | 6 | 7 | 6 | 11 | 7 | 15 | 9 | 64 |
| <i>Astraptes alector hopfferi</i> (Plötz, 1881) | | | | | 7 | 10 | | | 17 |
| <i>Astraptes anaphus annetta</i> Evans, 1952 | | | | | 2 | | | | 2 |
| <i>Autochton cellus</i> (Boisduval & Le Conte, 1837) | 6 | | | | 7 | | | | 13 |
| <i>Autochton cincta</i> (Plötz, 1882) | 1 | 4 | 9 | | 6 | 5 | 5 | | 30 |
| <i>Autochton neis</i> (Geyer, 1832) | 7 | 4 | 6 | 7 | | | | | 24 |
| <i>Achalarus toxeus</i> (Plötz, 1882) | 8 | 5 | 9 | 4 | 5 | 5 | 3 | 8 | 47 |
| <i>Thorybes pylades albosuffusa</i> H. Freeman, 1943 | | | | | 6 | | | | 6 |
| <i>Cabares potrillo potrillo</i> (Lucas, 1857) | 8 | 7 | 9 | 7 | 3 | 8 | 5 | 7 | 54 |
| <i>Spathilepia clonius</i> (Cramer, 1775) | | 2 | 4 | 5 | | | | | 11 |
| <i>Cogia hippalus biska</i> Evans, 1953 | 3 | 8 | 7 | 7 | | | | | 25 |
| Pyrginae Burmeister, 1878 | | | | | | | | | |
| Carcharodini Verity, 194 | | | | | | | | | |
| <i>Arteurotia tractipennis tractipennis</i> Butler & H. Druce, 1872 | 7 | 4 | | | 5 | 7 | | | 23 |
| <i>Polyctor enops</i> (Godman & Salvin, 1894) | 3 | | | | 7 | | | | 10 |
| <i>Noctuana lactifera bipuncta</i> (Plötz, 1884) | | | | | 7 | 5 | | | 12 |
| <i>Bolla brennus brennus</i> (Godman & Salvin, 1896) | 4 | 6 | | | 6 | 4 | 5 | | 25 |

| Taxon | Dry season | | | | Rainy season | | | | General (MMZ) |
|--|------------|-----|-----|-----|--------------|-----|-----|-----|---------------|
| | S 1 | S 2 | S 3 | S 4 | S 1 | S 2 | S 3 | S 4 | |
| <i>Staphylus mazans</i> (Reakirt, 1867) | 8 | 6 | 4 | 8 | 10 | 6 | 11 | 14 | 67 |
| <i>Staphylus azteca</i> (Scudder, 1872) | 7 | | | | 6 | | | | 13 |
| <i>Pholisora catullus</i> (Fabricius, 1793) | 3 | 7 | 6 | 4 | 7 | 8 | 8 | 11 | 54 |
| Erynnini Brues & F. Carpenter, 1932 | | | | | | | | | |
| <i>Gorgythion begga pyralina</i> (Möschler, 1877) | 9 | 4 | 5 | 3 | 7 | 9 | 4 | 7 | 48 |
| <i>Sostrata nordica</i> Evans, 1953 | 7 | | | | | | | | 7 |
| <i>Grais stigmaticus stigmaticus</i> (Mabille, 1883) | 8 | 9 | 6 | | 8 | 3 | | | 34 |
| <i>Timochares ruptifasciata</i> (Plötz, 1884) | | | | | 10 | | | | 10 |
| <i>Chiomara georgina georgina</i> (Reakirt, 1868) | 5 | 6 | 5 | 9 | 7 | 14 | 9 | 13 | 68 |
| <i>Gesta invisus</i> (Butler & H. Druce, 1872) | 4 | 7 | 3 | 6 | 2 | 6 | 8 | 5 | 41 |
| <i>Erynnis funeralis</i> (Scudder & Burgess, 187) | 1 | 3 | 6 | 8 | | | | | 18 |
| Achlyodidini Burmeister, 1878 | | | | | | | | | |
| <i>Eantis tamenund</i> (W. H. Edwards, 1871) | 5 | 6 | 10 | 5 | 12 | 7 | 11 | 8 | 64 |
| <i>Zera hyacinthinus hyacinthinus</i> (Mabille, 1877) | 5 | 7 | 6 | 6 | 4 | | | | 28 |
| Pyrgini Burmeister, 1878 | | | | | | | | | |
| <i>Carrhenes canescens canescens</i> (R. Felder, 1869) | 3 | | | | | | | | 3 |
| <i>Systasea pulverulenta</i> (R. Felder, 1869) | 7 | 8 | | 9 | 6 | 7 | 6 | 4 | 53 |
| <i>Celotes nessus</i> (W. H. Edwards, 1877) | | | 8 | 6 | | | 4 | 6 | 24 |
| <i>Pyrgus albescens</i> Plötz, 1884 | 8 | 10 | 7 | 3 | 12 | 8 | 13 | 16 | 77 |
| <i>Pyrgus oileus</i> (Linnaeus, 1767) | 6 | 11 | 6 | 5 | 22 | 7 | 14 | 19 | 90 |
| <i>Pyrgus philetas</i> W. H. Edwards, 1881 | 1 | 1 | 1 | 3 | | | | | 6 |
| <i>Heliopyrgus sublinea</i> (Schaus, 192) | 6 | 6 | 7 | | 8 | 5 | | | 32 |
| <i>Heliopetes laviana laviana</i> (Hewitson, 1868) | 9 | 5 | 5 | 5 | 8 | 4 | 9 | 8 | 53 |
| <i>Heliopetes macaira macaira</i> (Reakirt, 1867) | | | | | 9 | | | | 9 |
| Hesperiinae Latreille, 189 | | | | | | | | | |
| Thymelicini Tutt, 195 | | | | | | | | | |
| <i>Ancyloxypha arene</i> (W. H. Edwards, 1871) | 7 | 7 | 3 | 7 | 12 | 4 | 2 | 9 | 51 |
| <i>Copaeodes aurantiaca</i> (Hewitson, 1868) | 4 | 3 | 6 | 4 | 7 | 11 | 3 | 10 | 48 |
| <i>Copaeodes minima</i> (W. H. Edwards, 187) | 2 | 5 | 5 | 6 | 12 | 12 | 10 | 10 | 62 |
| Calpodini A. Clark, 1948 | | | | | | | | | |
| <i>Panoquina lucas</i> (Fabricius, 1793) | | | | | 2 | 5 | | | 7 |
| Anthoptini A. Warren, 29 | | | | | | | | | |
| <i>Synapte pecta</i> Evans, 1955 | | | | | 1 | | | | 1 |
| Moncini A. Warren, 28 | | | | | | | | | |
| <i>Remella rita</i> (Evans, 1955) | | | | | 2 | | | | 2 |
| <i>Amblyscirtes toteca toteca</i> Scudder, 1872 | 2 | | | | | | | | 2 |
| <i>Cymaenes trebius</i> (Mabille, 1891) | | | | | 5 | | | | 5 |
| <i>Lerodea eufala eufala</i> (W. H. Edwards, 1869) | 4 | 3 | 8 | | 4 | 6 | | | 25 |
| <i>Lerema accius</i> (J. E. Smith, 1797) | 5 | 5 | 3 | 6 | 6 | 10 | 9 | 7 | 51 |
| <i>Lerema liris</i> Evans, 1955 | 5 | 7 | 4 | 5 | 7 | 3 | 6 | 6 | 43 |
| <i>Vettius fantasos</i> (Cramer, 178) | | | | | 2 | 4 | | | 6 |
| Hesperiini Latreille, 189 | | | | | | | | | |
| <i>Hylephila phyleus phyleus</i> (Drury, 1773) | 3 | 3 | 3 | 2 | 3 | 5 | 8 | 7 | 34 |
| <i>Polites vibex praeceps</i> (Scudder, 1872) | 4 | 5 | 3 | 4 | 7 | 7 | 2 | 5 | 37 |
| <i>Wallengrenia otho otho</i> (J. E. Smith, 1797) | | | | | 4 | | | | 4 |
| <i>Atalopedes campestris huron</i> (W. H. Edwards, 1863) | 1 | 2 | 4 | 3 | 5 | 4 | 4 | 4 | 27 |
| <i>Poanes melane vitellina</i> (Herrich-Schäffer, 1869) | 4 | 4 | | | | | | | 8 |
| <i>Anatrytone mazai</i> (H. Freeman, 1969) | | | | | 3 | | | | 3 |
| <i>Quasimellana eulogius</i> (Plötz, 1882) | 4 | 2 | | | | 3 | 4 | 3 | 16 |
| <i>Quinta cannae</i> (Herrich-Schäffer, 1869) | | | | | 6 | 2 | | | 8 |
| <i>Nyctelius nyctelius nyctelius</i> (Latreille, 1824) | 5 | 3 | 5 | 6 | 6 | 9 | 7 | 9 | 50 |

The tree snail on Rota Island, Northern Mariana Islands, long identified as *Partula gibba* (Partulidae), is a different species

David R. Sischo^{1,2}, Michael G. Hadfield¹

1 Kewalo Marine Laboratory, Pacific Biosciences Research Center, University of Hawai'i at Mānoa, 41 Ahui St., Honolulu, 96813 Hawai'i, USA **2** Department of Land and Natural Resources, Division of Forestry and Wildlife, State of Hawai'i, 1151 Punchbowl St. Rm. 325, Honolulu, 96813 Hawai'i, USA

Corresponding author: David R. Sischo (david.r.sischo@hawaii.gov)

Academic editor: T. Backeljau | Received 8 July 2020 | Accepted 13 March 2021 | Published 17 May 2021

<http://zoobank.org/CE4FE521-0DEC-485F-863E-32CB91BAAA67>

Citation: Sischo DR, Hadfield MG (2021) The tree snail on Rota Island, Northern Mariana Islands, long identified as *Partula gibba* (Partulidae), is a different species. ZooKeys 1037: 105–118. <https://doi.org/10.3897/zookeys.1037.56303>

Abstract

Tree snails in the family Partulidae are widespread across the tropical Pacific, with endemic species occurring on most high islands. Partulid species have faced catastrophic range reductions and extinctions due primarily to introduced predators. Consequently, most extant species are threatened with imminent extinction. The U.S. administered Mariana Islands, consisting of Guam in the South and the Commonwealth of the Northern Mariana Islands (CNMI) in the north, historically harbored six endemic partulid species, half of which are thought to be extinct. While conducting a phylogenetic assessment of *Partula gibba*, an extant tree-snail with a range spanning at least seven islands within the archipelago, it was discovered that what has been identified as *P. gibba* on the island of Rota is a misidentified cryptic species. Here we use molecular phylogenetics, shell morphometrics and reproductive anatomy to describe it as a new species, *Partula lutaensis* **sp. nov.** Because the new species has suffered population declines and has a restricted range, consisting solely of the small island of Rota, we highlight the urgent need for conservation measures.

Keywords

Cryptic species, Mariana Islands, Micronesia, Mollusca, narrow-range endemic, systematics

Introduction

The tree-snail family Partulidae is known from islands across the tropical Pacific (Cowie 1992). While most of the known diversity occurs in the eastern portion of the family's range, particularly the Society Islands for the genus *Partula* and the Samoan Islands for the genus *Samoana*, the progenitors of both genera likely came from further west (Lee et al. 2014). The 15 islands of the Mariana Archipelago in the western Pacific (Fig. 1) historically harbored six described species. Two of them, *Partula radiolata* (Pfeiffer, 1846), and *Partula salifana* Crampton, 1925, were known only from the island of Guam, while *Partula desolata* Bauman & Kerr, 2013, described from sub-fossil shells, and *Partula langfordi* Kondo, 1970, were described as single-island endemics from Rota and Aguigan, respectively. The only two Mariana species with multi-island distributions are *Samoana fragilis* (Férussac, 1821), known from both Guam and Rota, and *Partula gibba* Férussac, 1821, known from seven islands, from Guam, in the south, to Pagan Island in the north. In a recent publication, we described the discovery of a cryptic species of *Partula* on the island of Rota, based on molecular evidence (Sischo and Hadfield 2017). Due to greatly similar shell shape, this species had been identified as *Partula gibba* in prior surveys and publications (Kondo 1970; Bauman 1996; Bauman and Kerr 2013; Hadfield 2015). Adding further taxonomic confusion, a colony of *Partula* once maintained at the Invertebrate Conservation Center, Zoological Society of London in London, was labeled *Partula langfordi*, although it was originally collected on Rota (Goodacre and Wade 2001; Sischo and Hadfield 2017). Because *P. langfordi* was described as endemic to the island of Aguigan, snails bearing that name in the London collection were likely not *P. langfordi* (Kondo 1970). Unfortunately, *P. langfordi* is now thought to be extinct (Smith 2013; J. Liske-Clark, Northern Mariana Department of Fish and Wildlife, personal communication). The name of Aguigan Island is variously spelled on different maps and in different resources, including: Agiguan, Agijuan and Aguijan. We apply here the spelling currently in use by CNMI bureaus, the NOAA and elected officials in the CNMI.

To distinguish the new Rota *Partula* species from other extant species in the Mariana Archipelago, we paired our previously published phylogeny (Sischo and Hadfield 2017) with anatomy of the male reproductive tract, the latter having been used extensively as a diagnostic trait for *Partula* species (Pilsbry 1909; Pilsbry and Cooke 1934; Kondo 1955, 1968, 1970; Gerlach 2016; Slapcinsky and Kraus 2016). Because we were not able to extract useful DNA from preserved tissue of *Partula langfordi*, we were unable to carry out molecular phylogenetics with that species. In addition to anatomy of the male reproductive tract, we further distinguished *P. langfordi* from the species on Rota by replicating the shell morphometric analysis originally conducted by Kondo (1970) in his study of *P. langfordi* and co-occurring *Partula gibba* on the island of Aguigan. Here we describe *Partula lutaensis* sp. nov. and designate type material.

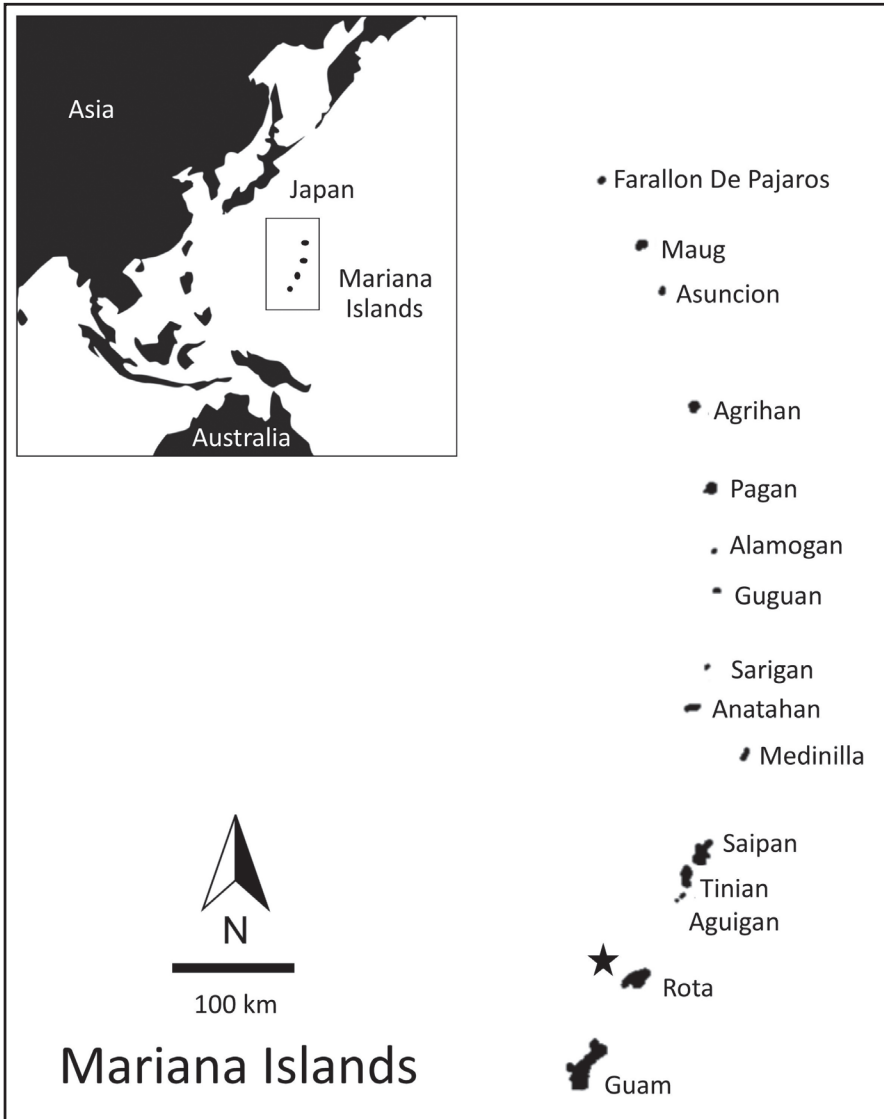


Figure 1. Map of the Mariana Archipelago with a star indicating the location of Rota Island.

Material and methods

Due to the endangered status of all partulid species from Guam and the Commonwealth of the Northern Mariana Islands, we have elected to not include specific location information of any of the extant colonies or type specimen material in this paper. However, this information has been deposited in the Bernice Pauahi Bishop Museum with each specimen.

Shell morphological assessment

Kondo (1970) found no differences in conchology, aside from non-overlapping shell sizes, between *P. langfordi* and sympatric *P. gibba* on the island of Aguigan. Because *Partula* from Rota had been mistakenly identified as *P. langfordi*, we carried out a similar comparison. Shells of *P. langfordi* from the mollusc collection housed at the Bernice Pauahi Bishop Museum (BPBM) in Honolulu, Hawai'i were used for analysis. BPBM lot numbers 213092, 21309, 213104, 213012, 213024, originally collected by Y. Kondo from Aguigan Island were compared with shells from what was then labeled as *P. gibba* (BPBM lot numbers, 217155, 213251, 213248, 213151, 213241) originally collected on Rota (Fig. 2). Lengths and widths were measured to 0.01 mm from 48 shells of *P. langfordi* and 47 shells of *P. gibba* with precision calipers. Shell length was measured parallel to the shell axis from the apex to the base of the aperture, and width was measured perpendicular to the shell axis across the widest portion of the shell. Means (M) and standard deviations (s.d.) are reported. Adult *Partula* spp.

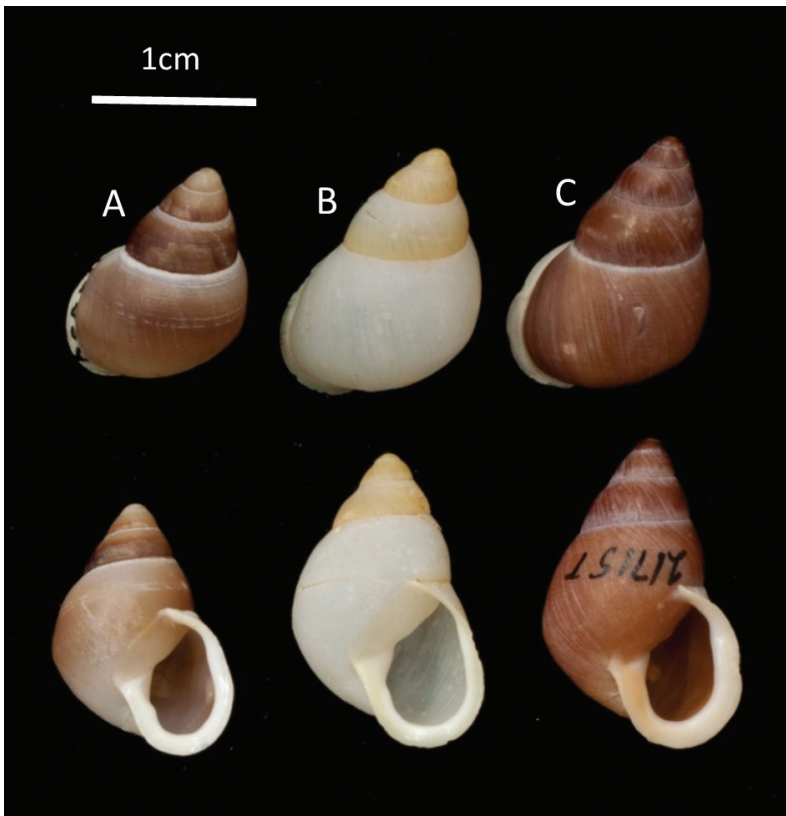


Figure 2. A typical shell of *P. langfordi* from Aguigan (**A**) compared to light and dark shell morphs of *P. lutaensis* sp. nov. from Rota (**B** and **C**). The three shells are shown in abapertural view in the upper row and apertural view below.

stop growing and become sexually mature when they form a characteristic thickened flare around the aperture of their shells, here referred to as a lip. All shells measured were lipped, indicating they were mature adults (Cowie 1992). Mean shell length and width were compared with independent-samples, two-sided t-tests, assuming unequal variances, using Microsoft Excel (version 16.44). Extensive shell metrics and comparisons for all partulid species of the Mariana Islands are found in historical publications (Crampton 1925; Kondo 1955, 1970). More recently Gerlach (2016) carried out extensive morphometric analyses of partulid shells, including *P. lutaensis* sp. nov., there referred to as *Partula* sp. (Rota). We therefore have made no other shell size comparisons. Lacking phylogenetic data for *P. langfordi*, our objective here was to replicate Kondo's shell size comparison between *P. langfordi* and sympatric *P. gibba* to determine whether *P. langfordi* and *P. lutaensis* sp. nov. are similarly distinct.

Morphology of the male reproductive tract

Many taxonomic descriptions of partulid snails have emphasized reproductive anatomy, particularly differences in the male part of the reproductive tract, to differentiate species (Pilsbry 1909; Pilsbry and Cooke 1934; Kondo 1955, 1968; Gerlach 2016; Slapcinsky and Kraus 2016). For this purpose, we obtained preserved specimens of *Partula radiolata* (lot nos. 21462 [2] and 213605 [1]) and *P. gibba* (lot nos. 214256 [2] and 214179 [1]) from Guam and those recorded as *P. gibba* from Rota (lot nos. 188958 [2], 213131 [2], 213152 [3]) from the extensive collections of the BPBM in Honolulu, Hawai'i. In selecting preserved museum specimens from Rota, we endeavored to obtain snails from the same or very near sites where snail tissue samples were collected for DNA analysis. Kondo and others who collected at these sites separated 'soft parts' from many shells for inclusion in the Bishop Museum collections and maintained the same lot numbers for the shells and preserved bodies for snails collected at one site at the same time. This allowed us to examine the shells before carrying out the dissections to make certain that the shells matched the shells of the snails from which we had collected small tissue samples for DNA analyses. In all cases, we were successful in this matching. Kondo (1970) found no difference in the male reproductive tracts of *P. langfordi* and *P. gibba*. We therefore did not dissect specimens of *P. langfordi*.

The following specimens were dissected.

- *Partula radiolata* (Pfeiffer, 1846) from Guam: BPBM no. 214262, 2 spms; BPBM no. 213605, 1 spm.
- *Partula gibba* Férussac, 1821 from Guam: BPBM no. 214256, 2 spms; 214179, 1 spm.
- *Partula* sp. nov. from Rota, as *P. gibba* in BPBM collections: BPBM no. 213151, 3 spms; 188958, 1 spm.; 213132, 2 spms; 213128, 1 spm.

The museum specimens were stored in 90% ethanol. Before dissecting them, we transferred them to three changes of fresh water and carried out the dissections under

water. The reproductive tracts of the snails were exposed by cutting the right-dorsal wall of the snail with a fine scalpel. Then, using fine forceps, the reproductive tract was carefully exposed and the ducts teased apart. Dissections were photographed with a Canon camera mounted on a Zeiss dissection microscope. Outline drawings were made by tracing duct contours from photos using Adobe Illustrator.

DNA analysis

During our collecting trip to Rota in 2010 only small tissue samples were collected for DNA analysis. Following the discovery of a cryptic species on Rota described in Sischo and Hadfield (2017), we were sent five newly collected voucher specimens from Rota by the CNMI Division of Fish and Wildlife to serve as type material for this new cryptic species. Unfortunately, our attempts to extract DNA from these ethanol-preserved specimens failed for unknown reasons. In the interim, all *Partula* species from Guam and the Commonwealth of the Northern Mariana Islands were listed as Endangered under the U.S. Endangered Species Act (US Fish and Wildlife Service 2015). Due to the rarity of the new species and its listing status, we have been unable to obtain another full voucher specimen. To move forward with describing this species, three non-lethal tissue samples were collected from individuals of the same population as the original shell vouchers provided by the CNMI Division of Fish and Wildlife, as well as three samples from a new site not visited by Sischo and Hadfield (2017). Non-lethal tissue samples were collected following the methodology of Thacker and Hadfield (2000), originally developed for sampling Hawaiian tree snails. These tissue vouchers were used to confirm that the shell vouchers are *P. lutaensis* and not *P. gibba*. Tissue sample collection, tissue preservation, total cell DNA extraction, CO1 DNA amplification and CO1 phylogenetic analyses were carried out using the methods described by Sischo and Hadfield (2017).

Results

Systematics

Class Gastropoda Cuvier, 1795

Subclass Heterobranchia Burmeister, 1837

Order Stylommatophora A. Schmidt, 1855

Superfamily Pupilloidea W. Turton, 1831

Family Partulidae Pilsbry, 1900

Genus *Partula* Férussac, 1821

Type species. *Helix faba* Gmelin, 1791.

***Partula lutaensis* sp. nov.**

<http://zoobank.org/65D4AC75-488B-4A29-9773-5E0F5FB25449>

Type material. *Holotype*. Bishop Museum BPBM 284888 Fig. 3. Entire specimen collected by Jill Liske-Clark, 20/11/2014 from type locality. *Paratypes*. BPBM 284889, 2 specimens collected by Jill Liske-Clark, 20/11/2014, from type locality, and BPBM 284890, 3 specimens collected by Jill Liske-Clark, same date, from a second location on Rota Island, Commonwealth of the Northern Mariana Islands.

Type locality. Rota Island, Commonwealth of the Northern Mariana Islands (CNMI).

Diagnosis. Shell. Shell dextral, moderately thin, ovate-conic, slightly perforate; umbilicus open; whorls moderately convex, suture adpressed; aperture ovate-elongate, slightly oblique; outer lip reflexed, thick, glossy; parietal lip glossy with light or dark coloration; color of embryonic whorls and post-embryonic whorls variable from shades of brown, buff, white and yellow with prominent white subsutural band; Measurements ($N = 48$ specimens from five lots in BPBM collections from Rota): height (= length) 15.98 mm, s.d. 0.75 mm; width, 10.64 mm, s.d., 0.24 mm. See Figure 4 for examples of shell color variation. Shell greatly resembles those of *Partula gibba* on Guam and Saipan (Crampton 1925).

Distinguishing shells of *P. lutaensis* from those of *P. langfordi*. Shell length of *P. langfordi* ($M = 13.83$ mm, s.d. = 0.37 mm, $N = 47$) was significantly shorter than the length of *P. lutaensis* sp. nov. ($M = 15.98$ mm, s.d. = 0.75 mm, $N = 48$), $t(82) = -13.91$,



Figure 3. Shell holotype of *P. lutaensis* sp. nov.



Figure 4. Left – Color morphs of *Partula lutaensis* sp. nov. found within a 10 × 10-meter quadrat. Right – Closeup of a *Partula lutaensis* sp. nov. with a dark shell.

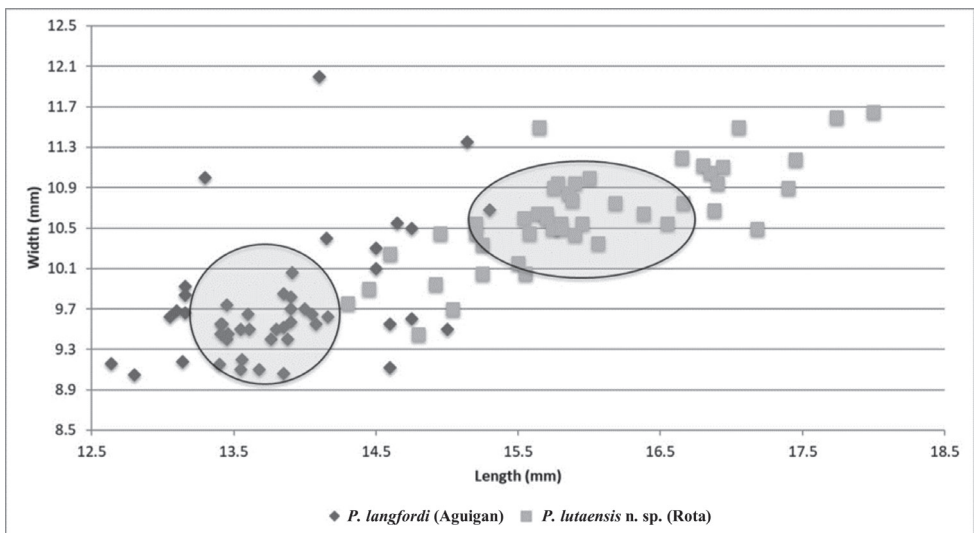


Figure 5. Scattergram of Bishop Museum shell measurements comparing shell width (y-axis) by shell length (x-axis) of 48 *P. langfordi* from Aguigan and 47 *P. lutaensis* sp. nov. from Rota. The mean shell length and width plus standard deviation of each species are encircled. All shells were lipped indicating snails were mature and had reached terminal growth.

$P < 0.001$. Similarly, shell width of *P. langfordi* ($M = 9.74$ mm, $s.d = 0.36$ mm) was significantly less than that of *P. lutaensis* sp. nov. ($M = 10.64$ mm, $s.d = 0.24$ mm), $t(90) = -8.02$, $P < 0.001$ (Fig. 5).

Male reproductive system. The male reproductive system of *Partula gibba* figured by Kondo (1955, 1970) and Gerlach (2016) is highly variable. In specimens we examined (Fig. 6A), the vas deferens entered the penis very near its top, leaving the upper

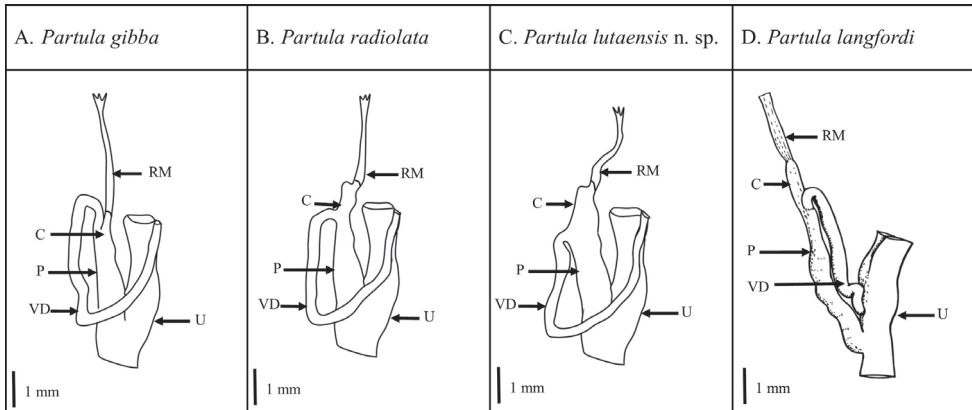


Figure 6. Outline drawings comparing the male reproductive tracks of four extant *Partula* species from the Mariana Islands. Male anatomy abbreviations are as follows: retractor muscle (RM), caecum (C), penis (P), vas deferens (VD), uterus (U). The figure of *Partula langfordi* is adapted from figure 5 of Kondo (1970). Note, Kondo found no difference between the male reproductive tracts of *P. gibba* and *P. langfordi*.

portion of the penis, attached to the retractor muscle and called the caecum by Gerlach (2016), to be very short. In specimens of *P. radiolata*, the entry of the vas deferens was about 1/5 to 1/4 of the length of the penis below the retractor-muscle attachment (Fig. 6B). However, the male duct was distinctive in *P. lutaensis* sp. nov. by the bulge or shoulder at the top of an expanded caecum, proximal to the vas deferens. In the male system of *P. lutaensis* sp. nov., the attachment of the vas deferens was consistently more distal than in either *P. gibba* or *P. radiolata* (Fig. 6C); the insertion was close to 1/3 of the length of the penis below the retractor-muscle attachment. In no other regard were there any distinctive differences among the penial structures of these three species. The lower attachment of the vas deferens to the retractor muscle in both *P. lutaensis* sp. nov. and *P. radiolata* is concordant with their placement as sister taxa in phylogenetic reconstructions of the group. Kondo (1970) found no differences between the male reproductive tract of *P. langfordi* and *P. gibba*. We include a modified version of his drawing with ours for comparison (Fig. 6D).

Ecology. Type and paratype specimens were found on *Epiprennum aureum* and *Tectaria crenata* (J. Liske-Clark, Northern Mariana Department of Fish and Wildlife, personal communication).

Etymology. The specific epithet *lutaensis* recognizes Luta, the indigenous Chamorro name for the island of Rota.

DNA analyses

Analyses of the mitochondrial CO1 fragment confirmed that the tissue samples collected from the two type and paratype collection localities on Rota are *P. lutaensis* sp. nov. From the six tissue samples collected, two additional CO1 haplotypes were recovered (GenBank Accession numbers MT720839 and MT720840). As described in

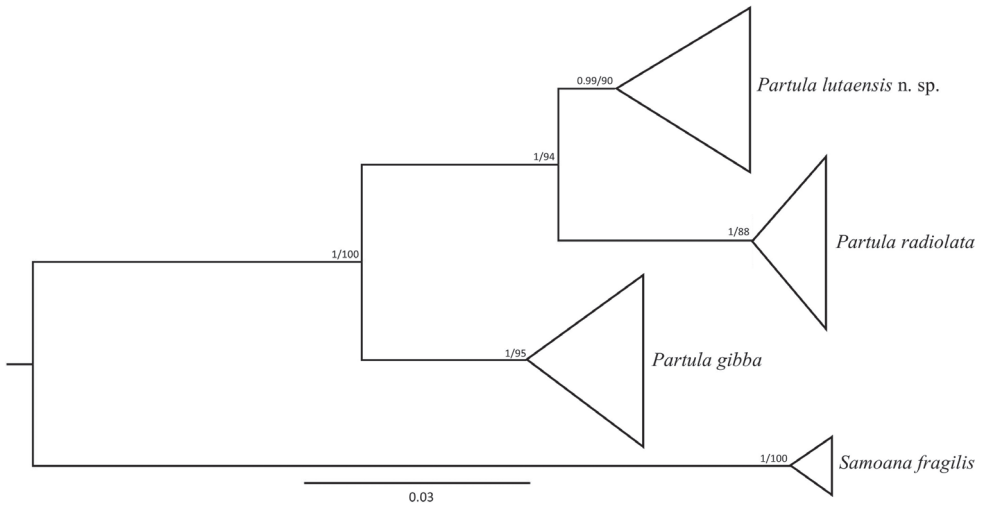


Figure 7. Bayesian phylogenetic tree representing the relationships between extant species in the family Partulidae from the Mariana Archipelago. This figure is an adaptation from one published in Sischo and Hadfield (2017). The phylogeny contains sequences from 24 individuals with unique haplotypes from seven islands and is based on a concatenated alignment of three genes (CO1, 16S and ITS2). The combined sequence length was 1683 base pairs. Maximum likelihood and Bayesian analyses recovered comparable topologies. Therefore, Bayesian posterior probabilities and maximum likelihood bootstrap values are reported on all nodes greater than 0.80 or 80% respectively. Branch ends have been collapsed to emphasize support for the species groups, rather than within group relationships. Also, note that this phylogeny does not include the newly sequenced haplotypes of *Partula lutaensis* sp. nov. mentioned above.

Sischo and Hadfield (2017), *P. lutaensis* sp. nov. is sister to *P. radiolata* from Guam despite having a shell more similar in appearance to *P. gibba* than to *P. radiolata* (Fig. 7). Currently all known extant colonies of *Partula* on Rota are *P. lutaensis* sp. nov.

Discussion

The phylogeographic assessment of the extant partulids in the Mariana Islands reported by Sischo and Hadfield (2017) strongly supports the presence of a cryptic species on Rota and is concordant with further analyses of the male reproductive tracts, with *P. lutaensis* sp. nov. and *P. radiolata* sharing a lower attachment of the vas deferens in relation to the retractor muscle. Because this cryptic species was not found on any other islands, we conclude it is endemic to the island of Rota and have given it the name *Partula lutaensis* sp. nov. to recognize the indigenous Chamorro name for the island.

Available data indicate that all known populations of the genus *Partula* on Rota are *P. lutaensis* sp. nov.. This does not rule out the possibility that *P. gibba* once was, or currently is, on the island. Further surveys for extant partulid populations and analysis of sub-fossil shell remains on Rota may provide further evidence as to the present and



Figure 8. A *Partula lutaensis* sp. nov. freshly depredated by *Platydemus manokwari* observed by authors on Rota.

historical distribution of these two species on the island. Moving forward, we strongly encourage that DNA barcoding be employed to determine species identification of any new living populations of *Partula* spp. discovered on Rota and elsewhere in the Mariana Islands. Furthermore, should *P. gibba* be located on Rota it should be attempted to find shell or body characters that might aid in distinguishing the two species without dissection or tissue sample collection.

Partula lutaensis sp. nov. was observed in locally high abundance on Rota, similar to observations of *P. radiolata* on Guam (Sischo and Hadfield 2017). Unfortunately, *P. gibba*, once the most abundant partulid on Guam, is now almost entirely extirpated (Hopper and Smith 1992; Sischo and Hadfield 2017; C. Fiedler personal communication June 2018). Persistence despite depredation by introduced predators may be further evidence of the shared ancestry between *P. lutaensis* sp. nov. and *P. radiolata*. Possibly, the *P. lutaensis* – *P. radiolata* clade shares behavioral and or life-history traits that have allowed the species to persist despite significant threats. For

example, a recent study found that *P. radiolata* has a higher reproductive rate than *P. gibba* (Bick et al. 2018).

Across the Pacific, partulid species have been driven to extinction by introduced predators, most notably North American carnivorous snail species in the genus *Euglandina*, and the New Guinea flatworm *Platydemus manokwari* (Clarke, Murray and Johnson 1984; Murray et al. 1988; Hopper and Smith 1992; Bauman 1996; Coote et al. 1999; Cowie and Cook 2001; Régnier, Fontaine and Bouchet 2009; Pelep and Hadfield 2011; Meyer et al. 2017; Sischo and Hadfield 2017; Hadfield 2020; Gerlach et al. 2020). This has been particularly true in the Mariana Islands where half of the described partulid species are thought to be extinct, and the remaining species are imperiled across their ranges. While we observed *P. lutaensis* sp. nov. in locally high numbers in 2010, known populations are few and geographically discrete. Sub-fossil shells of partulids are ubiquitous on Rota (Bauman 1996) and Saipan (personal observations, October 2014), suggesting severe range reductions (Bauman 1996). Additionally, we observed *Platydemus manokwari* depredating *P. lutaensis* sp. nov. while collecting tissue samples on Rota (Fig. 8). Because *P. lutaensis* sp. nov. is an island-endemic species with a very restricted range and is clearly under significant predation pressure from introduced species, its existence is imperiled. When the Rota populations were considered to be *Partula gibba*, they were protected by a federal Endangered Species declaration. For these reasons, it is imperative that *Partula lutaensis* sp. nov. be listed as Endangered as soon as possible.

Acknowledgements

This project was supported by the US Fish and Wildlife Service and by the University of Hawai‘i at Mānoa. We would like to thank Ms Regina Kawamoto and Dr Norine Yeung with the Bishop Museum of Honolulu for providing access to the mollusc collection and for allowing us to borrow and dissect historically collected specimens for anatomical analyses. We would like to thank Paul Pearce-Kelly, Angus Davison, Chris Wade, Justin Gerlach, and Barry Smith for helping us sort out the mystery of a possible captive colony of *P. langfordi* in England and for mailing us specimens. Additionally, we would like to thank Jill Liske-Clark of the Commonwealth of the Northern Mariana Islands – Division of Fish and Wildlife for her support in our efforts and for collecting voucher specimens and additional tissue samples from Rota.

References

- Bauman S (1996) Diversity and decline of land snails on Rota, Mariana Islands. *American Malacological Bulletin* 12: 13–27. <https://www.biodiversitylibrary.org/part/143145#/summary>
- Bauman S, Kerr AM (2013) *Partula desolata* sp. nov. (Pulmonata: Partulidae), an extinct land snail from Rota, Mariana Islands Micronesia. *Micronesica* 5: 1–12. http://micronesica.org/sites/default/files/2013-05_bauman-kerr_partula.pdf

- Bick CS, Pearce-Kelly P, Coote T, Ó Foighil D (2018) Survival among critically endangered partulid tree snails is correlated with higher clutch sizes in the wild and higher reproductive rates in captivity. *Biological Journal of the Linnean Society* 125(3): 508–520. <https://doi.org/10.1093/biolinnean/bly124>
- Clarke B, Murray J, Johnson MS (1984) The extinction of endemic species by a program of biological control. *Pacific Science* 38(2): 97–104. <http://hdl.handle.net/10125/844>
- Coote T, Clarke D, Loeve E, Meyer JY (1999) Extant populations of endemic partulids on Tahiti, French Polynesia. *Oryx* 33(3): 215–222. <https://doi.org/10.1046/j.1365-3008.1999.00065.x>
- Cowie RH (1992) Evolution and extinction of Partulidae, endemic Pacific island land snails. *Philosophical Transactions of the Royal Society of London B – Biological Sciences* 335: 167–191. <https://doi.org/10.1098/rstb.1992.0017>
- Cowie RH, Cook RP (2001) Extinction or survival: partulid tree snails in American Samoa. *Biodiversity and Conservation* 10: 143–159. <https://doi.org/10.1023/A:1008950123126>
- Crampton HE (1925) Studies on the variation, distribution, and evolution of the genus *Partula*. The species of the Mariana Islands, Guam and Saipan. Carnegie Institution of Washington Publication 228a: 1–116.
- Gerlach J (2016) Icons of evolution: Pacific Island tree-snails, family Partulidae. Cambridge Phelsuma Press, 336 pp.
- Gerlach J, Barker GM, Bick CS, Bouchet P, Brodie G, Cristensen CC, Collins T, Coote T, Cowie RH, Fiedler CG, Griffiths OL, Florens FBV, Hayes K, Kim J, Meyer J, Meyer WM, Richling I, Slapcinsky JD, Winsor L, Yeung NW (2020) Negative impacts of invasive predators used as biological control agents against the pest snail *Lissachatina fulica*: the snail *Euglandina 'rosea'* and the flatworm *Platydemus manokwari*. *Biological Invasions* 23: 997–1031. <https://doi.org/10.1007/s10530-020-02436-w>
- Goodacre SL, Wade CM (2001) Molecular evolutionary relationships between partulid land snails of the Pacific. *Proceedings of the Royal Society B – Biological Sciences* 268(1462): 1–7. <https://doi.org/10.1098/rspb.2000.1322>
- Hadfield MG (2015) The occurrence of the endangered tree snail *Partula gibba* in the Mariana Islands, with a focus on Pagan Island. *Bishop Museum Bulletin in Zoology* 9: 147–167. <http://hbs.bishopmuseum.org/pubs-online/pdf/bz9-10.pdf>
- Hadfield MG (2020) Snails that eat snails. *The Feral Atlas* (Stanford University Press). <https://feralatlus.supdigital.org/poster/snails-that-eat-snails>
- Hopper DR, Smith BD (1992) Status of Tree Snails (Gastropoda: Partulidae) on Guam, with a Resurvey of Sites Studied by HE Crampton in 1920. *Pacific Science* 46: 77–85. <https://scholarspace.manoa.hawaii.edu/bitstream/10125/1675/v46n1-77-85.pdf>
- Kondo Y (1955) A revision of the family Partulidae (Gastropoda Pulmonata). PhD Thesis, Cambridge, Harvard University, Massachusetts.
- Kondo Y (1968) Partulidae: preview of anatomical revision. *Nautilus* 81: 73–77.
- Kondo Y (1970) Some aspects of Mariana Islands Partulidae (Mollusca, Pulmonata). *Bishop Museum Occasional Papers* 24(5): 73–90. <http://hbs.bishopmuseum.org/pubs-online/pdf/op24-5.pdf>
- Lee T, Li J, Churchill CK, Ó Foighil D (2014) Evolutionary history of a vanishing radiation: isolation-dependent persistence and diversification in Pacific Island partulid tree snails. *BMC Evolutionary Biology* 14: e202. <https://doi.org/10.1186/s12862-014-0202-3>

- Meyer WM, Yeung NW, Slapcinsky J, Hayes KA (2017) Two for one: inadvertent introduction of *Euglandina* species during failed bio-control efforts in Hawaii. *Biological Invasions* 19: 1399–1405. <https://doi.org/10.1007/s10530-016-1354-4>
- Murray J, Murray E, Johnson M, Clarke B (1988) The extinction of *Partula* on Moorea. *Pacific Science* 42: 150–153.
- Pelep PO, Hadfield MG (2011) The status of the endemic snails of the genus *Partula* (Gastropoda: Partulidae) on Pohnpei, Federated States of Micronesia. *Micronesica* 41(2): 253–262. https://micronesica.org/sites/default/files/17_pelep-hadfield_pp_253-262.pdf
- Pilsbry HA (1909–1910) *Manual of Conchology, Structural and Systematic vol 20: Caecilioides, Glessula and Partulidae*. Academy of Natural Sciences, Philadelphia, 154 pp.
- Pilsbry HA, Cooke CM (1934) Partulidae of Tonga and related forms. *Occasional Papers of the Bernice P. Bishop Museum* 10: 3–22. <http://hbs.bishopmuseum.org/pubs-online/pdf/op10-14.pdf>
- Régnier C, Fontaine B, Bouchet P (2009) Not knowing, not recording, not listing: numerous unnoticed mollusk extinctions. *Conservation Biology* 23(5): 1214–1221. <https://doi.org/10.1111/j.1523-1739.2009.01245.x>
- Slapcinsky J, Kraus F (2016) Revision of Partulidae (Gastropoda, Stylommatophora) of Palau, with description of a new genus for an unusual ground-dwelling species. *ZooKeys* 614: 27–49. <https://doi.org/10.3897/zookeys.614.8807>
- Sischo DR, Hadfield MG (2017) Phylogeographic relationships among multi-island populations of the tree snail *Partula gibba* (Partulidae) in the Mariana Islands. *Biological Journal of the Linnean Society* 121: 731–740. <https://doi.org/10.1093/biolinnean/blx031>
- Smith BD (2013) Taxonomic inventories and assessments of terrestrial snails on the islands of Tinian and Aguiguan in the Commonwealth of the Northern Mariana Islands. University of Guam Marine Laboratory Technical Report 154.
- Thacker RW, Hadfield MG (2000) Mitochondrial phylogeny of extant Hawaiian tree snails (Achatinellinae). *Molecular Phylogenetics and Evolution* 16: 263–270. <https://doi.org/10.1006/mpev.2000.0793>
- US Fish and Wildlife Service (2015) Endangered and Threatened Wildlife and Plants; Endangered Status for 16 Species and Threatened Status for 7 Species in Micronesia. *Federal Register* 80: 59424–59497. <https://www.govinfo.gov/content/pkg/FR-2015-10-01/pdf/2015-24443.pdf>

Taxonomic study of the Oriental genus *Catullioides* Bierman, 1910 (Hemiptera, Fulgoromorpha, Tropicuchidae), with description of a new species from China

Hao-Yu Zhu¹, Fang Yu¹, Si-Yuan Xu¹, Fang-Zhou Ma²,
Rong-Rong Wang³, Zhi-Shun Song¹

1 Institute of Insect Resources and Biodiversity, School of Life Sciences, Chemistry & Chemical Engineering, Jiangsu Second Normal University, Nanjing, China **2** Nanjing Institute of Environmental Sciences, Ministry of Ecology and Environment, Nanjing, China **3** Key Laboratory of Zoological Systematics and Evolution, Institute of Zoology, Chinese Academy of Sciences, Beijing, China

Corresponding authors: Rong-Rong Wang (wangrr@ioz.ac.cn); Zhi-Shun Song (songzs@jssnu.edu.cn)

Academic editor: Mike Wilson | Received 4 March 2021 | Accepted 19 April 2021 | Published 17 May 2021

<http://zoobank.org/10E8FE8D-686F-4C5E-9445-BCC7FCFA5E95>

Citation: Zhu H-Y, Yu F, Xu S-Y, Ma F-Z, Wang R-R, Song Z-S (2021) Taxonomic study of the Oriental genus *Catullioides* Bierman, 1910 (Hemiptera, Fulgoromorpha, Tropicuchidae), with description of a new species from China. ZooKeys 1037: 119–136. <https://doi.org/10.3897/zookeys.1037.65481>

Abstract

The tropiduchid genus *Catullioides* Bierman, 1910 is redescribed and illustrated. *Catullioides* includes two species, *C. rubrolineata* Bierman, 1910 (the type species) and *C. taishunensis* Zhu, Wang & Song, **sp. nov.** A key to the species of the genus is provided.

Keywords

Catullioini, Fulgoroidea, morphology, taxonomy

Introduction

The planthopper family Tropicuchidae Stål is one of twenty-one currently recognized extant families of Fulgoroidea (Hemiptera: Fulgoromorpha) (Wang et al. 2016; Bourgoin 2021). With more than 670 species in 196 extant and extinct genera, this family

is divided into two subfamilies, Elicinae Melichar and Tropicuchinae Stål (Bourgoin et al. 2019; Bourgoin 2021). Elicinae comprises four extant tribes and two extinct tribes (Gnezdilov 2013; Szvedo and Stroiński 2017; Bourgoin 2021). Distributed worldwide, Tropicuchinae comprises 17 extant tribes and two fossil tribes (Fennah 1982; Wang et al. 2016). Little research has been done on the phylogenetic relationships within Tropicuchidae (Stroiński et al. 2015), although recently, a morphological phylogeny was completed on Tropicuchini Stål (Wang et al. 2016).

In Tropicuchinae, the tribe Catulliini was first recognized by Fennah (1982) based on the type genus *Catullia* Stål and five other genera. Catulliini may be distinguished from other tribes in Tropicuchinae by the following combination of characters: frons unicarinate; pedicel of antennae with microsetae not extending to base; apical segment of rostrum very short, sometimes broader than long; hind tibiae with four lateral spines; posterior margin of mesonotum broadly rounded; forewings more than 2.5 times as long as broad; vein MP not associated with vein CuA basally; subapical cell R (C2) relatively broad at base and narrowing, usually sinuately, to apex; gonostyles symmetrical, elongate, tapering in distal half, separated from base; anterior connective lamina of gonapophyses VIII with one tooth on ventral margin, and with less than four teeth on dorsal margin; gonopods without teeth at apex or ventrally, longer than gonapophyses VIII [slightly modified based on Fennah (1982)]. The Catulliini taxa are mainly distributed in the Old-World tropics and subtropics, including sub-Saharan Africa, India, Sri Lanka, southern China, Japan (Ryukyu Islands), and Southeast Asia (Bourgoin 2021). Recently, the seventh genus, the fossil genus *Catulliasites* Szvedo (*nomen novum* for *Hastites* Cockerell), from the Insect Limestone (latest Eocene) of the Isle of Wight, UK, was moved to this tribe (Szvedo et al. 2019).

The Oriental genus *Catullioides* was established by Bierman (1910) for a single species, *Catullioides rubrolineata* Bierman, 1910, from Java, Indonesia. *Catullioides rubrolineata* was considered mistakenly as a synonym of *Barunooides albosignatus* (Distant, 1906) by Melichar (1914), creating the erroneous synonymy of *Catullioides* with *Barunooides* Distant (*nomen novum* for *Baruna* Distant, 1906) (Melichar 1914). Distant (1916) corrected this error and observed that “both Bierman’s description and figure define the costal membrane of the tegmina as possessing numerous transverse veins, whereas my description and figure of *Barunooides* clearly show the contrary, costal membrane without transverse veins” (Distant 1916: 53). This taxonomic error was repeated in subsequent literature recording this monotypic genus (e.g., Muir 1931; Yang et al. 1989; Hayashi 1995).

While sorting and identifying planthopper material from the collection of the Insect Explorations of Taishun, Zhejiang, China, on August 21–30, 2020, we found a second and new species of *Catullioides*, *C. taishunensis* Zhu, Wang & Song, sp. nov., which is described and illustrated in this study.

Material and methods

The specimens studied in the course of this work are deposited in the Bernice P. Bishop Museum, Honolulu, HI, U.S.A. (BPBM); Institute of Zoology, Chinese Academy of

Sciences, Beijing, China (**IZCAS**); and Zoological Collection, Jiangsu Second Normal University, Nanjing, China (**JSSNU**).

The post-abdomens of the specimens used for dissections were cleared in 10% KOH at room temperature for ca. 6–12 hours, rinsed and examined in distilled water and then transferred to 10% glycerol and enclosed in microvials to be preserved with the specimens. Observations, measurements, and photography were conducted under a LEICA M205 C optical stereomicroscope with a Canon EOS 5D Mark IV digital camera at the Jiangsu Key Laboratory of Biofunctional Molecules, JSSNU. Some final images were compiled from multiple photographs using the Helicon Focus 6 image stacking software and improved in Adobe Photoshop CC.

The morphological terminology and measurements used in this study follow Wang et al. (2016) for most characters and Bourgoïn et al. (2015) for the forewing. Features noted in the genus description are not repeated in the species description except for clarity or additional description.

Taxonomy

Family Tropiciduchidae Stål, 1866

Genus *Catullioides* Bierman, 1910

Catullioides Bierman, 1910: 21. Type species: *Catullioides rubrolineata* Bierman, 1910; by original designation and monotypy.

Catullioides Bierman: Metcalf (1954: 58); Fennah (1982: 638); Yang et al. (1989: 74).

Diagnosis. *Catullioides* may be distinguished from other genera in Tropiciduchidae by the following combination of characters: vertex shorter than width, anterior margin distinctly arched, lateral carinae strongly elevated, posterior margin angularly concave, median carina complete; frons and clypeus with median carina broadly and strongly convex, intermediate carinae absent; rostrum very short and robust, apical segment abruptly truncate and concave at apex; antennae with pedicel cylindrical, with no more than 20 sensory plaque organs distributed in apical half; pronotum with anterior central part distinctly produced forwards, anterior margin strongly convex, median and intermediate carinae complete and sharp; mesonotum tricarinate, lateral carinae incurving and converging anteriorly; forewings narrow and long, with nodal line, costal area narrow with numerous transverse veinlets, number of apical cells between veins RA and CuA from 14 to 16; hind tibiae with four lateral spines and seven apical teeth, hind tarsomeres I with eight apical teeth; gonostyles symmetrical, elongate, outer ventral edge strongly carinate from base to apex; periandrium symmetrical, reniform and compressed; aedeagus asymmetrical, elongate, cylindrical, with four sclerotised processes; segment X of male slender and elongate, with long lateroapical angles.

Redescription. Head including compound eyes slightly narrower than pronotum (Figs 3A, 7A). Vertex (Figs 3A, 7A) broad, shorter in midline than width at base;

anterior margin ridged and distinctly arched anteriorly, lateral carinae strongly elevated and subparallel, posterior margin carinate and angularly concave at about 100° angle, median carina distinct and complete; disc slightly depressed. Frons (Figs 3C, 7C) large and broad, convex in midline, longer than breadth, lateral margins weakly carinate, slightly converging below antennae; median carina broadly and strongly convex, intermediate carinae absent. Frontoclypeal suture (Figs 3B, C, 7B, C) distinct and straight. Clypeus (Figs 3C, 7C) about half as long as frons, median carina broadly and strongly convex. Rostrum (Figs 3C, 7C) very short and broad, reaching to middle coxae, apical segment short, as long as breadth, abruptly truncate and concave at apex. Compound eyes (Figs 3A–C, 7A–C) oval. Ocelli (Figs 3B, 7B) small, reddish, close to eye and away from base of antennae. Antennae (Figs 3A–C, 7A–C) with scape small, ring-like; pedicel cylindrical, covered with fine setulae and no more than 20 sensory plaque organs distributed in apical half.

Pronotum (Figs 3A–C, 7A–C) longer than vertex in midline, distinctly shorter than mesonotum in midline; anterior central part distinctly produced forwards with anterior margin keeled and strongly convex; disc large, strongly elevated, tricarinate and delimited by intermediate carinae, median and intermediate carinae complete and sharp, median carina with a lateral pit on each side; lateral marginal areas deeply concave with a longitudinal carina on each side from eye to tegula; posterior margin subangulately concave. Mesonotum (Figs 3A, 7A) clearly tricarinate on disc, lateral carinae incurving, converging anteriorly, and reaching end of median carina. Forewings (Figs 3D, F, 7D) hyperpterous, narrow and long, membranous, without granulation, with nodal line (just past midlength); costal area present, narrower than costal cell, beyond level of tip of clavus, with numerous transverse veinlets; vein ScP+R forked basad before midlength and well basad nodal line, ScP+RA separated beyond nodal line; vein MP bifurcating into MP_{1+2} and MP_{3+4} at level of nodal line; vein CuA forked before ScP+R forking; Pcu and A_1 veins fused into a long Pcu+A1 vein at apical 1/3 in clavus; number of apical cells between veins RA and CuA from 14 to 16. Hindwings (Figs 3E, G, 7E) hyaline, ScP+R, MP and CuA bifurcating only once; ScP+R and CuA bifurcating near apical third, anterior to bifurcation of MP; veins CuP and Pcu unbranched, running close and parallel at their base; vein A_1 bifurcating into A_{1a} and A_{1b} near middle, A_2 unbranched; transverse veinlets *r-m* and *m-cua1* anterior to bifurcation of MP. Legs moderately long, hind tibia with four lateral spines (rarely three with the extreme basal spine absent) and seven apical teeth; hind tarsomere I with eight apical teeth and hind tarsomere II with two lateral apical teeth.

Male genitalia. Pygofer (Figs 4A–D, 8A–D), in lateral view (Figs 4A, B, 8A, B), much wider ventrally than dorsally, posterior margin more or less convex medially, without process, anterior margin produced in a pair of broad and large sclerotised processes ventrolaterally, inserted in former segment; in dorsal view (Figs 4C, 8C), dorsal margin slightly excavated to accommodate segment X. Gonostyles (Figs 4A, B, D, 8A, B, 8D) symmetrical, elongate, in ventral view (Figs 4D, 8D), inner margin more or less sinuate; in lateral view (Figs 4A, B, 8A, B), narrow at base, broadest in middle, gradually convergent and tapering toward apex, acute apically; dorsal margin

irregularly sinuate, with a finger-like process raised from dorsolateral margin at base, directed dorsolaterad; outer dorsal edge with a hook-like process near basal third, directed caudad and curved ventrolaterad, acute at apex, twisted; outer ventral edge strongly carinate from base to apex. Periandrium (Figs 4E–H, 8E–H) symmetrical, moderately large, in lateral view (Figs 4F, G, 8F, G), reniform, compressed, its opening declined dorsoventrally, loosely attached to aedeagus basally. Aedeagus (Figs 4E–H, 8E–H) asymmetrical, elongate, cylindrical, sclerotised basally, and inflated apically, with four various sclerotised processes; in dorsal view (Figs 4E, 8E), two right processes produced on the membranous lobe: apical process elongate, tapering laterocaudad, basal one broad, triangular, pointed dorsocephalad; dorsal process small, somewhat triangular, directed dorsocephalad; left process large and broad, knife-like, directed laterocaudad. Segment X (Figs 4A–C, 8A–C) slender and elongate, in lateral view (Figs 4A, B, 8A, B), dorsal margin straight then declined ventrocaudad; ventral margin slightly incurved, lateroapical angles truncated apically; in dorsal view (Figs 4C, 8C), slender, expanded at base, narrowed in middle, apex deeply excavated to accommodate anal style, lateroapical angles strongly produced caudad. Anal style cylindrical, relatively small, not reaching to apex.

Female genitalia. Gonocoxae VIII (Figs 5B, C, E, G) with one membranous, slender, flattened endogonocoxal processes on endogonocoxal lobe. Gonapophyses VIII (Figs 5B, C, E, F) with anterior connective lamina strongly sclerotized, narrow and straight, in lateral view, tapering distad, with five minute teeth on dorsal margin, ventral margin slightly curved dorsad at apical fourth with three large blunt teeth. Gonapophyses IX (Figs 5G, H) converging apically, suddenly protruding laterad, truncate at apex. Gonoplasts (Figs 5A–C, I) fused at basal fourth, with two sclerotized lobes fully fused together and delimited by a longitudinal membranous suture: dorsal lobe elongate and tapering caudad, ventral lobe large, longer, apical part rounded, smooth. Segment X (Figs 5A, B, D, I) very small, in lateral view (Fig. 5I), triangular, broaden caudally, caudal margin reclined caudoventrad; in dorsal view (Fig. 5D), apex excavated to accommodate anal style. Anal style (Fig. 5D) relatively small, almost as long as length of caudal margin.

Biology. Collecting data show that adults of both *C. rubrolineata* and *C. taishunensis* sp. nov. were collected from *Miscanthus floridulus* (Lab.) Warb. ex Schum et Laut. (common name: giant *Miscanthus*; Poaceae), the largest of the *Miscanthus* species. It has coarse foliage with a distinct central rachis on a feathery inflorescence. *Catullioides rubrolineata* exhibits phototaxis as most specimens were collected by light trapping (see also Yang et al. 1989; Hayashi 1995), while *C. taishunensis* sp. nov. was never collected in this way.

Diversity and distribution. The genus contains two species widely distributed in the Oriental region.

Remarks. *Catullioides* is externally similar to the genus *Catullia* Stål, but can be separated from the it by the following features: the general color of the body, especially the broad red stripes along the median carinae of the vertex, frons, clypeus, pronotum and mesonotum; the vertex with a complete median carina and angularly concave

posterior margin (median carina absent and posterior margin broadly concave in *Catullia*); and the number of apical cells between veins RA and CuA of forewings from 14 to 16 (about ten in *Catullia*).

Key to species of *Catullioides*

- 1 Forewings almost flat, central area of basal two-thirds and apical third dark brown to black, clavus, apices of costal area, postcostal cell, and veins C1 and C2 yellowish green in males (Figs 2C, 3D); hindwings relatively broad, ratio of length to width about 1.9–2.0:1 (Fig. 3E, G) ***C. rubrolineata* Bierman, 1910**
- Forewings tectiform, membrane distinctly incurved, mostly fuscous to black, clavus yellowish-green to dark brown in males (Figs 6C, 7D); hindwings narrow and long, ratio of length to width about 2.6:1 (Fig. 7E)..... ***C. taishunensis* Zhu, Wang & Song, sp. nov.**

***Catullioides rubrolineata* Bierman, 1910**

Figures 1–5

Catullioides rubrolineata Bierman, 1910: 22, pl. 1, fig. 9a–d.

Barunoides albosignata (Distant): Melichar (1914: 140) [error].

Catullioides albosignatus (Distant): Yang et al. (1989: 74, fig. 3); Hayashi (1995: 65, fig. 1) [error].

Redescription. Body length from apex of head to tip of forewings: ♂ 8.4–9.5 mm, ♀ 9.4–10.3 mm; head length from apex of cephalic process to base of eyes: ♂ 0.7–0.8 mm, ♀ 0.8–0.9 mm; head width including eyes: ♂ 1.3–1.4 mm, ♀ 1.4–1.5 mm; forewing length: ♂ 7.0–7.7 mm, ♀ 8.1–8.6 mm.

Coloration. Sexual dimorphism in general color (Fig. 1). Females distinctly paler on body than males (Fig. 2). General color pale green and red on head and thorax, and dark brown on body. Head excluding eyes, pronotum and mesonotum mostly pale green to yellowish green, broad stripes along median carinae of vertex, frons, clypeus, pronotum and mesonotum, lateral margins of frons, lateral areas of pronotum and mesonotum behind eyes red, clypeus and apical margins of paranotal lobes dark brown to black. Compound eyes red to fuscous with posterior margin pale green, ocelli purplish red. Forewings, in males (Fig. 3D), with central area of basal two-thirds and apical third dark brown to black, clavus, apices of costal area, postcostal cell, veins C1 and C2 yellowish green; in females (Fig. 3F), much paler than in males, mostly yellowish green, central area of basal two-thirds and Medial area dark brown to black. Thorax and abdomen mostly black in males (Fig. 2C); in females (Fig. 2D), much paler than in males, mostly yellowish brown.



Figure 1. Habitus of *Catullioides rubrolineata* Bierman **A** male **B** female. Photographed by Z-S Song.

Structure. Vertex (Fig. 3A) wider than length, with ratio of length at midline to width between eyes 0.5:1. Frons with ratio of length at midline to maximum width 1.6:1 (Fig. 3C). Forewings (Fig. 3D, F) almost flat, ratio of length to width about 2.9–3.2:1. Hindwings (Fig. 3E, G) with ratio of length to width about 1.9–2.0:1.

Male genitalia. Pygofer, in lateral view (Figs 4A, 4B), with posterior margin slightly sinuate, more or less convex medially, anterior margin produced in a pair of broad and large sclerotised processes ventrolaterally; in ventral view (Fig. 4D), far longer than in dorsal view (Fig. 4C), with ratio of ventral to dorsal width about 4.5:1. Gonostyles (Fig. 4A, B, D) elongate, in ventral view (Fig. 4D), inner area along ventrolateral carina less sclerotised and filmy, dorso-basal process directed dorsolaterad; in lateral view (Fig. 4A, B), ventrolateral carina strongly ridged from base to apex. Aedeagus (Fig. 4E–H) large and elongate, as long as gonostyles; in right lateral view (Fig. 4F), right apical process directed dorsad and curved laterocaudad; in left lateral view (Fig. 4G), left process large and broad, base narrow and twisted, remaining cultrate, directed laterocaudad. Segment X (Fig. 4C) slender and elongate, anal style relatively small, not reaching to apex.

Female genitalia (Figs 5A–I) as in generic description.

Material examined. CHINA: 7♂♂, 6♀♀, Zhejiang, Taishun, Beikengdi (27°28'30"N, 119°54'28"E), 469 m, light trap, 28.viii.2020, F.Z. Ma, S.Y. Xu

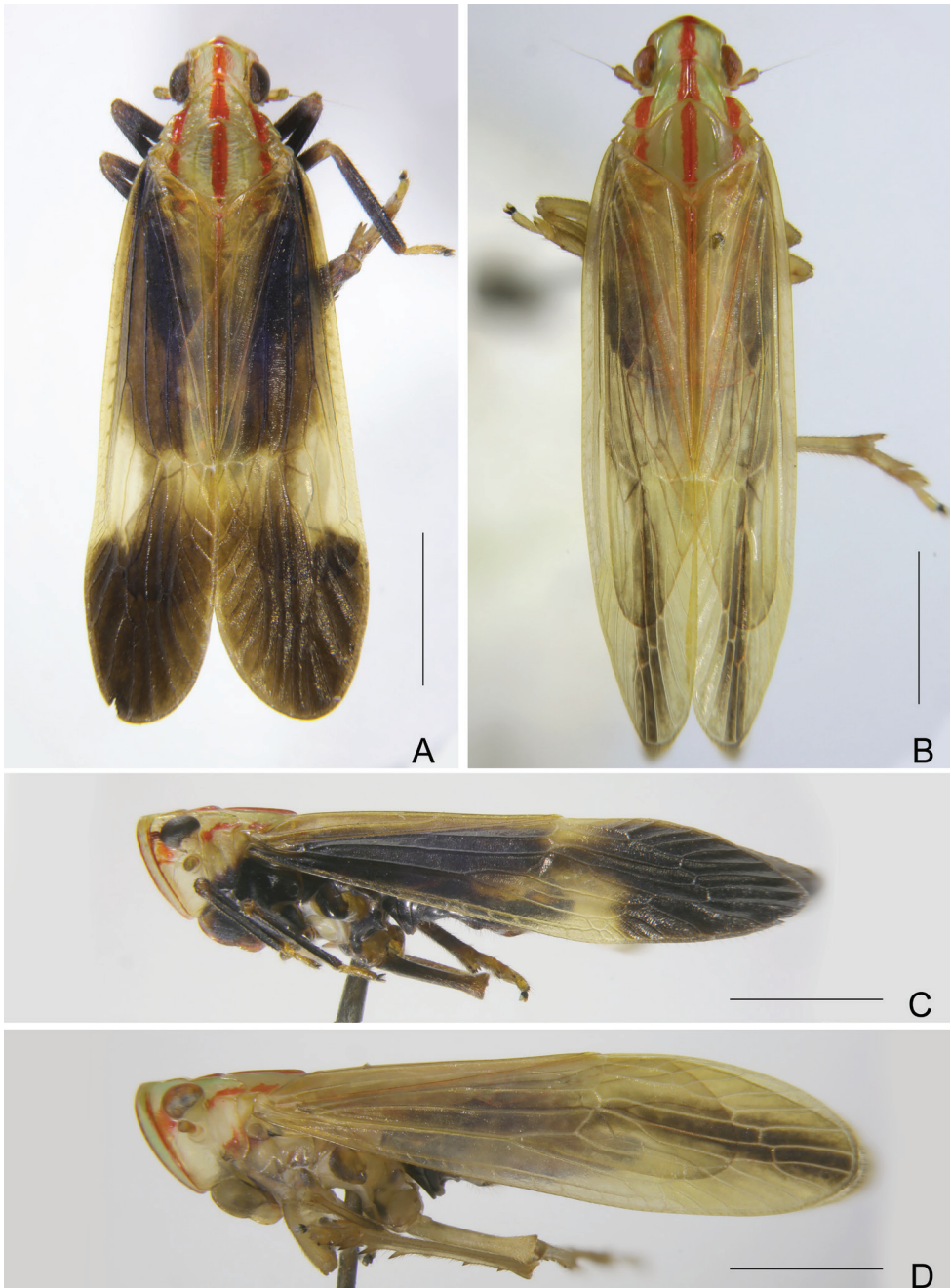


Figure 2. *Catullioides rubrolineata* Bierman **A** male, dorsal view **B** female, dorsal view **C** male, lateral view **D** female, lateral view. Scale bars: 2 mm.

& H.Y. Zhu; 2♂♂, 2♀♀, same collecting locality and time, F.Z. Ma, S.Y. Xu & H.Y. Zhu (all in JSSNU); 1♀, Hainan, Shuiman, 640 m, 29.v.1960, S.F. Li; 8♂♂, 3♀♀, Fujian, Jiangle, Longqi Mountain, 200 m, 10.viii.1991, S.M. Song; 1♀, Fujian,

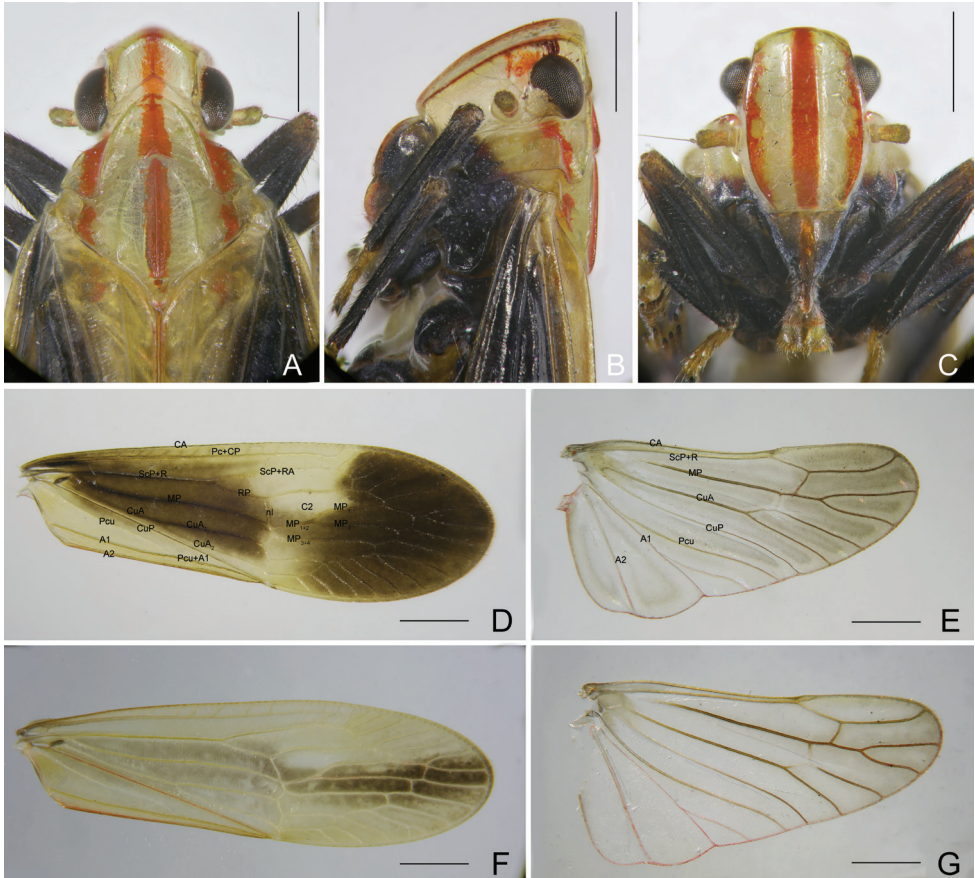


Figure 3. *Catullioides rubrolineata* Bierman **A** head, pronotum and mesonotum, dorsal view **B** head and pronotum, lateral view **C** head and pronotum, ventral view **D** forewing of male **E** hindwing of male **F** forewing of female **G** hindwing of female. Abbreviations: nl, nodal line. Scale bars: 1 mm.

Jiangle, Longqishan, 500 m, 13.viii.1991, X.C. Zhang; 8♂♂, 2♀♀, Yunnan, Hekou, 80 m, light trap, 7.vi.1956, K.R. Huang; 1♂, Yunnan, Xishuangbanna, Mengla, 620–650 m, 9.vi.1959, S.F. Li; 1♀, Yunnan, Jinghong, Damenglong, 30.ix.1979, J.X. Cui (all in IZCAS). **VIETNAM:** 1♂, Kontum N of Pleiku, 550 m, 13.v.1960, L.W. Quate. **LAOS:** 1♀, Borikhane Prov. Paksane, 20.xii.1965, native collector; 1♂, Vientiane Prov. Tha Ngone, 30.xi.1965, native collector. **MALAYSIA:** 1♀, Borneo, Sarawak Sadong, Kampong Tapuh, 300–450 m, 10.vii.1958, T.C. Maa (all in BPBM).

Host plant. *Miscanthus floridulus*.

Distribution. China (Zhejiang, Hainan, Fujian, Yunan, Taiwan); Japan (Ryukyu Islands); Vietnam; Laos; Malaysia; Indonesia.

Remarks. *Catullioides rubrolineata* is newly recorded from Vietnam and Laos. Our specimens are distinctly larger than those recorded from Taiwan, China by Yang et al. (1989). Their data showed the body length of *C. rubrolineata* from Nantou, Taiwan as 5.27 ± 0.11 mm in males and 5.76 ± 0.33 mm in females

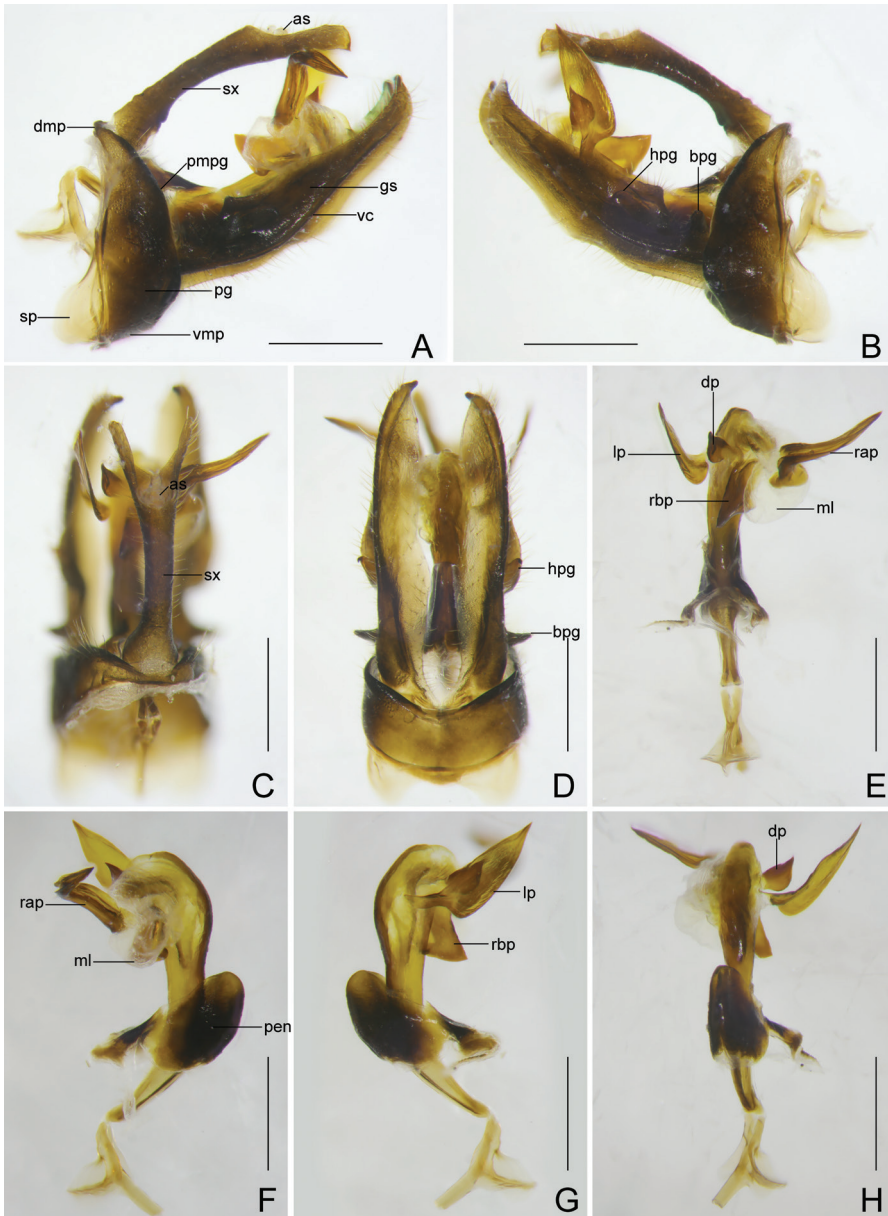


Figure 4. *Catullioides rubrolineata* Bierman **A** male pygofer, gonostyles, and segment X, left lateral view **B** male pygofer, gonostyles, and segment X, right lateral view **C** male segment X and pygofer, dorsal view **D** male pygofer and gonostyles, ventral view **E** aedeagus, dorsal view **F** aedeagus, left lateral view **G** aedeagus, right lateral view **H** aedeagus, ventral view. Abbreviations: as, anal style; bpg, basal process of gonostyle; dmp, dorsal margin of pygofer in profile; dp, dorsal process of phallosome; gs, gonostyle; hpg, hook-like process of gonostyle; lp, left process of phallosome; ml, membranous lobe of phallosome; pen, perianthrium; pg, pygofer; pmpg, posterior margin of pygofer in profile; rap, right apical process of phallosome; rbp, right basal process of phallosome; sp, sclerotised processes of pygofer; sx, segment X; vc, ventrolateral carina of gonostyle; vmp, ventral margin of pygofer in profile. Scale bars: 0.5 mm.

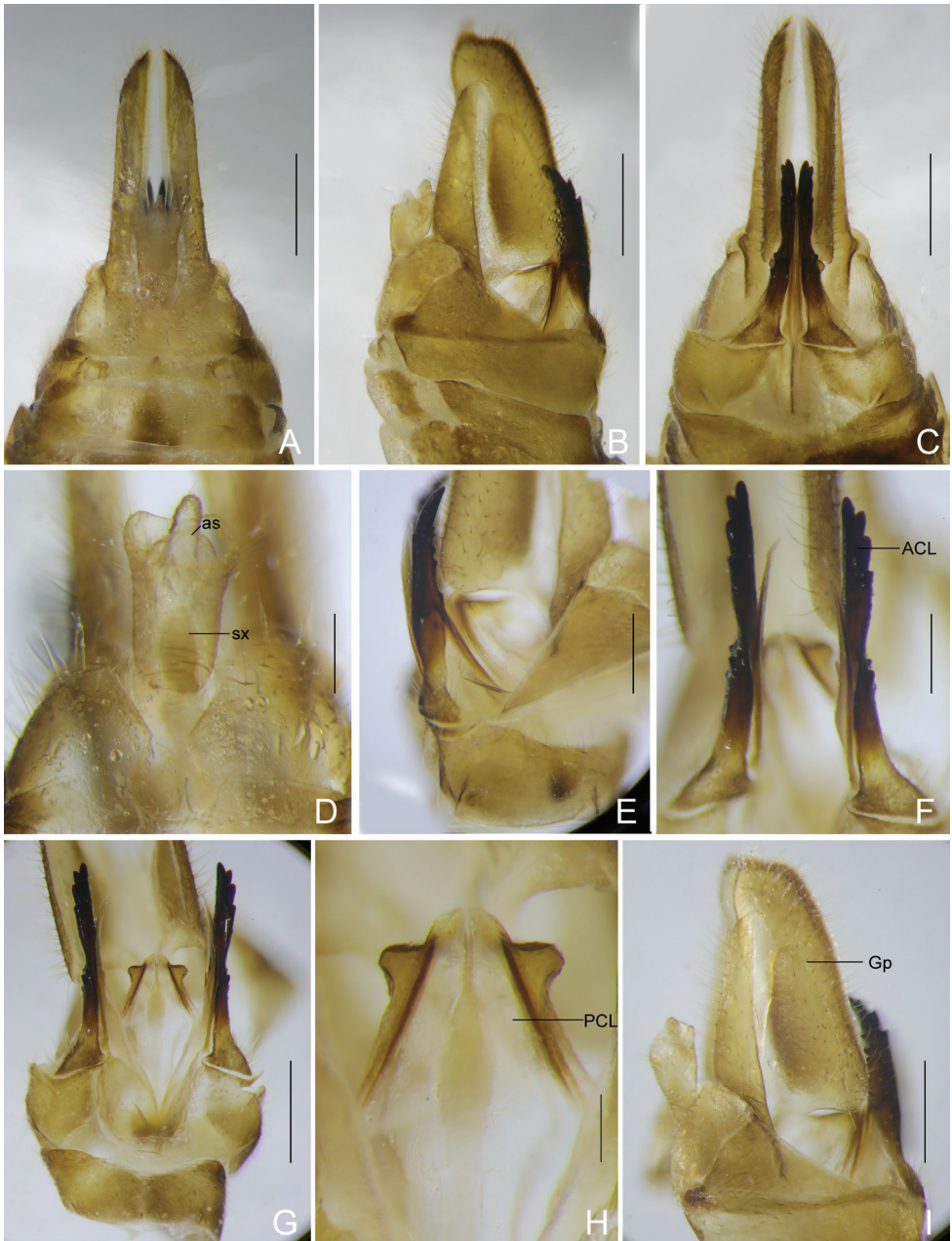


Figure 5. *Catullioides rubrolineata* Bierman **A** female terminalia, dorsal view **B** female terminalia, lateral view **C** female terminalia, ventral view **D** female segment X, dorsal view **E** gonapophyses VIII, lateral view **F** gonapophyses VIII, ventral view **G** gonapophyses VIII and IX, ventral view **H** gonapophyses IX, ventral view **I** gonoplace, lateral view. Abbreviations: ACL, anterior connective lamina of gonapophysis VIII; as, anal style; Gp, gonoplace; PCL, posterior connective lamina of gonapophysis IX; sx, segment X. Scale bars: 0.5 mm (**A-C, G, I**); 0.2 mm (**D-F, H**).

(Yang et al. 1989). The type specimens of *C. rubrolineata* from Indonesia (6.5–8.0 mm) are also a little shorter than the specimens we examined (Bierman 1910). Unfortunately, we did not examine the syntypes of Bierman (1910) and the specimens of Yang et al. (1989), and identified this species based on our critical review of the literature.

***Catullioides taishunensis* Zhu, Wang & Song, sp. nov.**

<http://zoobank.org/96FB5511-9536-49AD-A02A-E8CCA3827555>

Figures 6–8

Type material. *Holotype* ♂, CHINA: Zhejiang, Taishun, Beikengdi (27°28'30"N, 119°54'28"E), 28.viii.2020, Z.S. Song (JSSNU). *Paratypes*, CHINA: 3♂♂, same data as holotype, F.Z. Ma, S.Y. Xu & H.Y. Zhu (JSSNU); 3♂♂, same data as holotype, Z.S. Song (IZCAS).

Diagnosis. The new species may be easily distinguished from *C. rubrolineata* by the distinctly incurved, non-flat forewings; the narrow and long hindwings; and the different general coloration.

Description. ♂, body length from apex of head to tip of forewings: 7.7–7.9 mm; head length from apex of cephalic process to base of eyes: 0.6–0.7 mm; head width including eyes: 1.2–1.3 mm; forewing length: 6.1–6.3 mm.

Coloration. General color in males pale green and red on head and thorax, and black on body (Fig. 6). Head excluding eyes, pronotum and mesonotum mostly pale green to yellowish green, broad stripes along median carinae of vertex, frons, clypeus, pronotum and mesonotum, lateral margins of frons, lateral areas of pronotum and mesonotum behind eyes red, clypeus and apical margins of paranotal lobes black (Fig. 2C). Compound eyes red to fuscous with posterior margin pale green, ocelli purplish red. Forewings mostly fuscous to black, clavus yellowish green to dark brown (Fig. 7D). Lateral parts of pro- and meso-thorax black, meta-thorax yellowish green; legs black except coxae and tarsomeres yellowish green. Abdomen with terminalia mostly black.

Structure. Vertex (Fig. 7A) wider than long, with ratio of length at midline to width between eyes 0.5:1. Frons with ratio of length at midline to maximum width 1.6:1 (Fig. 7C). Forewings (Fig. 7D) tectiform, membrane distinctly incurved at nodal line, ratio of length to width about 3.1:1. Hindwings (Fig. 7E) narrow and long, ratio of length to width about 2.6:1.

Male genitalia. Similar to those of *C. rubrolineata*. Pygofer relatively narrow and small, in lateral view (Fig. 8A, B), posterior margin slightly sinuate, more or less convex medially, anterior margin produced in a pair of broad and large sclerotised processes ventrolaterally; in ventral view (Fig. 8D) far longer than in dorsal view (Fig. 8C), with ratio of ventral to dorsal width about 4.5:1. Gonostyles (Fig. 8A, B, D) elongate, in ventral view (Fig. 8D), inner area along ventrolateral carina less sclerotised and filmy, dorso-basal process directed dorsolaterad; in lateral view (Fig. 8A, B), ventrolateral



Figure 6. *Catullioides taishunensis* sp. nov. **A** male, photographed by Z-S Song **B** male, dorsal view **C** male, lateral view. Scale bars: 2 mm.

carina strongly ridged from base to apex. Aedeagus (Fig. 8E–H) large and elongate, as long as gonostyles; in right lateral view (Fig. 8F), right apical process directed dorsad and curved laterocaudad; in left lateral view (Fig. 8G), left process large and broadly flat, base narrow and twisted, remaining cultrate, directed laterocaudad. Segment X (Fig. 8C) slender and elongate, anal style relatively small, not reaching to apex.

Female unknown.

Etymology. The new species is named for its occurrence in Taishun, Zhejiang, China. The specific epithet *taishunensis* is to be treated as a latinized adjective in the nominative singular.

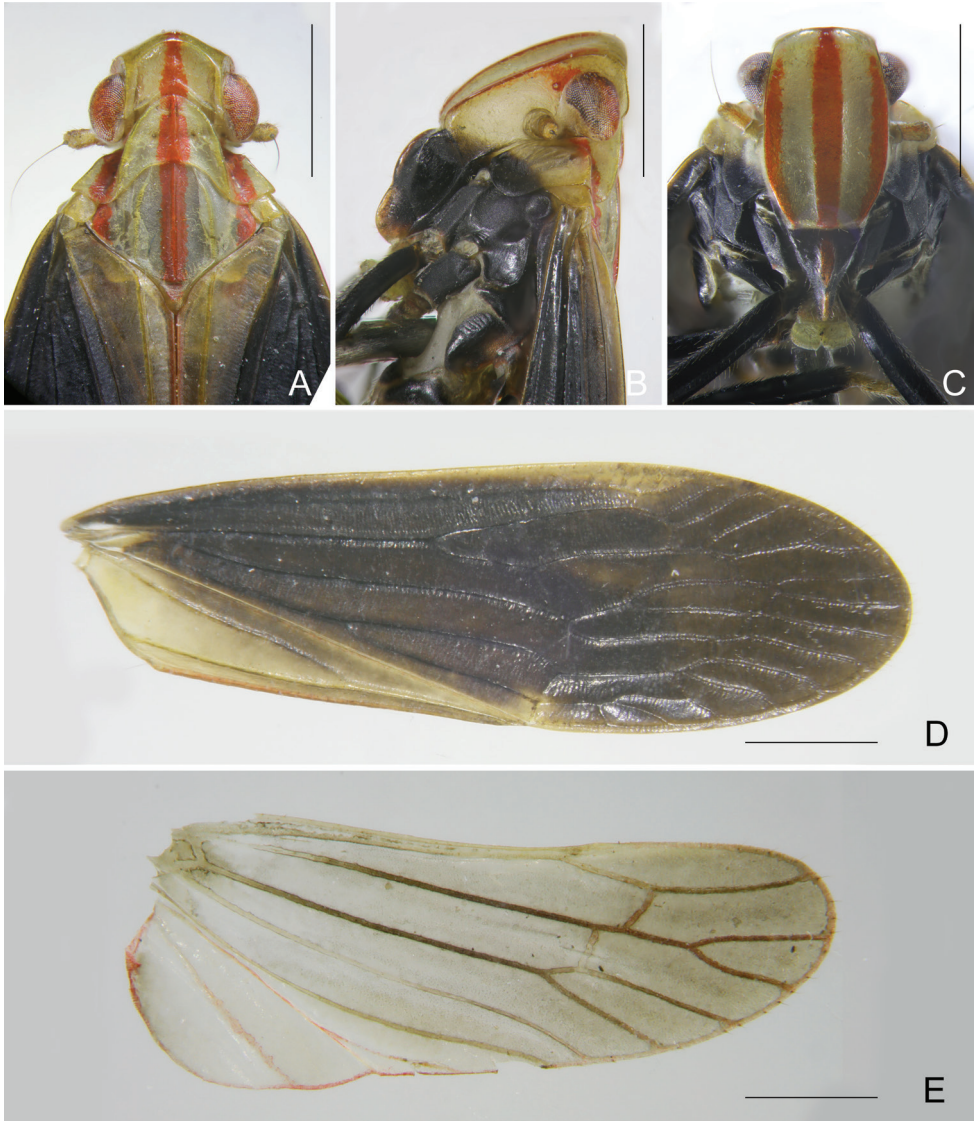


Figure 7. *Catullioides taishunensis* sp. nov. **A** head, pronotum and mesonotum, dorsal view **B** head and pronotum, lateral view **C** head and pronotum, ventral view **D** forewing **E** hindwing. Scale bars: 1 mm.

Host plant. *Miscanthus floridulus*.

Distribution. So far only known from Taishun, Zhejiang, China.

Remarks. Bierman (1910) erected *Catullioides rubrolineata coriacea* Bierman (1910) for its smaller body and different coloration of the forewings. He did not describe and illustrate it in detail. It needs to be further studied and compared with our new species *C. taishunensis* sp. nov.

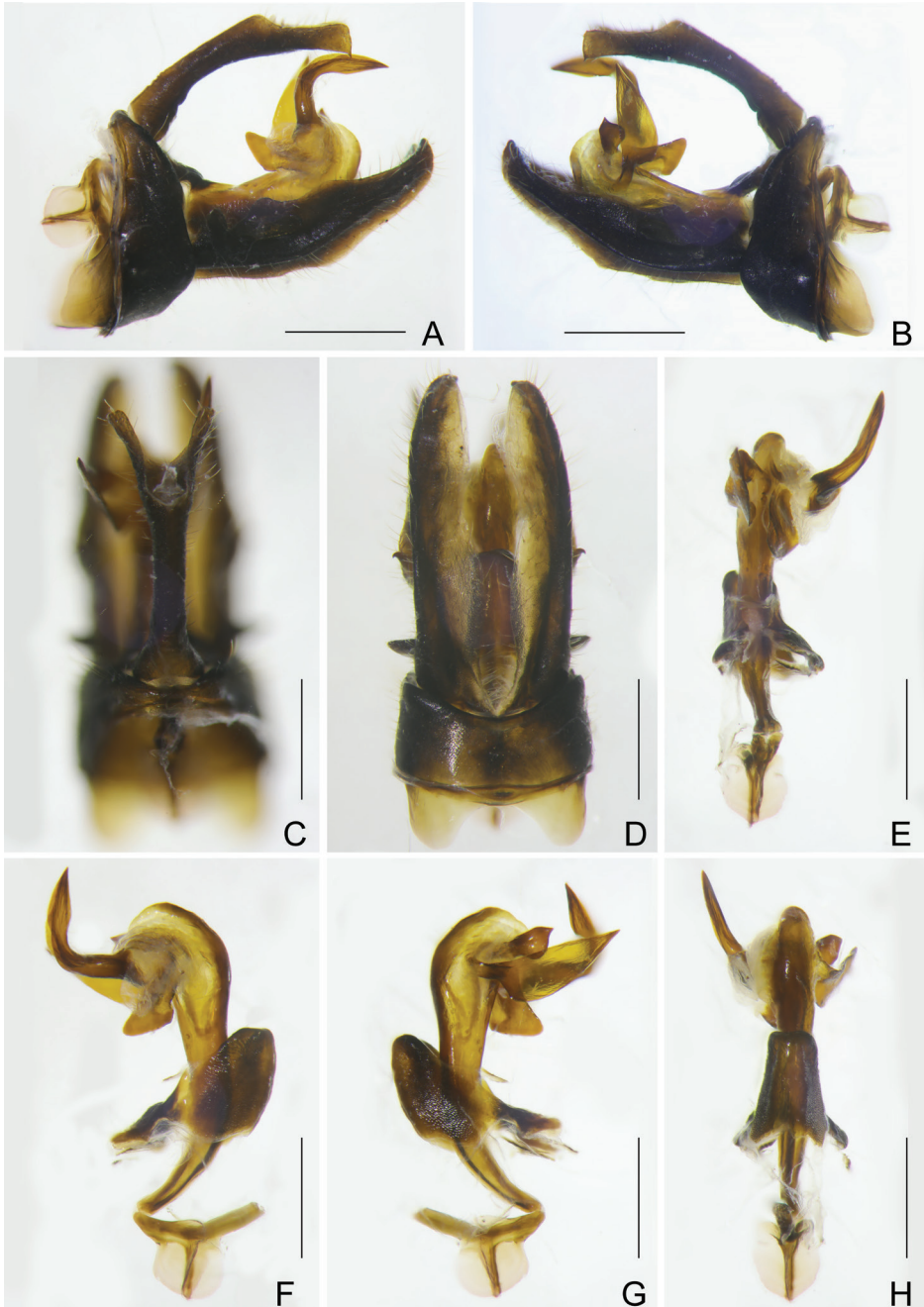


Figure 8. *Catullioides taishunensis* sp. nov. **A** male pygofer, gonostyles, and segment X, left lateral view **B** male pygofer, gonostyles, and segment X, right lateral view **C** male segment X and pygofer, dorsal view **D** male pygofer and gonostyles, ventral view **E** aedeagus, dorsal view **F** aedeagus, left lateral view **G** aedeagus, right lateral view **H** aedeagus, ventral view. Scale bars: 0.5 mm.

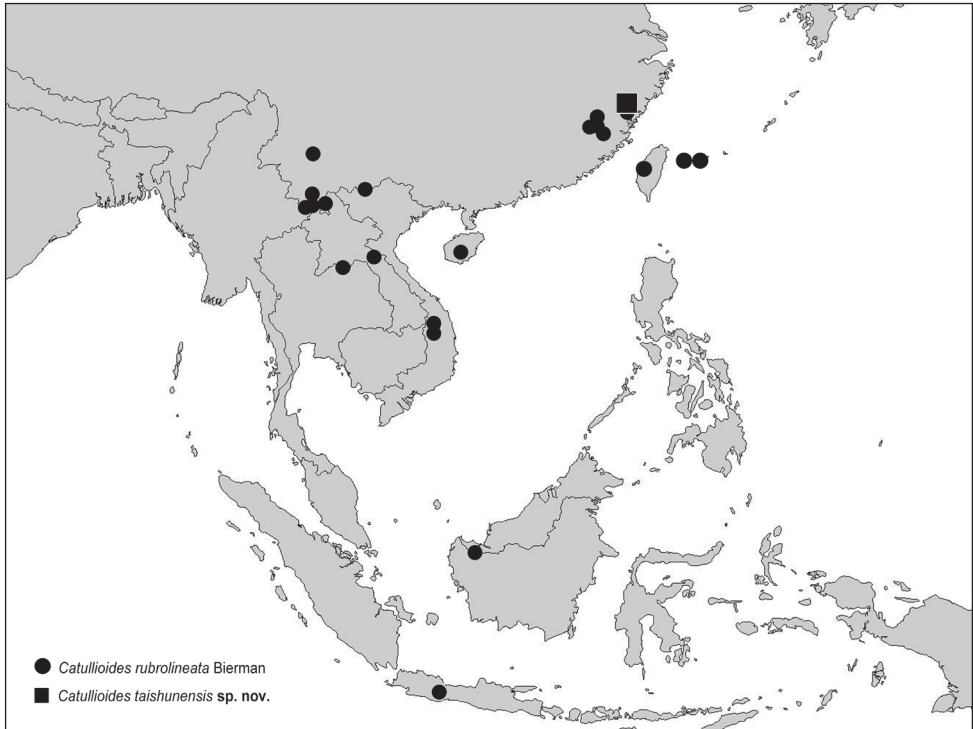


Figure 9. Geographical distribution of *Catullioides* species.

Acknowledgements

We wish to thank Keith Arakaki and David Preston (BPBM) for loans of specimens. We are grateful to Thierry Bourgoin, Muséum National d’Histoire Naturelle, Paris, France and Charles Bartlett, University of Delaware, U.S.A. for their efforts in improving this paper. We also thank Mike Wilson for his kind editorial help and comments on the manuscript. We extend our appreciation to Ai-Ping Liang, Institute of Zoology, Chinese Academy of Sciences, Beijing, China for his continued help and support. The work on which this paper is based was supported by grants from the National Natural Science Foundation of China (nos. 31961143002 and 31970442), and Biodiversity Survey, Monitoring and Assessment Project of the Ministry of Ecology and Environment, China (2019HB2096001006).

References

- Bierman CJH (1910) Homopteren aus Niederländisch Ost-Indien. II herausgegeben von D. MacGillavry und K. W. Dammerman. Notes from the Leyden Museum 33: 1–68.
- Bourgoin T (2021) FLOW (Fulgoromorpha Lists On the Web): a world knowledge base dedicated to Fulgoromorpha. Version 8. <http://hemiptera-databases.org/flow/> [accessed on 1 March 2021]

- Bourgoin T, Wang R-R, Asche M, Hoch H, Soulier-Perkins A, Stroiński A, Yap S, Szwedó J (2015) From micropterism to hyperpterism: recognition strategy and standardized homology-driven terminology of the forewing venation patterns in planthoppers (Hemiptera: Fulgoromorpha). *Zoomorphology* 134: 63–77. <https://doi.org/10.1007/s00435-014-0243-6>
- Bourgoin T, Wang R-R, Szwedó J, Li X-Y, Chen X (2019) A new early Miocene fossil genus from Dominican amber extends the Eastern Asia distribution of Paricanini (Hemiptera: Fulgoromorpha: Tropiciduchidae) to the Neotropics. *Palaeontologia Electronica* 22.3.77: 1–15. <https://doi.org/10.26879/958>
- Distant WL (1906) The Fauna of British India, Including Ceylon and Burma. Rhyrhota Vol. III (Heteroptera-Homoptera). Taylor & Francis, London, 503 pp.
- Distant WL (1912) Descriptions of new genera and species of Oriental Homoptera. *Annals and Magazine of Natural History* 8: 181–194. <https://doi.org/10.1080/00222931208693118>
- Distant WL (1916) The Fauna of British India, Including Ceylon and Burma. Rhyrhota Vol. VI. Homoptera: Appendix. Taylor & Francis, London, 248 pp.
- Fennah RG (1982) A tribal classification of the Tropiciduchidae (Homoptera: Fulgoroidea), with the description of a new species on tea in Malaysia. *Bulletin of Entomological Research* 72: 631–643. <https://doi.org/10.1017/S0007485300008658>
- Gnezdilov VM (2013) Contribution to the taxonomy of the family Tropiciduchidae Stål (Hemiptera, Fulgoroidea) with description of two new tribes from Afrotropical Region. *Deutsche Entomologische Zeitschrift* 60: 179–191.
- Hayashi M (1995) Discovery of *Catullioides albosignatus* (Homoptera, Tropiciduchidae) from the Ryukyu Islands, Japan. *Japanese Journal of Entomology* 63: 65–66.
- Melichar L (1914) Monographie der Tropiciduchinen (Homoptera). *Verhandlungen des Naturforschenden Vereines in Brünn* 53: 1–145.
- Melichar L (1915) Monographie der Lophopinen. *Annales Historico-Naturales Musei Nationalis Hungarici*. Budapest 13: 337–385.
- Metcalf ZP (1954) General Catalogue of the Homoptera, Fascicule IV Fulgoroidea. Part 11 Tropiciduchidae. North Carolina State College, Raleigh, North Carolina, 167 pp.
- Muir F (1931) New and little-known Fulgoroidea in the British Museum (Homoptera). *Annals of the Magazine of Natural History* 7: 297–314. <https://doi.org/10.1080/00222933108673318>
- Stroiński A, Wang R-R, Bourgoin T, Liang A-P, Szwedó J (2015) Review of the Paricanini (Hemiptera: Fulgoromorpha: Tropiciduchidae). *Annales Zoologici Warszawa* 65: 579–597. <https://doi.org/10.3161/00034541ANZ2015.65.4.006>
- Szwedó J, Stroiński A (2017) Who's that girl? The singular Tropiciduchidae planthopper from the Eocene Baltic amber (Hemiptera: Fulgoromorpha). *Palaeontologia Electronica* 20.3.60A: 1–20. <https://doi.org/10.26879/784>
- Szwedó J, Drohojowska J, Popov Y, Simon E, Wegierek P (2019) Aphids, true hoppers, jumping plant-lice, scale insects, true bugs and whiteflies (Insecta: Hemiptera) from the Insect Limestone (latest Eocene) of the Isle of Wight, UK. *Earth and Environmental Science Transactions of the Royal Society of Edinburgh* 110: 331–396. <https://doi.org/10.1017/S175569101900001X>
- Wang R-R, Li X-Y, Szwedó J, Stroiński A, Liang A-P, Bourgoin T (2016) Testing Tropiciduchini Stål 1866 (Hemiptera: Tropiciduchidae) monophyly, a young inter-tropical taxon of mainly

insular species: taxonomy, distribution patterns and phylogeny, with the description of a new genus from Papua New Guinea. *Systematic Entomology* 42: 359–378. <https://doi.org/10.1111/syen.12219>

Yang J-T, Yang C-T, Wilson MR (1989) Tropicuchidae of Taiwan (Homoptera: Fulgoroidea). *Collected Papers on Homoptera of Taiwan, Taiwan Museum Special Publication* 8: 65–115.

The complete mitochondrial genomes of two erythroneurine leafhoppers (Hemiptera, Cicadellidae, Typhlocybininae, Erythroneurini) with assessment of the phylogenetic status and relationships of tribes of Typhlocybininae

Xiaoxiao Chen¹, Can Li², Yuehua Song¹

1 School of Karst Science, Guizhou Normal University/ State Key Laboratory Cultivation Base for Guizhou Karst Mountain Ecology Environment of China, Guiyang, Guizhou 550001, China **2** Guizhou Provincial Key Laboratory for Rare Animal and Economic Insect of the Mountainous Region, Guiyang University, Guiyang, Guizhou 550001, China

Corresponding author: Yuehua Song (songyuehua@163.com)

Academic editor: Mick Webb | Received 27 January 2021 | Accepted 28 April 2021 | Published 17 May 2021

<http://zoobank.org/7B1C98B4-26F1-4125-861D-BFA7E41B741C>

Citation: Chen X, Li C, Song Y (2021) The complete mitochondrial genomes of two erythroneurine leafhoppers (Hemiptera, Cicadellidae, Typhlocybininae, Erythroneurini) with assessment of the phylogenetic status and relationships of tribes of Typhlocybininae. ZooKeys 1037: 137–159. <https://doi.org/10.3897/zookeys.1037.63671>

Abstract

The number and classification of tribes in the leafhopper subfamily Typhlocybininae are not yet fully clear, and molecular data has recently been used to help resolve the problem. In this study, the mitochondrial genomes of *Mitjaevia shibingensis* Chen, Song & Webb, 2020 and *M. dworakowskiae* Chen, Song & Webb, 2020 of the tribe Erythroneurini (Cicadellidae, Typhlocybininae) were sequenced. Most protein-coding genes (PCGs) start with ATN and end with TAA or TAG, and the AT content of these three codons were found differ from previous results that show that the first codon has the highest incidence. Two rRNA genes are highly conserved, and the AT content in *16S* is higher than that of *12S*. The nucleotide diversity and genetic distance among 13 PCGs of the four tribes from Typhlocybininae show that Empoascini nucleotide diversity is significantly less than in the other three tribes, and have the largest distance from the others, while Typhlocybini and Zyginellini have the smallest distance, indicating that the relationship between the two is the closest. The *nad2*, *nad4*, *nad4L*, and *nad5* genes have greater nucleotide diversity, showing potential for use as the main markers for species identification. The phylogenetic analysis yielded a well-supported topology with most branches receiving maximum support and a few branches pertaining to relationships within Zyginellini and Typhlocybini receiving lower support. The species of these two

tribes are intertwined, and it was impossible to resolve them into separate branches. In addition, the tribes Empoascini and Erythroneurini were recovered as monophyletic, and Alebrini was placed at the base of the tree as the most primitive. These results are broadly in line with other molecular phylogenetical studies which differ from traditional morphological classification.

Keywords

Mitjaevia dworakowskiae, *Mitjaevia shibingensis*, mitochondrial genome, phylogenetic analysis, tribal taxonomic status

Introduction

Cicadellidae (leafhoppers) are the largest family of the order Hemiptera. Representatives are important agricultural and forestry pests that feed on a variety of plants such as cereal crops, vegetables, and fruit trees, and they are also vectors of plant pathogens (Morris 1971; Guo 2011; Roddee et al. 2018). Leafhoppers also have many interesting characteristics, such as varied lifestyles and feeding strategies (including utilizing different endosymbionts), covering their bodies with brochosomes, and producing courtship signals through the plant substrate. These characteristics make leafhoppers suitable material for studies on biological evolution and geographical research (Chen et al. 2020a, b). The subfamily of Typhlocybinae is the second largest group of Cicadellidae and is widely distributed in the six major zoogeographic regions of the world. Erythroneurini, the largest tribe of Typhlocybinae, includes ~2,000 species worldwide (Wang et al. 2012).

The traditional classification of leafhopper has attracted much research attention, including the classification of Typhlocybinae. At present, Typhlocybinae contains six tribes (Alebrini, Empoascini, Erythroneurini, Zyginellini, Typhlocybini, Dikraneurini) but this division remains controversial (Hamilton 1998; Balme 2007; Dietrich 2013). Today, the emergence of next-generation sequencing technology is a breakthrough for solving this problem enabling mitochondrial genomic data to verify and reference the existing family-level classification of Typhlocybinae. Many previous attempts have been made to estimate phylogenetic relationships among leafhoppers mostly by using either morphological data or sequence data from a few gene regions (Hamilton 1983; Dietrich et al. 2001; Zahniser and Dietrich 2013; Krishnankutty et al. 2016), but there is very little research on Typhlocybinae. So far, in the National Center for Biotechnology Information (NCBI), Typhlocybinae only has complete mitochondrial genomic data for 19 species (Table 1).

The insect mitochondrial genome (mtDNA) is usually a closed double-stranded DNA molecule with a molecular weight of 14–20 kb. Usually, it contains 37 genes, including 13 protein-coding genes (PCGs), NADH dehydrogenase 1-6 and 4L (*nad1-6* and *nad4L*), cytochrome c oxidase subunits 1-3 (*cox1-3*), ATPase subunit 6 and 8 (*atp6* and *atp8*), cytochrome b (*cytb*), two ribosomal RNAs genes (*16S* and *12S*) and 22 transfer RNA (tRNA) genes. A region rich in A + T, the control region, is also present (Boore 1999; Wang et al. 2018). Compared with the nuclear genome, the in-

Table 1. List of the mitochondrial genomes analyzed in the present study.

| Tribe | Species | Length (bp) | GenBank accession no. |
|----------------|----------------------------------|-------------|-----------------------|
| Empoascini | <i>Empoasca flavescens</i> | 15,152 | MK211224.1 |
| | <i>Empoasca onukii</i> | 15,167 | NC_037210.1 |
| | <i>Empoasca vitis</i> | 15,154 | NC_024838.1 |
| | <i>Ghauriana sinensis</i> | 15,491 | MN699874.1 |
| Erythroneurini | <i>Empoascanara dwalata</i> | 15,271 | MT350235.1 |
| | <i>Empoascanara gracilis</i> | 14,627 | MT576649 |
| | <i>Empoascanara sipra</i> | 14,827 | NC_048516.1 |
| | <i>Empoascanara wengangensis</i> | 14,830 | MT445764 |
| | <i>Illinigina</i> sp. | 14,803 | KY039129.1 |
| | <i>Mitjaevia dworakowskiae</i> | 16,399 | MT981880 |
| | <i>Mitjaevia protuberanta</i> | 15,472 | NC_047465.1 |
| | <i>Mitjaevia shibingensis</i> | 15,788 | MT981879 |
| Typhlocybini | <i>Bolanusoides shaanxiensis</i> | 15,274 | MN661136.1 |
| | <i>Eupteryx minuscula</i> | 16,944 | MN910279.1 |
| | <i>Typhlocyba</i> sp. | 15,223 | KY039138.1 |
| Zyginellini | <i>Limasolla lingchuanensis</i> | 15,716 | MN605256.1 |
| | <i>Parabahimia luodianensis</i> | 16,497 | NC_047464.1 |
| | <i>Parathailocyba orla</i> | 15,382 | MN894531.1 |
| | <i>Zyginella minuta</i> | 15,544 | MT488436.1 |

sect mitochondrial genome has the characteristics of a simple structure, low molecular weight, stable composition, conservative arrangement, maternal inheritance, and easy detection. It is very suitable for the study of evolutionary genomics and is widely used to identify the phylogenetic relationships and population structures at different taxonomic levels (Saccone et al. 2002; Cook et al. 2005; Wilson et al. 2008).

To further enrich the mitochondrial genome data of leafhoppers and provide comparative data for closely related species, we sequenced and analyzed the complete mitochondrial genomes of *Mitjaevia shibingensis* and *M. dworakowskiae* and analyzed their phylogenetic relationship with other Typhlocybinae. The new molecular data obtained will help in the identification of leafhopper species, kinship comparison, and future studies on population genetics and evolution.

Materials and methods

Mitogenome sequencing, assembly, and annotation

For this study, samples of *Mitjaevia shibingensis* and *M. dworakowskiae* were collected in 100% alcohol and stored at -20°C in the laboratory. Total DNA was extracted from the entire body without the abdomen and wings. The mitochondrial gene sequences were obtained through second-generation sequencing. Primers were designed to amplify the mtDNA sequence in PCR reactions. The PCR reaction was performed using the LA Taq polymerase. The PCR conditions were as follows: initial denaturation at 94°C for 2 min, then 35 cycles of denaturation at 94°C for 30 sec, annealing at 55°C for 30 sec, and extension at 72°C for 1 min/kb, followed by the final extension at 72°C for 10 min. The PCR products were sequenced directly, or,

if needed, first cloned into a pMD18-T vector (Takara, JAP) and then sequenced, by the dideoxynucleotide procedure, using an ABI 3730 automatic sequencer (Sanger sequencing) using the same set of primers. After quality-proofing of the obtained fragments, the complete mt genome sequence was assembled manually using DNASTar (Burland 2000), and a homology search was performed by the Blast function in NCBI to verify the amplified sequence as the target sequence (Meng et al. 2013; Yu et al. 2017). The nucleotide base composition, codon usage, and A + T content values were analyzed with MEGA 6.06 (Tamura et al. 2013). The secondary structure of tRNA genes was annotated using online tools tRNAscan-SE 1.21 and ARWEN (Lowe and Eddy 1997; Laslett and Canbäck 2008). The tandem repeat sequence in the control area was determined by the online search tool Tandem Repeats Finder (Benson 1999). The base skew values for a given strand were calculated using the formulae: AT skew = $[A - T] / [A + T]$ and GC skew = $[G - C] / [G + C]$ (Perna and Kocher 1995). The nucleotide diversity (Pi) and sliding window analysis (sliding window: 200 bp, step size: 20 bp) of 13 PCGs among four tribes of Typhlocybiinae species were conducted with DnaSP 5.0 software (Rozas et al. 2017). And the genetic distance of the four tribes was estimated in MEGA 6.06.

Phylogenetic analysis

The phylogenetic analysis included two sets of data. First, the phylogenetic tree was constructed based on 29 *cox1* data among six tribes of Typhlocybiinae and two outgroups. Secondly, phylogenetic tree analysis was conducted using a dataset including the complete mitochondrial genomes of the two newly sequenced erythroneurine species, 17 typhlocybiinae species, and two outgroups, of which nine sets of data were from team sequencing, while the remaining 10 were obtained from the NCBI database (Table 1).

The Gblocks Server online platform was used to eliminate poorly aligned positions and divergent regions of DNA protein alignment, and all alignments were checked and corrected in MEGA 6.06 prior to the phylogenetic analysis (Tamura et al. 2013). Five datasets were generated: (1) *cox1* with 573 nucleotides (2) 13 PCGs with 10,452 nucleotides (PCGs); (3) the first and second codon positions of the 13 PCGs with 6968 nucleotides (PCG12); (4) 13 PCGs with 10,452 nucleotides and 2 rRNA with 1615 nucleotides (PCGR); (5) and amino acid sequences of the 13 PCGs with 2666 amino acids (PCGAA).

The trimmed datasets were used to estimate the phylogeny by maximum likelihood (ML) using IQ-TREE and Bayesian inference (BI) using MrBayes 3.2.7 (Zhou et al. 2011; Du et al. 2017). ML constructed with the IQ-TREE used an ultrafast bootstrap approximation approach with 10,000 replicates and calculated bootstrap scores for each node (BP). BI selected GTR + I + G as the optimal model, running 10 million generations twice, sampling once every 1000 generations, after the average standard deviation of the segmentation frequency drops below 0.01, with the first 25% of the samples are discarded burn-in, and the remaining trees used to generate a consensus tree and calculate the posterior probability (PP) of each branch.

Results and discussion

Organization and composition of the genome

The genomic organization and nucleotide composition of the two new mitogenomes sequenced in this study are similar to those of other previously reported Typhlocybina (Tan et al. 2020; Yuan et al. 2020). The complete mitogenomes of *M. shibingensis* and *M. dworakowskiae* are double-stranded plasmids with 15,788 and 16,399 bp, respectively. Both species contain the usual 13 PCGs, 22 tRNA genes, 2 rRNA genes, and a control region (Fig. 1). Fourteen genes encode in the minority strand (L-strand) while the others encode in the majority strand (H-strand). *Mitjaevia shibingensis* has a total of 46 bp intergenic space in 12 regions ranging from 1 to 8 bp. Eleven genes were found to overlap by a total of 47 bp. *Mitjaevia dworakowskiae* has a total of 84 bp intergenic space in 12 regions ranging from 2 to 15 bp, and seven genes were found to overlap by a total of 23 bp (Table 2).

The AT contents and skew statistics are shown in Table 3. The mitochondrial genomes of *M. shibingensis* and *M. dworakowskiae* show heavy AT nucleotide bias, with A + T% content for the whole sequence was 78.4% and 79.0%, respectively. Similar patterns of nucleotide composition are also found in other leafhopper species (Du et al. 2017; Wang et al. 2018; Xian et al. 2020). The control region (CR) has the strongest A + T% bias, while the PCGs shows the lowest A + T% among whole genes. The whole genome has positive AT skews (0.042, 0.051) and negative GC skews (−0.074, −0.104). Analysis of 37 individual genes of the two species show that AT skews are mostly positive, while for GC skews, the genes of both species are mostly negative (Fig. 2). Positive AT skews indicates that the content of base A is higher than that of base T. However, in a few genes, although the AT skews is negative, the difference in absolute value was very small. For negative GC skew, a negative value indicates that the content of base G is lower than that of base C, while a positive value indicates the opposite. In general, the basic composition of these two species is biased towards A and C.

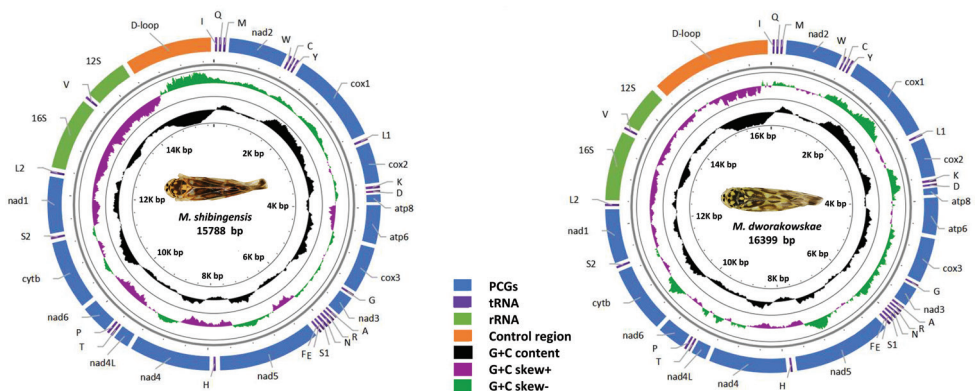


Figure 1. Circular maps of the mitochondrial genome of *Mitjaevia shibingensis* and *M. dworakowskiae*.

Table 2. Organization of the *Mitjaevia shibingensis* and *M. dworakowskiae* mitochondrial genome.

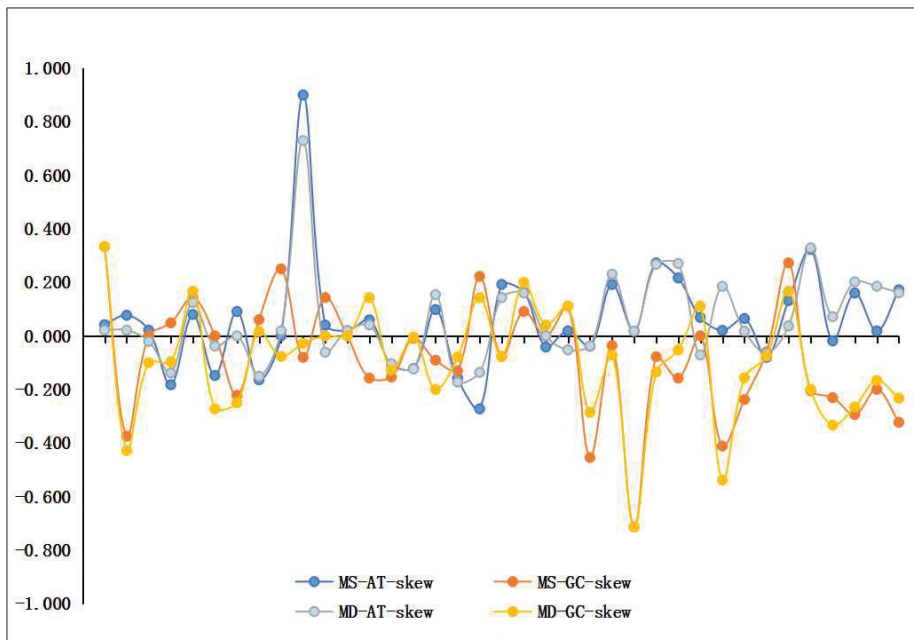
| Gene | <i>M. shibingensis</i> | | <i>M. dworakowskiae</i> | | Intergenic | Start codon | Stop codon | Strand |
|--------------|------------------------|-----------|-------------------------|-----------|------------|-------------|------------|---------|
| | Position | Size (bp) | Position | Size (bp) | | | | |
| tRNA-Ile | 1–63 | 63 | 1–63 | 63 | 0 | | | H |
| tRNA-Gln | 61–128 | 68 | 61–128 | 68 | –3 | 0 | | L |
| tRNA-Met | 151–219 | 69 | 137–205 | 69 | 8 | 9 | | H |
| <i>nad2</i> | 220–1191 | 972 | 206–1177 | 972 | 0 | ATA | TAA | H |
| tRNA-Trp | 1190–1253 | 64 | 1176–1235 | 60 | –2 | 2 | | H |
| tRNA-Cys | 1246–1307 | 62 | 1233–1295 | 63 | –8 | | | L |
| tRNA-Tyr | 1307–1368 | 62 | 1299–1364 | 66 | 5 | 3 | | L |
| <i>cox1</i> | 1378–2913 | 1536 | 1374–2909 | 1536 | 1 | 2 | ATG | TAA TAG |
| tRNA-Leu | 2915–2980 | 66 | 2911–2976 | 66 | 0 | 2 | | H |
| <i>cox2</i> | 2981–3659 | 679 | 2977–3655 | 679 | 0 | ATT | T | H |
| tRNA-Lys | 3660–3730 | 71 | 3656–3726 | 71 | 0 | | | H |
| tRNA-Asp | 3733–3793 | 61 | 3727–3789 | 63 | –1 | 0 | | H |
| <i>atp8</i> | 3792–3944 | 153 | 3799–3942 | 144 | –1 | –2 | TTG ATA | TAA |
| <i>atp6</i> | 3938–4591 | 654 | 3936–4589 | 654 | –7 | 0 | ATG | TAA |
| <i>cox3</i> | 4592–5371 | 780 | 4590–5369 | 780 | 2 | 8 | ATG | TAA |
| tRNA-Gly | 5376–5437 | 62 | 5370–5431 | 62 | 0 | | | H |
| <i>nad3</i> | 5438–5791 | 354 | 5432–5785 | 354 | 0 | ATT ATA | TAA | H |
| tRNA-Ala | 5796–5857 | 62 | 5791–5855 | 65 | 4 | –2 | | H |
| tRNA-Arg | 5857–5921 | 65 | 5861–5922 | 62 | 2 | 15 | | H |
| tRNA-Asn | 5912–5986 | 66 | 5922–5981 | 60 | –2 | 0 | | H |
| tRNA-Ser | 5986–6053 | 68 | 5986–6052 | 67 | –4 | –1 | | H |
| tRNA-Glu | 6055–6118 | 64 | 6058–6123 | 66 | 8 | 11 | | H |
| tRNA-Phe | 6135–6197 | 63 | 6128–6195 | 68 | 4 | 2 | | L |
| <i>nad5</i> | 6200–7873 | 1674 | 6200–7873 | 1674 | 0 | TTG | TAA | L |
| tRNA-His | 7874–7937 | 64 | 7874–7937 | 64 | 0 | | | L |
| <i>nad4</i> | 7937–9265 | 1329 | 7937–9265 | 1329 | –7 | –1 | ATG | TAA |
| <i>nad4L</i> | 9259–9537 | 279 | 9259–9537 | 279 | 1 | –7 | ATG | TAA |
| tRNA-Thr | 9540–9605 | 66 | 9540–9604 | 65 | 2 | 0 | | H |
| tRNA-Pro | 9606–9671 | 66 | 9605–9671 | 67 | 0 | 7 | | L |
| <i>nad6</i> | 9674–10159 | 486 | 9674–10159 | 486 | 2 | 5 | ATT | TAA |
| <i>cytb</i> | 10166–11302 | 1137 | 10162–11298 | 1137 | 7 | 0 | ATG | TAG TAA |
| tRNA-Ser | 11309–11372 | 64 | 11298–11363 | 66 | –2 | 9 | | H |
| <i>nad1</i> | 11363–12304 | 942 | 11366–12296 | 931 | –10 | –2 | ATT | TAA T |
| tRNA-Leu | 12305–12370 | 66 | 12297–12364 | 68 | 0 | | | L |
| <i>16S</i> | 12371–13562 | 1192 | 12365–13549 | 1185 | 0 | | | L |
| tRNA-Val | 13563–13627 | 65 | 13550–13615 | 66 | 0 | | | L |
| <i>12S</i> | 13628–14359 | 732 | 13616–14351 | 736 | 0 | | | L |
| D-loop | 14360–15788 | 1429 | 14352–16399 | 2048 | | | | |

Protein-coding genes and codon usage

Similar to other Typhlocybinae mitochondrial genomes, of the 13 PCGs of *M. shibingensis* and *M. dworakowskiae*, nine genes (*cox1*, *cox2*, *cox3*, *atp8*, *atp6*, *nad2*, *nad3*, *nad6*, and *cytb*) are located on the major strand (H-strand) while the other four PCGs (*nad4*, *nad4L*, *nad5*, and *nad1*) are located on the minor strand (L-strand). The largest gene was the *nad5* gene, and the smallest was the *atp8* gene in erythroneurine mitogenomes. The average AT content values of PCGs were 75.4% and 76.7% in *M. shibingensis* and *M. dworakowskiae*, respectively. The A + T content of the first codon positions (76.5%, 77.5%) was much higher than that of the second (76.1%, 75.4%) and the third (74.5%, 77.3%) positions. This result was different from most other

Table 3. Nucleotide compositions, AT skew, and GC skew in different regions of *Mitjaevia shibingensis* and *M. dworakowskiae* mitochondrial genomes.

| Feature | A% | C% | G% | T% | A+T% | AT skew | GC skew | Length (bp) |
|--------------------------------|------|------|------|------|------|---------|---------|-------------|
| <i>M. shibingensis</i> | | | | | | | | |
| Whole | 40.8 | 11.6 | 10.0 | 37.6 | 78.4 | 0.042 | -0.074 | 15,788 |
| PCGs | 39.3 | 12.8 | 11.5 | 36.4 | 75.7 | 0.038 | -0.053 | 10975 |
| 1 st codon position | 41.6 | 12.1 | 11.5 | 34.9 | 76.5 | 0.087 | -0.026 | 3659 |
| 2 nd codon position | 38.3 | 12.2 | 11.7 | 37.8 | 76.1 | 0.007 | -0.018 | 3658 |
| 3 rd codon position | 38.0 | 14.1 | 11.3 | 36.6 | 74.5 | 0.019 | -0.111 | 3658 |
| tRNA | 40.6 | 10.9 | 10.1 | 38.4 | 79.0 | 0.028 | -0.037 | 1427 |
| 16S | 48.1 | 11.1 | 6.0 | 34.8 | 82.9 | 0.160 | -0.294 | 1192 |
| 12S | 48.0 | 12.0 | 6.1 | 33.9 | 81.8 | 0.172 | -0.323 | 732 |
| CR | 42.7 | 3.5 | 3.8 | 50.0 | 92.7 | -0.079 | 0.038 | 1429 |
| <i>M. dworakowskiae</i> | | | | | | | | |
| Whole | 41.5 | 11.6 | 9.4 | 37.5 | 79.0 | 0.051 | -0.104 | 16,399 |
| PCGs | 40.1 | 12.5 | 10.8 | 36.6 | 76.7 | 0.046 | -0.073 | 10955 |
| 1 st codon position | 42.4 | 11.9 | 10.6 | 35.1 | 77.5 | 0.095 | -0.055 | 3652 |
| 2 nd codon position | 38.0 | 12.9 | 11.7 | 37.3 | 75.4 | 0.009 | -0.047 | 3652 |
| 3 rd codon position | 39.9 | 12.7 | 10.0 | 37.4 | 77.3 | 0.032 | -0.119 | 3651 |
| tRNA | 40.6 | 11.6 | 9.9 | 37.9 | 78.5 | 0.034 | -0.081 | 1435 |
| 16S | 49.6 | 11.1 | 6.4 | 32.9 | 82.5 | 0.202 | -0.266 | 1185 |
| 12S | 47.6 | 11.1 | 6.9 | 34.4 | 81.9 | 0.161 | -0.233 | 736 |
| CR | 43.1 | 6.9 | 4.2 | 45.8 | 88.9 | -0.030 | -0.246 | 2048 |

**Figure 2.** AT and GC skews calculated for the 37 mitochondrial genomes of *Mitjaevia shibingensis* and *M. dworakowskiae*. Each point indicates an individual gene.

studies which show that the third codon has the highest AT content (Du et al. 2019; Yang et al. 2020). AT skews of all codon positions is positive while GC skews are negative. Most PCGs have the standard ATN (ATA/ATT/ATG/ATC) as the start codon,

while *nad5* and *atp8* genes have TTG, a pattern also observed in other leafhopper mitogenomes (Wang et al. 2017; Wang et al. 2020). Conventional stop codons (TAA or TAG) appear in most PCGs, except that *cox2* and *nad1* use an incomplete codon (a single T-) as the stop codon (see Tables 2, 3).

Research determined the behavior of the PCG codon families and found that codon usage was very similar among Cicadellidae mitogenomes when the results of two species were calculated and summarized (see Table 4, Fig. 3). All 62 available codons (excluding TAA and TAG) are present in *M. shibingensis* and *M. dworakowskiae*. Synonymous codon usage bias was observed in both mitochondrial genomes, and 22 codons were used more frequently than other codons. The four most abundant codons were AAU (Asn), AAA (Lys), AUU (Ile), and UUA (Leu2). The preferred codons all end with A or U, which contribute to the high A + T bias of the entire mitogenomes.

Table 4. Codon and Relative Synonymous Codon Usage (RSCU) of 13 PCGs in the mt genomes of *Mitjaevia shibingensis* and *M. dworakowskiae*.

| Amino acid | Codon | Count/RSCU | | | | Amino acid | Codon | Count/RSCU | | | |
|------------|-------|------------------------|-------------|-------------------------|-------------|------------|-----------|------------------------|-------------|-------------------------|-------------|
| | | <i>M. shibingensis</i> | | <i>M. dworakowskiae</i> | | | | <i>M. shibingensis</i> | | <i>M. dworakowskiae</i> | |
| Phe | UUU | 190^a | 1.49 | 200 | 1.5 | Tyr | UAU | 190 | 1.56 | 185 | 1.57 |
| | UUC | 65 | 0.51 | 66 | 0.5 | | UAC | 53 | 0.44 | 51 | 0.43 |
| Leu2 | UUA | 234 | 3.15 | 245 | 3.33 | His | CAU | 57 | 1.37 | 49 | 1.48 |
| | UUG | 63 | 0.85 | 45 | 0.61 | | CAC | 26 | 0.63 | 17 | 0.52 |
| Leu1 | CUU | 46 | 0.62 | 39 | 0.53 | Gln | CAA | 56 | 1.58 | 66 | 1.71 |
| | CUC | 28 | 0.38 | 20 | 0.27 | | CAG | 15 | 0.42 | 11 | 0.29 |
| | CUA | 56 | 0.75 | 69 | 0.94 | Asn | AAU | 269 | 1.49 | 281 | 1.54 |
| | CUG | 19 | 0.26 | 24 | 0.33 | | AAC | 91 | 0.51 | 84 | 0.46 |
| Ile | AUU | 226 | 1.5 | 225 | 1.55 | Lys | AAA | 242 | 1.62 | 246 | 1.57 |
| | AUC | 75 | 0.5 | 66 | 0.45 | | AAG | 56 | 0.38 | 67 | 0.43 |
| Met | AUA | 201 | 1.58 | 213 | 1.68 | Asp | GAU | 35 | 1.32 | 35 | 1.52 |
| | AUG | 54 | 0.42 | 40 | 0.32 | | GAC | 18 | 0.68 | 11 | 0.48 |
| Val | GUU | 52 | 1.66 | 53 | 1.93 | Glu | GAA | 56 | 1.51 | 62 | 1.65 |
| | GUC | 12 | 0.38 | 11 | 0.4 | | GAG | 18 | 0.49 | 13 | 0.35 |
| | GUA | 47 | 1.5 | 41 | 1.49 | Cys | UGU | 27 | 1.26 | 37 | 1.42 |
| | GUG | 14 | 0.45 | 5 | 0.18 | | UGC | 16 | 0.74 | 15 | 0.58 |
| Ser2 | UCU | 47 | 1.29 | 48 | 1.28 | Trp | UGA | 49 | 1.24 | 54 | 1.33 |
| | UCC | 19 | 0.52 | 11 | 0.29 | | UGG | 30 | 0.76 | 27 | 0.67 |
| | UCA | 66 | 1.81 | 81 | 2.15 | Arg | CGU | 14 | 1.27 | 13 | 1.44 |
| | UCG | 8 | 0.22 | 5 | 0.13 | | CGC | 5 | 0.45 | 2 | 0.22 |
| Pro | CCU | 26 | 1.11 | 42 | 1.65 | CGA | 20 | 1.82 | 14 | 1.56 | |
| | CCC | 30 | 1.28 | 27 | 1.06 | | CGG | 5 | 0.45 | 7 | 0.78 |
| | CCA | 34 | 1.45 | 31 | 1.22 | Ser1 | AGU | 53 | 1.46 | 48 | 1.28 |
| | CCG | 4 | 0.17 | 2 | 0.08 | | AGC | 16 | 0.44 | 26 | 0.69 |
| Thr | ACU | 49 | 1.26 | 54 | 1.26 | AGA | 53 | 1.46 | 51 | 1.36 | |
| | ACC | 42 | 1.08 | 38 | 0.89 | | AGG | 29 | 0.8 | 31 | 0.82 |
| | ACA | 55 | 1.41 | 63 | 1.47 | Gly | GGU | 31 | 1.11 | 34 | 1.31 |
| | ACG | 10 | 0.26 | 16 | 0.37 | | GGC | 15 | 0.54 | 10 | 0.38 |
| Ala | GCU | 26 | 1.89 | 23 | 1.74 | GGA | 25 | 0.89 | 31 | 1.19 | |
| | GCC | 6 | 0.44 | 9 | 0.68 | | GGG | 41 | 1.46 | 29 | 1.12 |
| | GCA | 18 | 1.31 | 19 | 1.43 | * | UAA | 177 | 1.61 | 170 | 1.61 |
| | GCG | 5 | 0.36 | 2 | 0.15 | UAG | 43 | 0.39 | 41 | 0.39 | |

^aThe higher values of preferentially used codons are given in bold.

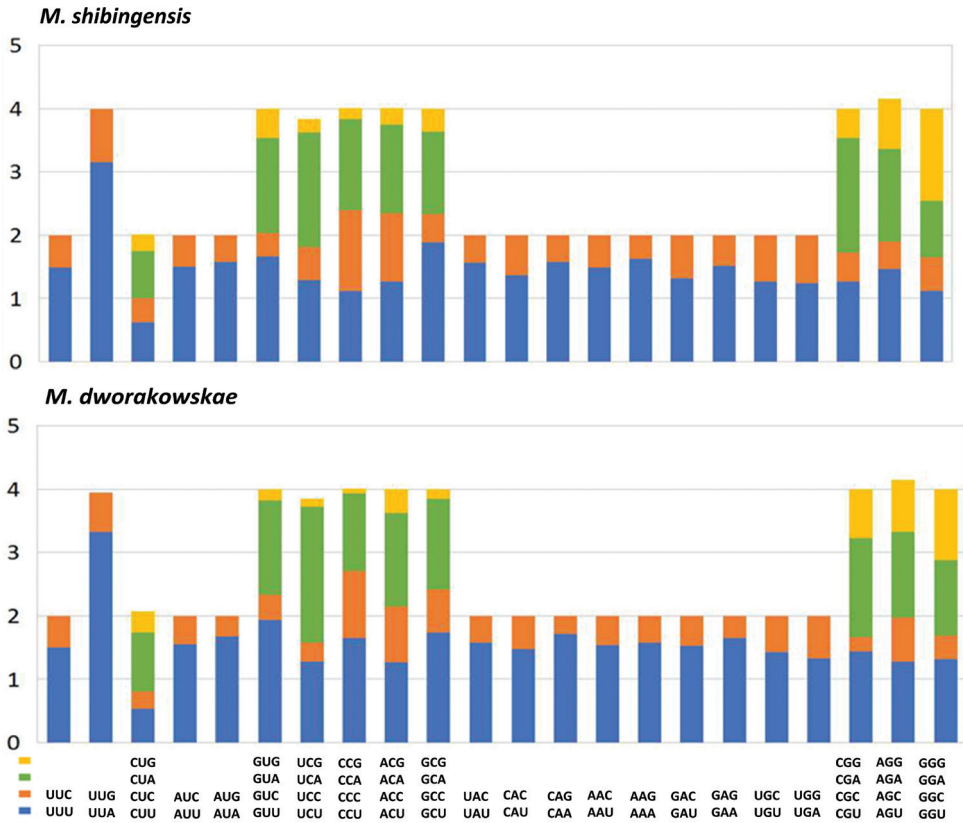


Figure 3. Relative Synonymous Codon Usage (RSCU) of mitochondrial genomes for *Mitjaevia shibingensis* and *M. dworakowskiae*.

Transfer RNA and ribosomal RNA genes

All 22 typical tRNA genes are present in the *M. shibingensis* and *M. dworakowskiae* mitochondrial genomes, of which 14 genes were oriented on the major strand (H-strand), whereas the others were transcribed on the minor strand (L-strand). Their nucleotide lengths are almost identical between species, ranging from 60 bp to 71 bp (Table 2). The average AT content values of tRNAs is 78.5% and 79% in each species, respectively, and the tRNA genes have negligible AT and GC skews (Table 3). Compared to the ancestral insect mitochondrial gene order, no tRNA gene rearrangements were found. All of the tRNA genes can be folded into typical clover-leaf secondary structures except for the *trnS1* in both species' mitochondrial genomes, which lacks the dihydrouridine (DHU) stem and forms a simple loop. In the metazoan mt genome, lack of the DHU arm was very common in *trnS1* (Yang et al. 2020). Based on the secondary structure, a total of 24 and 22 G-U weak base pairs were found in tRNAs of *M. shibingensis* and *M. dworakowskiae*, respectively (Figs 4, 5). Most mismatched nucleotides were G-U

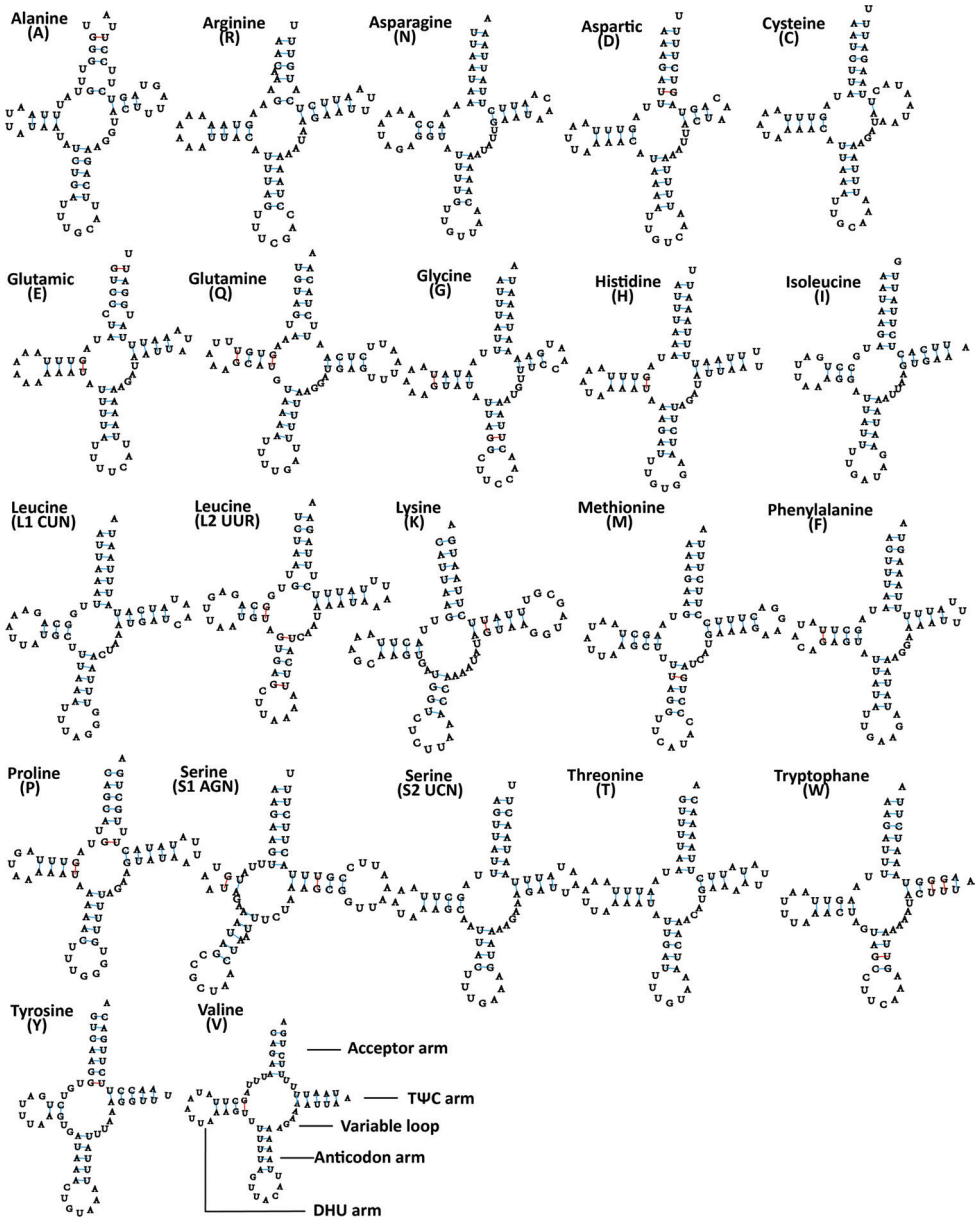


Figure 4. Inferred secondary structures of 22 tRNAs from *Mitjaevia shibingensis*. Watson-Crick base pairings are illustrated by lines (-), whereas GU base pairings are illustrated by red lines (-). Structural elements in tRNA arms and loops are illustrated as for *trnV*.

pairs, which form weak bonds in tRNA and non-classical pairs in tRNA secondary structure, similar to other Cicadellidae (Jia et al. 2010).

Leafhopper ribosomal RNA (rRNA) includes *16S* RNA and *12S* RNA. These two genes are highly conserved and are encoded on the minor strand (L-strand). Similar to other known insects, the content of A + T% in *16S* was higher than that of *12S*.

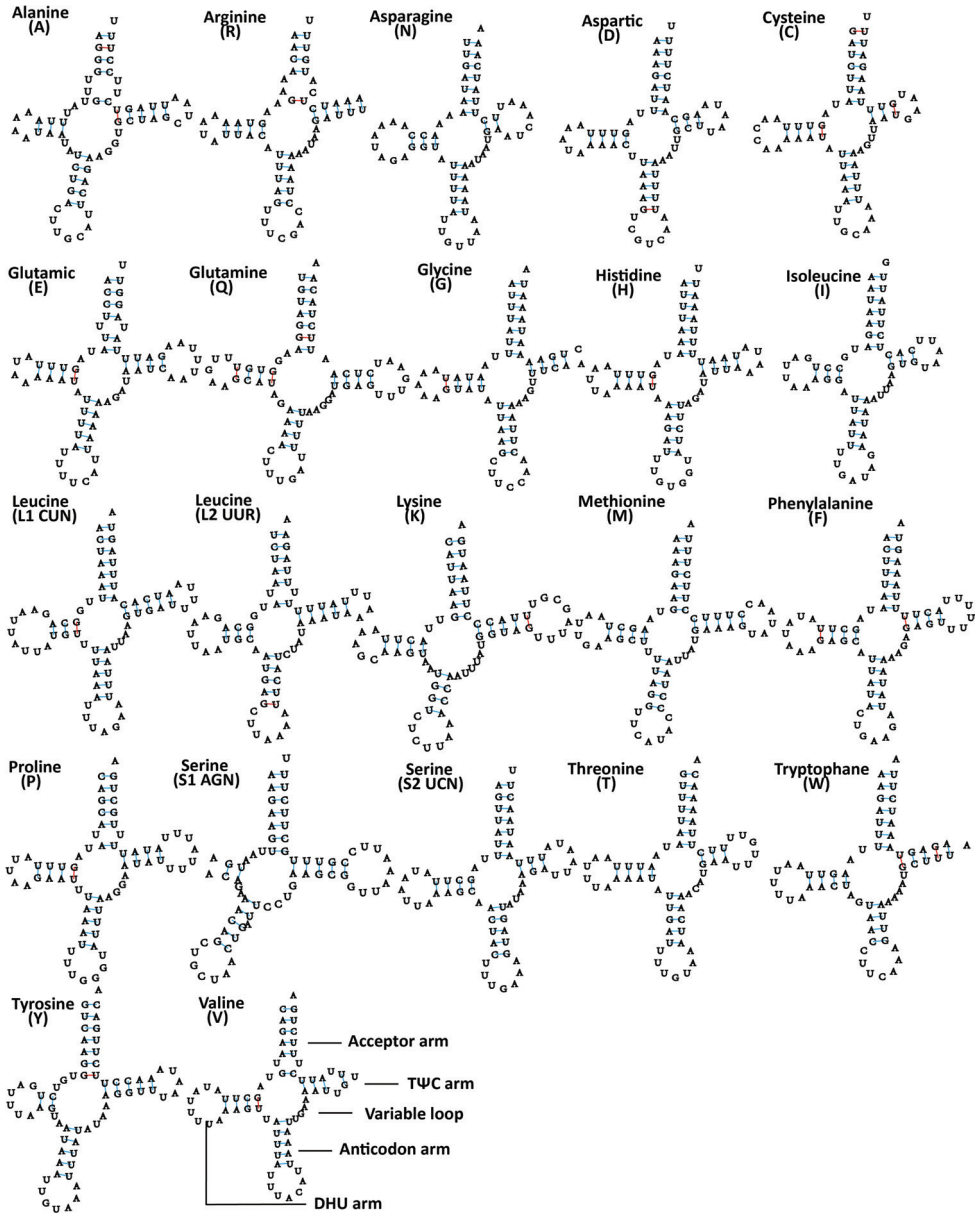


Figure 5. Inferred secondary structures of 22 tRNAs from *Mitjaevia dworakowskiae*. Watson-Crick base pairings are illustrated by lines (-), whereas GU base pairings are illustrated by red lines (-). Structural elements in tRNA arms and loops are illustrated as for *trnV*.

The *16s* genes of *M. shibingensis* and *M. dworakowskiae* were 1192 bp and 1852 bp in length, with AT contents of 82.90% and 82.50%, respectively, and located between *trnL2* and *trnV*. The *12S* rRNA genes of both were 732 bp and 736 bp in length, with AT contents of 81.80% and 81.90%, respectively, and located after *trnV*. The rRNA genes showed a positive AT skew and negative GC skew (Table 3).

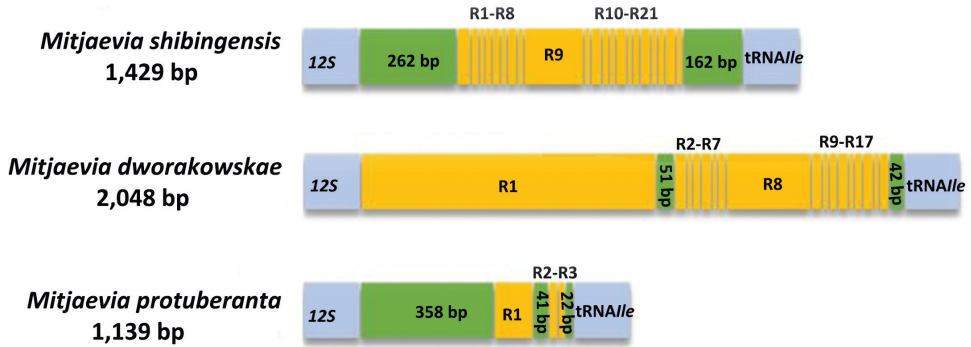


Figure 6. Organization of the control region structure in the mitochondrial genomes of three *Mitjaevia* species. R: repeat unit.

Control region

Like the typical insect mitochondrial genome, the mt genomes of *M. shibingensis* and *M. dworakowskiae* have a large non-coding region, which was identified as the control region and located downstream of *12S*. Control regions of both species were rich in AT, with lengths of 1429 bp and 2048 bp AT contents of 92.7% and 88.9%, respectively (Table 3). The control regions in the three available *Mitjaevia* mitogenomes were variable and not highly conserved, and their lengths ranged from 15 and 784 bp with variable numbers of repeat sequences (Fig. 6). *Mitjaevia shibingensis* included 21 types of repeat unit (R), 17 kinds of repeats (R1, R2) were found in *M. dworakowskiae* with various lengths and copy numbers, and three repeat units were present in *M. protuberanta*. At present, we were unable to find any correlation in repeating units in the different species, probably because of the limited number of species analyzed in this study. Further comparative studies of additional leafhopper mitogenomes are needed.

Nucleotide diversity and genetic distance analysis

The sliding window analysis shows highly variable nucleotide diversity (Pi values) among 13 PCGs sequences of the four tribes of Typhlocybinae (Fig. 7). Empoascini nucleotide diversity is significantly lower than of the other three tribes. The genes *nad2*, *nad4*, *nad4L*, and *nad5* had higher nucleotide diversity, while the genes *cox3*, *cox2*, *cytb*, and *cox1* had comparatively low nucleotide diversity when using MEGA 6.06 software, based on Kimura-2 Parameter, and Bootstrap resampling 1000 times to test and analyze the genetic distance of the four tribes of Typhlocybinae. The results show that the genetic distance between Empoascini and the other three tribes is the largest, and between Typhlocybini and Zyginellini are the smallest (Table 5).

Nucleotide diversity analysis, a primary method for identifying the regions with large nucleotide divergence, is especially useful for designing species-specific markers.

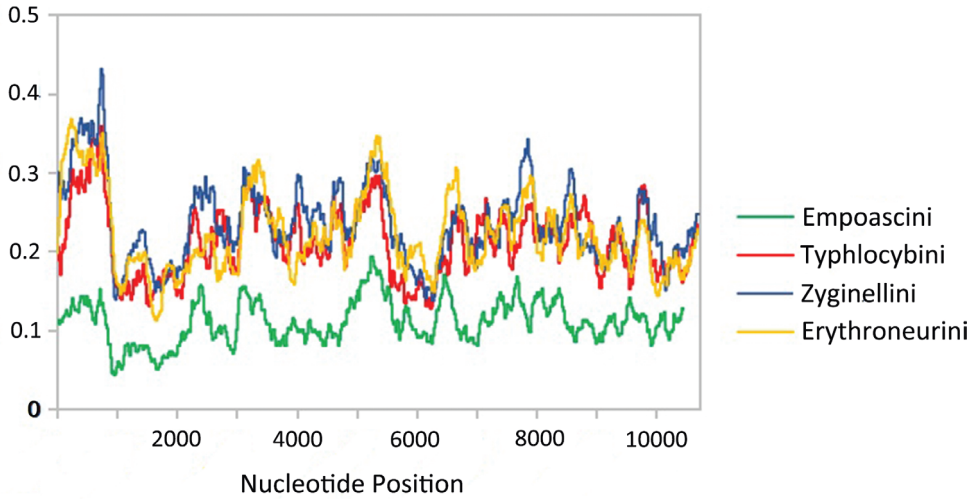


Figure 7. Nucleotide diversity (π) and sliding window analysis of 13 PCGs of the four tribes of Typhlocybinae.

These are useful for taxa with highly variable morphological characteristics, especially Typhlocybinae species which belong to groups that are difficult to distinguish by morphology alone (Jia et al. 2010; Ma et al. 2019). Among the four tribes, *nad2*, *nad4*, and other highly variable genes have garnered our attention. Whether they can be used as the main marker for species identification or the main related genes that control the appearance of the subfamily is worthy of further study. The genetic distance reflects the distance of the genetic relationships between each tribe. Among the four tribes, Typhlocybini and Zyginellini have the smallest genetic distance, indicating that the relationship between the two is the closest, which is consistent with the results of morphological studies (Zhang 1990; Huang 2013).

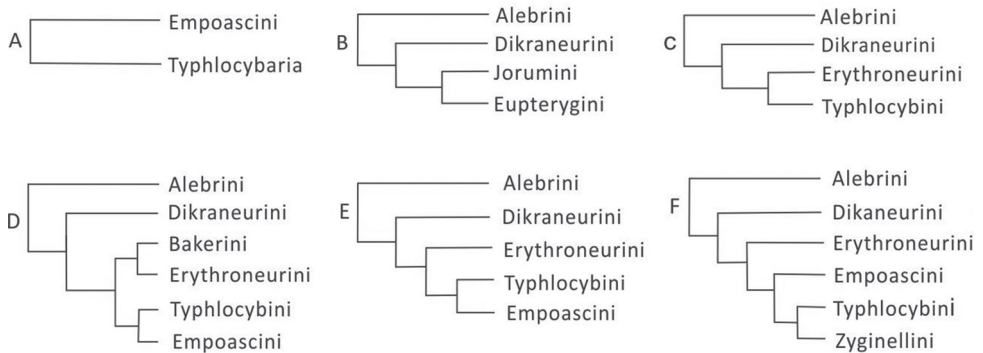
Phylogenetic relationships

Historical review

Typhlocybinae has been divided into tribes based mainly on the characteristics of the wing veins for the past 90 years. Melichar (1903), Distant (1908, 1918), and Matsumura (1931), among others, divided Typhlocybinae into Empoascaria and Typhlocybaria according to whether the hindwing apical cell is closed (Fig. 8A). McAtee (1934) further divided Typhlocybinae into four tribes, Alebrini, Dikraneurini, Jorumiini, and Eupterygini (Fig. 8B), based on the wing veins. Young (1952), also using the male genitalia, recognised the tribes Alebrini, Dikraneurini, Erythroneurini, and Typhlocybini (Fig. 8C). According to whether the peripheral vein of the hind wings exceeds the end of the R+M vein, it was believed that Erythroneurini evolved from Dikraneurini but Mahmood (1967), when adding the tribe Bakerini, believed this

Table 5. The genetic distance between the four tribes of Typhlocybinae.

| | Empoascini | Typhlocybini | Zyginellini |
|----------------|------------|--------------|-------------|
| Typhlocybini | 0.3663 | | |
| Zyginellini | 0.3645 | 0.2663 | |
| Erythroneurini | 0.3623 | 0.3288 | 0.3262 |

**Figure 8.** The traditional classification process of tribe levels in the subfamily Typhlocybinae.

condition to be an acquired mutation. At the same time, Mahmood (1967) postulated that Erythroneurini might be more closely related to Typhlocybini, but the relationship between Erythroneurini and the other tribes still need to be determined by studying a large number of specimens. Mahmood and Ahmed (1968a), using the characteristic of the peripheral vein of the hind wings extending to the end of the R vein, separated Empoascini from the former Typhlocybini, and Typhlocybinae was divided into six tribes (Fig. 8D). Dworakowska (1970) compared the characteristics of Bakerini, Typhlocybini, and Erythroneurini, and postulated that Bakerini may be a relatively primitive branch of Erythroneurini (Fig. 8E). Dworakowska (1977, 1990) discussed Typhlocybini with respect to other tribes, and postulated that the different connection modes of the hindwing peripheral vein and CuA represented different branches, and divided Zyginellini from Typhlocybini resulting in six tribes: Alebrini, Dikraneurini, Empoascini, Erythroneurini, Typhlocybini, and Zyginellini, while Zhang (1990) postulated that Erythroneurini evolved from Empoascini. Since then, Typhlocybinae-related research has followed Dworakowska's six-tribe classification system (Fig. 8F). However, Dietrich (2013) found that the hind wings of leafhoppers have both Zyginellini and Typhlocybini hindwing characteristics when studying the leafhoppers in South America and postulated that the venation characters may not be a stable feature for classification. In terms of overall morphology, Zyginellini and Typhlocybini have similarities present in certain genera and species. Therefore, there is no clear and strong evidence at present to determine whether or not Zyginellini belongs to a natural monophyletic group, and its taxonomic status needs to be further clarified, probably with molecular data.

More recent studies

In recent years, molecular sequencing technology has been widely used in phylogenetic analysis, which can test and verify the results of different levels of more morphology based traditional classifications. Within Typhlocybae, only a few studies have used the combination of morphological characteristics and molecular data to construct phylogenetic relationships. The amount of data is sparse at present and further data is needed.

Dietrich and Dmitriev (2006) used PAUP 4.0b10 to analyze the phylogeny of Typhlocybae for the first time based on morphological characteristics and concluded that Erythroneurini and Dikraneurini are closely related. However, their analysed samples came mainly from the New World, and whether their results represent the relationship between the tribes of Typhlocybae remains to be clarified. Balme (2007) combined morphological characteristics with molecular characteristics (*16S* rDNA, *H3*) to perform a phylogenetic analysis of Typhlocybae, and obtained the following topological structure: Alebrini + ((Empoascini + Typhlocybini) + Dikraneurini), but due to the small sample, the results need to be verified.

Jiang (2016) used *28S* rDNA D2–D3, *16S* rDNA sequence and morphological characteristics to make a preliminary exploration of the phylogenetic relationships of Typhlocybae and obtained the following topological structure: Alebrini + (Empoascini + Erythroneurini), implying that Erythroneurini is a monophyletic group. Song et al. (2020) constructed a phylogenetic tree of Typhlocybae using 13PCGs of eight species and obtained the following topology: Empoascini+ (Typhlocybini+ (Erythroneurini+Zyginellini)). These four tribes are all monophyletic, and Erythroneurini and Zyginellini are sister groups, differing only slightly from the traditional morphological classification. Jiao (2017) used MP and NJ methods to analyze the phylogenetic relationship between Alebrini and Dikraneurini based only on morphological data. The results showed that the two tribes' monophyly was well supported, and its position in the evolutionary tree was similar to that of Zhang (1990) and showed that Alebrini is more primitive.

Results

This study, based on 29 species of *cox1*, 19 species of 13 PCGs, and two rRNA mitochondrial genes data of Typhlocybae produced a slightly different result to the traditional classification with respect to Typhlocybini and Zyginellini. Maximum Likelihood (ML) method was used with IQ-TREE using an ultrafast bootstrap approximation approach with 10,000 replicates. The Bayesian Inference (BI) analysis was performed using MrBayes 3.2.7, with the best fit model GTR+I+ G (Vogler and DeSalle 1993).

Cox1 is one of the mitochondrial protein-coding genes and its bi-terminal sequence is more conservative than *cox2*. It has a rapid evolution rate and large differences between species, and can provide rich phylogenetic information, hence is an ideal mito-

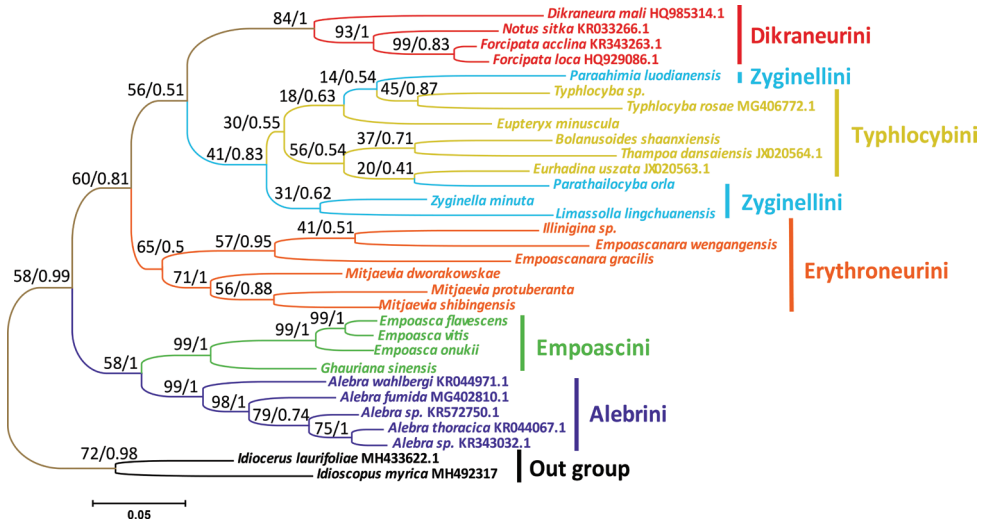


Figure 9. ML and BI Phylogenetic tree inferred from *coxI* of Typhlocybinae. The first number at each node is a bootstrap proportion (BP) of maximum likelihood (ML) analyses, and the second number is Bayesian posterior probability (PP).

chondrial molecular marker. The gene sequences were obtained in the current study by downloading the *coxI* gene sequence of 29 species of Typhlocybinae and two outgroups of Idiocerinae from NCBI to construct a phylogenetic tree. BI and ML analyses generated the same tree topology: (Alebrini + Empoascini) + (Erythroneurini + ((Zyginellini + Typhlocybini) + Dikraneurini))). Most relationships were highly supported, and a few branches pertaining to relationships within Zyginellini and Typhlocybini received lower support (Fig. 9). Also, the tree topology is different from previous research, with Alebrini + Empoascini forming sister groups, and the species of Zyginellini and Typhlocybini are interconnected and cannot be resolved into separate branches. The remaining tribes are monophyletic groups. Alebrini is placed at the base of the tree and is therefore the most primitive. The phylogenetic relationship is generally consistent with the results of previous studies based on morphology and molecules (Balme 2007; Jiang 2016).

At present, the complete mitochondrial genome data of Alebrini and Dikraneurini have not been added to NCBI. Thus, the phylogenetic relationships were analyzed based on the concatenated nucleotide sequences of 13 PCGs and two rRNA from 19 Typhlocybinae (the remaining four tribes) species and two outgroups. Although ML and PB analyses produced inconsistent topologies across the different datasets and models, most relationships were highly supported and consistent in the analyses, and the main difference is the relationship of species between Zyginellini and Typhlocybini. (Figs 10, 11). In this study, Empoascini and Erythroneurini were recovered as monophyletic, always forming a clade with high support values, while Zyginellini and Typhlocybini formed a single branch in every tree, and neither tribe was ever resolved

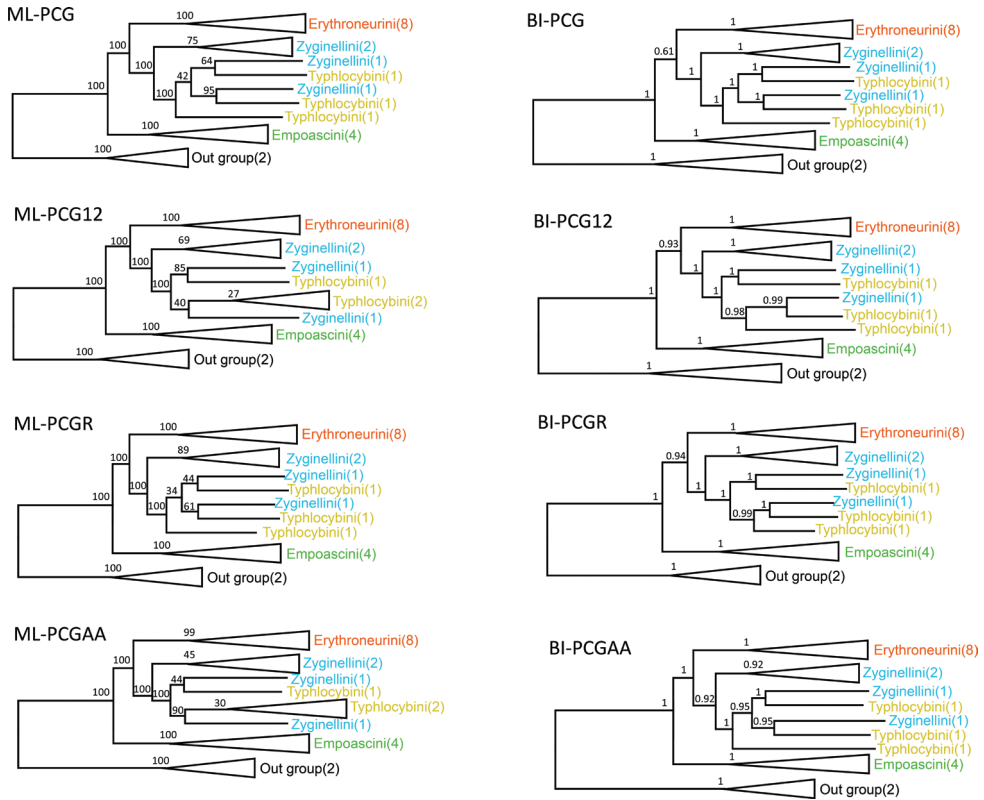


Figure 10. Phylogenetic trees of Typhlocybinae inferred by maximum likelihood (ML) and PhyloBayes (PB) methods based on 13 PCGs and 2 rRNA.

as monophyletic, which suggests that the hind wing character traditionally used to separate these two tribes is not reliable and that the tribes should probably be treated as synonyms, as was suggested previously by Dietrich (2013). Within the Typhlocybinae, the four species of Emposcini studied constituted one clade and tended to be placed at the basal position of the tree as the sister group to the other tribes. Unlike the previous analyses, our results support the combination of Zyginiellini and Typhlocybini as a tribe. As with other recent studies, our results indicate that sequence data from leafhopper mitogenomes is informative of phylogenetic relationships in the taxonomic hierarchy of this group. Also, the results of the phylogenetic tree and nucleotide diversity are consistent. Emposcini has the lowest nucleotide diversity and is clearly distinguished from the other three tribes. Therefore, we speculate that the richness of nucleotide diversity has an impact on the phylogenetic relationship of Typhlocybinae. However, data are available for only a tiny fraction of species so the addition of more species, and representatives of other major lineages, will be needed to determine the extent to which mitogenome sequence data can resolve leafhopper phylogeny.

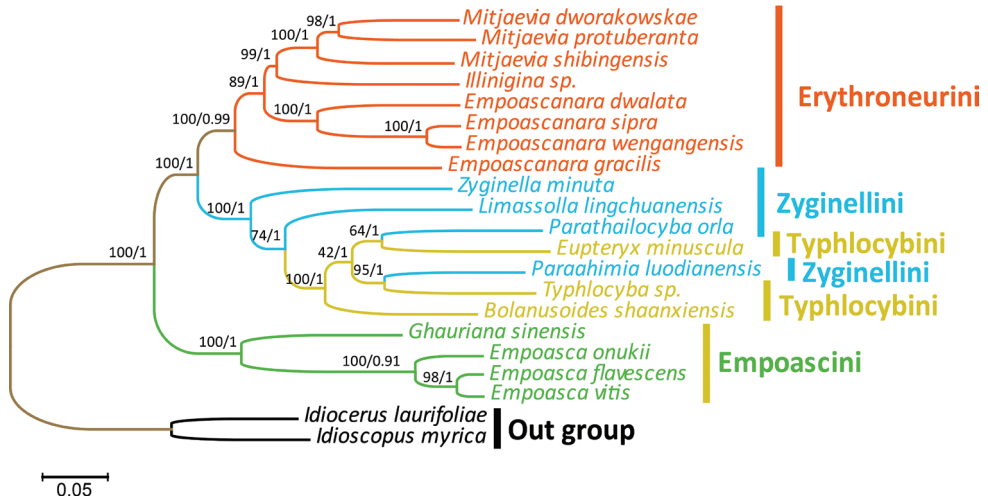


Figure 11. ML and BI Phylogenetic tree inferred from 13 PCGs of Typhlocybinae. The first number at each node is a bootstrap proportion (BP) of maximum likelihood (ML) analyses, and the second number is Bayesian posterior probabilities (PP).

Conclusions

This paper describes the complete mitochondrial genomes of *M. shibingensis* and *M. dworakowskiae*, analyzes the basic composition, location, secondary structure, and other characteristics of PCGs, tRNA genes, rRNA genes, and control regions, and compares them to other Typhlocybinae mitochondrial genomes. The mitogenomes of these two species closely resemble those of most other sequenced leafhoppers in various structural and compositional aspects. The sliding window analysis shows a highly variable nucleotide diversity (P_i values) among 13 PCGs sequences of the four tribes of Typhlocybinae. Empoascini nucleotide diversity is significantly lower than in the other three tribes, and the other three tribes have little difference between them. The genes *nad2*, *nad4*, *nad4L*, and *nad5* have higher nucleotide diversity, and whether they can be used as the main markers for species identification or the main related genes that control the appearance of the subfamily is worthy of further study. The genetic distance of the four tribes of Typhlocybinae shows that the Empoascini and the other three tribes are the largest while Typhlocybini and Zyginellini are the smallest and indicates that the relationship between the two is the closest, which is consistent with the results of morphological studies. Phylogenetic analysis of 31 *cox1* yielded a well-supported topology with most branches receiving maximum support and a few branches pertaining to relationships within Zyginellini and Typhlocybini receiving lower support; the species of these two tribes are intertwined and cannot be resolved into separate branches, and Alebrini is placed at the base of the tree as the most primitive. Phylogenetic relationships were analyzed based on the concatenated nucleotide sequences of 13 PCGs and two rRNA show that although ML and PB analyses produced inconsistent topologies across the different datasets and models, and most relationships were highly supported and constant in the analyses.

In this study, Emposcini and Erythroneurini were recovered as monophyletic while Zyginellini and Typhlocybini gathered into a single branch and Emposcini tended to be placed at the basal position of the tree as the sister group to the other tribes. This study indicated that mitochondrial genome sequences are informative for leafhopper phylogeny, but unlike the previous analysis (Zhang 1990), the results of this study re-located the taxonomic status and phylogenetic relationship of the six tribes of Typhlocybinae and supported the combination of Zyginellini and Typhlocybini as a single tribe. Also, the results of the phylogenetic tree and nucleotide diversity are consistent. Emposcini has the lowest nucleotide diversity and is clearly distinguished from the other three tribes. Therefore, we speculate that the richness of nucleotide diversity has an impact on the phylogenetic relationship of Typhlocybinae.

Based on the current and previous studies, the classification of the tribes of Typhlocybinae is not yet fully resolved with respect to Typhlocybini and Zyginellini, i.e., one or two tribes. From a molecular perspective, more sequencing data is needed to build a more complete phylogenetic tree to support or modify the traditional morphological classification. To this aim, it is hoped that the new data provided here will facilitate future comparative studies of leafhopper mitogenomes and demonstrate the need for more comparative data.

Acknowledgements

We thank Chris Dietrich for reviewing the manuscript and Mick Webb for checking and revising the manuscript. This work was funded partly by the World Top Discipline Program of Guizhou Province: Karst Ecoenvironment Sciences (No. 125 2019 Qianjiao Keyan Fa), the Guizhou Provincial Science and Technology Foundation ([2018]1411), the Guizhou Science and Technology Support Project ([2019]2855), the Science and Technology Project of Guiyang City ([2020]7-18), the Innovation Group Project of Education Department of Guizhou Province ([2021]013), the Training Program for High-level Innovative Talents of Guizhou Province ([2016]4020) and the Project for Regional Top Discipline Construction of Guizhou Province: Ecology in Guiyang University (Qianjiao Keyan Fa [2017]85).

References

- Balme GR (2007) Phylogeny and Systematics of the Leafhopper Subfamily Typhlocybinae (Insecta: Hemiptera: Typhlocybinae). Ph.D. thesis, North Carolina State University, Raleigh.
- Benson G (1999) Tandem repeats finder: a program to analyze DNA sequences. *Nucleic Acids Research* 27: 573–580. <https://doi.org/10.1093/nar/27.2.573>
- Boore JL (1999) Animal mitochondrial genomes. *Nucleic Acids Research* 27: 1767–1780. <https://doi.org/10.1093/nar/27.8.1767>
- Burland TG (2000) DNASTAR's Laser Gene sequence analysis software. *Methods in Molecular Biology* 132: 71–91. <https://doi.org/10.1385/1-59259-192-2:71>

- Chen X, Song Y, Webb (2020) Two new species of the leafhopper genus *Mitjaevia* Dworakowska from China (Hemiptera, Cicadellidae, Typhlocybinae). *ZooKeys* 964: 31–40. <https://doi.org/10.3897/zookeys.964.48655>
- Chen XX, Tan C, Yuan ZW, Song YH (2020b) Cluster analysis of geographical distribution patterns of Erythroneurini in China. *Journal of Environmental Entomology* 42(5): 1141–1153.
- Chen XX, Yuan ZW, Yuan XW, Song YH (2020a) Advances in mitochondrial genome complete sequence structure of Leafhopper. *Genomics and Applied Biology* 39(06): 2565–2577. <https://doi.org/10.13417/j.gab.039.002565>
- Cook CE, Yue QY, Akam M (2005) Mitochondrial genomes suggest that hexapods and crustaceans are mutually paraphyletic. *Proceedings of the Royal Society B* 272: 1295–1304. <https://doi.org/10.1098/rspb.2004.3042>
- Dietrich CH, Dmitriev DA (2007) Revision of the New World leafhopper genus *Neozygina* Dietrich & Dmitriev (Hemiptera: Cicadellidae: Typhlocybinae: Erythroneurini). *Zootaxa* 1475: 27–42.
- Dietrich CH, McKamey SH, Deitz LL (2010) Morphologybased phylogeny of the treehopper family Membracidae (Hemiptera:Cicadomorpha: Membracoidea). *Systematic Entomology* 26: 213–239. <https://doi.org/10.1046/j.1365-3113.2001.00140.x>
- Dietrich CH (2013) South American leafhoppers of the tribe Typhlocybini (Hemiptera: Cicadellidae: Typhlocybinae). *Zoologia* 30: 519–568. <https://doi.org/10.1590/S1984-46702013000500008>
- Distant WL (1908) *Rhynchota* (Vol. IV). Homoptera and Appendix (Pt.). The Fauna of British India, Including Ceylon and Burma. Taylor and Francis, London, 501 pp.
- Distant WL (1918) *Rhynchota* (Vol. VII). Homoptera: Appendix. Heteroptera: Addenda. The fauna of British India, Including Ceylon and Burma. Taylor & Francis, London, 872–1009.
- Du YM, Dai W, Dietrich CH (2017) Mitochondrial Genomic Variation and Phylogenetic Relationships of Three Groups in the Genus *Scaphoideus* (Hemiptera: Cicadellidae: Deltocephalinae). *Scientific Reports* 7: e16908. <https://doi.org/10.1038/s41598-017-17145-z>
- Du YM, Dietrich CH, Wu Dai (2019) Complete mitochondrial genome of *Macrosteles quadrimaculatus* (Matsumura) (Hemiptera: Cicadellidae: Deltocephalinae) with a shared tRNA rearrangement and its phylogenetic implications. *International Journal of Biological Macromolecules* 122: 1027–1034. <https://doi.org/10.1016/j.ijbiomac.2018.09.049>
- Du YM, Zhang CN, Dietrich CH, Zhang YL, Dai W (2017) Characterization of the complete mitochondrial genomes of *Maiestas dorsalis* and *Japananus hyalinus* (Hemiptera: Cicadellidae) and comparison with other Membracoidea. *Scientific Reports* 7: e14197. <https://doi.org/10.1038/s41598-017-14703-3>
- Dworakowska I (1977) *Jimara* gen. n. of Dikraneurini from Africa. *Reichenbachia* 16(37): 337–346.
- Dworakowska I (1979) On some Typhlocybinae from India and adjoining areas (Homoptera, Auchenorrhyncha, Cicadellidae). *Reichenbachia* 17(18): 143–162.
- Dworakowska I (1970) Remarks on the tribe Bakerini Mahm with description of one new genus of Typhlocybini (Cicadellidae, Typhlocybinae). *Bulletin de l'Academie Polonaise des Sciences (Serie des Sciences Biologiques)* 17(11–12): 691–696.
- Guo HF (2011) Major tea pests-advances in research on pseudo-eye leafhopper. *Jiangsu Agricultural Sciences* 1: 132–134. <https://doi.org/10.15889/j.issn.1002-1302.2011.01.093>

- Hamilton KGA (1983) Classification, morphology and phylogeny of the family Cicadellidae (Rhynchota: Homoptera). In: Knight WJ, Pant NC, Robertson TS, Wilson MR (Eds) Proceedings, 1st International Workshop on Biotaxonomy, Classification and Biology of Leafhoppers and Planthoppers of Economic Importance. Commonwealth Institute of Entomology, London, 15–37.
- Hamilton KGA (1998) New World species of *Chlorita*, *Notus*, and *Forcipata* (Rhynchota: Homoptera: Cicadellidae: Typhlocybinae) with a new tribe Forcipatini. Canadian Entomologist 130: 491–507. <https://doi.org/10.4039/Ent130491-4>
- Huang M (2003) Systematic study of Typhlocybini from China (Homoptera: Cicadellidae: Typhlocybinae). Ph.D. thesis, Northwest A&F University, Yanglin.
- Jia WZ, Yan HB, Guo AJ, Zhu XQ, Wang YC, Shi WG, Chen HT, Zhan F, Zhang SH, Fu BQ (2010) Complete mitochondrial genomes of *Taenia multiceps*, *T. hydatigena* and *T. pisiformis*: additional molecular markers for a tapeworm genus of human and animal health significance. BMC Genomics 8(11): e447. <https://doi.org/10.1186/1471-2164-11-447>
- Jiang H (2016) Taxonomy and phylogeny of the tribe Erythroneurini from China based on molecular and morphological characters (Hemiptera: Cicadellidae: Typhlocybinae). M.S. thesis, Northwest A&F University, Yanglin.
- Jiao M (2017) Systematics study on tribes Alebrini and Dikraneurini from China. Ph.D. Thesis, Guizhou University, Guiyang.
- Krishnankutty SM, Dietrich CH, Dai W, Siddappaji MH (2016) Phylogeny and historical biogeography of leafhopper subfamily Iassinae (Hemiptera: Cicadellidae) with a revised tribal classification based on morphological and molecular data. Systematic Entomology 41 (3): 580–595. <https://doi.org/10.1111/syen.12175>
- Laslett D, Canbäck B (2008) ARWEN: a program to detect tRNA genes in metazoan mitochondrial nucleotide sequences. Bioinformatics 24: 172–175. <https://doi.org/10.1093/bioinformatics/btm573>
- Lowe TM, Eddy SR (1997) TRNAscan-SE: a program for improved detection of transfer RNA genes in genomic sequence. Nucleic Acids Research 25: 955–964. <https://doi.org/10.1093/nar/25.5.955>
- Ma LY, Liu AF, Chiba B, Yuan AX (2019) The mitochondrial genomes of three skippers: insights into the evolution of the family HesperIIDae (Lepidoptera). Genomics 112(1): 432–441. <https://doi.org/10.1016/j.ygeno.2019.03.006>
- Mahmood SH, Ahmed M (1968) Problems of higher classification of Typhlocybinae (Cicadellidae–Homoptera). University Studies, University of Karachi 5(3): 72–79.
- Mahmood SH (1967) A study of the typhlocybinae genera of the Oriental region (Thailand, the Philippines and adjoining areas). Pacific Insects Monographs 12: 1–52.
- Matsumura S (1931a) 6000 Illustrated Insects of the Japan Empire. Insecta Matsumurana, Tokyo, 1496 pp.
- McAtee WL (1934) Genera and subgenera of Eupteryginae (Homoptera: Jassidae). Proceedings of the Zoological Society of London 104: 93–117. <https://doi.org/10.1111/j.1469-7998.1934.tb06225.x>
- Meng ZH, Yang MF, Zhou YF, Lu ZY, Ni JQ (2013) Molecular phylogenetic analysis of some species of Cicadellinae based on mitochondrial *Cyt b* Gene. Guizhou Agricultural Sciences 41: 1–5.

- Morris MG (1971) Differences between the invertebrate faunas of grazed and ungrazed chalk grassland, IV. Abundance and diversity of Homoptera–Auchenorrhyncha. *Journal of Applied Entomology* 8: 37–52. <https://doi.org/10.2307/2402126>
- Nguyen LT, Schmidt HA, Von HA, Minh BQ (2015) IQ-TREE: a fast and effective stochastic algorithm for estimating maximum-likelihood phylogenies. *Molecular Biology and Evolution* 32: 268–274. <https://doi.org/10.1093/molbev/msu300>
- Perna NT, Kocher TD (1995) Patterns of nucleotide composition at fourfold degenerate sites of animal mitochondrial genomes. *Journal of Molecular Evolution* 41: 353–358. <https://doi.org/10.1007/BF00186547>
- Roddee J, Kobori Y, Hanboonsong Y (2018) Multiplication and distribution of sugarcane white leaf phytoplasma transmitted by the leafhopper, *Matsumuratettix hiroglyphicus* (Matsumura) (Hemiptera: Cicadellidae), in infected sugarcane. *Sugar Tech* 20: 445–453. <https://doi.org/10.1007/s12355-017-0559-x>
- Rozas J, Ferrer-Mata A, Sánchez-DelBarrio JC, Guirao-Rico S, Librado P, Ramos-Onsins SE, Sánchez-Gracia A (2017) DnaSP 6: DNA sequence polymorphism analysis of large data sets. *Molecular Biology and Evolution* 34(12): 3299–3302. <https://doi.org/10.1093/molbev/msx248>
- Saccone C, Gissi C, Reyes A, Larizza A, Sbisà E, Pesole G (2002) Mitochondrial DNA in Metazoa: degree of freedom in a frozen event. *Gene* 286: 3–12. [https://doi.org/10.1016/S0378-1119\(01\)00807-1](https://doi.org/10.1016/S0378-1119(01)00807-1)
- Song YH, Yuan XW, Li C (2020) The mitochondrial genome of *Paraahimia luodianensis* (Hemiptera: Cicadellidae: Typhlocybinae), a new genus and species from China. *Mitochondrial DNA B* 5(2): 1351–1352. <https://doi.org/10.1080/23802359.2020.1735280>
- Tamura K, Stecher G, Peterson D, Filipski A, Kumar S (2013) MEGA6: molecular evolutionary genetics analysis version 6.0. *Molecular Biology and Evolution* 30: 2725–2729. <https://doi.org/10.1093/molbev/mst197>
- Tan C, Chen XX, Li C, Song YH (2020) The complete mitochondrial genome of *Empoasca canara sipra* (Hemiptera: Cicadellidae: Typhlocybinae) with phylogenetic consideration. *Mitochondrial DNA B* 5(1): 260–261. <https://doi.org/10.1080/23802359.2019.1698990>
- Vogler AP, DeSalle R, Assmann T (1993) Molecular population genetics of the endangered tiger beetle, *Cicindela dorsalis* (Coleoptera: Cicindelidae). *Annals of the Entomological Society America* 86: 142–152. <https://doi.org/10.1093/aesa/86.2.142>
- Wang JJ, Li H, Dai RH (2017) Complete mitochondrial genome of *Taharana Fasciana* (Insecta, Hemiptera: Cicadellidae) and comparison with other Cicadellidae Insects. *Genetica* 145: 593–602. <https://doi.org/10.1007/s10709-017-9984-8>
- Wang JJ, Wu YF, Dai RH, Yang MF (2020) Comparative mitogenomes of six species in the subfamily Iassinae (Hemiptera: Cicadellidae) and phylogenetic analysis. *International Journal of Biological Macromolecules* 149: 1294–1303. <https://doi.org/10.1016/j.ijbiomac.2020.01.270>
- Wang XS, Huang M, Zhang YL (2012) Cluster analysis of Typhlocybinae (Hemiptera: Cicadellidae) distributional pattern in China. *Journal of Northwest A & F University (Natural Science Edition)* 40: 86–94. [+ 101.] <https://doi.org/10.13207/j.cnki.jnwafu.2012.04.004>
- Wang XY, Wang JJ, Fan ZH, Dai RH (2019) Complete mitogenome of *Olidiana ritcheriina* (Hemiptera: Cicadellidae) and phylogeny of Cicadellidae. *PeerJ* 7: e8072. <https://doi.org/10.7717/peerj.8072>

- Wilson AC, Cann RL, Carr SM, George M, Gyllensten UB, Helmsbychowski KM, Stoneking M (2008) Mitochondrial DNA and two perspectives on evolutionary genetics. *Biological Journal of the Linnean Society* 26: 375–400. <https://doi.org/10.1111/j.1095-8312.1985.tb02048.x>
- Xian Z, Dietrich CH, Min H (2020) Characterization of the complete mitochondrial genomes of two species with preliminary investigation on phylogenetic status of Zyginiini (Hemiptera: Cicadellidae: Typhlocybae). *Insects* 11: e684. <https://doi.org/10.3390/insects11100684>
- Yang Y, Liu HY, Qi L, Kong LF, Li Q (2020) complete mitochondrial genomes of two toxin-accumulated nassariids (Neogastropoda: Nassariidae: *Nassarius*) and their implication for phylogeny. *International Journal of Molecular Sciences* 21: e3545. <https://doi.org/10.3390/ijms21103545>
- Young DA (1952) A reclassification of Western Hemisphere Typhlocybae (Homoptera, Cicadellidae). *The University of Kansas Science Bulletin* 35: 3–217. <https://doi.org/10.5962/bhl.part.4327>
- Yu PF, Wu GH, Han BY (2017) Sequencing and analysis of the mitochondrial genome of *Kolla paulula* (Walker) (Hemiptera: Cicadellidae). *Journal of the Anhui Agricultural University* 44: 874–881. <https://doi.org/10.13610/j.cnki.1672-352x.20171017.032>
- Yuan XW, Li C, Song YH (2020) Characterization of the complete mitochondrial genome of *Mitjaevia protuberanta* (Hemiptera: Cicadellidae: Typhlocybae). *Mitochondrial DNA B* 5(1): 601–602. <https://doi.org/10.1080/23802359.2019.1710601>
- Zahniser JN, Dietrich CH (2013) A review of the tribes of Deltocephalinae (Hemiptera: Auchenorrhyncha: Cicadellidae). *European Journal of Taxonomy* 45: 1–211. <https://doi.org/10.5852/ejt.2013.45>
- Zhang YL (1990) A taxonomic study of leafhoppers in China (Homoptera: Cicadellidae). Tianze Press, Hong Kong, 139–144.
- Zhou J, Liu X, Stones DS, Xie Q, Wang G (2011) MrBayes on a graphics processing unit. *Bioinformatics* 27(9): 1255–1261. <https://doi.org/10.1093/bioinformatics/btr140>

Supplementary material I

Datasets of phylogenetic analysis

Authors: Xiaoxiao Chen, Can Li, Yuehua Song

Data type: phylogenetic

Copyright notice: This dataset is made available under the Open Database License (<http://opendatacommons.org/licenses/odbl/1.0/>). The Open Database License (ODbL) is a license agreement intended to allow users to freely share, modify, and use this Dataset while maintaining this same freedom for others, provided that the original source and author(s) are credited.

Link: <https://doi.org/10.3897/zookeys.1037.63671.suppl1>

A new genus and species of Hydrobiidae Stimpson, 1865 (Caenogastropoda, Truncatelloidea) from Peloponnese, Greece

Andrzej Falniowski¹, Jozef Grego², Aleksandra Rysiewska¹,
Artur Osikowski³, Sebastian Hofman⁴

1 Department of Malacology, Institute of Zoology and Biomedical Research, Jagiellonian University, ul. Gronostajowa 9, 30-387 Kraków, Poland **2** Horná Mičíná 219, SK-97401 Banská Bystrica, Slovakia **3** Department of Animal Reproduction, Anatomy and Genomics, University of Agriculture in Krakow, al. Mickiewicza 24/28, 30-059 Kraków, Poland **4** Department of Comparative Anatomy, Institute of Zoology and Biomedical Research, Jagiellonian University, ul. Gronostajowa 9, 30-387 Kraków, Poland

Corresponding author: Sebastian Hofman (s.hofman@uj.edu.pl)

Academic editor: Eike Neubert | Received 5 February 2021 | Accepted 22 April 2021 | Published 18 May 2021

<http://zoobank.org/2B9A12E1-65A9-43EE-9978-C02CCDBCD4EA>

Citation: Falniowski A, Grego J, Rysiewska A, Osikowski A, Hofman S (2021) A new genus and species of Hydrobiidae Stimpson, 1865 (Caenogastropoda, Truncatelloidea) from Peloponnese, Greece. ZooKeys 1037: 161–179. <https://doi.org/10.3897/zookeys.1037.64038>

Abstract

Minute caenogastropod brackish-water gastropods, formerly classified as *Hydrobia*, are important elements of the brackish-water fauna and were objects of intensive study for many years. Until now, five genera have been distinguished, most of them represented by a number of species, but rather indistinguishable without molecular data (cytochrome oxidase subunit I – COI). In the eastern Mediterranean region, they are still poorly studied. In this paper, we present a new species of “*Hydrobia*” from the brackish Moustos spring, Arkadia, eastern Peloponnese, Greece. The shell, protoconch, radula, female reproductive organs, and penis are described and illustrated, together with the molecular (COI) relationships with other hydrobiids. All data confirm that these snails represent a distinct taxon, which must be classified as a new species belonging to a new genus. The formal descriptions are given. The closest, sister taxon is *Salenthydrobia* Wilke, 2003. The molecularly estimated time of divergence, 5.75 ± 0.49 Mya, coincides with 5.33 Mya, which is the time of the Oligocene flooding that terminated the Messinian salinity crisis. During the latter period, brackish “Lago-Mare” habitats were most probably suitable for the last common ancestor of *Salenthydrobia* and the newly described genus. Later, the Pliocene flooding isolated the Apennine and Peloponnese populations, promoting speciation.

Keywords

Cytochrome oxidase subunit I, morphology, phylogeny, Pliocene flooding, speciation

Introduction

The typically brackish-water caenogastropod snails formerly known as *Hydrobia* inhabit estuaries and other brackish habitats around the northern Atlantic and adjacent seas; in many places, these small, tiny snails are numerous and their biomass is large. Thus, they form an important component of the brackish water fauna and have been studied for many aspects (for details see Muus 1967; Falniowski 1987; Fretter and Graham 1994). The simple shells show a set of plesiomorphic character states and are extremely variable, making species determination hardly possible (e.g., Muus 1963, 1967; Falniowski et al. 1977; Wilke and Falniowski 2001). Muus (1963, 1967) demonstrated clear and stable differences in the penis morphology and snout and tentacle pigmentation between the three Baltic species, although the pigmentation was later found to be more variable but still useful for species determination (Falniowski 1986). However, later studies (e.g., Radoman 1973, 1977, 1983; Giusti and Pezzoli 1984; Wilke and Davis 2000; Wilke et al. 2000; Wilke and Pfenninger 2002; Wilke 2003), including those applying molecular data (mostly the partial sequences of mitochondrial cytochrome oxidase), confirmed these morphological differences, but as discriminating the genera. The discrimination of species within these genera was found possible only with molecular data. Currently, five genera are distinguished within *Hydrobia* s.l.

The genus *Hydrobia* Hartmann, 1821 (type species *Cyclostoma acutum* Draparnaud, 1805) is represented by several molecularly distinct species with rather restricted ranges, both Atlantic and Mediterranean. The nomenclatural problems (e.g., Bank et al. 1979; Falniowski and Szarowska 2002) were solved by the ICZN Opinion 2034 (Case 3087) (International Commission on Zoological Nomenclature 2003). The genus *Peringia* Paladilhe, 1874 (type species *Turbo ulvae* Pennant, 1777) is monotypic. *Peringia ulvae*, capable to live in salinity as high as at the open sea and having a lecithotrophic veliger, is widely distributed along the Atlantic coast, including the Baltic sea, but does not inhabit the Mediterranean Sea. The genus *Ventrosia* Radoman, 1977 (type species *Turbo ventrosus* Montagu, 1803) has been considered a junior synonym of *Ecrobia* Stimpson, 1865, since Davis et al. (1989) suggested that North American *Ecrobia truncata* (Vanatta, 1924) was introduced from Europe and would then be a synonym of *Ventrosia ventrosa*. This was later confirmed by molecular data (Osikowski et al. 2016). *Ecrobia* (its type species, following the ICZN rules, *Turbo ventrosus* Montagu, 1803) is represented by a few molecularly distinguishable species (Szarowska and Falniowski 2014; Osikowski et al. 2016) known from the Baltic Sea to the Black Sea. The genus *Adriohydrobia* Radoman, 1977 (type species *Paludina gagatinella* Küster, 1852) is known from the Adriatic Sea only; a few nominal spe-

cies assigned earlier to *Adriohydrobia* are molecularly identical with *A. gagatinella*, and thus they became synonyms (Wilke and Falniowski 2001). The monotypic genus *Salenthydrobia* Wilke, 2003 (type species *Salenthydrobia ferreri* Wilke, 2003), was found at three closely situated populations in the southernmost part of the Apennine Peninsula (Wilke 2003).

Reliable data are scarce on the group formerly known as *Hydrobia* in the eastern Mediterranean brackish habitats. The numerous records that exist of *Peringia ulvae* from the eastern Mediterranean are a good example, as this species does not occur in the Mediterranean Sea. Another example is the monograph on the Greek Hydrobiidae (Schütt 1980), which does not mention any representatives of “*Hydrobia*”. Even though shells cannot be used for species determination, many hydrobiologists and marine biologists still record species determined by shell characters alone (e.g., Koutsoubas et al. 2000; Evagelopoulos et al. 2009). As stated above, the head pigmentation and penis morphology make identification of genera possible (Muus 1963, 1967; Falniowski 1986, 1987), while female reproductive organs are taxonomically less useful (Falniowski 1988). At species level, all morphological characters are hardly applicable because of morphostatic evolution (Davis 1992). Non-adaptive radiation, marked by the rapid proliferation of species without ecological differentiation (Gittenberger 1991), results in a flock of species that need not differ either morphologically or ecologically. Thus, at the species level in the Hydrobiinae, morphological characters cannot be used for species recognition alone, and molecular data are inevitably necessary to distinguish taxa.

So far, two species of *Ecrobia* have been recorded from six localities in Greece (Kevrekidis et al. 2005; Szarowska and Falniowski 2014; Osikowski et al. 2016), one of them (*E. ventrosa*) at the western coast of the Peloponnese Peninsula. In summer 2009, a few specimens of “*Hydrobia*” were collected at the brackish Moustos spring at Arkadia, on the eastern coast of the Peloponnese. The aim of the present paper is to establish their phylogenetic position, applying morphological and molecular data.

Material and methods

The snails were collected in 2009 by sieve at the Moustos spring (Fig. 1), Arkadia, eastern Peloponnese, Greece (2 km N of Aghios Andreas, under the road from Astros to Korakovouni, 37.3845, 22.7444). The spring is situated about 500 m from the Aegean Sea. This large, brackish spring with sulphide content, rising from calcareous breccia, feeds a larger seashore lagoon called Limni Moustos with adjacent swamps hosting a bird reserve. The specimens were taken from the spring and the stony ridge towards the lagoon. No specimens were found in the lagoon.

The snails were fixed in 80% ethanol. The shells were photographed with a Canon EOS 50D digital camera, under a Nikon SMZ18 microscope with a dark field. The dissections were done under a Nikon SMZ18 microscope with a dark field, equipped



Figure 1. Moustos spring, type locality of *Achaiohydrobia moreana*.

Table 1. Taxa used for phylogenetic analyses with their GenBank accession numbers and references.

| Species | COI/H3 GB numbers | References |
|---|-----------------------------|---|
| <i>Adriohydrobia gagatinella</i> (Küster, 1852) | AF317857/- | Wilke and Falniowski 2001 |
| <i>Belgrandiella kuesteri</i> (Boeters, 1970) | MG551325/MG551366 | Osikowski et al. 2018 |
| <i>Bythinella cretensis</i> Schütt, 1980 | KT353689/- | Szarowska et al. 2016b |
| <i>Ecrobia grimmii</i> (Clessin in W. Dybowski, 1887) | MN167716/- | Vandendorpe et al. 2019 |
| <i>Ecrobia maritima</i> (Milaschewitsch, 1916) | KX355830, KX355834/MG551322 | Osikowski et al. 2016/Grego et al. 2017 |
| <i>Ecrobia spatiatiana</i> (Radoman, 1973) | MN167737/- | Vandendorpe et al. 2019 |
| <i>Ecrobia truncata</i> (Vanatta, 1924) | MN167740, MN167741/- | Vandendorpe et al. 2019 |
| <i>Ecrobia ventrosa</i> (Montagu, 1803) | KX355837, KX355840/- | Osikowski et al. 2016 |
| <i>Hydrobia acuta</i> (Draparnaud, 1805) | AF278808/- | Wilke et al. 2000 |
| <i>Hydrobia acuta neglecta</i> Muus, 1963 | AF278820/- | Wilke et al. 2000 |
| <i>Hydrobia glyca</i> (Servain, 1880) | AF278798/- | Wilke et al. 2000 |
| <i>Littorina littorea</i> (Linnaeus, 1758) | KF644330/KP113574 | Layton et al. 2014/Neretina 2014, unpublished |
| <i>Montenegraspeum bogici</i> (Pešić & Glöer, 2012) | KM875510/MG880218 | Falniowski et al. 2014/Grego et al. 2018 |
| <i>Peringia ulvae</i> (Pennant, 1777) | AF118292, AF118302/- | Wilke and Davis 2000 |
| <i>Pontobelgrandiella</i> sp. | KU497012/MG551321 | Rysiewska et al. 2016/Grego et al. 2017 |
| <i>Pseudamnicola pieperi</i> Schütt, 1980 | KT1710670/ KT1710741 | Szarowska et al. 2016a |
| <i>Pseudorientalia</i> sp. | KJ920477/- | Szarowska et al. 2014 |
| <i>Salenthydrobia ferrerii</i> Wilke, 2003 | AF449201, AF449213/- | Wilke 2003 |

with Nikon DS-5 digital camera, whose captured images were used to draw anatomical structures with a graphic tablet. Morphometric parameters of the shell were measured by one person using a Nikon DS-5 digital camera and ImageJ image analysis software (Rueden et al. 2017). The penes were photographed under Motic microscope with a dark field. The radulae were extracted with Clorox, applying the techniques described by Falniowski (1990), and examined and photographed using a HITACHI S-4700 scanning electron microscope.

Snails for molecular analysis were fixed in 80% ethanol. DNA was extracted from whole specimens; tissues were hydrated in TE buffer (3 × 10 min); then, total genomic DNA was extracted with the SHERLOCK extraction kit (A&A Biotechnology), and the final product was dissolved in 20 µl of tris-EDTA (TE) buffer. The extracted DNA was stored at -80 °C at the Department of Malacology, Institute of Zoology and Biomedical Research, Jagiellonian University in Kraków (Poland).

Mitochondrial cytochrome oxidase subunit I (COI) and nuclear histone 3 (H3) loci were sequenced. Details of PCR conditions, primers used, and sequencing were given by Szarowska et al. (2016a). Sequences were initially aligned in the MUSCLE (Edgar 2004) program in MEGA 7 (Kumar et al. 2016) and then checked in BI-OEDIT 7.1.3.0 (Hall 1999). Uncorrected *p*-distances were calculated in MEGA 7. The estimation of the proportion of invariant sites and the saturation test (Xia 2000; Xia et al. 2003) were performed using DAMBE (Xia 2013). In the phylogenetic analysis additional sequences from GenBank were used as reference (Table 1). The data were analysed using approaches based on Bayesian inference (BI) and maximum likelihood (ML). We applied the GTR model whose parameters were estimated by RaxML (Stamatakis 2014). The Bayesian analyses were run using MrBayes v. 3.2.3 (Ronquist et al. 2012) with defaults of most priors. Two simultaneous analyses were

performed, each with 10,000,000 generations, with one cold chain and three heated chains, starting from random trees and sampling the trees every 1,000 generations. The first 25% of the trees were discarded as burn-in. The analyses were summarised as a 50% majority-rule tree. The ML analysis was conducted in RAxML v. 8.2.12 (Stamatakis 2014) using the RAxML-HPC v. 8 on XSEDE (8.2.12) tool via the CIPRES Science Gateway (Miller et al. 2010). To calibrate the molecular clock for COI, the divergence time between *Peringia ulvae* and *Salenthydrobia ferrerii* (Wilke 2003), with correction according to Falniowski et al. (2008), were used. The likelihoods for trees with and without the molecular clock assumption in a likelihood ratio test (LRT) (Nei and Kumar 2000) were calculated with PAUP. The relative rate test (RRT) (Tajima 1993) was performed in MEGA. As Tajima's RRTs and the LRT test rejected an equal evolutionary rate throughout the tree, time estimates were calculated using a penalized likelihood method (Sanderson 2002) in r8s v. 1.7 for Linux (Sanderson 2003).

Abbreviations

| | |
|--------------|--|
| GNHM | Goulandris Natural History Museum. Athens, Greece; |
| HNHM | Hungarian Natural History Museum, Budapest; |
| NHMW | Natural History Museum Vienna, Austria; |
| NHMUK | The Natural History Museum, London UK. |

Results

The shells (Fig. 2) are broad, ovate-conic with a few flat whorls, rapidly growing and separated by moderately deep suture. Shell measurements are presented in Table 2. Nearly all adult shells have a corroded apex, and most display some injuries, and secondarily healed crevices, perhaps caused by the corrosion by sulphides. Very frequently there are scalariform shells, looking like they were secondarily formed after dissolution of the “normal” shell. The snout and tentacles are uniformly and intensively black pigmented. The female reproductive organs (Fig. 3) have a prominent spiral of black-

Table 2. Shell measurements of *Achaihydrobia moreana*; specimen symbols as in Fig. 2; measured variables: see Fig. 2.

| | <i>a</i> | <i>b</i> | <i>c</i> | <i>d</i> | <i>e</i> | α | β |
|---------------------|-------------|-------------|-------------|-------------|-------------|------------|-----------|
| A – holotype | 2.25 | 1.29 | 1.06 | 0.63 | 0.82 | 111 | 11 |
| B – 2A19 | 2.69 | 1.34 | 1.10 | 0.80 | 0.91 | 95 | 12 |
| C – 2A20 | 1.68 | 0.99 | 0.92 | 0.38 | 0.67 | 98 | 8 |
| D | 1.93 | 1.02 | 0.90 | 0.60 | 0.63 | 93 | 13 |
| E | 2.09 | 1.22 | 0.96 | 0.56 | 0.72 | 104 | 15 |
| F | 2.45 | 1.33 | 1.10 | 0.69 | 0.87 | 109 | 13 |
| <i>M</i> | 2.18 | 1.20 | 1.01 | 0.61 | 0.77 | 101.67 | 12.00 |
| <i>SD</i> | 0.363 | 0.156 | 0.091 | 0.140 | 0.113 | 7.474 | 2.366 |
| <i>MIN</i> | 1.68 | 0.99 | 0.90 | 0.38 | 0.63 | 93.00 | 8.00 |
| <i>MAX</i> | 2.69 | 1.34 | 1.10 | 0.80 | 0.91 | 111.00 | 15.00 |

Table 3. Pairwise genetic *p*-distances calculated for COI within *Hydrobia* s. lato.

| <i>p</i>-distances between and within genera | | | | | |
|--|-----------------------|--------------------------|--------------------|------------------|----------------|
| | <i>Achαιοhydrobia</i> | <i>Salenthydrobia</i> | <i>Peringia</i> | <i>Hydrobia</i> | <i>Ecrobia</i> |
| <i>Achαιοhydrobia</i> | 0.000 | | | | |
| <i>Salenthydrobia</i> | 0.109 | 0.016 | | | |
| <i>Peringia</i> | 0.123 | 0.121 | 0.021 | | |
| <i>Hydrobia</i> | 0.142 | 0.131 | 0.115 | 0.028 | |
| <i>Ecrobia</i> | 0.167 | 0.151 | 0.145 | 0.150 | 0.050 |
| <i>p</i>-distances between <i>Ecrobia</i> species | | | | | |
| | <i>E. spatiatiana</i> | <i>E. ventrosa</i> | <i>E. truncata</i> | <i>E. grimmi</i> | |
| <i>E. spatiatiana</i> | | | | | |
| <i>E. ventrosa</i> | 0.038 | | | | |
| <i>E. truncata</i> | 0.064 | 0.060 | | | |
| <i>E. grimmi</i> | 0.066 | 0.062 | 0.064 | | |
| <i>E. maritima</i> | 0.057 | 0.050 | 0.057 | 0.040 | |
| <i>p</i>-distance between <i>Hydrobia</i> species | | | | | |
| | <i>H. glyca</i> | <i>H. acuta_neglecta</i> | | | |
| <i>H. glyca</i> | | | | | |
| <i>H. acuta_neglecta</i> | 0.037 | | | | |
| <i>H. acuta</i> | 0.034 | 0.013 | | | |
| <i>p</i>-distance within <i>Peringia ulvae</i> 0.021 | | | | | |
| <i>p</i>-distance within <i>Salenthydrobia ferrerii</i> 0.016 | | | | | |

pigmented renal oviduct. The penis (Fig. 4) has a broad proximal part and long and narrow filament, without any outgrowth. The character states listed briefly above allow the classification to neither known species nor any known genus in the Hydrobiidae.

We obtained two new sequences of COI (479 bp, GenBank Accession Numbers MW741741-MW741742), and two new sequences of H3 (309 bp, GenBank Accession Numbers MW776415-MW776416). The tests by Xia et al. (2003) for COI and H3 revealed no saturation. In all analyses, the topologies of the resulting phylograms were identical in both the ML and BI. The phylogram based on the cytochrome oxidase (Fig. 5) clearly show the position of this taxon within the “*Hydrobia*” as widely understood, and as a sister taxon (bootstrap support 75%) of *Salenthydrobia ferrerii*, with an estimated divergence time of 5.75 ± 0.49 Mya. The pairwise *p*-distances (Table 3) calculated for the taxa shown in the phylogram (Fig. 5) are typical rather for inter-generic level.

Family Hydrobiidae Stimpson, 1865

Genus *Achαιοhydrobia* Falniowski, gen. nov.

<http://zoobank.org/B18334FD-AB44-421A-80FE-568854549087>

Type species. *Achαιοhydrobia moreana* by monophyly.

Diagnosis. Shell broad, ovate-conic with a few flat whorls, rapidly growing and separated by a moderately deep suture; female reproductive organs with prominent, massive swelling of the spiral of the oviduct; oval bursa copulatrix with the duct longer than the bursa, receptaculum seminis prominent but smaller than the bursa, with the

duct slightly distinguishable; penis tapering, widened at the base, without any outgrowths (nonglandular lobes) and without the distal papilla.

Derivatio nominis. The genus name refers to Achaia, one of the ancient names of Greece and the Greek people.

Remarks. The tapering penis with its broad base distinguishes *Achaiohydrobia* from *Hydrobia* and *Peringia*. The lack of any non-glandular outgrowths (lobes) distinguishes it from *Hydrobia*, *Peringia*, and *Ventrosia*. The lack of the distal papilla on the penis distinguishes it from *Salenthydrobia*. The massive swelling of the long spiral renal oviduct differentiates *Achaiohydrobia* from all other genera besides *Hydrobia*. The molecular divergence between *Achaiohydrobia* and the other genera ($p = 0.109\text{--}0.167$ for mitochondrial COI) is typical of the genus-level in Hydrobiidae.

***Achaiohydrobia moreana* Hofman & Grego, sp. nov.**

<http://zoobank.org/165D82EB-2F0A-47DB-BB52-A216E12A99DF>

Figure 2

[GenBank no. for COI: MW741741–MW741742; for H3: MW776415–MW776416]

Holotype. GNHM 39589, leg. M. Szarowska and A. Falniowski, 16.07.2009; ethanol-fixed specimen (Fig. 2A), brackish water of Moustos spring, 2 km N of Aghios Andreas, Arkadia, eastern Peloponnese, Greece (37.3845, 22.7444), creeping on the stones and gravel.

Paratypes. Ten paratypes, ethanol-fixed, in the collection of the Department of Malacology of Jagiellonian University. GNHM 39590/20, HNHM Moll.105301/30 wet specimens; NHMW 113630/10 wet specimens; NHMUK 20210006/10; coll. Eröss 10 wet specimens; coll. Grego 32 wet and 36 dry specimens.

Diagnosis. Shell broad, ovate-conic with a few flat whorls, rapidly growing and separated by a moderately deep suture; female reproductive organs with a prominent, massive swelling of the spiral of the oviduct; oval bursa copulatrix with the duct longer than the bursa, receptaculum seminis prominent but smaller than the bursa, with the duct slightly distinguishable; penis tapering, widened at the base, without any outgrowths (no glandular lobes) and without the distal papilla (diagnosis the same as for this monotypic genus).

Description. *Shell* (Fig. 2) broad, thick-walled, brownish, moderately translucent, up to 2.69 mm high and 1.34 mm broad, ovate-conic with about five flat whorls, growing rapidly and separated by moderately deep suture. Conical spire height about 0.25 of the shell height; body whorl prominent and broad. Aperture narrow, elongate-elliptical; peristome complete and thin, in contact with the wall of the body whorl; umbilicus slit-like or completely covered by the parietal lip. Shell surface smooth, with growth lines hardly visible, often corroded.

Measurements of holotype and sequenced and illustrated shells: Table 2. Shell variability slight (Fig. 2).

Protoconch (Fig. 6) smooth, often corroded.

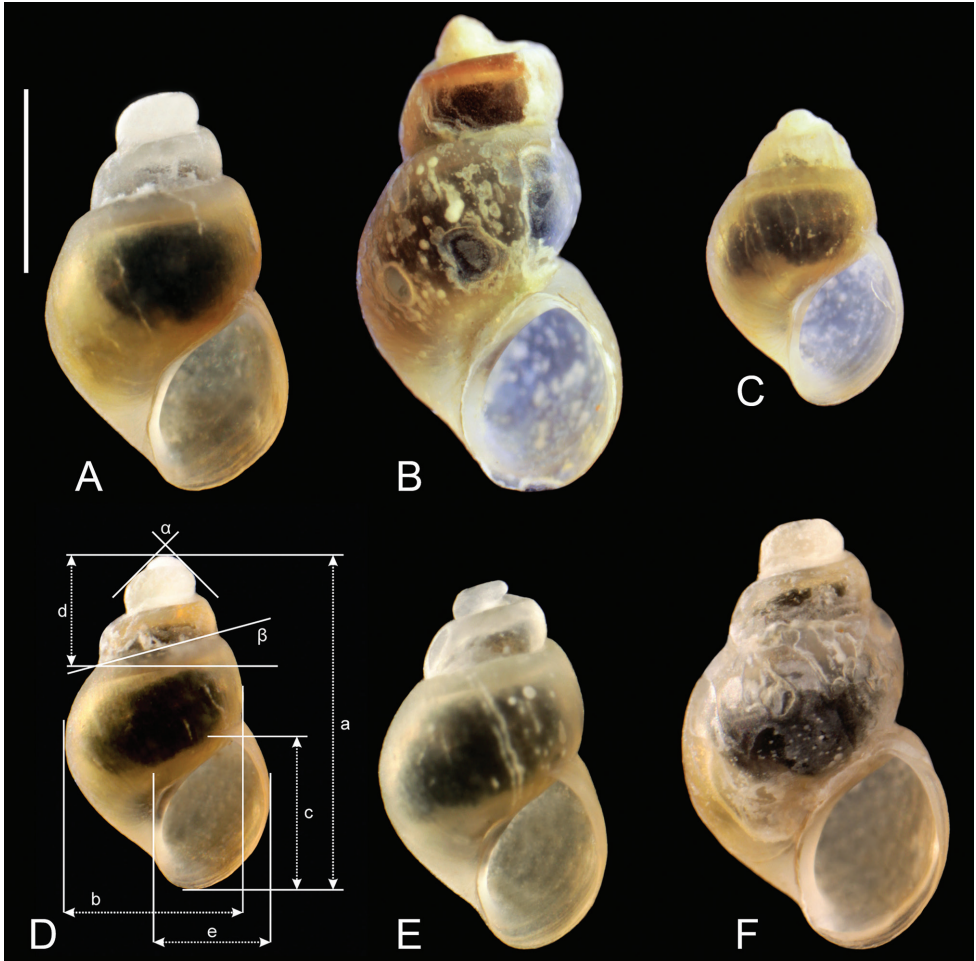


Figure 2. Shells of *Achaiohydrobia moreana* **A** holotype; shell measurements are shown: a = shell height, b = body whorl breadth, c = aperture height, d = spire height, e = aperture breadth, α = apex angle, β = angle between body whorl suture and horizontal surface. Scale bar: 1 mm.

Radula (Fig. 7) typically taenioglossate, with prominent basal cusps and the central cusp on the central tooth; central tooth formula:

$$\frac{3-1-3}{1-1} \text{ or } \frac{(4)3-1-3(4)}{1-1} \text{ or } \frac{4-1-4}{1-1}$$

The lateral tooth with 2 – 1 – 2 prominent and broad cusps, especially the bigger one. Inner marginal tooth with about 11, and outer marginal one with 16–19 cusps.

Soft parts morphology and anatomy. The mantle, snout, and tentacles intensively pigmented uniformly black. The female reproductive organs (Fig. 3) with a prominent,

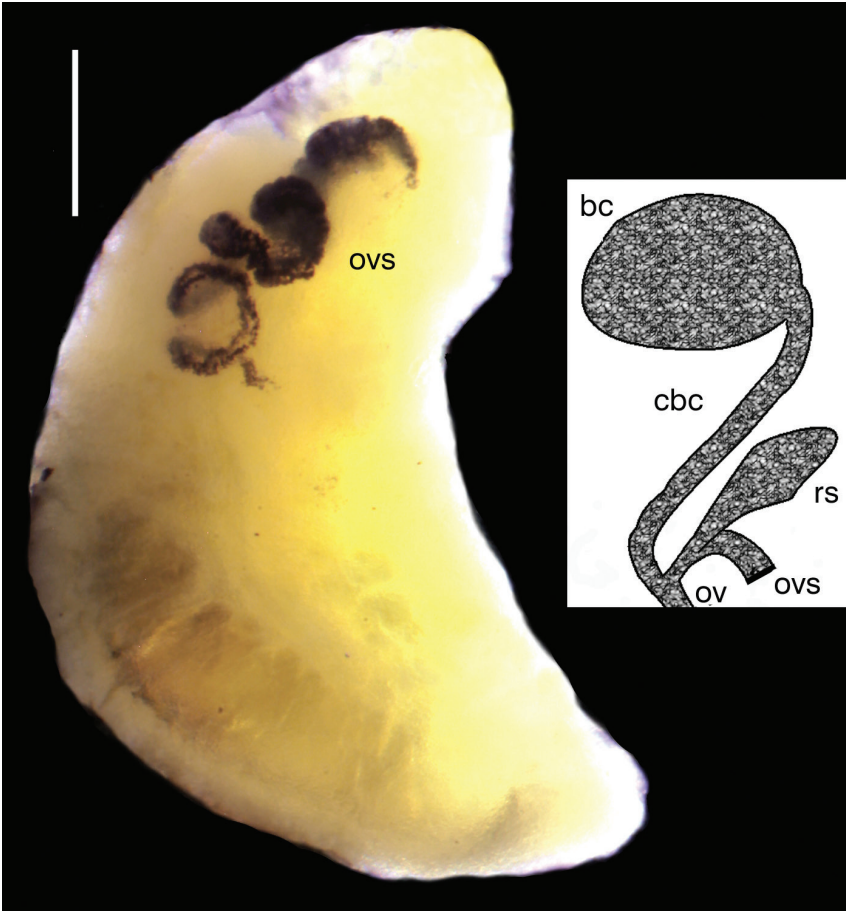


Figure 3. Renal and pallial section of female reproductive organs of *Achaiohydrobia moreana*; drawing not to the scale (bc – bursa copulatrix, cbc – duct of the bursa, ov – oviduct, ovs – spiral of renal oviduct, rs – receptaculum seminis). Scale bar: 200 μ m.



Figure 4. Penis of *Achaiohydrobia moreana*. Scale bar: 200 μ m.

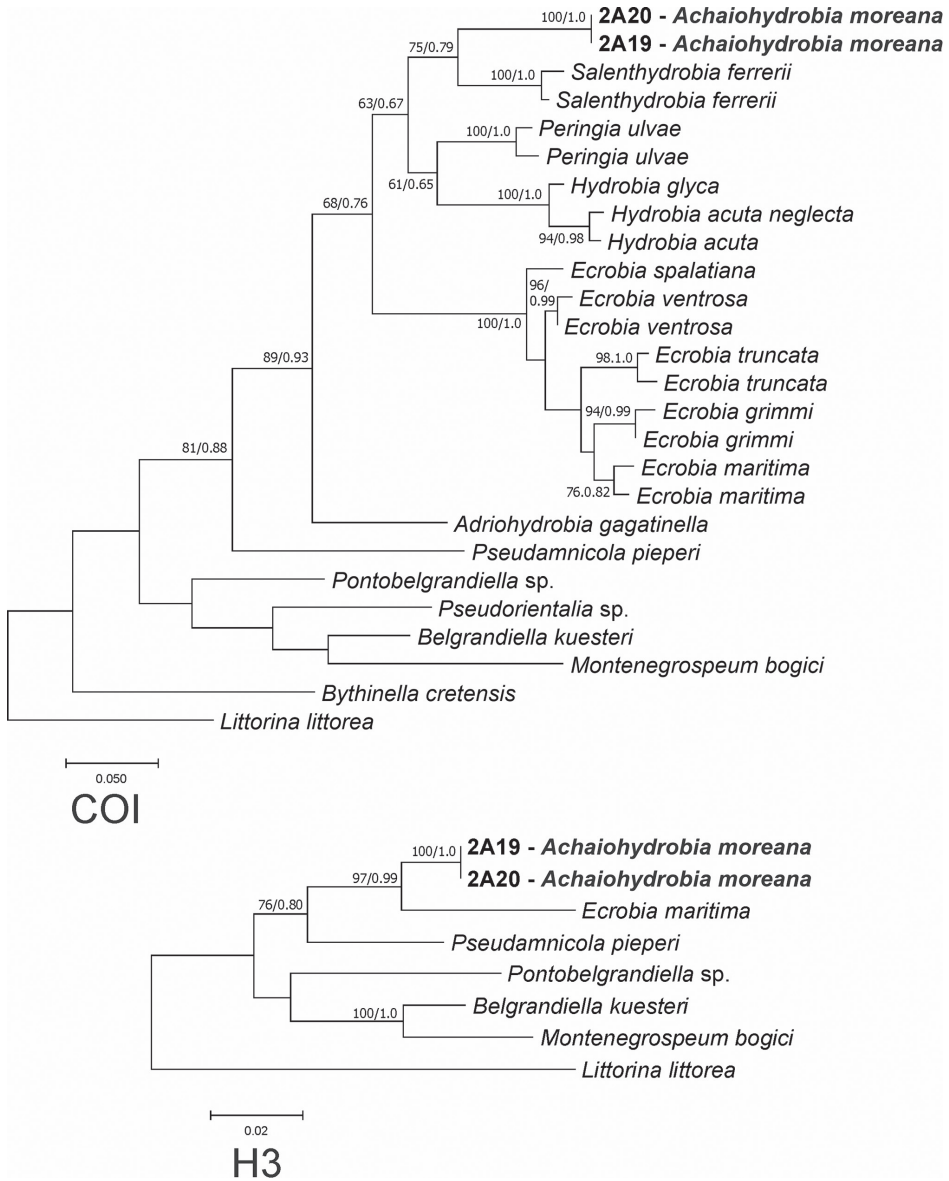


Figure 5. Phylogenetic relationships between the species formerly classified as *Hydrobia*.

massive swelling of the spiral of the intensively pigmented black renal oviduct. The bursa copulatrix oval, situated dextro-lateral to the style sac, with the duct longer than the bursa, the receptaculum seminis big, but smaller than the bursa, elongated, with the duct slightly distinguishable from the receptaculum. The penis (Fig. 4) tapering, widened at the base, without any nonglandular lobes, no papilla, its proximal section slightly broadened (if at all; see Fig. 4D).

Derivatio nominis. The specific epithet *moreana* refers to Morea, the medieval name of Peloponnese Peninsula.



Figure 6. Protoconchs of *Achaiohydrobia moreana*. Scale bar: 200 μm .

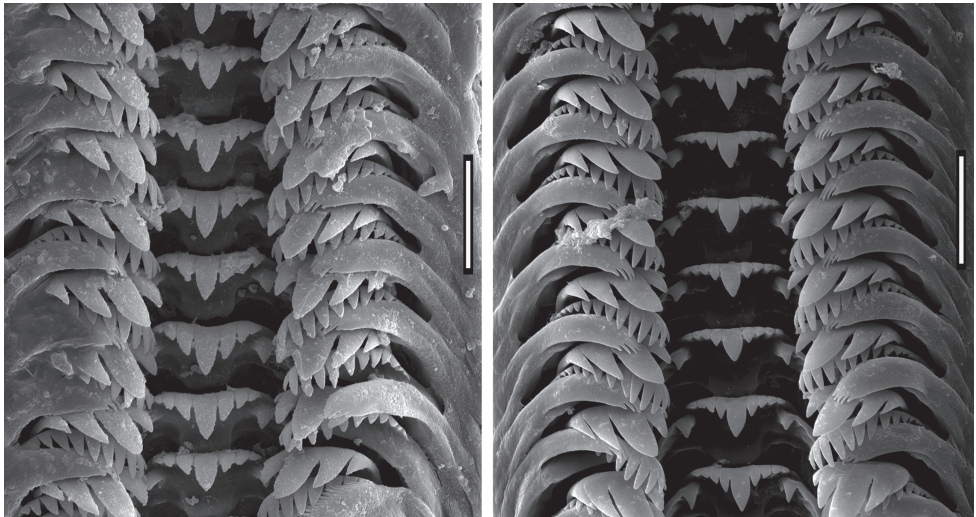


Figure 7. Radulae of *Achaiohydrobia moreana*. Scale bar: 25 μm .

Discussion

The radula was the first internal structure considered in the gastropod systematics. In the snails formerly known as *Hydrobia*, whose shells especially lack taxonomically useful characters, the radulae were studied for a long time (Meyer and Möbius 1872; Woodward 1891; Kuhlitz 1898; Krull 1935; Seifert 1935; Feliksiak 1938; Muus 1963, 1967; Bishop 1976; Falniowski et al. 1977; Bank and Butot 1984; Giusti and Pezzoli 1984; Wilke 2003). However, no constant differences were found to distinguish species, although some not quite stable differences in cusp basal cusp number, etc., were observed. The radula of our *Achaiohydrobia* also bears no unique character states.

The penis morphology of *Achaiohydrobia* is most similar to that of *Adriohydrobia*, but in the newly described genus it is more massive. Differentiating character states are the shape of the bursa copulatrix, its shorter duct and the massive swelling of the oviduct, traits not observable in *Adriohydrobia*. There are detailed data describing the differences in the female reproductive organs (for a summary see Wilke 2003). However, the examination of more numerous specimens (Falniowski 1988) has shown a much variability (also artefactual, physiological, etc.) which gives doubts to the usefulness of these character states for species or genus discriminations (Falniowski 1987, 1989, 1990). The broad base of the penis, listed by Wilke (2003) as one of the apomorphic traits of *Salenthydrobia*, can hardly be recognized as a synapomorphy characterizing all the specimens of our *Achaiohydrobia*. Only three specimens of *Achaiohydrobia* were photographed, and in one of them, no broad base was observed (Fig. 4D).

Brackish-water snails are considered to form isolated populations in suitable habitats, isolated by land, but also by the sea with its full salinity (e.g., Giusti and Pezzoli 1984; Falniowski 1987; Fretter and Graham 1994; Wilke and Davis 2000; Wilke et al. 2000; Wilke 2003). Only *P. ulvae*, capable of living in full sea salinity and with lecithotrophic, although short-living, veliger larva, forms populations less affected by isolation. However, considering all data available (see Fretter and Graham 1994 for details), all "*Hydrobia*" taxa studied so far may be able to survive in open-sea salinity. Anyway, partial isolation promotes allopatric speciation in these gastropods. The type locality of *Achaiohydrobia moreana* is one of the springs fed by the complicated system of poljes and sink-holes in Arcadia (Higgins and Higgins 1996). In the geologic history of the region (e.g., Rögl 1998, 1999) there were many events, such as transgressions of the sea, that must have created conditions that would promote speciation.

The estimated time of divergence between *Achaiohydrobia* and the phylogenetically close *Salenthydrobia* (5.75 ± 0.49 Mya) coincides with 5.33 Mya, which is the time of the Oligocene flooding that ended the Messinian salinity crisis; the estimate is comparable to the divergence time between *Salenthydrobia* and *Peringia* (Wilke 2003) and little older than the two species of *Ecrobia* (Osikowski et al. 2016). An estimated 1.7% divergence per million years is comparable with other estimated times of divergence for Hydrobiidae (Wilke 2003; Osikowski et al. 2016).

The Messinian salinity crisis affected all the Recent basins of the Mediterranean (Krijgsman et al. 1999; McKenzie 1999). The uplift of the northern African and southern Iberian margins, probably due to the roll back of the Tethys oceanic lithosphere delaminating bands of lithospheric mantle from beneath the continental margin (Duggen et al. 2003), blocked the passage between the Atlantic and Mediterranean about 5.96 Mya. This resulted in the regression of the sea and a lowering of the water level by more than 1000 m. In the place of the Recent Mediterranean, there was a desert, crossed by the vast canyons of large rivers, with some water bodies too rich and others too poor in salt; thus, it was impossible for marine organisms to inhabit the area. There were at least 10 sea transgressions in the Mediterranean during the Messinian (Hsü 1983). The region of the Recent Sea of Marmara served as a gateway between the Paratethys and the Mediterranean. Frequent marine introgressions fed water bodies (basins) of a “Lago-Mare” character: large and deep, although with brackish habitats. Apart from brackish water bodies, there were also highly saline ones, but nowhere in the Mediterranean there were normal marine conditions. We should note, however, that such brackish water “Lago-Mare” basins were probably inhabitable for brackish-water snails. Later, 5.33 Mya at boundary between the Miocene from Pliocene, the abrupt catastrophic Pliocene transgression of water from the Atlantic, probably caused by gravity-induced slumping from the western margin of the Gibraltar arch into the Atlantic abyssal plains (Duggen et al. 2003), filled the Mediterranean basin with sea water again. The rapid, drastic changes formed barriers for the fresh- and brackish-water fauna, promoting speciation processes in many animals (e.g., Wilke 2003; Huys et al. 2004; Falniowski et al. 2007).

Acknowledgements

This study was supported by a grant from the National Science Centre 2017/25/B/NZ8/01372 to Andrzej Falniowski. We are grateful for the assistance of Anna Łatkiewicz (Laboratory of FE Scanning Microscopy and Microanalysis, Institute of Geological Sciences, Jagiellonian University, Krakow, Poland) for her help with the SEM. We would like to express our thanks to Zoltán Fehér, Zolán-Péter Erőss and András Hunyadi from Hungarian Natural History Museum in Budapest for supporting our research.

References

- Bank RA, Butot LJM (1984) Some more data on *Hydrobia ventrosa* (Montagu, 1803) and “*Hydrobia*” *stagnorum* (Gmelin, 1791) with remarks on the genus *Semisalsa* Radoman, 1974 (Gastropoda, Prosobranchia, Hydrobioidea). *Malakologische Abhandlungen, Staatliches Museum für Tierkunde Dresden* 10: 5–15.
- Bank RA, Butot LJM, Gittenberger E (1979) On the identity of *Helix stagnorum* Gmelin, 1791, and *Turbo ventrosus* Montagu, 1803 (Prosobranchia, Hydrobiidae). *Basteria* 43: 51–60.

- Bishop MJ (1976) *Hydrobia neglecta* Muus in the British Isles. *Journal of Molluscan Studies* 42: 319–326. <https://doi.org/10.1093/oxfordjournals.mollus.a065340>
- Davis GM (1992) Evolution of prosobranch snails transmitting Asian *Schistosoma*: coevolution with *Schistosoma*: a review. *Progress in Clinical Parasitology* 3: 145–204. https://doi.org/10.1007%2F978-1-4612-2732-8_6
- Davis GM, McKee M, Lopez G (1989) The identity of *Hydrobia truncata* (Gastropoda: Hydrobiidae): Comparative anatomy, molecular genetics, ecology. *Proceedings of the Academy of the Natural Sciences of Philadelphia* 140: 247–266. <https://www.jstor.org/stable/4064963>
- Draparnaud J-P-R (1805) Histoire naturelle des mollusques terrestres et fluviatiles de la France. Levrault & Schoell, Paris [2 pp. (Avertissement a sa Majesté l'Impératrice), 2 pp. Rapport, i–viii (Préface) +] 164 pp. [+ pls 1–13, 1 p. Errata.] <https://doi.org/10.5962/bhl.title.12856>
- Duggen S, Hoernie K, van den Bogaard P, Rüpke L, Morgan JP (2003) Deep roots of the Messinian salinity crisis. *Nature* 422: 602–606. <https://doi.org/10.1038/nature01553>
- Edgar RC (2004) MUSCLE: multiple sequence alignment with high accuracy and high throughput. *Nucleic Acids Research* 32: 1792–1797. <https://doi.org/10.1093/nar/gkh340>
- Evagelopoulos A, Spyarakos E, Koutsoubas D (2009) Phytoplankton and macrofauna in the low salinity ponds of a productive solar saltworks: spatial variability of community structure and its major abiotic determinants. *Global NEST Journal* 11: 64–72. <https://doi.org/10.30955/gnj.000576>
- Falniowski A (1986) Pigmentation in *Hydrobia ulvae* (Pennant, 1777) and *H. ventrosa* (Montagu, 1803) (Hydrobiidae, Prosobranchia) from the Polish Baltic. *Acta Hydrobiologica* 28: 443–449. <https://doi.org/10.12657/folmal.028.025>
- Falniowski A (1987) Hydrobioidea of Poland (Prosobranchia: Gastropoda). *Folia Malacologica* 1: 1–122. <https://doi.org/10.12657/folmal.001.001>
- Falniowski A (1988) Female reproductive organs of *Hydrobia ulvae* (Pennant, 1777) and *H. ventrosa* (Montagu, 1803) from Puck Bay (Southern Baltic Sea) (Gastropoda, Prosobranchia, Hydrobioidea). *Malakologische Abhandlungen, Staatliches Museum für Tierkunde Dresden* 13: 27–31.
- Falniowski A (1989) A critical review of some characters widely used in the systematics of higher taxa of freshwater prosobranchs (Gastropoda: Prosobranchia), and a proposal of some new, ultrastructural ones. *Folia Malacologica* 3: 73–94. <https://doi.org/10.12657/folmal.003.005>
- Falniowski A (1990) Anatomical characters and SEM structure of radula and shell in the species-level taxonomy of freshwater prosobranchs (Mollusca: Gastropoda: Prosobranchia): a comparative usefulness study. *Folia Malacologica* 4: 53–142. <https://doi.org/10.12657/folmal.004.005>
- Falniowski A, Szarowska M (2002) Comment on the proposed conservation of *Hydrobia* Hartmann, 1821 (Mollusca, Gastropoda) and *Cyclostoma acutum* Draparnaud, 1805 (currently *Hydrobia acuta*) by the replacement of the lectotype of *H. acuta* with a neotype; proposed designation of *Turbo ventrosus* Montagu, 1803 as the type species of *Ventrosia* Radoman, 1977; and proposed emendation of spelling of *Hydrobiina* Mulsant, 1844 (Insecta, Coleoptera) to *Hydrobiusina*, so removing the homonymy with Hydrobiidae Troschel, 1857 (Mollusca). *Bulletin of Zoological Nomenclature* 59: 128–130.
- Falniowski A, Dyduch A, Smagowicz K (1977) Molluscs from Puck Bay (Baltic Sea) collected in 1973. *Acta Zoologica Cracoviensia* 12: 507–531.

- Falniowski A, Szarowska M, Grzmil P (2007) *Daphniola* Radoman, 1973 (Gastropoda: Hydrobiidae): shell biometry, mtDNA, and the Pliocene flooding. *Journal of Natural History* 41: 2301–2311. <https://doi.org/10.1080/00222930701630733>
- Falniowski A, Szarowska M, Sirbu I, Hillebrand A, Baciu M (2008) *Heleobia dobrogica* (Grossu & Negrea, 1989) (Gastropoda: Rissooidea: Cochliopidae) and the estimated time of its isolation in a continental analogue of hydrothermal vents. *Molluscan Research* 28: 165–170.
- Falniowski A, Pešić V, Glöer P (2014) *Montenegrospeum* Pešić et Glöer, 2013: a representative of Moitesseriidae? *Folia Malacologica* 22: 263–268. <https://doi.org/10.12657/folmal.022.023>
- Feliksiak S (1938) Radula von *Hydrobia ulvae* (Pennant) aus der *Littorina*-Zeit. *Zoologischer Anzeiger* 122: 186–189.
- Fretter V, Graham A (1994) British Prosobranch Molluscs. Their Functional Anatomy and Ecology. Revised and Updated Edition. The Ray Society, London, 755 pp.
- Gittenberger E (1991) What about non-adaptive radiation? *Biological Journal of the Linnean Society* 43: 263–272. <https://doi.org/10.1111/j.1095-8312.1991.tb00598.x>
- Giusti F, Pezzoli E (1984) Notulae malacologicae XXIX. Gli Hydrobiidae salmastri delle acque costiere Italiane: Primi cenni sulla sistematica del gruppo e sui caratteri distintivi delle singole morfospesie. *Lavori della Società Italiana di Malacologia* 21: 117–148.
- Grego J, Hofman S, Mumladze L, Falniowski A (2017) *Agrafia* Szarowska et Falniowski, 2011 (Caenogastropoda: Hydrobiidae) in the Caucasus. *Folia Malacologica* 25: 237–247. <https://doi.org/10.12657/folmal.025.025>
- Grego J, Glöer P, Rysiewska A, Hofman S, Falniowski A (2018) A new *Montenegrospeum* species from south Croatia (Mollusca: Gastropoda: Hydrobiidae). *Folia Malacologica* 26: 25–34. <https://doi.org/10.12657/folmal.026.004>
- Hall TA (1999) BioEdit: a user-friendly biological sequence alignment editor and analysis program for Windows 95/98/NT. *Nucleic Acids Symposium Series* 41: 95–98.
- Hartmann JDW (1821) System der Erd- und Flußschnecken der Schweiz. Mit vergleichender Aufzählung aller auch in den benachbarten Ländern, Deutschland, Frankreich und Italien sich vorfindenden Arten. In: Steinmüller JR (Ed.) *Neue Alpina*. Eine Schrift der Schweizerischen Naturgeschichte, Alpen- und Landwirtschaft gewidmet, Erster Band. Winterthur, 194–268. [pls 1, 2] <http://biodiversitylibrary.org/page/41756566>
- Higgins MD, Higgins R (1996) *A Geological Companion to Greece and the Aegean*. Cornell University Press, Ithaca / Duckworth Publishers, London, 240 pp.
- Hsü KJ (1983) *The Mediterranean was a Desert*. Princeton University Press, Princeton, 216 pp.
- Huysse T, Van Houdt J, Volckaert FAM (2004) Paleoclimatic history and vicariant speciation in the “sand goby” group (Gobiidae, Teleostei). *Molecular Phylogenetics and Evolution* 32: 324–336. <https://doi.org/10.1016/j.ympev.2003.11.007>
- International Commission on Zoological Nomenclature (2003) Opinion 2034 (Case 3087). *Hydrobia* Harmann, 1821: conserved by replacement of the lectotype of *Cyclostoma acutum* Draparnaud, 1805 (currently *Hydrobia acuta*; Mollusca, Gastropoda) with a neotype; *Ventrosia* Radoman, 1977. *Bulletin of Zoological Nomenclature* 60: 152–154.
- Kevrekidis T, Wilke T, Mogias A (2005) When DNA puts ecological works back on the right track: genetic assessment and distribution patterns of mudsnail populations in the Evros

- Delta lagoons. *Archiv für Hydrobiologie* 162: 19–35. <https://doi.org/10.1127/0003-9136/2005/0162-0019>
- Koutsoubas D, Arvanitidis C, Dounas C, Drummond L (2000) Community structure and dynamics of the Molluscan fauna in a Mediterranean lagoon (Gialova lagoon, SW Greece). *Belgian Journal of Zoology* 130: 131–138.
- Krijgsman W, Hilgen FJ, Raffi I, Sierro FJ, Wilson DS (1999) Chronology, causes and progression of the Messinian salinity crisis. *Nature* 400: 652–655. <https://doi.org/10.1038/23231>
- Krull H (1935) Anatomische Untersuchungen an einheimischen Prosobranchiern und Beiträge zur Phylogenie der Gastropoden. *Zoologische Jahrbücher (Anatomie Ontogenie)* 60: 399–464.
- Kuhlgatz T (1898) Untersuchungen über die Fauna der Schwentinemündung mit besonderer Berücksichtigung der Copepoden des Planktons. *Wissenschaftliche Meeresuntersuchungen*, Kiel, Neue Folge 3: 91–157.
- Kumar S, Stecher G, Tamura K (2016) MEGA7: Molecular Evolutionary Genetics Analysis version 7.0 for bigger datasets. *Molecular Biology and Evolution* 33: 1870–1874. <https://doi.org/10.1093/molbev/msw054>
- Küster HC (1852–1853) Die Gattungen *Paludina*, *Hydrocaena* und *Valvata*. In: *Abbildungen nach der Natur mit Beschreibungen. Systematisches Conchylien-Cabinet von Martini und Chemnitz*, 2. Edition. Nürnberg: Bauer & Raspe. Bd 1, Abt. 21: 1(21) (113): 1–24, pls 1, 2 (1852); (115): 25–56, pls 3–8 (1852); (119): 57–96, pls 9–14.
- Layton KK, Martel AL, Hebert PD (2014) Patterns of DNA barcode variation in Canadian marine molluscs *PLoS ONE* 9: E95003. <https://doi.org/10.1371/journal.pone.0095003>
- McKenzie JA (1999) From desert to deluge in the Mediterranean. *Nature* 400: 613–614. <https://doi.org/10.1038/23131>
- Meyer HA, Möbius K (1872) *Fauna der Kieler Bucht*. Bd. 2. Die Prosobranchia und Lamelli-branchia, nebst einem Supplement zu den Opisthobranchia. W. Engelmann, Leipzig, 139 pp.
- Miller MA, Pfeiffer W, Schwartz T (2010) Creating the CIPRES Science Gateway for inference of large phylogenetic trees. In: *Proceedings of the Gateway Computing Environments Workshop (GCE)*, 14 Nov., New Orleans, LA: 1–8. <https://doi.org/10.1109/GCE.2010.5676129>
- Montagu G (1803) *Testacea Britannica, or natural history of British shells, marine, land, and fresh-water, including the most minute: systematically arranged and embellished with figures*. Romsey, London, 606 pp. <https://doi.org/10.5962/bhl.title.33927>
- Muus BJ (1963) Some Danish Hydrobiidae with the description of a new species *Hydrobia neglecta*. *Proceedings of Malacological Societies London* 35: 131–138. <https://doi.org/10.1093/oxfordjournals.mollus.a064910>
- Muus BJ (1967) The fauna of Danish estuaries and lagoons. *Meddelelser fra Danmarks Fiskeri og Havundersogelser* 5: 1–316.
- Nei M, Kumar S (2000) *Molecular Evolution and Phylogenetics*. Oxford University Press, Oxford, 333 pp.
- Osikowski A, Hofman S, Georgiev D, Kalcheva S, Falniowski A (2016) Aquatic snails *Ecrobia maritima* (Milaschewitsch, 1916) and *E. ventrosa* (Montagu, 1803) (Caenogastropoda: Hydrobiidae) in the East Mediterranean and Black Sea. *Annales Zoologici* 66: 477–486. <https://doi.org/10.3161/00034541ANZ2016.66.3.012>

- Osikowski A, Hofman S, Rysiewska A, Sket B, Prevorčnik S, Falniowski A (2018) A case of biodiversity overestimation in the Balkan *Belgrandiella* A. J. Wagner, 1927 (Caenogastropoda: Hydrobiidae): molecular divergence not paralleled by high morphological variation. *Journal of Natural History* 52: 323–344. <https://doi.org/10.1080/00222933.2018.1424959>
- Paladilhe A (1874) Monographie de nouveau genre *Peringia*, suivie des descriptions d'espèces nouvelles de Paludines françaises. *Annales des Sciences Naturelles, series 6, Zoologie et Paléontologie* 1: 1–38.
- Pennant T (1777) *British zoology*. Vol. IV. Crustacea. Mollusca. Testacea. White, London, 154 pp.
- Radoman P (1973) New classification of fresh and brackish water Prosobranchia from the Balkans and Asia Minor. *Posebna Izdanja, Prirodnjacki muzej u Beogradu* 32: 1–30.
- Radoman P (1977) Hydrobiidae auf der Balkanhalbinsel und in Kleinasien. *Archiv für Molluskenkunde* 107: 203–223.
- Radoman P (1983) Hydrobioidea a superfamily of Prosobranchia (Gastropoda). I Systematics. *Serbian Academy of Sciences and Arts, Monographs* 547, *Department of Sciences* 57: 1–256.
- Ronquist F, Teslenko M, van der Mark P, Ayres DL, Darling A, Höhna S, Larget B, Liu L, Suchard MA, Huelsenbeck JP (2012) Efficient Bayesian phylogenetic inference and model choice across a large model space. *Systematic Biology* 61: 539–542. <https://doi.org/10.1093/sysbio/sys029>
- Rueden DT, Schindelin J, Hiner MC, DeZonia BE, Walter AE, Arena ET, Eliceiri KW (2017) ImageJ2: ImageJ for the next generation of scientific image data. *BMC Bioinformatics* 18: e529. <https://doi.org/10.1186/s12859-017-1934-z>
- Rögl F (1998) Palaeogeographic considerations for Mediterranean and Paratethys seaways (Oligocene to Miocene). *Annalen des Naturhistorischen Museums in Wien* 99A: 279–310.
- Rögl F (1999) Mediterranean and Paratethys. Facts and hypotheses of an Oligocene to Miocene paleogeography (short overview). *Geologica Carpathica* 50: 339–349.
- Rysiewska A, Georgiev D, Osikowski A, Hofman S, Falniowski A (2016) *Pontobelgrandiella* Radoman, 1973 (Caenogastropoda: Hydrobiidae): a recent invader of subterranean waters? *Journal of Conchology* 42: 193–203.
- Sanderson MJ (2002) Estimating absolute rates of molecular evolution and divergence times: a penalized likelihood approach. *Molecular Biology and Evolution* 19: 101–109. <https://doi.org/10.1093/oxfordjournals.molbev.a003974>
- Sanderson MJ (2003) R8s: inferring absolute rates of molecular evolution, divergence times in the absence of a molecular clock. *Bioinformatics* 19: 301–302. <https://doi.org/10.1093/bioinformatics/19.2.301>
- Schütt H (1980) Zur Kenntnis griechischer Hydrobiiden. *Archiv für Molluskenkunde* 110: 115–149.
- Seifert TR (1935) Bemerkungen zur Artunterscheidung der deutschen Brackwasser-Hydrobiiden. *Zoologischer Anzeiger* 110: 233–239.
- Stamatakis A (2014) RaxML Version 8: a tool for phylogenetic analysis and post-analysis of large phylogenies. *Bioinformatics* 30: 1312–1313. <https://doi.org/10.1093/bioinformatics/btu033>
- Szarowska M, Falniowski A (2014) *Ventrosia maritima* (Milaschewitsch, 1916) and *V. ventrosa* (Montagu, 1803) in Greece: molecular data as a source of information about species ranges

- within the Hydrobiinae (Caenogastropoda: Truncatelloidea). *Folia Malacologica* 22: 61–67. <https://doi.org/10.12657/folmal.022.006>
- Szarowska M, Hofman S, Osikowski A, Falniowski A (2014) Divergence preceding Island formation among Aegean insular populations of the freshwater snail genus *Pseudorientalia* (Caenogastropoda: Truncatelloidea). *Zoological Science* 31: 680–686. <https://doi.org/10.2108/zs140070>
- Szarowska M, Osikowski A, Hofman S, Falniowski A (2016a) *Pseudamnicola* Paulucci, 1878 (Caenogastropoda: Truncatelloidea) from the Aegean Islands: a long or short story? *Organisms Diversity and Evolution* 16: 121–139. <https://doi.org/10.1007/s13127-015-0235-5>
- Szarowska M, Osikowski A, Hofman S, Falniowski A (2016b) Do diversity patterns of the spring-inhabiting snail *Bythinella* (Gastropoda, Bythinellidae) on the Aegean Islands reflect geological history? *Hydrobiologia* 765: 225–243. <https://doi.org/10.1007/s10750-015-2415-x>
- Tajima F (1993) Simple methods for testing molecular clock hypothesis. *Genetics* 135: 599–607. <https://doi.org/10.1093/genetics/135.2.599>
- Wilke T (2003) *Salenthydrobia* gen. nov. (Rissooidea: Hydrobiidae): a potential relict of the Messinian salinity crisis. *Zoological Journal of the Linnean Society* 137: 319–336. <https://doi.org/10.1046/j.1096-3642.2003.00049.x>
- Wilke T, Davis GM (2000) Intraspecific mitochondrial sequence diversity in *Hydrobia ulvae* and *Hydrobia ventrosa* (Hydrobiidae: Rissoacea: Gastropoda): Do their different life histories affect biogeographic patterns and gene flow? *Biological Journal of the Linnean Society* 70: 89–105. <https://doi.org/10.1006/bijl.1999.0388>
- Wilke T, Falniowski A (2001) The genus *Adriohydrobia* (Hydrobiidae: Gastropoda): polytypic species or polymorphic populations? *Journal of Zoological Systematics and Evolutionary Research* 39: 227–234. <https://doi.org/10.1046/j.1439-0469.2001.00171.x>
- Wilke T, Pfenninger M (2002) Separating historic events from recurrent processes in cryptic species: phylogeography of mud snails (*Hydrobia* spp.). *Molecular Ecology* 11: 1439–1451. <https://doi.org/10.1046/j.1365-294X.2002.01541.x>
- Wilke T, Rolán E, Davis GM (2000) The mudsnail genus *Hydrobia* s.s. in the northern Atlantic and western Mediterranean: a phylogenetic hypothesis. *Marine Biology* 137: 827–833. <https://doi.org/10.1007/s002270000407>
- Woodward BB (1892) On the radula of *Paludestrina jenkinsi* Smith and that of *P. ventrosa* Mont. *Annales and Magazine of Natural History* 9: 376–378. <https://doi.org/10.1080/00222939208677341>
- Vandendorpe J, van Baak CGC, Stelbrink B, Delicado D, Albrecht C, Wilke T (2019) Historical faunal exchange between the Pontocaspian Basin and North America. *Ecology and Evolution* 9: 10816–10827. <https://doi.org/10.1002/ece3.5602>
- Xia X (2000) *Data analysis in molecular biology and evolution*. Kluwer Academic Publishers, Boston, Dordrecht & London, 280 pp.
- Xia X (2013) DAMBE: A comprehensive software package for data analysis in molecular biology and evolution. *Molecular Biology and Evolution* 30: 1720–1728. <https://doi.org/10.1093/molbev/mst064>
- Xia X, Xie Z, Salemi M, Chen L, Wang Y (2003) An index of substitution saturation and its application. *Molecular Phylogenetics and Evolution* 26: 1–7. [https://doi.org/10.1016/S1055-7903\(02\)00326-3](https://doi.org/10.1016/S1055-7903(02)00326-3)

